PRE-INJURY STATINS IN EARLY RESUSCITATION OF COMPLEX BATTLEFIELD INJURIES

By

HENRIETTA POON

A thesis submitted to
The University of Birmingham
for the degree of
DOCTOR OF PHILOSOPHY

Institute of Inflammation and Ageing
College of Medical and Dental Sciences
University of Birmingham
December 2019

Abstract

The Defence Medical Services faces many challenges when treating personnel injured on the battlefield. These include logistical constraints, such as limited resources, and prolonged evacuation times, as well as the physiological and immunological responses in the host as a result of traumatic injury. Injuries from explosions can include injuries caused by the shock wave that interact with the physiological and inflammatory responses to 'conventional' trauma. The result can be an augmented inflammatory state, which may lead to systemic disease and remote organ damage. The use of pharmacological adjuncts to resuscitation may mitigate these inflammatory responses. Statins are potential candidates because of their pleiotropic properties such as organ protection and anti-inflammatory effects. The beneficial pleiotropic have been widely reported in ischaemia-reperfusion injury, and to a much lesser extent after haemorrhagic shock.

The study utilised a rat model of complex battlefield injury, which comprised femur fracture (tissue injury) and haemorrhage, with and without blast injury. The study was conducted in two strands (injury with and without blast), and within each strand the animals were randomised to receive either simvastatin or placebo. Outcome measures include DAMPS, cytokines, chemokines, circulating endothelial cells and histological changes, as well as physiological parameters such as blood pressure and acid-base status (degree of shock).

The injury, shock state and the resuscitation regimen in this model generated the expected physiological changes, and a measurable inflammatory response, which were both statistically and clinically significant. However, there was no statistically significant difference between treatment groups in either injury strand. These results suggest that treatment with simvastatin does not modify the response to trauma in either of the models of trauma used in this study.

Dedication

This work is dedicated to the casualties of war.

Acknowledgements

First and foremost, I would like to thank Professor Mark Midwinter, who gave me the opportunity to embark on this project during his tenure as Professor of Military Surgery, without which no part of this thesis would have been possible.

I would also like to thank my supervisor at University of Birmingham, Dr Paul Harrison, for his support.

I would like to thank Surg Capt Rory Rickard, the current Professor of Military Surgery, who is ever so patient and encouraging.

As a surgical trainee new to translational research, I relied heavily on the advice and goodwill from the team at DSTL Porton Down. Everyone was welcoming, kind and patient, and offered me essential guidance and support throughout this endeavour.

I would like to thank Dr Abigail Spear for her expertise and guidance in molecular biology techniques. Abigail - your patience, encouragement and words of wisdom (which also extend to new motherhood) is much appreciated, thank you.

I would like to acknowledge Dr Dominic Jenner for his expertise in developing the imaging flow cytometry protocol and for analysing the samples.

Dr Lyndsey Robertson, Dr Rachael Ireland and Dr Robert Purcell - please accept my gratitude for helping a surgical trainee navigate the world of immunology.

Thanks also to Sara Macildowie and Jo Choules for showing me the ropes in molecular biology techniques, and particularly for helping with RNA extraction.

I would like to acknowledge the Analytical Chemistry team at DSTL Porton Down for their expertise in developing the plasma simvastatin detection assay and for analysing the samples.

Thank you to Professor Karim Brohi and his team at Centre for Trauma Sciences for the collaboration on gene expression profiling after trauma.

These experiments would not have been possible without the support from the team at Medical and Trauma Science, DSTL Porton Down. Thank you Esther, Callie, Harry, Clare, Mark, Charles and Keith. You guys have made those long hours in the laboratory much shorter, both figuratively and literally.

Thank you to my friends for keeping up my spirits and listening to my laments these couple of years.

To my DSTL supervisors Dr Sarah Watts and Dr Emrys Kirkman, I am seldom without words but no words can express my gratitude to you. Your kindness, patience, encouragement, expertise and guidance have supported me throughout this journey. I am humbled by how generous you have been with your time (knowing how busy you both are), and going above and beyond the call of duty to support this endeavour. For your friendship, I am eternally grateful.

Finally I would like to thank my family. To my parents, who have supported me in everything I have chosen to do in life, no matter how unachievable it may seem. To Tim, Georgiana, Sandy, and Darwin, thank you for putting up with my occasional absence and providing the unwavering love that has kept me going.

Statement of Copyright

TABLE OF CONTENTS

List of illustrations

List of tables

List of abbreviations

AAA	abdominal aortic aneurysm
ALI	acute lung injury
ALT	alanine aminotransferase
ANOVA	one way analysis of variance
AP-1	activator protein-1
ARDS	adult respiratory distress syndrome
ATC	acute traumatic coagulopathy
ATP	adenosine triphosphate
CaO_2	oxygen content of arterial blood
CCL	C-C motif ligand
CCR	C-C motif receptor
cDNA	complementary DNA
CECs	circulating endothelial cells
CO	cardiac output
COX-2	cycloocygenase-2
CX3CL	C-X3-C motif ligand
CXCL	C-X-C motif ligand
CXCR	C-X-C motif receptor
CYP	cytochrome
DAMPS	damage- associated molecular patterns
DHEA	dehydroepiandrosterone
DNA	deoxyribonucleic acid
DO_2	oxygen delivery
DO_2 crit	point of critical oxygen delivery
Dstl	Defence Science and Technology Laboratory
EGF	epidermal growth factor
ELISA	enzyme-linked immunosorbent assay
EMSA	electrophopretic mobility shift assay
eNOS	endothelial NOS
EPC	endothelium progenitor cells
FDA	US food and drug administration
FWB	fresh whole blood
G-CSF	granulocyte colony stimulating factor
GDC	genomic DNA control
GM-CSF	granulocyte-macrophage colony-stimulating factor
GRO	growth-regulated oncogene
GSW	gun shot wound
HAT	histone acetyl transferases
Hb	haemoglobin
Hct	haematocrit
HDAC	histone deacetylase
HFOV	high frequency oscillatory ventilation
HGE	haemorrhage
HIF	hypoxia inducible factor

HMG-CoA	3-hydroxy-ethylglutaryl coenzyme A
HMGB1	high-mobility group box-1
HO-1	heme oxygenase-1
HR	heart rate
HS	haemorrhagic shock
HS/R	haemorrhagic shock and resuscitation
ICAM	interceullular adhesion molecule
IED	improvised explosive device
IFN	interferon
IL	interleukin
iNOS	inducible NOS
ip	intraperitoneal
IP	interferon gamma-induced protein
IQR	interquartile range
IRI	ischaemia-reperfusion injury
IRI	ischaemia-reperfusion
ISS	injury severity score
IV	intravenous
kPa	kilopascal
LC-QQQ-MS	liquid chromatography triple quadrupole tandem mass spectrometry
LC/MS	liquid chromatography-tandem mass spectrometry
LFA	lymphocyte function associated antigen
LFTs	liver function tests
MAP/MBP	mean arterial pressure
MBBA	multiplexed bead array assay
Mcl	myeloid cell leukaemia
MCP	monocyte chemoattractant protein
MERT	Medical Emergency Response Team
MIP	macrophage inflammatory protein
mM	millimolar
mmHg	millimetre of mercury
MoD	Ministry of Defence
MOF	multiple organ failure
MP	microparticles
MPO	myeloperoxidase
mtDNA	mitochondrial DNA
NAD(P)H	nicotinamide adenine dinucleotide phosphate
NF-kB	nuclear factor kappa B
NH	novel hybrid
NO	nitric oxide
NOS	nitric oxide synthase
NRQ	normalised relative quantities
O_2ER	oxygen extraction ratio
og	orogastric
PaO_2	partial pressure of oxygen in arterial blood

PBI	primary blast injury
PBLI	primary blast lung injury
PBS	phosphate buffered saline
PCA	perchloric acid
PECAM	platelet endothelial cell adhesion molecule
PGE_2	prostaglandin E2
PM	*post-mortem*
PP	pyrophosphate
PPC	positive PCR control
pRBC	packed red blood cell
PRR	pattern recognition receptors
qPCR	quantitative polymerase chain reaction
RANTES	regulated on activation, normal T cell expressed and secreted
RCT	randomised controlled trial
RNA	ribonucleic acid
RNS	reactive nitrogen species
ROS	reactive oxygen species
RT-qPCR	quantitative reverse transcription PCR
RTC	road traffic collision
RTC	reverse transcription control
SaO_2	arterial haemoglobin saturation
SBP	systolic blood pressure
SEM	standard error of mean
SI	seriously ill
SIRS	systemic inflammatory response syndrome
STAT3	signal transducer and activator of transcription 3
SV	stroke volume
THBD	thrombomodulin
TLR	toll-like receptors
TNF	tumour necrosis factor
TRALI	transfusion-related acute lung injury
TXA	tranexamic acid
U&Es	urea and electrolytes
UK	United Kingdom
US	United States
VCAM	vascular cell adhesion protein
VEGF	vascular endothelial growth factor
VO_2	whole body oxygen consumption
VPA	valproic acid
VSI	Very seriously ill

CHAPTER 1 INTRODUCTION

1.1. Trauma Overview

1.1.1. Epidemiology

Trauma is the leading cause of death in the first four decades of life in the western world; with each fatality there are at least two severely injured casualties with life changing, debilitating injuries that require long term care [1]. In England, approximately 20,000 cases of major trauma happen each year resulting in approximately 5400 deaths per year [2]. Traumatic brain injury, followed by haemorrhage, is the leading cause of early death in civilian trauma [3]. In Europe, traumatic brain and spinal injury pose the highest morbidity burden due to permanent disability [4]. The annual lost economic output from these deaths and severe injuries in the UK is estimated to be between £3.3 billion and £3.7 billion [2]. Trauma is therefore not only a major cause of death but also a significant social-economical burden.

Road traffic collision (RTC) is the most common mechanism of injury in the civilian population in the United Kingdom (UK), with blunt force trauma as the main mode of injury [2]. Penetrating injuries, including gunshot wounds (GSW) and stabbings, account for two percent of major trauma [5]. Seventy-five percent of major trauma patients are male, with the highest concentration between age group 16 to 20 [1]. Differences exist in other countries, penetrating trauma deaths are the most common in the United States (US); with GSW accounting for 42% of trauma deaths, followed by RTC at 26% [6].

In order to quantify the degree of traumatic injuries for research and registry purposes, scoring systems are used. The Injury Severity Score (ISS) is an

anatomical scoring system based on three worse injured parts of the body, the range of scores are from 0 to 75 (with 75 deemed unsurvivable) [7].

Trauma has become a hot topic for research, given the political and public interest in the recent UK military operations in Iraq and Afghanistan. Since 2001, 447 UK Military or Ministry of Defence (MoD) personnel have died in the Afghanistan conflict, of which 404 were killed as a result of hostile action [8]. There were 2173 field hospital admissions from those wounded in action, of which 303 casualties were classified as “very seriously ill” (VSI) and 307 as “seriously ill” (SI) since the beginning of the Afghanistan campaign [9]. VSI is defined by Joint Casualty and Compassionate Policy and Procedures to be ”injury of such severity that life or reason is imminently endangered; SI is used where the patient’s condition of such severity that is a cause for immediate concern but no imminent danger to life or reason” [10].[1]

1.1.2. Military Trauma

The main mechanisms of injury in the military casualties differ from those of the civilian population. Blast or explosion, from munitions or commonly Improvised Explosive Devices (IEDs) has been the main injury mechanism of coalition troops in Iraq and Afghanistan [11, 12]. Such injuries are uncommon in the civilian population but unfortunately do occur in rare incidences of terrorist attacks, such as the recent attack at Manchester arena in 2017 [13-16].

Blast produced significant tissue damage and life-changing injuries in combat casualties. Demographic data taken prospectively from the British Military Field

[1] The terms “VSI” and “SI” are not strictly ‘medical categories’, but designed to give an indication of severity of injury to inform the next of kin and chain of command. In this context, “reason” indicates mental capacity.

Hospital in Iraq documented all casualties from roadside IEDs sustained open wounds [17]. MoD trauma registry data identified 105 UK military personnel with significant multiple amputations and 291 with injuries resulting in single or partial amputations from Iraq and Afghanistan [18]. Fatalities with traumatic lower extremity amputations caused by IEDs have also been shown to have associated severe head, chest or abdomen injuries [19]. Over the summer of 2010 in Afghanistan, there was a surge in the number of casualties with lower extremity amputations in additional to pelvic, genitourinary and or abdominal injuries; the term “dismounted complex blast injury” was therefore coined by the US military to described these high-energy injuries [20].

Although explosion is the most common mechanism of battlefield injury in the recent conflicts of Iraq and Afghanistan, haemorrhage is the most common cause of battlefield deaths [21]. This has been true historically and is of no surprise given the nature of the injury patterns. The arrest of bleeding is crucial for survival hence the revised <C>ABC trauma emergency care paradigm was introduced into the common pre-deployment Battlefield Advanced Trauma Life Support (BATLS) course and incorporated into the Clinical Guidelines for Operations [22]. Copious research efforts have been made on the control of exsanguination at the point of injury; novel haemostatic products such as the Combat Application Tourniquets (CAT), chitosan dressing (e.g. HemCon) and the QuikClot were used by the UK Defence Medical Services during the Iraq and Afghanistan conflicts [23-25]. Efficacy of these products on the battlefield has been reported in retrospective clinical studies [26, 27]. However, such immediate measures are temporary and it is imperative that the combat casualties are rapidly evacuated to surgical facilities.

Timeliness of treatment has always been a fundamental principle of medical support within the UK Armed Forces, as the window of opportunity for successful medical intervention is often narrow and specific, the evacuation timeline needs to be as short as possible [28]. The casualty evacuation chain had evolved with UK medical support planning as the country moved from fixed plans of the Cold War on the European front, to supporting forces covering huge area and far away from the home base such as the 1991 Gulf War [29]. Subsequently, lessons from Iraq and Afghanistan led to the introduction of the Operational Patient Care Pathway "10-1-2 medical planning guideline" in the Joint Medical Doctrine; advocating bleeding and airway control for the most severe casualties within ten minutes, followed by enhanced field care delivered by Defence Medical Services (DMS) medical personnel within one hour, Damage Control Surgery (DCS) and critical care support within two hours [30, 31]. Advances in en-route care capabilities have developed over the past decade; the most defining development is the UK Medical Emergency Response Team (MERT), where a doctor with critical care skills is deployed forward in a CH-47 Chinook helicopter to retrieve the casualty [32]. In patients with severe injuries of ISS between16 and 50, evacuation via the MERT is associated with increased survival [33].

However short evacuation time and the availability of advanced evacuation platforms are not always guaranteed despite careful planning, as military operations often face challenges such as tactical constraints and available resources in austere environments. UK civilian pre-hospital timeline data indicated time of wounding to hospital is less than 80 minutes [1]. A timeline study based on Iraq data between 2003 and 2004 (Operation Telic 3) described the mean time from casualty report was logged to the arrival at field hospital to be 4 hours 31 minutes [34]. In the earlier

phases of the Afghanistan conflict between 2006 to 2007, the median time from wounding to arrival at the field hospital emergency department was reported to be 120 minutes [35]. Evacuation timelines tend to be longer in the early phase of conflict, which military commanders and trauma researchers need to keep in mind when planning for contingency and research focus.

1.1.3. Distribution of trauma deaths

Trunkey first described the trimodal distribution of trauma death: immediate (within the first hour), early (first few hours) and late (days or weeks) in his landmark civilian trauma epidemiology study in 1983 [36]. These same peaks were not observed in subsequent U.S. civilian trauma epidemiology studies in the nineties and noughties, in which the authors postulated that this was related to the implementation and maturation of trauma systems [6, 37]. Demetriades *et al* described two peaks of death: (1) within an hour, (2) between one to six hours after hospital admission; there was a sustained but no pronounced peak in the 'late' deaths as previously described by Trunkey [37]. The magnitude of these peaks differed between mechanisms; higher proportion of deaths from penetrating trauma died within an hour and a greater proportion of blunt trauma deaths occurred in the later stages [37]. Gofrit *et al* echoed in their study based on data from the Lebanon War; the highest peak was immediate deaths and there were no later peaks [38]. Retrospective review of UK casualties who survived to a medical facility in Iraq and Afghanistan found that over 50% died within 24 hours, mainly from head injuries; no obvious distribution in timing of death was seen [39].

1.1.4. Mortality and morbidity of multiple organ failure in trauma

Despite the change of trauma death distributions reported above, there remain a significant number of trauma patients that succumb to their injuries in the later stages due to sepsis and multiple organ failure (MOF). Ten percent of patients with major trauma develop sepsis, which increases the mortality rate and the incidence of MOF significantly [40]. An increase in the incidence of MOF after major trauma was observed over the past decade and had been reported to be as high as 32% [41].

The implications of MOF are enormous; the risk of death after trauma increases to six times in the presence of MOF and organ failure was reported by Sauia *et al* to be the cause in 61% of the late hospital trauma deaths [6, 42]. Civilian clinical data suggests advanced age is an independent risk factor for late multi-organ failure; whilst high ISS, blood transfusion of six packs of red cells within 12 hours, and systolic pressure of less than 90 on arrival to emergency department is associated with early multi-organ failure [43]. Although military casualties have the advantage of being in the younger age group, the injuries sustained are often severe and susceptible to high volume blood loss, therefore likely to require significant fluid (blood) resuscitation and likely to have reduced blood pressure.

The length of stay in intensive care unit (ICU) and overall hospital stay in trauma patients are increased in the presence of sepsis or MOF, which would compound on the healthcare cost and delay discharge to rehabilitation units [40, 41]. Furthermore, poor long term functional status and quality of life after major trauma are associated with MOF, length of in-hospital stay and intensive care days [42, 44].

1.1.5. Summary

As we make advances in military pre-hospital care such as tackling the problem of exsanguination, better forward resuscitation and shorter time to damage control surgery; more patients with severe injuries are likely to survive in the early phases. This translates to more combat casualties that are prone to manifestations of trauma inflammatory response, leading to later morbidity and mortality. Strategies to mitigate such late complications of trauma should be the next focus for trauma research.

1.2. Cardiovascular response to injury

1.2.1. Circulatory system

The main purposes of the circulatory system are to deliver oxygen and nutrients around the body, remove waste in addition to forming part of the immune system. Cardiac output (CO) is the total blood flow from either side of the heart, a product of the volume of blood pumped by one ventricle (SV, stroke volume) and the number of beats made by the heart per unit time (HR, heart rate) (Equation 1). Oxygen delivery (DO_2) is the amount of oxygen delivered to the body from the lungs per unit time; it is the product of cardiac output (CO) and the oxygen content of arterial blood (CaO_2) (Equation 2). The oxygen content of arterial blood depends on the haemoglobin concentration (Hb), arterial haemoglobin saturation (SaO_2) and the amount of oxygen dissolved in plasma (minor portion, which is linearly related to the partial pressure of oxygen in arterial blood, PaO_2) (Equation 3). Whole body oxygen consumption (VO_2) represents the amount of oxygen consumed by the tissues per unit time to sustain normal metabolism, which varies according to the individual circumstances.

Cardiac output: $CO = SV \times HR$

Equation 1

Oxygen delivery: $DO_2 = CO \times CaO_2$

Equation 2

Arterial oxygen content: $CaO_2 = (k_1 \times Hb \times SaO_2) + (k_2 \times PaO_2)$, where k_1 is the Hufner's constant and k_2 is the solubility coefficient of oxygen at body temperature

Equation 3

Mean Arterial Pressure (MAP) = CO x SVR

Equation 4

1.2.2. Shock and oxygen

The term "shock" is used to describe inadequate tissue oxygen delivery to meet basic metabolic requirements. Conventionally, shock is classified into four categories: hypovolaemic, obstructive, cardiogenic and distributive. "Shock" is usually due to a hypoperfused state as a consequence of hypovolaemia and incomplete resuscitation in combat casualties; blood loss via damaged blood vessels results in a smaller circulating volume, reduced cardiac output and haemoglobin levels. In addition, there can be hypoxaemia as a result of blast lung injury (section 1.3.2.4) All these factors contribute to reduced oxygen delivery and hence "shock".

In normal circumstances the global amount of oxygen extracted from arterial blood is approximately 25% of that delivered. This provides a significant reserve that allows for increased extraction when delivery is reduced. When DO_2 is reduced e.g.

due to lower cardiac output, the body initially compensate by increasing oxygen extraction (O_2ER) to maintain VO_2. However this cannot be sustained indefinitely; if DO_2 continues to fall, a point is reached where extraction is maximal; any fall in DO_2 results in a fall in VO_2 (Figure 1). The transition point between VO_2 being independent and becoming dependent on DO_2 is called the point of critical oxygen delivery (DO_{2crit}) (the inflection point in Figure 1) and can be determined globally for the whole body or for individual organs. Once DO_2 falls below DO_{2crit}, tissues resort to anaerobic metabolism, which if prolonged leads to tissue damage and irreversible organ damage.

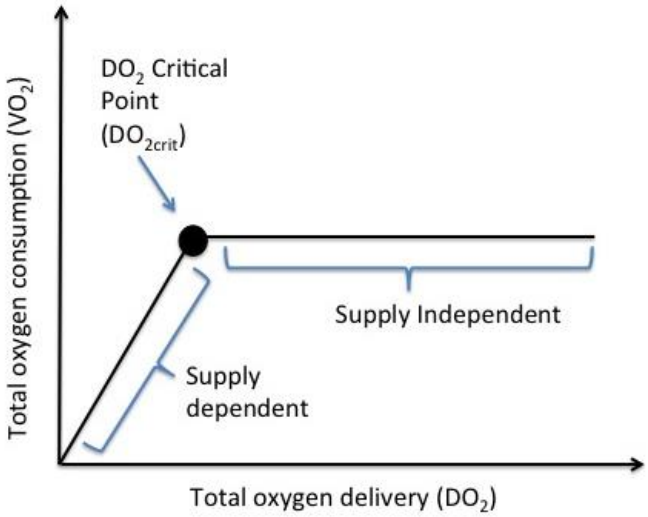

Figure 1 Schematic relationship of VO_2 and DO_2.

1.2.3. Effects of simple haemorrhage on cardiovascular system

1.2.3.1. Biphasic response to haemorrhage

The cardiovascular system has mechanisms in place to maintain homeostasis; part of this involves sustaining adequate tissue oxygen delivery to the most critical or the least tolerant organs during circulatory hypovolaemia. Barcroft *et*

al (1940s) studied the cardiovascular response to progressive haemorrhage until syncope in volunteers and reported a biphasic response (Figure 2) [45]. In the first phase of the response, tachycardia was observed with an increased peripheral vascular resistance, while arterial blood pressure was maintained. In the second phase, the heart rate and peripheral vascular resistance fell, and the volunteers became hypotensive (and syncopal). Return of the shed blood led to an immediate recovery in all volunteers [45].

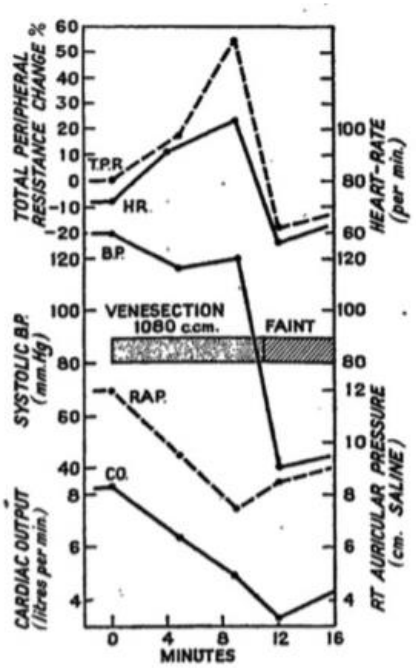

Figure 2 Barcroft's experiment demonstrating biphasic response of haemorrhage [45].

1.2.3.2. First phase of haemorrhage

When blood is lost from the circulation, the reduction in venous return decreases diastolic filling of the heart. According to Starling's Law of the Heart, the end diastolic volume influences the stroke volume [46]. During haemorrhage, reduction in end diastolic volume (preload) therefore leads to a decreased cardiac stroke volume, which in turn leads to a lower cardiac output as per Equation 1.

However, arterial blood pressure is maintained during the first 10-15% of blood loss due to the action of the arterial baroreceptor reflex leading to an increase in vascular resistance (Equation 4) [47]. The arterial baroreceptors are located in the medio-adventitial border of the vessel wall of the aortic arch and carotid sinus, where they respond to the stretch of the arterial wall exerted by the intraluminal pressure of the vessel, and play an important role in maintaining the arterial blood pressure within a normal range [48, 49]. These mechanoreceptors react to the rate of change of arterial blood pressure, in addition to the absolute pressure [50]. When cardiac output decreases, the stroke volume decreases (Equation 1), which in turn leads to a lowered arterial pulse pressure.

This change of arterial pulse pressure, even in the absence of alteration in overall pressure, causes an unloading of the baroreceptors resulting in reduced afferent activity. This leads to the immediate withdrawal of cardiac vagal activity to the sinoatrial (SA) node; thereby initiating tachycardia as first part of the response [51, 52]. In addition to inhibiting the vagal cardiac efferent fibres, the reduced baroreceptor afferent signal increases sympathetic efferent activity to the heart to produce tachycardia and increase myocardial contractility, and via sympathetic vasoconstrictor nerves increases total peripheral resistance of the vessels [53]. It is important to note that this vasoconstriction reflex is selective and varies with different vascular beds; vascular resistance in some organs such as the brain and heart tend not to increase while other organs such as gut and kidney experience vasoconstriction, thus diverting the remaining available blood flow to preferentially protect perfusion in cerebral and coronary beds during moderate blood loss [54].

The increased myocardial contractility and tachycardia limit (but do not overcome) the fall in cardiac output due to the reduced venous return, as per

Equation 1; and together with the increased in systemic vascular resistance from the vasoconstriction (Equation 4), the mean arterial pressure is maintained in first phase of simple haemorrhage.

1.2.3.3. Second phase of haemorrhage

As exsanguination continues to beyond approximately 20-30% of total blood volume, the cardiac output will drop significantly to 50-60% of the resting level; at this point blood pressure will drop drastically as 'phase two' takes over [55]. This is due to the stimulation of unmyelinated cardiac vagal C-fibres afferents that originate from a group of mechanoreceptors located in the left ventricular myocardium; which are activated when the ventricular wall becomes distorted by the forceful contractions of an incompletely filled chamber [56]. Vagal efferent activity to the heart is increased and sympathetic vasoconstrictor activity is reduced, to produce the 'depressor reflex' of bradycardia, hypotension and decrease in vascular resistance and skeletal muscles [57, 58].

The reduction in heart rate is thought to transiently improve diastolic filling, which in turn would give a modest rise in stroke volume and increase perfusion to the coronary arteries during the increased diastolic phase; thus potentially protect the heart. Evidence that this is indeed cardio-protective is gleaned from observations when clinicians had reported detrimental effects when atropine was used in attempt to reverse the paradoxical bradycardia in patients with haemorrhagic shock [59]. This second phase is not irreversible and can be reversed with the restoration of circulating blood volume [45].

1.2.3.4. Other cardiovascular responses in simple haemorrhage

Arterial chemoreceptors, located in the carotid sinus and aortic arch, are stimulated by stagnant hypoxia due to the reduction of chemoreceptor blood flow during hypotension [60]. Later, the increased H^+ ions from metabolic acidosis heighten the sensitivity of these chemoreceptors, whose stimulation results in an increase in the rate and effort of breathing [61, 62]. This change in respiratory rate may reduce the reflex bradycardia described earlier and prevent the arterial pressure from falling further [57, 63].

Jacobsen *et al* reported a 'third phase of haemorrhage'; an increase in heart rate and a further fall of mean arterial pressure was observed with progressive haemorrhage beyond 46% of total blood volume [64]. This is thought to be a terminal phase; associated with increased sympathetic activity and related to cerebral ischaemic response but the precise mechanisms remain unclear [65].

1.2.4. Effects of tissue injury on cardiovascular system

Tissue injury stimulates nociceptors that trigger a series of autonomic responses, resulting in altered cardiovascular control. Unlike the biphasic response in simple haemorrhage, hypertension and tachycardia is observed with tissue injury [66-68]. This was first described in experiments in which volunteers exercised one limb with the arrest of its circulation [66, 67]; this activated the nociceptive afferents, alike to damaged tissues. The increase in sympathetic vasoconstrictor activity to the vasculature raises the total peripheral resistance, hence giving a rise to the blood pressure [68]. Muscle perfusion is relatively preserved in this instance, unlike in simple haemorrhage. However, this systemic vasoconstriction from tissue injury

may divert blood flow from organs susceptible to ischaemia, such as the kidneys and gut, which potentially lead to organ damage.

As discussed earlier, a key role of baroreceptors is to maintain blood pressure within a normal range; one would expect a reduction in heart rate to adjust for the injury-induced rise in blood pressure. Instead, tachycardia is observed due to the suppression of the 'baroreflex' after tissue injury; the reflex resets to a higher arterial pressure and there is a concurrent reduction in reflex sensitivity [69]. This baroreflex sensitivity is lowered within three hours of moderate injury (in human), reaching the maximum suppression at day three from injury; and begins partial recovery progressively after two weeks of injury [70].

The exact mechanism of the reduction in baroreflex sensitivity remains unclear but is thought to be similar to the body's defence reaction, which allows high readiness for the 'fight or flight' situation [71]. Nociceptive afferent signals produced by the damage tissue travel via the anterolateral (spinothalamic) tract of the spinal cord to the brain; whilst the efferent signals are transmitted through the sympathetic outflow [69, 72]. The integration and organisation of the central nervous pathways in the cardiovascular response to injury is complex and is outside the scope of this thesis [73].

1.2.5. Interactions between the response to 'simple' haemorrhage and tissue injury

Bleeding seldom occurs in isolation without tissue injury in trauma casualties. The cardiovascular response to haemorrhage is altered in patients by an interaction with the responses to tissue injury. In an animal study by Little *et al*, clear differences have been shown in animals with controlled bleeding and 30 minutes of

limb ischaemia (ischaemia was used as means of inducing nociception); the second phase of haemorrhage response was delayed [74]. This alteration may give the false impression that the wounded exsanguinating trauma patient is 'less shocked' when using blood pressure as the clinical parameter to assess the extent of haemorrhage. The combination of tissue injury and haemorrhage indeed has been shown to be associated with higher mortality in a canine model [75]. It has been suggested that the delay of the phase two response (blood pressure is maintained) to haemorrhage in experimental animals with concomitant injury, is via vasoconstriction, particularly in organs such as gut and kidney, leading to ischaemic damage due to reduced end organ perfusion.

1.2.5.1. Changes in oxygen transport

Further studies, using the stimulation of somatic afferent nerves to mimic injury, have been conducted to investigate factors contributing to the poorer outcome associated with concomitant tissue injury and haemorrhage. Rady *et al* observed in a porcine model undergoing haemorrhage in the background of nociceptive stimulation (to simulate the nociceptive barrage of injury); there was greater reduction in the cardiac function, oxygen delivery and consumption, and higher serum lactate levels when compared to animal with haemorrhage alone [76]. In a subsequent porcine study, a smaller blood loss volume was required to reach target reduction in cardiac function and oxygen delivery in animals where actual musculoskeletal injury was induced at the hind leg using the captive bolt prior to haemorrhage [77]. It is evident that the loss of blood volume was not as well tolerated in conjunction with tissue injury. This may be explained by the suggestion of critical oxygen delivery is increased with neural stimulation and the body's ability

to obtain oxygen from the existing blood supply is lowered, which in turn may be related to the changes in regional blood flow discussed below [78].

1.2.5.2. Changes in regional blood flow and its consequences

As discussed earlier, blood flow is selectively redistributed from tissue of high ischaemic tolerance such as the skeletal muscles to those of lower ischaemic tolerance during the compensated phase of 'simple' haemorrhage [54]. In the cardiovascular response during tissue injury, muscle perfusion is relatively preserved despite the global constriction in vasculature. The interaction between haemorrhage and tissue injury modifies this cardiovascular response; vascular resistance is increased globally but the reduction of the intestinal circulation is significantly higher than the skeletomuscular circulation [79, 80]. An analogy can be drawn between this response and the defence mechanism in which blood flow is relatively diverted to skeletal muscles at the expense of vital organs in order to 'flee or fight'.

This redistribution of blood flow from metabolically active organs (gut) to the less active ones (skeletal muscle), translate to "inefficient" use of the cardiac output in an already compromised patient. The DO_{2crit} is affected by this change in blood flow distribution; as discussed earlier DO_{2crit} can be defined globally and locally, in this instance intestinal tissue would reach its DO_{2crit} prior to skeletal muscles, leading to gut ischaemia (Figure 3).

These findings are of concern for the trauma patient, as evidence has shown systemic insult to the intestines, such as ischaemia, would increase gut mucosal permeability, leading to translocation of bacteria and endotoxins, increased inflammatory response that contributes to the later sequelae of multi-organ dysfunction [81].

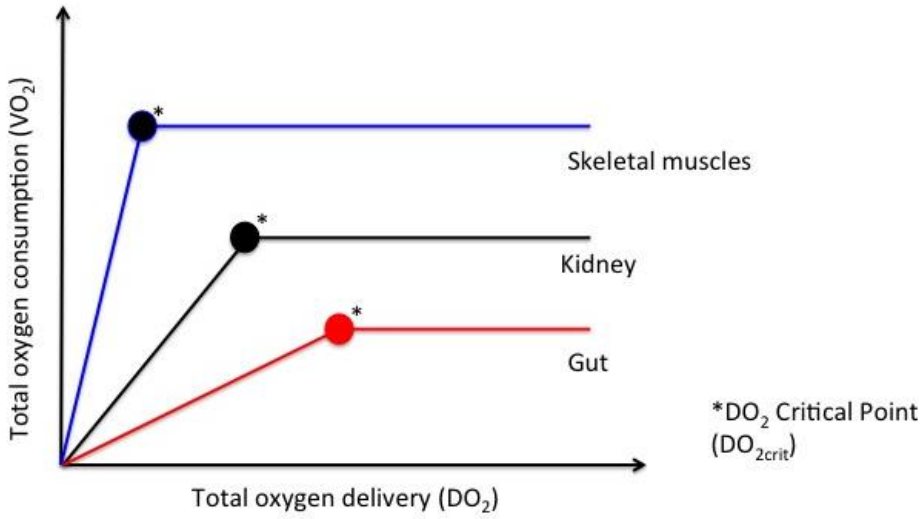

Figure 3 Schematic diagram to illustrate different DO_{2crit} in various tissues [82].

1.2.6. Summary

In the ethos of the famous American surgeon George Crile who advocated the importance of understanding the physiological functions of every tissue in his research on shock, this chapter explored the cardiovascular responses in three components: simple haemorrhage, tissue injury and their interactions. The consequence of unmet tissue oxygen demand would lead to subsequent organ failure, an understanding in the mechanisms behind the haemodynamic responses in trauma is necessary in the optimisation of trauma resuscitation strategies.

1.3. Blast mechanics and physiology

1.3.1. Blast physics

An explosion, in simple terms, is the rapid release of energy that is liberated by either burning or detonation. An explosive is a chemical compound that is capable of producing an explosion using its own energy. Gunpowder is classified as a 'low' explosive, as defined by its rate of decomposition. Low explosives burn to

release energy that propagates through the explosive at a velocity below the speed of sound. Nitroglycerin and trinitrotoluene (TNT) are examples of 'high' explosives (HE), the same class of explosives often found in terrorist devices and military ordnance.

When a charge detonates in a HE, a '**detonation wave**' is formed from the energy released from this exothermic process. Detonation wave travels through the explosive material at supersonic velocities and triggers further cascade of chemical reaction within the explosive. Upon reaching the limits of the explosive, pressure from detonation wave compresses the surrounding air molecules. This drives an instantaneous rise in pressure at the vicinity immediate to the explosive. The climb in pressure reaches '**peak overpressure**' in few microseconds and is propagated as a wave from the point of explosion at speeds in excess of sound. This is known as the '**shock wave**', and this short event lasts for few milliseconds when the explosion is caused by a conventional explosive. The overpressure decay often drops below the ambient pressure to sub-atmospheric level, before returning to ambient level. This is illustrated by the Friedlander waveform (Figure 4). The peak overpressure declines rapidly in its magnitude at inverse proportion to the cube distance from the explosive source as it travels outwards.

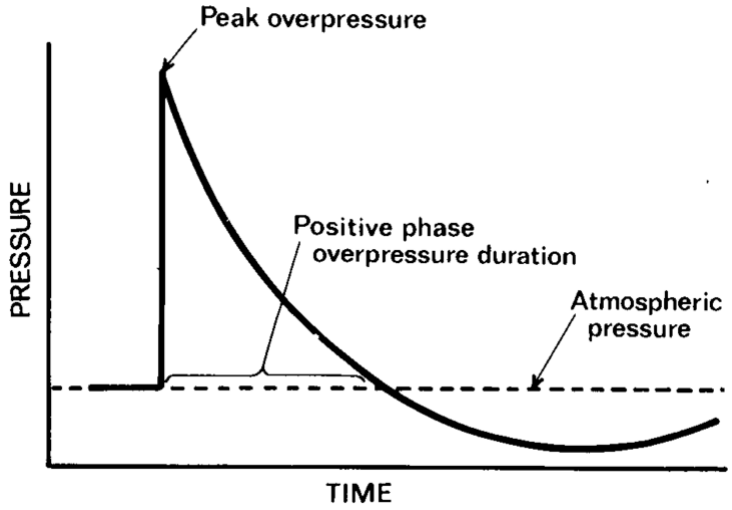

Figure 4 Friedlander waveform produced by the detonation of an air explosive in a free field [83].

During detonation as the solid or liquid explosive decompose into high volume of gaseous products and heat; the surrounding air is pushed rapidly outwards, this movement of air is known as '**blast wind**' or '**dynamic overpressure**'. This component of the explosion is relatively longer, where objects including people could be hurled over some distance. '**Blast wave**' is a collective term used to describe the combination of blast wind and shock wave produced from an explosion [84].

Fragments from the ammunition casing, objects (nails, ball bearings) contained within the explosive device and surrounding debris forms part of the explosion phenomena. Energy from the explosion is transmitted to these objects, which accelerate outwards, potentially causing harm. Lastly, heat from this highly exothermic process forms the fourth component of an explosion.

1.3.2. Blast injury pathophysiology

Each component of the explosion (shock wave, blast wind, fragments and heat) contributes to blast injury and the nature of the injury varies with different

components. Zuckerman classified blast injury into four categories based on the mechanisms by which they were produced: primary, secondary, tertiary and quaternary [85]. The basis of this classification remains in use today, with an additional 'quinary' category to include the clinical consequences of post detonation contaminants such as bacteria and radiation [86]. Table 1 summaries the mechanisms of blast injury [83].

Type of Blast injury	Mechanism	Organs affected
Primary	Impact of shock wave upon body.	Gas containing structures: ears, lungs, and bowel.
Secondary	Impact of fragment and other missiles energised by the explosion or accelerated by the dynamic pressure.	Penetrating or non-penetrating wounds on any part of the body.
Tertiary	Acceleration of the whole or part(s) of body by the blast wind to impact onto the ground or fixed objects.	Blunt injuries. Traumatic amputations of body parts, stripping of soft tissues. Crush injuries from the collapse of buildings.
Quaternary	Miscellaneous injuries from explosive products, e.g. heat, toxic fumes.	Burns, inhalation injury. May affect any part of the body.
Quinary	Clinical consequences of post detonation environmental contaminants, e.g. bacteria, radiation.	Sepsis. May affect any part of the body.

Table 1 Summary table on the mechanisms of blast injuries and organs affected.

1.3.2.1. Primary blast injury

The impact from the shock wave on the body wall is responsible for **primary blast injury (PBI)** in blast casualties. Energy is transferred onto the body from the shock wave at the point of impact, moving the body wall in the direction of the shock wave; this initiates movement of the internal organs by mechanism known as

‘**acceleration**’. However difference in the speed and direction of travel exists between the body wall and the viscera, this inertia mismatch results in damage such as mesentery tears.

Spalling, although not observed directly in blast casualties or biological models, has been suggested as a mechanism inducing blast injury [87]. When the shock wave moves from a high density medium (liquid) to low density (air), the compressed wave in the denser medium is reflected at the interface, this disrupts the boundary between the two medium, resulting in the displacement and fragmentation of the denser medium into the less dense medium [88]. An example would be a hammer striking onto a metal plate and the rust from the metal plate falls off. Pressure from the shock wave may transiently compress gas bubble, which re-expands rapidly when the pressure wave has passed. The re-expansion damages local tissue and is known as **implosion**.

Stress and shear waves are generated through tissues from the dissipation of energy to produce various degrees of injury. **Stress waves** are compression waves which are small and distort tissue rapidly; they do not produce gross laceration to tissue but instead influence damage at microvascular level to result in blood extravasation [89]. A mild example of stress wave is produced from percussing the chest wall in a physical examination for lung consolidation. **Shear waves** are transverse waves which produce gross organ distortion and lacerations [89].

The tympanic membrane is the most frequent site of primary blast injury, and can occur even at low overpressure [90]. The second most susceptible organ to primary blast injury is the lung, given its extensive air-tissue interface, and such pulmonary injuries are the most life threatening for initial survivors; which merits further elaboration later in the chapter. The true incidence of PBI is unclear, since it

is often underestimated in epidemiology studies. For example, casualties with concurrent secondary or tertiary blast injuries were excluded from analysis in a retrospective study on the incidence of primary blast lung or intestinal injury in the Iraq conflict [91].

1.3.2.2. Secondary, Tertiary, quaternary and quinary blast injury

The classification of blast injury is detailed in Table 1. **Secondary** blast injury is most commonly seen in survivors during mass casualty scenarios, followed by **tertiary** blast injury [13, 92]. Fragments and debris energised by the explosion or propelled by the blast winds collide with the casualty, resulting in secondary blast injuries that can be blunt or penetrating. **Tertiary** blast injury is the acceleration of the whole or body part(s) of the casualty by the blast wind onto the ground or fixed objects, for example traumatic amputations or degloving tissue injuries. **Quaternary** blast injury is a group of miscellaneous injuries from explosive products such as flash burns and inhalation injuries from toxic fumes. Kluger *et al* described a case series of patients following a terrorist bombing in Israel with 'hyperinflammatory state' related to the materials used in the manufacture of the explosives, as the '**quinary'** blast injury pattern [93].

1.3.2.3. Factors contributing to pattern and severity of blast injury

The balance of variety and severity of injuries seen in casualties depends on factors such as the size and component of the explosive used, the distance from the explosive source, and the local topography. Incidence of PBI is likely to be higher when larger explosive devices are used (higher magnitude of peak overpressure) and to those closest to the device (short duration of overpressure). Mellor *et al*

reviewed the victims from explosives in Northern Ireland in four groups, according to the blast load based on the size of the bomb and distance of the blast [94]. Unsurprisingly, their results showed that the group with highest blast load had the highest number of fatalities and survivors with the most severe injuries.

Perpetrators of terror use pre-formed fragments such as nails and ball bearings in devices to inflict maximum secondary blast injuries in order to create mass casualty scenarios. This was a common tactic used during 'The Troubles' in Northern Ireland, and recently used in the Boston Marathon bombing [95]. Enhanced-blast munitions such as fuel-air explosives were used by the Soviet Forces in Afghanistan to induce injury mostly via primary blast effects, as the vapour clouds from these weapons introduce blast effects over larger areas [96].

Confined space explosions are associated with a higher incidence of PBI and mortality, this is due to the reflected pressure waves and prolonged exposure to peak overpressure [97]. When the blast wave reflects on a surface at various angles or with a structure (e.g. wall) or person, the parameters of the incident wave are magnified [98]. Incidence of primary blast lung injury is significantly higher in vehicle occupants from a post mortem study of UK military personnel killed by IEDs [99]. In the Madrid train bombings, 63% of their critically ill patients were reported to have PBI to the lungs [100].

1.3.2.4. Primary blast injury to the lung

Primary blast lung injury (PBLI) is the most common fatal primary blast injury amongst initial blast survivors [101]. It is important to note that not all lung injuries sustained in a blast are due to the primary blast effects; energised fragments can lead to penetrating injuries to the thorax. Lung contusions could also be the

result of direct impact on the thorax from victims thrown against fixed objects (tertiary effects) or from flying debris (secondary effects). In this section, I will elaborate on the pathophysiological effects of primary blast injury of the lung.

It is now accepted that the coupling of shock wave with the thoracic wall is responsible for the damage seen in the lungs. Energy from blast wave is transmitted to lung parenchyma, generating spalling and implosion forces described earlier; to produce pulmonary contusions. Capillaries are lacerated by the forces and blood pool into the alveolar space, breakdown of alveolo-capillary barrier allows interstitial fluid to extravasate into lung tissue causing oedema [102]. These haemorrhagic contaminations result in disturbances to the ventilation/perfusion balance, creating a shunt and reduce the overall partial pressure oxygen in systemic arterial blood [103]. Haemoglobin exposed to extra-cellular environment may become oxidised to generate free radical reactions and potentiate the oxidative damage [104]. In addition, the progressive accumulation of leucocytes at the haemorrhagic area also escalates the inflammation process (section 1.4.3.4) [105].

Clinically the patient may present with cough, tachypnea, and cyanosis; respiratory failure develops as pulmonary function continues to decline. If the lung parenchyma is lacerated, patients may present with haemothorax; or with pneumothorax if air enters the pleural space from the alveolar disruption [106]. Formation of bronchopulmonary fistula from the disruption of the broncho-vascular tree in high blast exposure allows air to enter the circulation (air embolism), leading to instantaneous death [107, 108]. Table 2 summarises the evolution of PBLI.

Event	Clinical consequences	Time
Shock wave damage - Rupture of alveolar capillaries - Blood in alveoli and interstitium	Reduced gas transfer - Hypoxia - Cyanosis - Tachypnea Haemothorax/Pneumothorax Air embolism	0
Free Hb and blood - Free radical reactions and oxidative stress	Reduced gas transfer Inflammation Oedema	0
Leucocyte accumulation - More oxidative stress and oedema	Inflammation Oedema Respiratory failure	3 hours
Epithelial cell damage	Further deterioration of lung function	12-24 hours
Endothelial cell damage	Further deterioration of lung function	24-56 hours

Table 2 Summary table on the evolution of PBLI [105].

1.3.3. Physiological response to primary blast injury to the thorax

Bradycardia and hypotension in patients exposed to blast were reported by Barrow [109], and Krohn *et al* observed an immediate fall of systolic blood pressure and period of apnoea post blast exposure in animal studies [110]. Contrarily, Ruskin reported temporary hypertension observed in blast victims [111]. However, it is now established that the triad of apnoea followed by shallow breathing, bradycardia and prolonged hypotension is the characteristic response of primary blast to the thorax from a series of experiments performed under controlled laboratory conditions [112, 113].

This cardiopulmonary response is understood to be reflex in nature as there is a delay between the onset of the bradycardia (4 seconds) and hypotension (2 seconds) to blast exposure; in contrary one would expect the physiologic response to be instantaneous if it is cardiac or central nervous system in origin [114]. The vagal nerve is essential in mediating the reflex, as demonstrated by Irwin *et al* [115]. Efferent and afferent vagal pathways are likely to mediate the bradycardic response,

given that it is obliterated after either cervical vagotomy or atropine; whilst the afferent vagal pathway is accountable for the apnoeic response, as it is abolished by vagotomy only [114].

Hypotension is observed in primary blast to the thorax but not to the abdomen [113]. The vagal nerve partially contributes to the hypotensive response and the fall in blood pressure appears not to be a consequence of the bradycardia; this is evident from the observation of hypotension attenuated in vagotomised animals but not those treated by atropine alone [114]. Modulation of the baroreceptor reflex has been suggested since hypotension occurs without the presence of tachycardia [114]. Cardiac output is reduced due to myocardial impairment in exposure to blast, together with the decrease in peripheral resistance this could account for the sustained decrease in blood pressure [112, 116]. In addition, Zunic *et al* has shown an overproduction of Nitric Oxide (NO) in pulmonary blast injury, this potent vasodilator could also contribute to hypotension [117].

It has been postulated that the activation of pulmonary afferent C fibres or the pulmonary J receptors could be responsible for the reflex of apnoea, bradycardia and hypotension [113, 114]. These pulmonary J receptors are located at interstitial tissues close to the pulmonary capillaries, which could be stimulated by pulmonary oedema consequent to PBLI [118]. However one would expect pulmonary oedema to give a gradual reflex response, hence this is unlikely the case given the rapid reflex observed; therefore the exact mechanism of activation and nature of afferent pathway mediating the reflex response to primary blast injury remains unclear [119].

1.3.4. Impact of blast injury on the response to haemorrhage

The biphasic response of simple haemorrhage and the interaction between the cardiovascular response to haemorrhage and tissue injury was discussed in sections 1.2.3 - 1.2.5. Casualties with primary blast injury often present with other injuries resulting in haemorrhage, hence it is important to understand the altered physiological response within this combination [21].

Sawdon *et al* established in their experimental study that following thoracic blast the initial compensatory (phase one) tachycardia was absent and hypotension started earlier, at 10% loss of blood volume in animals [120]. Either the first phase of haemorrhage is shortened or the second phase of haemorrhage becomes more prominent in the presence of blast injury. The first possible explanation could be due to the modulation of baroreflex, as seen in the prolonged hypotension accompanied by bradycardia demonstrated by Ohnishi *et al* [114]. However, Sawdon *et al* also demonstrated that animals with thoracic blast injury and haemorrhage showed an attenuation of the depressor phase when treated with morphine [120]. Since it is known that the use of morphine in simple haemorrhage blocks the depressor effects, the latter explanation, that thoracic blast injury augments the haemorrhage depressor response sufficient enough to override the baroreflex, is the most likely [121].

1.3.5. Physiological response to primary blast injury with haemorrhage and tissue injury

Seriously injured blast victims may have a combination of primary blast injury, severe haemorrhage and tissue injury. Retrospective studies showed that casualties who sustained primary blast lung injury and traumatic amputations have an overall

poor outcome [94]. The biphasic response of haemorrhage is altered in the presence of a concomitant musculo-skeletal injury; characterised by maintenance of blood pressure achieved through vasoconstriction and vagal inhibition (section 1.2.5). However, the exact cardiovascular response to haemorrhage with combination of primary blast injury and tissue injury has yet to be investigated.

1.3.6. Summary

Blast injuries interact with the physiological and inflammatory response to trauma. Mass casualty scenarios from explosions add to the existing logistic constraints such as evacuation time and limited resuscitation resources. Collectively, this can escalate the manifestation of inflammation and add to the challenges of managing battlefield casualties.

1.4. Inflammation

1.4.1. Overview

Inflammation is the body's defence mechanism to insults such as infection or injury. The immune response is conventionally classified into innate or adaptive, with the aim to limit or repair damage and restore homeostasis. Celsus first described the four clinical signs and symptoms of localised inflammation in the first century A.D.: *rubor et tumor com calore et dolore*; which is still being taught to medical students today. Much research effort has been undertaken since Celsus to comprehend the complex molecular and signalling pathways in which inflammation is initiated and regulated. Various models of immunity had been proposed: the self-nonself model [122], the infectious-nonself model [123] and the danger model [124].

Direct tissue trauma, as well as the consequences of ischaemia caused by hypoperfusion characteristic in the cardiovascular response to haemorrhage, and subsequent reperfusion during fluid resuscitation, all lead to inflammation via different mechanisms (Figure 5). Each of these circumstances contributes to the complex inflammatory pathways but the exact mechanisms and interlinks are yet to be fully established. It is not possible to completely dissect the inflammatory response according to each of these trauma components since much overlap exists (Figure 5, Figure 6). However, there are some unique features in each that merit further discussion.

Inflammation classically starts with threat recognition, followed by recruitment of the immune system to remove this threat, and finally its termination once the damage has been repaired. This chapter will cover some of the mechanisms for threat recognition, immune system recruitment and threat removal, as well as the underlying mechanisms of inflammatory dysfunction that leads to the dire consequences of secondary tissue and organ damage.

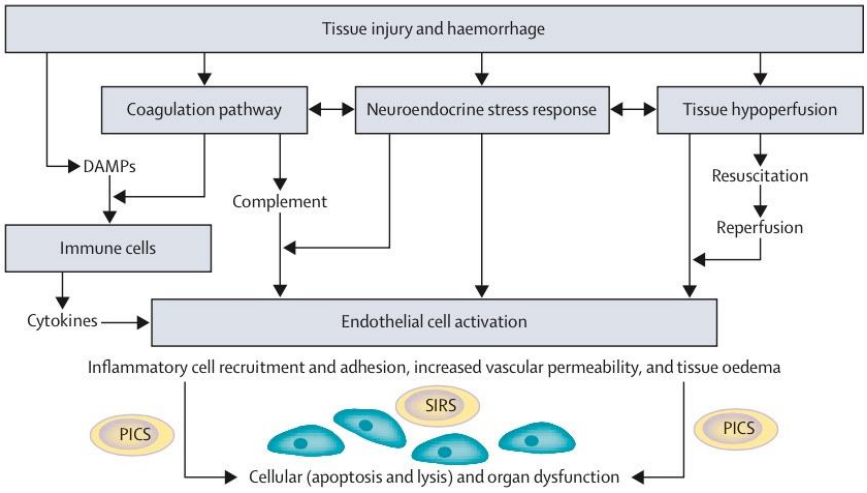

Figure 5 Pathways leading to tissue and organ damage after trauma [125].
DAMPs; damage-associated molecular patterns. SIRS; systemic inflammatory response syndrome. PICS; persistent inflammation, immunosuppression and catabolism syndrome.

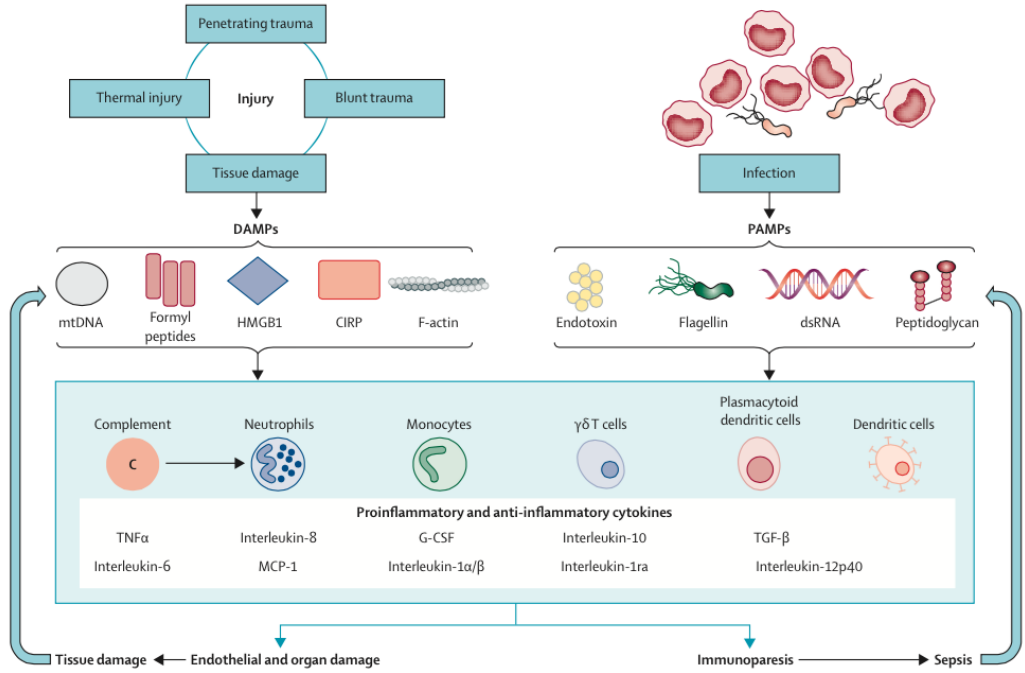

Figure 6 Activation of immune system after tissue injury [125].

1.4.2. Inflammatory response to tissue damage

1.4.2.1. Recognition

Local tissue damage in trauma leads to the release of endogenous substances termed as damage-associated molecular patterns (DAMPs) or alarmins [126]. DAMPs can be intracellular contents released following cell necrosis or substances secreted by other cells within the immune system, or part of the extracellular matrix components [127]. High-mobility group box-1 (HMGB1) and mitochondrial DNA (mtDNA) are two examples of DAMPs identified to play a role in trauma (Figure 6) [128, 129]. DAMPs act as 'inducer' or 'danger signals' to initiate the response of inflammation, their presence is detected by molecular receptors on cells known as pattern recognition receptors (PRR) [130]. An example of PRR is the Toll-

like receptors (TLR) family, TLR2 and TLR4 has been identified as the receptor for HMGB1 and TLR9 for mtDNA [131].

Stimulation of PRR up-regulates the transcription of genes for inflammatory mediators responsible in orchestrating the inflammatory response. Inflammatory mediators are classified according to their biochemical properties: vasoactive amines, vasoactive peptides, complement component fragments, lipid mediators, cytokines, chemokines and proteolytic enzymes [132]. It is beyond the scope of the thesis to discuss all the inflammatory mediators in detail, but certain cytokines have been identified to be elevated in early stages of trauma and in trauma patients with MOF.

Cytokines are low molecular proteins that influence other cellular and molecular effectors in the downstream pathway of inflammation positively (pro-inflammatory) or negatively (anti-inflammatory). Pro-inflammatory cytokines such as Interleukin-6 (IL-6), interleukin-1 (IL-1) and tumour necrosis factor (TNF) are released in tissue damage [133-135]. There is evidence to suggest the magnitude of pro-inflammatory cytokines elevation is related to the degree of tissue injury; e.g. the level IL-6 is found higher in open surgical procedures than in laparoscopic surgery where there is less tissue trauma [136]. Although 'dose response' of these cytokines is observed with the severity of injury, the magnitude of elevation is not always a predictor of the development of multiple organ failure [137]. Common pro-inflammatory actions include the production of more inflammatory mediators, activation and proliferation of leukocytes, endothelial cell activation and the induction of acute phase response [132].

Complement system is a collection of proteins, which is part of the innate immune response. Three conventional pathways have been described in the

activation of the complement system: 1) classical 2) lectin and 3) alternative; however the relative contribution of each pathway in the overall complement activation is less well understood. Thrombin from the coagulation system has been proposed as a fourth complement activation pathway [138]. Once activated, the release of various complement peptides follows. C3a and C5a are two pro-inflammatory peptides from the complement cascade released in the early phase of tissue injury [139]. As part of the 'signalling', C3a and C5a are strong chemo-attractants that prime neutrophils, an important step before neutrophils are recruited [140]. Complement anaphylatoxins (C3a and C5a) and cytokines draw the primed neutrophils from the circulation towards the site of injury in a process known as chemotaxis. Other functions of the complement system in the inflammatory pathway include: degranulation of mast cells, upregulation of adhesion molecules, release of vasoactive mediators and enhancement of hepatic active phase response.

Evidence from small clinical studies demonstrated correlation between the depletion of C3 serum levels and ISS; trauma patients with higher ISS had lower detected C3 serum level [141, 142]. The authors postulated the C3 serum depletion to be the result of complement system activation, and non-viable tissue generated from mechanical injury may have activated the complement system [142]. A recent larger study supports the notion of immediate 'complementopathy' in multiple trauma patients; elevated measurements of C3a and C5a and reduced haemolytic complement activity (measured as CH-50) were found in blood samples taken from patients at scene, these values remained altered for up to ten days after injury [143].

Increased complement activation correlates to the development of organ failure, as suggested by Zilow *et al* [144]. They observed a significant C3a increase from 6 hours after admission in trauma patients who later developed adult respiratory

distress syndrome (ARDS). Ganter *et al* in their prospective single centre observational study, not only identified a positive correlation between injury severity and early activation of alternative complement pathway, but this activation was also related to poor outcomes such as mortality, acute lung and kidney injury [145]. The complement activation pathway in trauma is uncertain, the authors suggested the initiation is via either the lectin or classical pathways and the alternative pathway is the central pathway [145].

1.4.2.2. Recruitment

Once recognition and signalling of the inflammation response have been initiated, the next crucial step is recruitment of neutrophils to the site of injury. This process involves the crossing of the endothelium via the sequential process of: tethering, rolling, activation, adhesion and migration [146]. The endothelium, in addition to its barrier functions, is active in the control of vascular tone, haemostasis, coagulation and inflammatory response [147]. Endothelial cells are located at the intima (inner layer) of vasculature and although they arise from the same embryonic origin, endothelial cells vary in different morphological and physiological properties, depending on anatomical location [148]. Membrane-bound molecules such as proteins, glycolipids, glycoproteins and proteoglycans form the glycocalyx, which lies on top to protect the endothelium and maintain the barrier function [147].

The movement of neutrophils from the circulation to the site of injury is partly facilitated by the adhesion molecules expressed on the surface of neutrophils and endothelial cells. Selectins aid the 'tethering and rolling' of primed neutrophils on the endothelium via rapid transient adhesive bond formation and dissociation (Figure 7) [149]. Selectins are a family of glycoproteins and its three known members are

denoted by prefixes L- (leukocytes), E- (endothelium) and P- (platelets), representing the cell types on which they were first identified. Rolling neutrophils become activated by selectins and other activating signals, the activated neutrophils become flattened to increase contact area for binding, and the integrin binding affinity is upregulated by this neutrophil activation [150]. Integrins on neutrophils bind with immunoglobulins (e.g. VCAM-1, ICAM-1) expressed on endothelial cells, this arrests the transient rolling interactions and neutrophils adhere firmly onto the endothelium [151]. Activated neutrophils 'migrate' across the endothelium via endothelial cell junctions or non-junctional locations, regulated by endothelial transmembrane proteins such as PECAM-1 (Figure 8) [152].

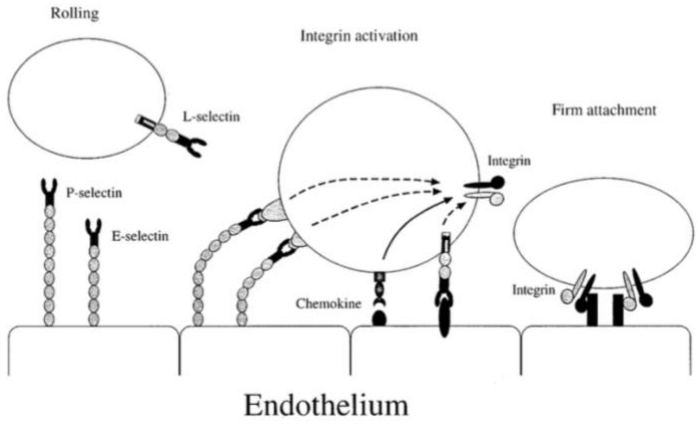

Figure 7 Neutrophil-endothelial interactions facilitated by selectins and integrins [149].

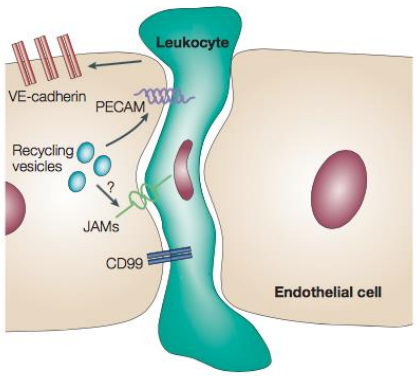

Figure 8 Transmigration of neutrophil through endothelial cell junction [153].

1.4.2.3. Threat removal

The intention of activated neutrophils entering the injured area is to contain and remove the damaged tissue; however this is not without 'collateral' damage. Activated neutrophils degranulate at the site of the injury and release substance such as pro-inflammatory cytokines, proteolytic enzymes, reactive oxygen species[2] (ROSs) and reactive nitrogen species (RNSs) [154]. Consequently endothelial function is adversely affected, which lead to capillary permeability changes, tissue oedema and neutrophil accumulation in tissue (Figure 5). Neutrophil extracellular traps (NETs), which are networks of neutrophil DNA fibres, histones, granule-derived peptides and enzymes, are released by neutrophils which can induce further endothelial injury and thrombosis [155, 156]. Furthermore, activated neutrophils release membrane microparticles, which act on the endothelium as inflammatory agonists, this interaction stimulates the release of additional pro-inflammatory cytokines, the up-regulation of adhesion molecules and increases inflammatory gene expression [157, 158].

Under normal circumstances neutrophils have a short half-life in circulation of 8-12 hours and 1-4 days in tissues, before undergoing spontaneous apoptosis [159]. Pro-inflammatory cytokines such as TNF-alpha, IL-1 and IL-6 released after trauma have been shown to accelerate or suppress neutrophil apoptosis [160]. Lifespan of neutrophils is significantly prolonged after traumatic injury and neutrophils from trauma patients have a lower rate of apoptosis [159]. Anti-apoptotic and pro-apoptotic proteins from the Bcl-2 family regulate the mitochondrial membrane potential, which is part of the intrinsic apoptotic pathway (two recognised apoptosis pathways: intrinsic and extrinsic) [160]. Severely injured patients have neutrophils

[2] Reactive oxygen species (ROS): O_2-derived free radicals e.g. O_2^-, OH^-, $ONOO^-$.

with greater expression of anti-apoptotic protein myeloid cell leukaemia (Mcl-1) and lower amount of pro-apoptotic protein Bax, leading to a balance that favours cell (neutrophil) survival [159]. The extrinsic pathway of apoptosis is initiated via the activation of death receptors found on the cell surface, such as Fas from the TNF-alpha superfamily [161]. This resistance to pro-apoptotic signals in neutrophils may contribute to systemic inflammatory response syndrome (SIRS) development in trauma patients [159].

The understanding of the effect of trauma on the regulation and functions of neutrophils is not complete; a comprehensive review on current perspectives has been summarised by Hazeldine *et al* [127]. The neutrophil-endothelium interaction is believed to play a decisive role in whether the inflammation process would resolve locally or escalate systemically to result in remote organ dysfunction and failure [154]. Evidence also suggests impaired neutrophil apoptosis regulation lead to accumulation of activated neutrophils, leading to SIRS after trauma [162]. The early sequestration of neutrophils in end organs after injury is believed to be an early event preceding to multiple organ failure and will be further discussed later in this chapter [163].

1.4.3. Inflammatory response components of trauma

1.4.3.1. Inflammatory response to haemorrhage

Trauma inflammatory response is multifaceted; this section will explore the various aspects brought on by the trauma components in sequence starting with haemorrhage.

Multiple studies have tried to elucidate the implications of global ischaemic stress from acute blood loss in the inflammatory response. In a swine model of

uncontrolled haemorrhage (grade V vascular liver injury), Brundage *et al* showed that the production of liver IL-6 mRNA increased proportionally to the severity of haemorrhagic shock [164]. This relationship was also demonstrated for nuclear factor kappa B (NF-κB), a transcription factor for pro-inflammatory genes including IL-6, and the downstream transcription amplification factor STAT3 that is part of further amplification of inflammation.

In a different rat model, complement activation was observed within 30 minutes from the beginning of haemorrhage, represented by the persisted significant fall of CH50 [165]. Altavilla *et al* reported raised NF-κB within minutes of bleeding, hepatic TNF-α mRNA and plasma TNF-α were also elevated [166]. NF-κB activation was blocked in animals treated with an antioxidant compound immediately after haemorrhage, suggesting that NF-κB was likely to be activated by ROSs released as a result of haemorrhage [166].

These findings support the notion of haemorrhage leads to early upregulation of pro-inflammatory transcription factor cascade, which have downstream consequences such as inflammatory response dysfunction (discussed later in the chapter).

1.4.3.2. Inflammatory response from tissue injury and concomitant haemorrhage

Interactions of haemorrhage and tissue injury have effects on the inflammatory response. The elevation of plasma IL-6 observed in animals subjected to tissue injury only was significantly lower when compared to a group given combined tissue injury and haemorrhage [133]. By six hours post haemorrhage, plasma IL-6 had fallen in both groups, but the levels in the injury plus haemorrhage group remained significantly higher than the injury alone group. In the same study,

plasma TNF levels were not detected in the injury alone group for the duration of the study. However, in the combined injury and haemorrhage group, after the first hour post tissue injury, plasma TNF became significantly elevated and attained the highest level at four hours post haemorrhage.

It is possible that the release of plasma IL-6 might have a closer link to soft tissue trauma, and that TNF is more closely linked to haemorrhage. In a clinical study that compared patients admitted with severe blunt trauma with patients suffering haemorrhagic shock from ruptured abdominal aorta aneurysm (AAA) and elective AAA repair, patients with ruptured AAA had significantly lower plasma IL-6 and higher plasma TNF on admission than the patients admitted with blunt trauma (who sustained less blood loss than the ruptured AAA group). Drawing conclusions from this type of comparison is fraught with difficulty because of the need to match patients in respect of all relevant factors other than the degree of haemorrhage. Unfortunately there was no matching of patients in the various groups in the study [167], rendering any conclusion of the relative impact of injury versus haemorrhage on cytokine release very tenuous.

1.4.3.3. Inflammatory response to ischaemia-reperfusion

Ischaemia-reperfusion injury (IRI) occurs locally and systemically in trauma patients. Local hypoperfusion is seen in injured tissue such as contusions, lacerations, or in damaged blood supply such as an arterial injury. Global hypoperfusion occurs when the patient is in haemorrhagic shock. Both instances result in reduced oxygen supply at cellular level, which if prolonged may cause irreversible damage. Reperfusion during or after resuscitation could be described as a ‘double-edged sword’, since rapid reversal of ischaemia is required for survival, yet

it can potentiate the damage sustained from ischaemia by triggering a complex cascade of events leading to secondary tissue damage and organ dysfunction.

Evidence of early inflammatory signalling from haemorrhage models (global ischaemia) was briefly mentioned in section 1.4.3.1. This current section focuses on the oxidative stress and inflammatory mediators arising from the sequelae of IR particularly in the context of haemorrhagic shock and resuscitation (HS/R), and their contributions to the perpetual inflammatory response.

1.4.3.3.1. Reactive Oxygen Species (ROS)

There are a plethora of pathways by which reactive oxidative species can be generated [168], although the most relevant pathways depend on the nature of the biological insult [169]. In addition to the ROS produced from activated neutrophils (section 1.4.2.3), hypoxia and reperfusion generates further ROS in its contribution to endothelial dysfunction. Xanthane oxidase (XO), NADPH oxidase (Nox2), mitochondrial electron transport chain and nitric oxide synthase uncoupling are the four potential enzymic sources of ROS in reperfusion injury [170]. XO has been extensively studied in IRI and H/R, and deemed as a major source of ROS in IRI, hence further elaboration below.

The generation of hypoxanthine during cellular hypoxia (reduced perfusion) depletes cellular second messenger cyclic adenosine monophosphate (cAMP) and subsequently reduces adenosine triphosphate (ATP) (Figure 9) [171]. This ATP deficiency leads to series of events resulting cellular membrane disintegration and DNA damage [171]. Apoptosis and necrosis occur in prolonged hypoxic conditions, leading to irreversible tissue damage and the further release of DAMPs to activate the inflammatory response (Figure 6).

During reperfusion of ischaemic tissue, the re-introduced oxygen reacts with hypoxanthine (accumulated during ischaemia) to produce superoxide anion (O_2^-), which leads to the release of hydroxyl ions (OH^-) that further exacerbates cellular disturbances and inflammatory mediators production (Figure 9) [171]. ROS act as redox messengers in intracellular regulation and signalling at physiological level; while in excess quantities they are known to be play key roles in apoptotic signalling mechanism [172].

In vivo microscopy studies have shown ROS production to be an early event in reperfusion, up to 80% surge in ROS generation was observed within five minutes of reperfusion post haemorrhage shock and this was associated with ten-fold increase in adherence of neutrophils to the endothelium a few minutes later [173]. Furthermore, oxidative stress generated from IR has been shown to induce an increased TLR4 surface expression, which amplifies the cascade of inflammatory response and subsequent organ injury (section 1.4.2.3) [174]. The production of ROS appears to be correlated to the severity of shock, as seen in an *ex vivo* study using plasma obtained from severely injured patients after resuscitation [175].

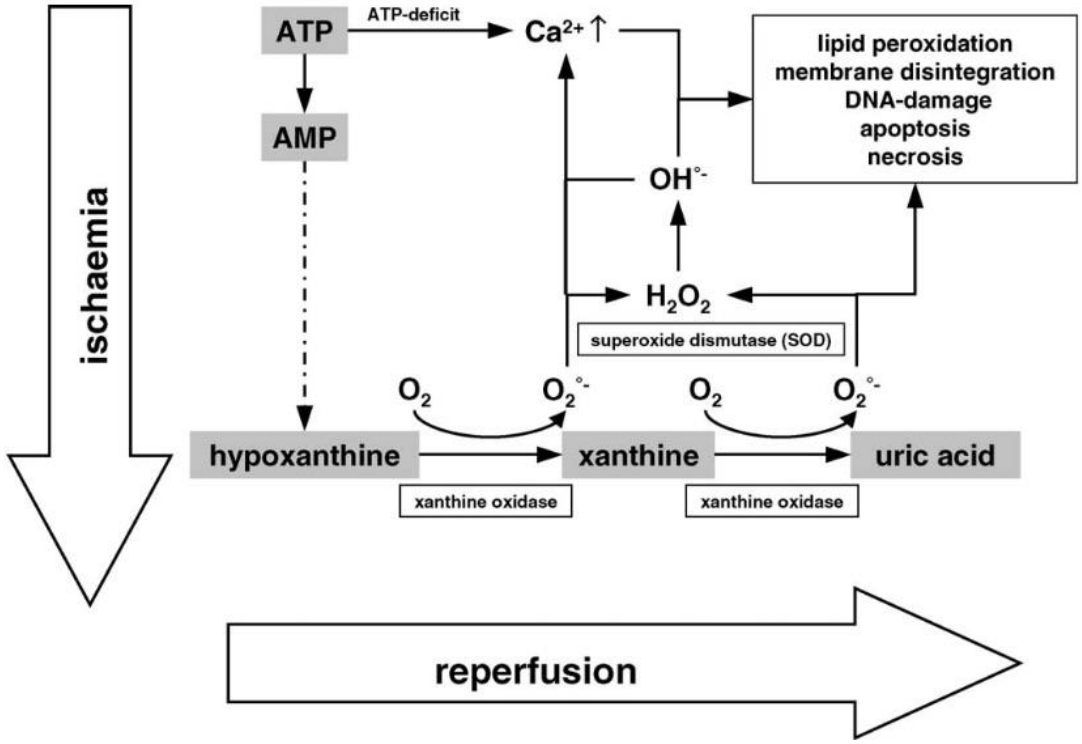

Figure 9 Mechanism of reactive oxygen species (ROS) generation in ischaemia and reperfusion injury [171].
O_2^-, superoxide; OH^-, hydroxyl ion.

1.4.3.3.2. Nitric oxide (NO)

NO is a free radical that plays an important part in the mediation of inflammatory response in IRI. NO may derive from one of the three nitric oxide synthase (NOS) isoforms and each isoform derivative differs in function. Evidence has shown the production of NO in haemorrhagic shock and hypoxic conditions arise mainly from inducible NOS (iNOS) [176].

Studies using iNOS inhibitors suggest iNOS-generated NO to be an amplifier of the inflammatory cascade in IRI. Hierholzer *et al* found NFkB and STAT3 activation, as well as IL6 and granulocyte colony stimulating factor (G-CSF) mRNA production in liver and lungs, to be iNOS dependent in their models of HS/R [177]. Lung wet-to-dry ratio and neutrophil accumulation were reduced in animals with iNOS inhibition [177]. A different HS/R study used NO donor to suppress iNOS-

derived NO bioavailability, found a decrease in hepatic mRNA expression of pro-inflammatory cytokines and liver injury on histology [178]. Other downstream consequences of iNOS upregulation in haemorrhagic shock include cycloocygenase-2 (COX-2) upregulation, which increases the production of toxic eicosanoid prostaglandin E2 (PGE_2) and more ROS, resulting in organ damage [179]

Endothelial-generated NO from endothelial NOS (eNOS) is likely to have organ protective effects in HS/R, given that animal studies have demonstrated L-arginine (a substrate for eNOS-derived NO) reduces hepatic injury [178]. However the calcium-dependent process of NO synthesis by eNOS appears to be impaired in haemorrhagic shock, possibly due to endothelial dysfunction and L-arginine depletion from increased vascular arginase activity [180, 181]. The alteration of biosynthesis of NO from eNOS attenuates the endothelium dependent vasodilating response to haemorrhage, hence may partly contribute to the tissue and organ ischaemia in haemorrhagic shock.

NO reacts with superoxide (O_2^-), which is in abundance in IR (section 1.4.3.3.1), to yield peroxynitrite ($ONOO^-$) [182]. Peroxynitrite, a potent oxidant, generates nitrosative stress to damage proteins, lipids and DNA [183]. In certain conditions such as L-arginine depletion, NOS can produce both NO and superoxide simultaneously, adding to the peroxynitrite cytotoxity and ROS availability [176, 184]. This ROS/RNS formation disrupts eNOS function, hence further reduces the bioavailability of endothelium-derived NO [185].

1.4.3.3.3. Cytokines

Evidence from experimental models (e.g. artery ligation of single organ) and clinical transplant studies have shown IR to induce a rapid release of pro-

inflammatory cytokines [186, 187]. However, HS/R differs from such IRI models; firstly ischaemia in HS/R is not the complete obstruction of vascular bed, and secondly reperfusion is not just the simple restoration of circulation, the type of resuscitation fluid used may contribute to cell survival [188].

In a HS/R rat model, serum TNF levels were detectable ten minutes after haemorrhage and peaked at 30 minutes of ischaemia, however TNF was no longer detectable after resuscitation (taken an hour from baseline sample) [189]. The results concur with a previous study of TNF association with haemorrhagic shock [133], but the clinical significance of its disappearance after resuscitation has not been explained. Yao *et al* postulated that sustained TNF release exists in the later stages of shock and is responsible for later complications, but may remain undetectable due to reasons such as complex formation [190].

In a different model, plasma IL-6 demonstrated a small statistical increase in the reperfusion phase from baseline measurements in a swine polytrauma-resuscitation but not in a HS/R swine model [191]. A marked increase in lung IL-6 mRNA levels was observed in the early phase of reperfusion (peaked at one hour post initiation of resuscitation) in a rat HS/R model and the degree of elevation was related to the duration of ischaemia [192]. Hierholzer *et al* subsequently showed this increase of IL-6 production in lungs after haemorrhagic shock and resuscitation contributes to neutrophil recruitment in lung injury [192]. Further discussion on remote organ injury will be discussed later in the chapter.

1.4.3.3.4. Complement activation

The complement system plays a major role in the early mediation IRI, as established using knock-out animals with IR to single organs and mainly myocardial

infarction clinical studies with complement inhibitors. These studies suggest the classical and the lectin pathway to be mainly responsible for complement activation [193]. Weiser *et al* examined the role of complement in mediating localised IRI using C3 depleted mice in a tourniquet hind-limb model and found 50% reduction in vascular leakage [194]. Same protection was noted in C4 depleted mice, hence the authors concluded that the classical pathway activates the complement system in IRI.

Complement consumption is seen in a rat HS/R model, represented by significant drop in CH50 within an hour post haemorrhage and remains low post resuscitation till the end the experiment [195]. Complement activation appears to have haemodynamic and metabolic effects in this model; complement (C3, CH50) depleted animals have significantly higher mean arterial pressure (MAP) after resuscitation and less severe metabolic acidosis, this was confirmed using animals with exacerbated complement activation. Better tissue perfusion as represented by the higher MAP, would suggest relative protection against tissue ischaemia and subsequent inflammatory sequelae. Indeed, a separate study showed C5 complement inhibition not only improved MAP after reperfusion but also attenuated remote organ injury such as the lungs [196].

1.4.3.3.5. Adhesion molecules

Adhesion molecules have been shown in single organ IR studies to be expressed at the early stages of ischemia, and blockade of adhesion molecules at the reperfusion stages reduced subsequent end organ injury [186].

Scalia *et al* reported a significant increase of P-selectin endothelial expression in a murine HS/R model which was associated with the upregulation of leukocyte-

endothelium interactions [197]. The number of rolling and adherent leukocytes was significantly elevated in the early phase of reperfusion; this observation was absent in animals with P-selectin gene deficiency or functional inactivation, hence demonstrating the key role of adhesion molecules in inflammatory response in IRI.

Furthermore, the expression of Intercellular adhesion molecule-1 (ICAM-1) and vascular adhesion molecule-1 (VCAM-1) in lungs and spleen were reported to be markedly elevated early during reperfusion (HR/S model) [198]. However this phenomena could be associated with type of fluid used rather than action of reperfusion *per se*, as this significant upregulation was only observed in animals receiving crystalloid solution but not those receiving fresh (shed) blood [198]. Nevertheless, since crystalloid fluid is still currently generally used as the very first line resuscitation fluid in a hypoperfused patient, these observations and their implications are still valid.

1.4.3.3.6. Neutrophils and endothelium

The upregulation of inflammatory mediators from the sequelae of ischaemia-reperfusion (sections 1.4.3.3.3 - 1.4.3.3.5) ultimately leads to increase in neutrophil recruitment, adhesion and transmigration across the endothelium. As a result, capillaries are plugged by neutrophils, which could interfere with blood flow restoration. Activated neutrophils exert their effects at the site of IRI by releasing ROS, pro-inflammatory cytokines and chemokines, hereby feeding to the vicious loop of further neutrophil recruitment and activation extending beyond the original site of injury [199].

Increased vascular permeability and interstitial sequestration of neutrophils are hallmarks of organ injury [200]. Results from intravital microscopy studies

suggest the number of rolling and adherent neutrophils in splanchnic microcirculation increases during the reperfusion phase post haemorrhagic shock [201]. Neutrophils infiltration to distal organs such as small bowel, are observed as early as 30 minutes after reperfusion post haemorrhagic shock [202]. Multiple neutrophil-depletion studies have demonstrated the central role of neutrophils in IR induced remote organ injury. Neutrophil-depleted mice with bilateral hind limb IRI displayed significantly reduced lung and liver injury, compared to control animals as indicated by measurements of pulmonary permeability and alanine aminotransferase (ALT) [203]. In a HS/R model, animals with neutrophil depletion prior to resuscitation had significantly attenuated liver and intestinal injuries at post-mortem [204].

Products of neutrophil degranulation, ROS and inflammatory mediators such as pro-inflammatory cytokines, complement and adhesion molecules released during IR are injurious to the endothelium. Endothelial dysfunction occurs early, which manifests as impaired endothelial NO production, more ROS and pro-inflammatory mediator generation and disruption of its barrier function to increase vascular permeability [173].

Wang and colleagues in their experiments showed the endothelium failure initiated during ischaemia in haemorrhagic shock persists for hours afterwards despite fluid resuscitation [205]. Admittedly they have used crystalloid fluid for resuscitation rather than shed blood, so the effects could be associated with types of fluid used rather than reperfusion, *per se*. Nonetheless, endothelial dysfunction in IRI plays an early role in development of organ and systemic failure, hence the restoration or maintenance of endothelial function would be a sensible therapeutic target in trauma resuscitation.

1.4.3.3.7. Remote organ injury

The consequences of IR extend beyond original affected site to initially uninjured remote organs such as lungs, liver, small bowel and kidneys [173, 174, 177-179, 192, 197, 198, 201-204]. Ample evidence has suggested that initial IRI results in systemic release of inflammatory mediators to orchestrate neutrophil-endothelial reactions in these distance organs. The exact mechanism remains to be fully elucidated and likely to involve multiple complex molecular signalling pathways. Recent studies using DNA micro-array approach have identified some early genes associated with the mitogen activated protein kinase (MAPK) pathway in IRI [206].

HMGB1 have been shown to be a key mediator in remote organ injury after haemorrhage. In mice subjected to 30% blood loss and subsequent reperfusion of shed blood, expression of pulmonary HMGB1 increased within four hours of haemorrhage and remained elevated for up to 72 hours [207]. This was not observed in neutropenic mice undergoing the same haemorrhage protocol; hence neutrophils are thought to be the source of increased HMGB1. In the same series of experiments, blockade of HMGB1 an hour after haemorrhage attenuated the activation of NF-κB and production of pro-inflammatory cytokines in the lungs.

In addition to generating inflammatory mediators and endothelial dysfunction (section 1.4.3.3.6), extravasated neutrophils have been shown to re-enter the vasculature during IRI due to the down-regulation of junctional adhesion molecule (JAMC) [208]. Reverse transmigration of these primed neutrophils with increased resistance to apoptosis and enhanced ROS production capabilities, could contribute to remote organ injury and systemic inflammation [199].

An alternative theory, the ‘gut hypothesis’, proposes that the intestines could be the main source of inflammatory mediators for systemic inflammatory responses

after trauma, given its vulnerability to ischaemia from splanchnic vasoconstriction in response to haemorrhage and concomitant tissue injury [209]. Gut bacterial and endotoxin translocation via the portal vein was initially thought to be the mechanism responsible, however this theory was *refuted* when neither bacteria nor endotoxin was found in portal blood of severely injured trauma patients despite 30% incidence of MOF in the cohort [210]. The current *newer* concept is mesenteric IR from HS/R result in gut barrier dysfunction and intestinal-derived bioactive factors enters the systemic circulation via mesenteric lymphatics, to induce pro-inflammatory actions such as neutrophils activation [211] and apoptosis in remote organs [212].

1.4.3.4. Inflammation response related to blast

As discussed in sections 1.3.2.1 and 1.3.2.4, hollow organs are susceptible to primary blast injury, which can directly lead to inflammatory response independent of IRI. Impact from the shock wave ruptures alveolar capillaries and blood floods into the lung parenchyma immediately. The extravasated blood and free haemoglobin (Hb; released from damaged blood cells) induce oxidative stress via antioxidant depletion and lipid peroxidation, which escalate the inflammatory response [213].

The early release of inflammatory mediators and chemoattractants has been attributed to the free Hb [214, 215]. The number of circulatory neutrophils increases within an hour from blast exposure, and activated neutrophils infiltrate into pulmonary haemorrhagic areas within three hours [215]. The accumulation of neutrophils and fluid in alveolar space continues, which results in the later shedding of endothelial cells from basement membrane into capillary lumen 24 hours after blast exposure, and the destruction of alveolar architecture [216].

Experimental animal studies reported early NO overproduction with associated plasma arginine depletion after pulmonary blast injury [117]. The authors postulated this was due to increased utilisation by NOS. Findings from another experiment where elevated levels of iNOS RNA were observed at 2 to 24 hours after moderate blast exposure, supported this suggestion [217]. Transient and early increase in NO production has also been reported in blast casualties [218]. The reason for the NO overproduction is unclear, but it had been proposed to be an anti-oxidant mechanism to oxoferryl Hb formation and thus prevent further free radical reactions [104].

NOS produce both NO and superoxide under L-arginine depleted conditions, resulting the formation of peroxynitrite (section 1.4.3.3.2). Indeed, significant increases in protein nitration (accepted as footprint of peroxynitrate formation) had been detected at two hours in animals after blast exposure compared to sham controls [217]. This potent oxidant adds to the redox disturbances already generated by ROS/RNS release in neutrophil degranulation and free radicals from free-Hb.

Restoration of redox balance using antioxidants in blast animal studies have been shown to restore Hb oxygenation and reduce lipid peroxidation, hence alleviating the free-radical mediated oxidative stress [219]. Significant decreases in pulmonary neutrophil infiltration and chemoattractants downregulation have also been reported in animals treated with antioxidants versus placebo [220]. The increased expression of heme oxygenase-1 (HO-1), an antioxidant enzyme, 24 to 48 hours after blast exposure has led to the speculation of its role in the compensatory mechanism to restore oxidative and inflammatory damage [217]. Chavko *et al* subsequently demonstrated increased survival in animals with pre-blast induction of

HO-1 upregulation using hemin [221]. These experiments add to the evidence of oxidative injury and its inflammatory consequences in pulmonary blast exposure.

It has been postulated that pulmonary blast injury can induce inflammatory responses in the systemic and central nervous system, however the underlying mechanism is unclear [222]. This proposed interlink is supported by subsequent experiments using *in vivo* myeloperoxidase (MPO) activity imaging; a significant increase in cerebral MPO activity intensity was observed in mice exposed to mild thoracic blast despite protective head gear over a one month period [223].

High blast dose to the lower extremities have been shown to activate and injure the endothelium in a rabbit model [224]. Significant increases in the number of circulating endothelial cells (CECs) were observed at six hours post injury compared with sham and animals exposed to lower blast doses. The same animals also have significantly increased tissue (gastrocnemius) expression of pro-inflammatory mediators (E-selectin, TNF-α, IL-6) and histological damage. This suggests the endothelial inflammatory response to blast is dose dependent and blast induced endothelial dysfunction potentially contributes to subsequent systemic inflammatory response. Remote organ injury and raised systemic inflammatory markers were reported in a more severe lower extremity blast model, however this could be attributed to the nature of the injuries sustained (haemorrhage, fracture, soft tissue and burn injury), rather than the effects of blast *per se* [225].

1.4.4. Inflammation and coagulation in trauma

Haemostasis and inflammation are two closely intertwined biological processes, with common evolutionary origins. Activation of one system would amplify the other, creating a positive feedback loop, potentially giving rise to a

vicious inflammation-haemostasis cycle [226]. The interactions between the two processes are complex; complicated by common pathways and shared components which crosstalk between the two systems at multiple levels. For example, inflammatory mediators (e.g. IL-1, IL-6 and TNF-α) induce disturbances across various components of the coagulation system (Figure 10) [226]; whilst thrombin promotes the inflammatory response via multiple avenues (Figure 11) [227]. The understanding of these interconnections is not complete and majority of mechanism-based evidence stem from thrombosis research [228]. Thus this section is not a concise review of inflammation-coagulation interactions, but a brief introduction of their bi-directional relationship in the context of trauma.

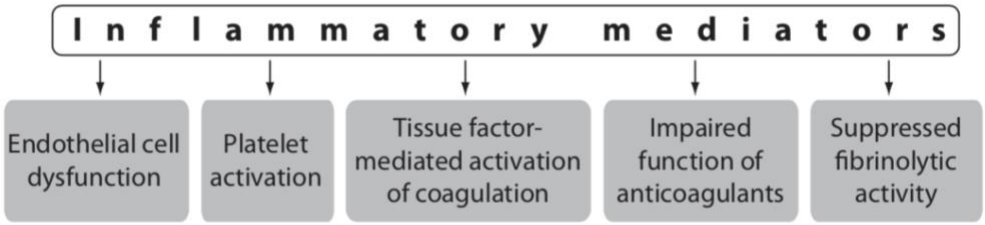

Figure 10 Effects of inflammatory mediators on haemostatic system [226].

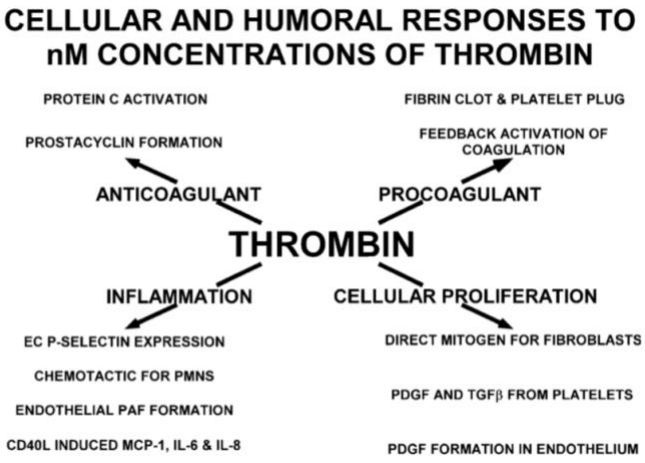

Figure 11 Thrombin as a multifunctional enzyme and promotes inflammation [227].

The coagulation system is part of body's protective response to injury, however similar to the inflammatory response, it can have detrimental effects when imbalanced and uncontrolled. Acute traumatic coagulopathy (ATC) describes an early coagulation abnormality that is recognised in trauma patients [229]. ATC is characterised by functional reduction in clot strength and increase in clotting times [230]. Its incidence correlates to severity of tissue trauma and systemic hypoperfusion [231], and is associated with adverse outcomes [232, 233]. The pathophysiology of ATC is not fully understood; proposed mechanisms include degradation of the endothelial glycocalyx induced by catecholamines, and hypoperfusion-induced activation of protein C pathway leading to anticoagulation, fibrinogen depletion and hyperfibrinolysis [234, 235].

ATC has consequences on inflammation, since proteins affected in ATC such as protein C and plasminogen-plasmin system, are shown to have immune regulatory properties in animal models of sepsis [236, 237]. Observational studies have shown that early protein C depletion in trauma patients is associated with increased risk of ventilator-associated pneumonia [238], and a dose-dependent relationship exists between the degree of protein C depletion and incidence of infection after trauma [239]. Darlington *et al* in their rat model of trauma-induced coagulopathy revealed strong correlations between coagulopathy progression (measured by prothrombin time, activated partial thromboplastic time and plasma fibrinogen) and plasma concentrations of some inflammatory mediators such as IL-1β, IL-10 and GM-CSF [240]. The authors suggested that this correlation is likely to be crosstalk between the two systems, as seen in other conditions for example atherosclerosis, and that this interaction is likely to involve pattern recognition receptors activation.

It is accepted that interactions exist between coagulation and inflammation, however in order to aid development of resuscitation strategies targeting these challenges in trauma care, more research is necessary to elucidate these intricate interactions in the context of trauma.

1.4.5. Systemic inflammatory response syndrome (SIRS)

A fine balance for survival exists between the beneficial effects of inflammation such as injury repair, and the potential detrimental effects of SIRS and subsequent MOF. There are two main paradigms on the development of SIRS after trauma (Figure 12A). The 'one hit, two hit' hypothesis states that pro-inflammatory response from the initial trauma is followed by a phase of compensatory anti-inflammatory response (CARS) [43]. Excessive initial innate immune responses lead to the development of early SIRS at 'first hit'; in the 'two hit' scenario, after an initial moderate pro-inflammatory response triggered by trauma, a second 'insult' (either infectious or non-infectious) boosts the pre-existing inflammatory state to develop SIRS at later stage (Figure 12B).

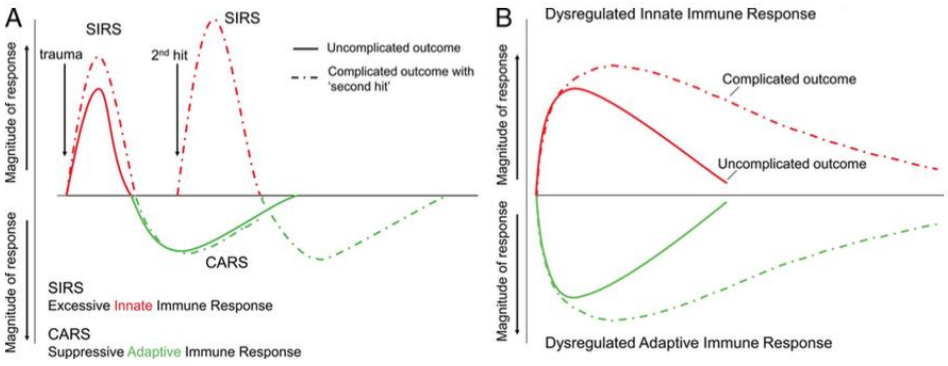

Figure 12 Two main paradigms on the development of SIRS after trauma. (A) Two-hit hypothesis. (B) Simultaneous dysregulation of both innate and adaptive immune response [241].

Xiao *et al* found in their civilian cohort of patients with severe blunt trauma the simultaneous increased in expression of genes involved in the pro-inflammatory and anti-inflammatory pathway within 4 hours lasting for days and weeks [241]. Hence a new paradigm has been proposed: the pro-inflammatory reactions from innate immune response and the anti-inflammatory reactions from adaptive immune response are initiated simultaneously; and the development of SIRS is due to the dysregulation of both innate and adaptive immune responses.

The inflammatory response from trauma is initiated via the various mechanisms described throughout the chapter, and potentially develops into SIRS and MOF. There is so far no proven effective treatment to reverse the process once MOF has been established, but individual organ support occurs using for example various ventilating strategies including high frequency oscillatory ventilation (HFOV); renal dialysis; and inotropes. Extracorporeal membrane oxygenation (ECMO) is often used as last resort for refractory ARDS and in extremis has been used in conjunction with HFOV [242]. They are extremely scarce and expensive resources compared to conventional organ support [243]. Resuscitation strategies have been tried and adopted to prevent the progression to organ failure and discussed in section 1.5.

1.4.6. Summary

Inflammatory response to injury is complex and complicated by effects of ischaemia-reperfusion, blast and coagulopathy. The understanding of the underlying mechanism is far from complete; mechanistic laboratory studies often consider few inflammatory mediators at each instance, whilst clinical reality of trauma inflammation is multifactorial. Evidence presented so far suggests the endothelium

to be a major contributor to the inflammatory response, and the common 'denominator' via the various proposed mechanisms. Hence the restoration of normal endothelial function would be a sensible target to attenuate the complications of inflammation.

1.5. Resuscitation strategies in trauma

The inflammatory response plays a key part in trauma casualty deterioration, pre-hospital resuscitation strategies such as intravenous fluids administration [244-256] and pharmacological adjuncts [257-261] have been used clinically, or evaluated in animal studies, to mitigate against this, and will be reviewed in the following section.

1.5.1. Fluid resuscitation

1.5.1.1. Intravenous fluids

The conventional aims of pre-hospital intravenous (IV) fluids administration in trauma are to replace lost blood volume from haemorrhage, to improve haemodynamics and reverse shock. Consensus remains elusive on the optimal IV fluids and the administration regimen (volume infused and timing in relation to definitive haemostasis) in trauma [262]. Battlefield use is further complicated by logistical constraints which might limit or influence fluid choice; not only the evacuation time to surgical haemorrhage control, but the weight of equipment carried by personnel whilst on long distance patrol would limit the volume and range of fluid available [263]. However, the key features of the ideal resuscitation fluid are accepted to be one that could provide rapid volume expansion to restore tissue

perfusion, cater to the metabolic needs of hypoxic cells and least likely to induce a dysfunctional inflammatory response [264].

Trauma fluid resuscitation strategy has evolved over the years. Before the nineties, hypotensive patients were promptly infused with large volume of isotonic fluid, in the rational that the need of restoring organ perfusion is paramount [265]. Concerns were raised on this practice, that the aggressive fluid administration before haemorrhage control could disrupt thrombus formation, resulting in further bleeding and decreased survival [266, 267]. Bickell *et al* suggested that delayed fluid resuscitation (till operating room) is superior to immediate fluid resuscitation, in terms of outcomes for hypotensive patients admitted with penetrating torso injuries [268]. Although this paved the concept of permissive hypotension resuscitation (section 1.5.1.1.2), the pre-hospital administration of large amount of IV fluids remained a common practice before the millennium.

1.5.1.1.1. Inflammatory effects of intravenous fluid

Resuscitation fluid could influence the inflammatory response after haemorrhagic shock, reported in animal studies that investigated resuscitation using various crystalloid and colloids [244-256]. The detailed discussion on these studies are beyond the scope of this thesis, however the take home message is that these experimental findings have altered the mindset towards IV fluids, which no longer appears innocuous but an intervention that could exacerbate the posttraumatic inflammatory response.

1.5.1.1.2. Permissive hypotension resuscitation and targeted resuscitation

Bickell *et al* alluded that delayed (in-hospital where surgical facilities are available) aggressive fluid resuscitation has better survival outcomes for patients with penetrating torso injuries than immediate fluid resuscitation [268]. This has challenged the traditional approach of aggressive fluid resuscitation, particularly in uncompressible haemorrhage. As a result, Tactical Combat Casualty Care (TCCC) battlefield guidelines at that time recommended: no IV fluid for casualties not in shock, and none for those in shock from uncontrolled haemorrhage [269]. However some tissue perfusion is required for survival, and since re-bleeding after fluid resuscitation is believed to occur above systolic BP 90 mmHg [270], the revised guidelines suggest IV fluids for casualties with altered mental state (no evidence of head injury) or weak peripheral pulses, to maintain the radial pulse which is still used today [269].

It is important to note that Bickell's study, which forms the basis for permissive hypotension resuscitation, had short evacuation time (approx.15 mins) and time to surgery (approx. 60 mins) [268]. Evidence from animal experiments appeared to support permissive hypotensive strategies, but most did not investigate its effects beyond two hours [271]. Animal models with injury such as aorta tear, are likely to be skewed towards re-bleeding, and may overly represent the 'popping the clot' theory [267, 270, 272-274].

UK military requirements in Iraq and Afghanistan led to further research in this area; which demonstrated prolonged (more than two hours) permissive hypotension resuscitation to be associated with poor outcome in a swine model of controlled haemorrhage and primary blast injury [275]. In the animals with severe haemorrhage only, prolonged hypotensive resuscitation allows survival but severely

compromise physiology evident from the worsening arterial base excess deficit [275]. Furthermore, the survival is markedly reduced in animals when haemorrhage is concomitant with blast lung injury [273].

A novel hybrid (NH) resuscitation strategy with two systolic blood pressure (SBP) targets; SBP 80 mmHg for first 60 minutes followed by revised target of SBP 110 mmHg, appears to overcome these drawbacks when evaluated in a swine model of initial controlled haemorrhage and grade four liver injury [276]. Such mixed arterial and venous models are more realistic in producing initial hypotension and potential re-bleeding at later stages [272]. Animals in the NH group had better physiology (base excess and oxygenation) and survival despite the additional blast injury. Furthermore, NH animals also had lower prothrombin time and peak IL-6 compared to those receiving hypotensive resuscitation; suggesting better coagulation and lesser inflammatory insult. This revised target approach to resuscitation is currently incorporated in UK military pre-hospital practice [277]. However, the need for a new resuscitation strategy remains, when the fine balance between 'popping the clot' and sufficient tissue perfusion for survival is disturbed by long evacuation time.

1.5.1.2. Blood products

1.5.1.2.1. Haemostatic resuscitation

The limitations of clear fluid resuscitation were progressively recognised during the conflicts in Iraq and Afghanistan, particularly in the treatment of trauma coagulopathy. Medical capabilities responded by developing pre-hospital resuscitation strategies within the principles of damage control resuscitation (DCR) to correct early abnormal physiology, which includes abnormal clotting [278].

Bringing blood components far forward to the casualty by the MERT [33], and the use of fresh whole blood (FWB) by forward surgical teams [279] are some of the resuscitation strategies adopted. Haemostatic resuscitation, features the early balanced use of packed red blood cells (pRBC), plasma and platelets, with the aims to reverse shock and preserve coagulation function [280, 281].

Usage of blood products is not without clinical risks, namely transfusion reaction and transmission of blood borne infections. Logistical challenges for remote use of blood products are immense; cold chain for storage, preparation process (e.g. platelets require continuous agitation at room temperature, fresh frozen plasma needs thawing prior usage) and short shelf life of products. Although blood has been used in battlefield casualties since World War I, there is no clear established evidence of its benefits. Retrospective observational studies from the recent military experience of Iraq and Afghanistan report survival benefits of pre-hospital blood products, however these studies have inherent limitations such as incomplete dataset, lack of control group and confounders [282]. As Cap *et al* have eloquently described forward resuscitation research – looking behind the past to find the future [283]. In order to translate military experience into civilian practice, trials such as RePHILL [284], PAMPer [285] and PUPTH [286] have been initiated to investigate the optimal use of pre-hospital blood products in civilian haemorrhagic shock.

1.5.1.2.2. Inflammatory effects of blood products

Evidence from animal studies suggests blood component therapy have inflammatory effects. Belizaire *et al* found in their experiments that stored pRBC units contain more microparticles (MP) than fresh units, and when these MPs were infused with RBCs into mice as part of resuscitation after haemorrhagic shock (HS),

accumulation of pulmonary neutrophils was increased in those animals [287]. The same team found post-HS mice resuscitated with old (15 days old) stored pRBC, to have increased levels of pro-inflammatory cytokines when compared to animals that had fresh RBC or washed old pRBC [288]. It is unclear if these MPs play a role in the contribution of transfusion-related acute lung injury (TRALI) [289]. TRALI is defined as acute lung injury (ALI) that occurs during or within 6 hours of a completed transfusion [290]

Leucocytes may have potentially contributed to the inflammatory effects of blood products. There is evidence to suggest the accumulation of inflammatory cytokines, bioactive lipids and proteins through leucocyte activities in the stored blood products, may prime neutrophils and activate endothelium in the recipient [291-293]. Adverse immunological transfusion effects such as febrile non-haemolytic transfusion reactions and TRALI, have been attributed to the presence of leucocytes in donor products [292, 294]. Some retrospective studies suggest leucoreduction is associated with lowered incidence of TRALI and other transfusion adverse effects [295, 296]. Pre-storage leucodepletion is routine in UK transfusion practice since 1999 for variant Creutzfeldt-Jakob disease (vCJD) risk reduction [297]. However, this practice is not universal in Europe and USA [298, 299]. Starkey *et al* retrospectively analysed the incidence of ALI amongst UK combat casualties who received at least 1 unit of pRBC transfusion, an incidence of 26% was reported over the 16-month period [300]. However, it was not possible to clearly distinguish if the ALI was related to primary blast lung injury or TRALI.

Certain blood components appear to offer some protection against HS-induced endothelial injury. For example, fresh plasma have been shown to partially restore [301] or reduce endothelial degradation [302]. Systemic inflammation and

remote organ injury appear to be attenuated in mice resuscitated with FWB compared to Ringer's lactate (RL), after a period of HS. Comparisons between plasma, pRBC, and various ratios of plasma to packed RBC (pRBC) using the above mouse model, has found the 1:1 plasma pRBC ratio to have the least systemic inflammatory response and remote organ injury [303]. Infusion of plasma to pRBC at 1:1 ratio is currently incorporated in the UK military haemostatic resuscitation strategy [277].

1.5.2. Pharmacological adjuncts to fluid resuscitation

The notion of using pharmaceutical resuscitation adjuncts to mitigate against casualty deterioration is an attractive prospect, particularly for the military, where the fine balance between tissue perfusion for survival and risk of initial clot disruption could be tipped by extended evacuation time and lack of early blood products.

The use of adjuncts is not a new concept in haemostasis. Tranexamic acid (TXA), an antifibrinolytic agent, has been used by UK military since 2009 and available on the evacuation platform MERT [304]. This practice was adopted by civilian practice and TXA is carried by UK civilian air ambulance since 2011 [305]. As plasmin has a role in the activation of the complement system, the attenuation of plasmin production by TXA might have additional anti-inflammatory effects [306]. A clinical study (NCT02535949) has been set up to evaluate TXA's pharmacokinetics and immunological effects in severely injured trauma patients [307].

This section is not a complete review of immunomodulatory drugs used/trialled in trauma (see [125] for overview), but focuses on drugs under investigation for their effects of in pre-hospital haemorrhagic-shock resuscitation.

1.5.2.1. Pharmacological adjuncts for inflammation

Post injury treatment via blockade or receptor antagonism of singular inflammatory mediator did not yield much success in early clinical trials [308, 309]. As the understanding of trauma immunology improves, there is a shift towards drugs that would modulate inflammation via multiple channels. Other pharmacological adjuncts to conventional resuscitation fluid have been investigated to address the inflammatory challenges posed by ischaemia-reperfusion during resuscitation [310]. Particularly, the interest in ethyl pyruvate began with the recognition of lactate's inflammatory effects in RL (section 1.5.1.1.1). Ethyl pyruvate, a stable lipophilic pyruvate derivative similar to molecular structure of lactate, is thought be a ROS scavenger with anti-inflammatory effects. Animal models of haemorrhage with tissue injury showed ethyl pyruvate used in conjunction with Hextend reduces serum and tissue expression of TNF [257, 259]. However, such benefits were not conferred in humans; a randomised controlled trial (RCT) of ethyl pyruvate in cardiac surgery patients has failed to demonstrate improved outcomes [311]. Recent animal studies on a chemically related compound, para-hydroxyphenylpyruvate (pHPP), demonstrated promising results [258].

Valproic acid (VPA), apart from its anti-epileptic properties, can impact inflammation by actions of histone deacetylase (HDAC) inhibition [312]. HDAC and histone acetyl transferases (HAT) are two counteracting enzymes that control the acetylation of nuclear histone, which plays a downstream role in cellular DNA transcription regulation [313]. Lin *et al* suggested that haemorrhage shock and resuscitation results in partial histone deacetylation, hence disturbing the HAT/HDAC balance [261]. Pre-treatment with VPA appears to reverse this imbalance, and improves survival in a lethal haemorrhage rat model [260]. Post injury administration

of VPA in the absence of resuscitation fluid also prolonged survival times after severe haemorrhagic shock [314], and in poly-trauma with haemorrhage [315].

The mechanisms by which VPA improves survival in haemorrhage is not entirely clear; suggested actions include attenuation of extracellular signal-regulated kinase 1/2 (ERK) activation [316], and reduction of c-Jun N-terminal kinase (JNK) phosphorylation and capses-3 activation [317]. A recent study has demonstrated VPA administration and resuscitation with albumin 4%, to have anti-inflammatory effects on endothelial cells in end organ after haemorrhagic shock [318]. Encouraged by the results from animal studies, a clinical study (NCT01951560) has been set up to determine the safety of VPA in healthy volunteers and trauma patients [319].

Multiple experimental and clinical observational studies have shown gender dimorphism in the immune and cardiovascular responses during haemorrhagic shock [320, 321]. Administration of male sex steroid following haemorrhage to female or castrated male mice appears to have immunosuppressive effects, and these adverse effects are attenuated in male or ovariectomised female mice given female sex hormone [322]. This leads to the notion of sex hormones and their intermediaries as possible pharmacological adjuncts in resuscitation.

Dehydroepiandrosterone (DHEA), an intermediary in the synthesis of testosterone and oestrogen, improved cardiac and hepatocellular function in a trauma-haemorrhage male rodent model when used with RL [323], and reduced systemic inflammatory response after tissue injury (bilateral femur fracture) [324]. Similarly, androstenediol, a metabolite of DHEA, also appears to have immunomodulatory effects after trauma and haemorrhage [325]. Extensive studies on oestrogen use after trauma-haemorrhage have shown promising results in

restoring normal immune function [326]. A clinical trial (NCT00973102) has recently been completed (results unpublished) on the benefits of intravenous oestrogen in patients with traumatic haemorrhagic shock [327].

1.5.3. Summary

Research so far has improved our understanding on the limitations of existing fluid resuscitation regimens, and the clinical consequences of defying the mantra "right fluid for the right patient at the right time". Far forward damage control resuscitation remains a balancing act, especially under logistical constraints. Pharmacological resuscitation adjuncts could act as 'bridging' therapies and have been the subject of research for more than a decade. There is some success in pharmaceutical haemostatic adjuncts, but so far no drug has been successfully introduced to modulate the early inflammation response in trauma.

1.6. Statins

1.6.1. Introduction

The 3-hydroxy-ethylglutaryl coenzyme A (HMG-CoA) reductase inhibitors, commonly known as statins, are a class of lipid-lowering drugs known for their use in primary and secondary prevention of cardiovascular disease. However, the cholesterol lowering properties are not the focus of this chapter.

Subgroup analysis in Cholesterol and Recurrent Events (CARE) trial suggests the benefit of statins in the prevention of further coronary events post myocardial infarction extends to patients with normocholesterolaemia [328]. Clinical findings such as increased myocardial perfusion, reduced angina episodes and minimal atheroma plaque regression on angiography, suggest cardiovascular benefits from

statins may not be solely attributed to cholesterol reduction; but via other mechanisms such as modulation of endothelium function, anti-inflammatory and anti-thrombotic actions [329-331]. Subsequently a substantial amount of evidence began to emerge in the past decade to explain the mechanisms responsible for such 'pleiotropic' properties of statins, a term coined to describe class of actions independent of cholesterol lowering [332].

This chapter aims to briefly cover the basic pharmacology of statins and focus on the existing evidence of their pleiotropic properties in the context of trauma.

1.6.2. Mechanisms of pleiotropic effects

Early mechanistic evidence for statins' pleiotropic effects mainly stem from cardiovascular research on atherosclerosis using endothelial cells, which focus on endothelial dysfunction, oxidative stress and inflammation (Figure 13). These effects are highly relevant to haemorrhagic shock and resuscitation in trauma, as they are part of the pathogenesis in ischaemia-reperfusion injury (IRI) (section 1.4.3.3). The mechanisms of these pleiotropic effects are partially understood; the three main theories that exist are:

- changes to isoprenoid intermediates synthesis
- disruption of lipid rafts
- direct blockage of interactions between $\alpha_1ß_2$ integrin and ICAM-1 to modulate the inflammatory response [333, 334]

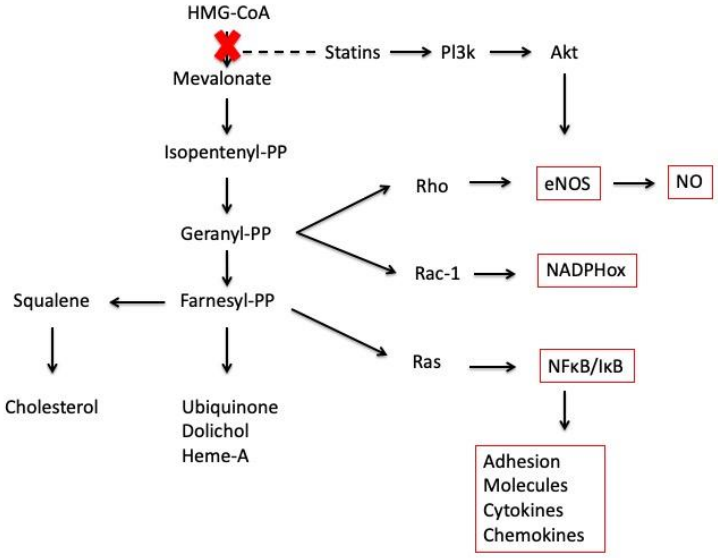

Figure 13 Pleiotropic effects of statins on inflammation. Figure adapted from [335]. Red cross indicates an inhibitory action of statins.

1.6.2.1. Changes to isoprenoid intermediates synthesis

Statins inhibit the multi-branching mevalonate pathway; besides limiting cholesterol biosynthesis, they also block the downstream production of isoprenoid intermediates such as farnesylpyrophosphate (Farnesyl-PP) and geranylpyrophosphate (Geranyl-PP) [332]. These intermediates are important lipid attachments for small GTP-binding proteins such as Rho, Rac and Ras, which act as molecular switches for a wide range of essential biochemical pathways [336]. This class of post-transcriptional lipid modification is known as 'prenylation' and is required for membrane-protein and protein-protein interactions that influence important intracellular signalling such as cell growth and differentiation [337]. Therefore, inhibition of isoprenoid intermediates may possibly account for some of the proposed pleiotropic effects.

1.6.2.2. Lipid membrane raft disruption

Another proposed mechanism by which statins exert pleotropic effect is the disruption of cholesterol rich lipid membrane rafts. Evidence suggests that intact lipid rafts act as signal transduction platforms in immunoreceptor signalling, and are required for cytokine, toll-like receptors (TLRs), immunoeffector cells signalling (T-cells, B cells, basophils and mast cells) [338, 339]. Statins impair lipid rafts by lowering cholesterol (Figure 13), this disrupts signalling to produce subsequent anti-inflammatory and anti-oxidative actions. Proteomic studies in human umbilical vein endothelial cells (HUVEC) suggest atorvastatin induces translocation of various proteins in and out of lipid rafts to produce anti-oxidative effects [340]. This proposed lipid raft disruption mechanism is less likely relevant to trauma, as protective effects of statins in IRI are reported in studies with short pre-treatment duration that are unlikely to have lowered cholesterol levels (section 1.6.5).

1.6.2.3. Direct blockage of interactions between $\alpha_1ß_2$ integrin and ICAM-1

Activated $\alpha_1ß_2$ integrin (also known as lymphocyte function associated antigen 1, LFA-1) on leucocyte surface interacts with its main ligand ICAM-1 as part of the inflammatory response and signalling cascade. Inhibition of LFA-1 using an antibody reduced neutrophil influx in a murine peritonitis model [333]. Simvastatin and mevastatin have been shown to block this interaction by locking the integrin at a low affinity state for its ligand [333]. This is observed at concentrations of statins at micromolar range, which is higher than the nanomolar range needed for HMG-CoA reductase blocking and achievable at the normal oral dose [334]. Blockage of $\alpha_1ß_2$ integrin and ICAM-1 binding reduces neutrophil recruitment in acute inflammation.

1.6.3. Protection against endothelial dysfunction and oxidative stress

Ischaemia-reperfusion injury (IRI) in trauma increases the production of iNOS, which leads to downstream effects such as organ damage (section 1.4.3.3). The cholesterol-dependent and cholesterol-independent mechanisms by which statins regulate NO have been extensively reviewed by Laufs *et al* [341]. NO is produced in large quantities over short time frame by iNOS, by contrast, eNOS production is sustained and at smaller quantities. One possibility is that statins restore the NO balance for organ protection by increasing eNOS production and inhibiting iNOS production. For example, mevastatin is found to increase eNOS mRNA and protein expression in human endothelial cells [342]. Figure 13 demonstrates that statins treatment reduces intracellular signalling molecules such as Rho GTPases. This in turn increases the production and bioavailability of eNOS. Atorvastatin appears to inhibit TNF-α and interferon-gamma (IFNγ) induced iNOS gene expression in rat endothelium, possibility via mechanisms independent of the HMG-CoA reductase pathway [343].

ROS generated from reperfusion amplifies the inflammatory response and injury to the endothelium. Statins may reduce ROS production by inhibiting membrane rac-1 protein expression which alters expression of NAD(P)H oxidase subunits (a key source of vasculature ROS production), as seen in vascular smooth muscle cells [344]. Furthermore, Statins increases circulating endothelium progenitor cells (EPC), which promote endothelium repair and revascularisation. *In vitro* studies suggest statins augment EPC differentiation in mononuclear cells via the PI3K/Akt pathway through the inhibition of mevalonate, but not its downstream product geranylgeranylpyrophosphate (GGPP) or Rho kinase [345]. EPC are known

to mobilise from the bone marrow in response to injured endothelium, hence useful in IRI.

1.6.4. Effect on inflammatory mediators

Transcription factor nuclear factor κB (NFκB), an inflammatory signalling pathway activated by pro-inflammatory cytokines as such IL-6 and TNF-α, is instrumental in the gene expression of cytokines, chemokines and adhesion molecules of the inflammation cascade. Statins have been shown to inhibit the activity of NFkB in cultured human endothelial cells and vascular smooth muscle cells, hence subsequent production of inflammatory mediators is also reduced [346, 347]. The most likely mechanism is inhibition of Ras protein prenylation (Figure 13) [335, 348]. However other mechanisms have also been proposed and include the following: increased inhibitor IkBa, which suppress IkB kinase (IKK), resulting in lowered activity level and binding capacity of NFkB [349] and modulation of the activation of activator protein-1 (AP-1) (regulates many inflammatory mediators genes) via the inhibition of Ras or Rho isoprenoids [346]. In addition, *in vitro* studies have proposed statins attenuate neutrophil trans-endothelial migration via RhoA inhibition [350].

1.6.5. Evidence of pleiotropic effects from animal studies

1.6.5.1. Ischaemia – reperfusion injury

Application of evidence from *in vitro* experiments are limited by the simplicity of cells compared to the complexity of tissues; the functional difference between cultured endothelial cells and arterial endothelial cells; as well as the statins concentrations achievable *in vitro* conditions compared to *in vivo*. Encouragingly, translational studies using animal models have demonstrated anti-inflammatory properties and endothelial protective effects of statins. Statins have been evaluated in focal ischaemia-reperfusion injury of various organs or in global IRI using models of haemorrhage and these are listed in Table 3. In focal organ ischaemia-reperfusion models, organs found to benefit from these effects include the heart [351], lungs [352], kidneys [353, 354], intestines [355], liver [356, 357], brain [358] and testicles [359]. Reduction of injury has also been reported in IRI models of spinal cord [360], peripheral nerves [361] and skeletal muscles [362, 363].

Study	Species	Details on IRI model	Statin dosage
[351]	Rat	Thoracotomy, occlusion of left anterior descending coronary artery 25 mins. Reperfusion for 2 hours.	Simvastatin 1 mg/kg i.v. 1 hour prior to ischaemia.
[352]	Rat	Thoracotomy, occlusion of left pulmonary artery, veins and main stem bronchus 90 mins. Reperfusion for 4 hours.	Simvastatin 0.5 mg/kg/day oral garage 5 days prior to thoracotomy.
[353]	Rat	Laparotomy, left nephrectomy, occlusion of right renal vascular pedicle 30 mins. Reperfusion for 2 to 24 hours.	Pravastatin 0.4 mg/kg/day oral gavage 5 days prior to laparotomy.
[354]	Rat	Laparotomy, clamping of both renal vascular pedicles for 45 mins. Reperfusion 4 hours.	Simvastatin 1mg/kg iv 30 mins prior to ischaemia.
[355]	Rat	Laparotomy, occlusion of superior mesenteric artery 60 mins. Reperfusion for 3 hours.	Simvastatin 10 mg/kg/day oral prior to laparotomy.
[356]	Rat	Laparotomy, occlusion of portal vein, hepatic artery and bile duct origin 30 mins. Reperfusion for 24 hours.	Simvastatin 10 mg/kg/day oral gavage 3 days prior to laparotomy.

Study	Species	Details on IRI model	Statin dosage
[351]	Rat	Thoracotomy, occlusion of left anterior descending coronary artery 25 mins. Reperfusion for 2 hours.	Simvastatin 1 mg/kg i.v. 1 hour prior to ischaemia.
[357]	Rat	Laparotomy, occlusion left hepatic artery 45 mins. Reperfusion 240 mins.	Simvastatin 1.25 to 5 mg/kg i.p. 24 hours prior to laparotomy.
[358]	Rat	Occlusion of left common and external carotid arteries 90 mins. Reperfusion 24 hours.	Rosuvastatin 1 to 10 mg/kg daily 7 days prior.
[359]	Rat	Occlusion of spermatic cord 40 mins. Reperfusion 30 mins.	Simvastatin 5 mg/kg i.p. 24 hours prior.
[360]	Rat	Occlusion of thoracic aorta 12 mins. Reperfusion 6 to 48 hours.	Simvastatin 10 mg/kg/daily 7 days prior.
[361]	Rat	Occlusion of femoral artery and vein for 3 hours. Reperfusion 3 hours to 14 days.	Simvastatin 1 mg/kg i.v. 1 hour prior.
[362]	Rat	Pneumatic tourniquets on bilateral hind limbs for 4 hours. Reperfusion 24 hours.	Simvastatin 0.2 to 20 mg/kg/day oral gavage 6 days prior.
[363]	Rat	Rubber bands on bilateral hind limbs for 2.5 hours. Reperfusion 12 hours.	Pravastatin 0.4 mg/kg/daily oral gavage 5 days prior.
[364]	Rat	Laparotomy, occlusion infra-renal aorta for 30 mins. Reperfusion 120 minutes.	Pravastatin 0.4 mg/kg/daily oral gavage 5 days prior.
[365]	Rat	Occlusion of bilateral femoral vessels for 2 hours. Reperfusion 3 hours.	Simvastatin 1 to 10 mg/kg/day o.g. 3 days prior.
[366]	Rat	Occlusion of bilateral femoral vessels for 2 hours. Reperfusion 3 hours.	Simvastatin 5 to 10 mg/kg/daily o.g. 3 days prior.
[367]	Rat	Pneumatic tourniquets on bilateral hind limbs for 4 hours. Reperfusion 24 hours.	Simvastatin 0.2 to 20 mg/kg/daily oral 5 days prior.
[368]	Rat	60% total blood volume over 30 mins. Resuscitation with equal volume of normal saline.	Fluvastatin 1 mg/kg i.v. prior.
[369]	Rat	MAP 30-32 mmHg in 5 mins. Resuscitation with 60% shed blood and volume of lactated Ringer's solution that equals 50% shed blood volume.	Simvastatin 5 mg/kg/daily i.p. 6 days prior.

Table 3 Existing statins studies using rat models of focal IRI or simple haemorrhage. IRI, ischaemia reperfusion injury. MAP, mean arterial pressure. i.v., intravenous. i.p., intraperitoneal. o.g., oral gastric.

Markers indicating of endothelial protection such as increased eNOS expression (to restore NO balance/endothelial function) and reduction of NADPH oxidase (inhibition of NADPH oxidase reduces generation of free radicals) are seen

in tissues from animals pre-treated with simvastatin and pravastatin in pulmonary [352] and renal IRI models [353]. In an intestinal IRI model, the reduction of glutathione peroxidase (GPx) and superoxide dismutase (SOD) in gut tissue (markers of anti-oxidative function) appeared to be attenuated in animals pre-treated with simvastatin [355]. Isoform HO-1 which is induced under stress conditions and are protective during hypoxia, are elevated in simvastatin treated animals compared to placebo in liver [357] and testicular IRI models [359].

Decreased amounts of pro-inflammatory cytokines such as TNF-α were found in serum and bronchoalveolar lavage of animals pre-treated with simvastatin in hepatic [356] and pulmonary IRI [352]. Histology examination suggests preservation of tissue architecture and reduced tissue oedema in organs exposed to focal IRI, when pre-treated with statins, these findings are also confirmed by two additional studies [352, 353, 356, 361]. Preservation of organ function post IRI with statins pre-treatment has been extrapolated from reduced motor deficit index score for hindlimb motor function post spinal IRI and decreased urine protein leakage [353, 360].

Organs such as lungs and kidneys are prone to secondary injury, as a consequence of the inflammatory sequelae from trauma and the associated blood loss and hypoperfusion. Animal studies have demonstrated that statins offer protection to organs remote from the initial insult [356, 364, 366, 367]. Pre-treatment with simvastatin or pravastatin for 3-10 days via oral gavage, prior to limb ischaemia-reperfusion or infra-renal aorta cross-clamping, reduced lung injury compared to placebo groups [364, 366]. Lung protection was also seen in liver IRI model [356]. Neutrophil tissue infiltration (measured by MPO activity), microvascular leakage (neutrophil concentration in bronchoalveolar fluid, lung wet-to-dry ratio) and histological features of lung injuries were less in the statins group compared to

placebo [356, 364, 366]. However, Cowled *et al* in their limb IR model demonstrated injured animals pre-treated with simvastatin had *reduced* renal MPO activity but *increased* pulmonary neutrophil infiltration compared to placebo group [367]. The reasons for the discrepancy in results are unclear.

Oxidative stress happens during ischaemia-reperfusion from traumatic haemorrhage, tissue injury, or primary blast injury. These conditions are stressful for cells and triggers a cascade of inflammatory responses. Heme oxygenase protein in its inducible form (HO-1) is expressed in response to conditions such as oxidative stress. It is believed to have antioxidant and anti-inflammatory functions, hence its induction may play a protective role. Sun *et al* in their limb IRI model demonstrated pre-treatment with simvastatin upregulates pulmonary HO-1 protein expression after IRI to the lower limbs, and a corresponding reduction in lung histological changes [366].

Inhibition of NOS using L-NIO, a potent irreversible inhibitor of both iNOS and eNOS, reduced neutrophil extravasation in both lungs and kidneys in a rat model of bilateral limb IRI [367]. This suggests NOS or NO contribute to mediating remote tissue damage during IRI. It has been shown that simvastatin treatment reduced renal neutrophil infiltration [367]. In order to investigate the mechanism of this protection, L-NIO was administrated in conjunction to simvastatin [367]. The combination further ameliorated the increased MPO activity (neutrophil infiltration) from IRI. The authors postulated each agent provided partial protection; that statins stabilised eNOS production during the early phase of reperfusion to inhibit adhesion molecule expression, whilst L-NIO inhibited peroxynitrite-mediated adhesion molecule expression in the later stages of reperfusion [367]. Further evidence that supports statins' role in eNOS came from Joyce M *et al,* when upregulation of eNOS

expression was demonstrated in lung tissue of rats undergoing abdominal aorta cross clamping pre-treated with pravastatin compared to placebo [364].

1.6.5.2. Haemorrhagic shock

In a rat model of simple haemorrhage, fluvastatin reduced the production of cytokines and organ damage [368]. Elevation of serum TNF-α and IL-10 from haemorrhage shock was attenuated with fluvastatin pre-treatment. Histological findings from liver, kidney, lung and small bowel demonstrated reduced injury score in the fluvastatin treated injured group. Interestingly, the decrease in MAP and increase in heart rate expected post haemorrhage (60% blood volume) was ***attenuated*** in the fluvastatin treated injured group. A lower heart rate and a higher MAP was noted in the statins group when compared to injured placebo group. The authors [368] did not postulate any explanation for these haemodynamic findings. Such differences in haemodynamics between statins and placebo were not observed in a pressure driven rat model of simple haemorrhage (target MAP 30 mmHg) by Relja *et al* [369].

However, very important differences between the models of haemorrhage employed in the two studies must be acknowledged. In the study reported by Lee *et al* [368] the haemorrhage was performed in conscious animals, which were restrained by tethering of their tails, while the haemorrhage in the study reported by Relja *et al* [369] was conducted under isoflurane anaesthesia. Use of anaesthetic agents, particularly those such as isoflurane which impact on cardiovascular reflexes, can substantially modify the initial and subsequent response to blood loss, and could attenuate a recovery in blood pressure. Stress, such as that which might have been caused by the method of restraint in Lee's study could also modify the

response to haemorrhage; in theory if it were to cause a defence-type response it might accentuate a resistance to fall in blood pressure during haemorrhage and augment a tendency to recovery of blood pressure. Furthermore, the volume of haemorrhage in Lee's study (60% blood volume) was substantially greater than that used by Relja *et al* (approximately 30% blood volume[3]), although the initial rate of blood loss was likely to have been substantially greater in Relja's study compared to Lee's. Unfortunately, with so many variables in play, it is impossible to make a meaningful prediction of whether any of these factors might have had an impact on the relative outcome of these two studies.

Despite the apparent differences in the impact of statins on the haemodynamic response to blood loss in the studies reported by Lee *et al* and Relja *et al* (see previous paragraph), the findings from the two studies regarding organ damage, inflammation and survival are congruent. Both studies showed statins to have protective effects with regard to organ damage, inflammation and survival. Simvastatin pre-treatment reduced mortality and attenuated hepatic injury [369]. Serum ALT, marker of hepatocellular damage was reduced along with histological evidence of hepatic neutrophil accumulation, oxidative stress, necrosis and apoptosis. Systemic inflammation indicated by serum IL-6 at 2 hours post resuscitation was also lowered in the statins group.

Haemorrhagic shock inhibits NO production by eNOS (endothelial dysfunction), and induces iNOS activity which produces large qualities of NO [181]. Simvastatin pre-treatment attenuated the expected rise in Rho/Rho-kinases (ROCK) protein and induced the production of HO-1 and eNOS post haemorrhage and

[3] Calculated from the reported volume of blood withdrawn as a proportion of an estimated total blood volume of 6.06 ml/100g body weight.

resuscitation [369]. In light of existing *in vitro* evidence, the authors postulate that ROCK inhibition is the mechanism by which statins influence eNOS expression (Figure 13). The increased hepatic HO-1 production corresponds to a decrease in hepatic injury in this haemorrhage model, which supports the observations from focal IRI models (paragraph 2 section 1.6.5.1).

In summary, these animal models described so far in this chapter are of some relevance in trauma but they do not reflect the physiological and immunological burden of 1) complex battlefield trauma, and 2) the impact of current resuscitation practices. Protective effects of statins treatment in IRI have been demonstrated using a variety of statins at different dosage administrated over a range of short periods prior to IRI (Table 3). This suggests IRI protection to be a class effect observed after a short pre-treatment duration, which makes the side effects of statins (apparent over long course treatment) less relevant.

1.6.6. Clinical studies

No clinical trial exists for the use of statins in major trauma, but some evidence from observational studies suggest pre-injury statins use is associated with improved outcomes. Benefits of pre-injury statins are also observed in specific forms of trauma such as head injury [370] and burns [371]. However, statins have been investigated in vascular and transplant patients, and the results may be indicative for trauma.

Observational studies of ruptured abdominal aorta aneurysm, where patients undoubtedly experienced haemorrhagic shock and reperfusion, suggest survival benefits with statins pre-treatment [372, 373]. Peri-operative use of statins is associated with reduced incidence of primary graft dysfunction (a form of acute lung

injury post transplantation) after lung transplant [374]. However, although some overlap exists in the pathophysiology between trauma, vascular and transplant surgery, results from studies in vascular or transplant surgery should not be applied directly to trauma due to some differences in cardiovascular responses such as regional blood flow (section 1.2.5.2).

Multivariable analysis of retrospective observational data of 1224 patients from 69 hospitals collected by Efron *et al* has identified pre-injury statins treatment as an independent predictor of reduced in-hospital mortality in elderly trauma patients (AIS≥3) without cardiovascular co-morbidities [375]. Another retrospective study with smaller sample size of 120 patients from a single centre, has also identified pre-injury statins use to be associated with lower mortality in traumatic haemorrhagic shock [376]. However, in contrast a secondary analysis from a multicenter prospective cohort study on trauma outcomes, suggested no difference in mortality with pre-injury statins treatment, but it did identify that statin treatment was independently associated with *higher* risk for developing multiple organ failure in blunt injury with haemorrhagic shock [377].

Since statins are generally used by the older population, these observations are based on patients at least 55 years old and above; no observational data is available in the younger population more aligned to military trauma patients. Secondly, registry studies have inherent limitations such as: the lack of details on the type or dose of statins used, and length of treatment (pre and post injury) [375-377]. Another possible confounder includes the ‘healthy user effect’; patients on regular statins treatment could reflect health-seeking behaviour and less likely to have untreated underlying co-morbidities that might affect outcome [378].

Furthermore, several discussion points arise from the contrary results from the study by Neal *et al* [377]. The cohort of patients examined are severely injured (ISS 30) with comorbidities, plausible explanations for the lack of effect could be an inflammatory storm generated in very severe injuries or the burden of existing comorbidities, may eclipse any protective effects of statins. Negative 'rebound' effects had been described in patients with acute withdrawal of chronic statins use (post vascular surgery), such as increased cardiac events, which could have contributed to these observations [379]. It is also possible that statins' pleiotropic properties wane with long term treatment [380].

So far, completed RCTs on trauma pre-injury statins use are limited to burns, undisplaced radial fracture or traumatic brain injury [381-384]. The findings of these trials are mixed; statins treatment had no effect in fracture healing, whilst in burns and traumatic brain injury statins reduced inflammatory markers. Their detailed discussion is beyond the remit of this thesis. No clinical trials have specifically explored the use of statins in conjunction with current resuscitation strategies in severe trauma patients with tissue injury and haemorrhage shock [125, 385].

Anti-inflammatory effects of statin have been reported in RCTs designed to investigate patients with established infections or organ failure, all but one of these RCTs used progression of sepsis or mortality as primary outcomes. A meta-analysis of five RCTs on the effect of statins treatment on mortality did not find any benefits in septic patients [386]. However, subgroup analysis of patients who previously were on statins and those randomised into the statins group by Kruger *et al*, demonstrated significantly improved mortality outcome over placebo treatment [387]. Other trials planned or underway measure outcomes such as inflammatory markers (IL-6) [388], time to clinical stability (normalisation of vital signs) [389] and time to shock reversal

in sepsis [390, 391]. Organ specific studies were initiated to investigate statins treatment in ARDS; one trial found significant improvements in pulmonary and systemic inflammation with statins treatment over placebo [392] but a larger trial did not find any patient outcome benefits (ventilation-free days, non-pulmonary organ failure free days, mortality) [393]; another trial was terminated due to futility [394]. A study designed to investigate the role of statins in the reduction of ALI post blunt chest trauma is currently underway [395].

Although clinical trials of statins for their pleiotropic application in sepsis or ARDS are less optimistic, the potential of statins to improve outcomes in battlefield trauma should not be dismissed. Firstly, the patients from sepsis or ARDS studies are of a different population compared to the majority of trauma patients who are generally younger and with less co-morbidities. Secondly, in these RCTs patients are critically unwell with established inflammatory process for some duration prior to statins treatment, hence perhaps beyond the remit of statins intervention. This is different to the military trauma setting where the aim is to give the drug early as part of far forward resuscitation. *In vitro* and *in vivo* studies provide evidence that statins influence multiple mechanisms at various stages in the inflammatory response. Given the complex nature of inflammation (evident from the lack of success with specific antagonist of inflammatory mediator), statins which acts at multi-level via numerous mediators, might potentially influence the overall inflammatory process from trauma.

1.6.7. Pharmacology

Many factors affect the pharmacokinetic properties of statins. Firstly, they are either administered in lactone pro drug which is enzymatically hydrolysed *in vivo* to

active hydroxyl-acid form, or given in its active state hydroxy acid [396]. Most statins are administrated as hydroxyl acids, except lovastatin and simvastatin. Absorption is quick, peak plasma concentration is reached within 4 hours after administration. Food intake has variable effects on statins absorption rates, but not for simvastatin and rosuvastatin.

Statins have low systematic bioavailability due to effective first pass uptake in the liver (mostly) or gastrointestinal tract. The lipophilic or hydrophilic rate determines the solubility and first-pass uptake. Lipophilic statins such as simvastatin and atorvastatin diffuse passively through hepatic cell membrane, whilst hydrophilic pravastatin and rosuvastatin depend on carrier-mediated uptake into hepatocytes. Hydrophilic statins are deemed to be more hepato-selective than lipophilic ones, as less likely to penetrate extrahepatic tissues. As the liver is the site of cholesterol biosynthesis hence the target organ for drug action in statins licensed use, the effective first pass uptake is deemed advantageous in the treatment of hypercholesterolaemia.

Statins are predominately metabolised via cytochrome P450 (CYP450) family enzymes, except for pravastatin [397]. The CYP3A4 isoenzyme metabolises many statins into their active derivatives, which attribute the activity of the drug. Statin elimination is mostly in bile (faeces) and the rest via renal excretion, with the exception for pravastatin where 60% excretion is by tubular secretion. Most statins have short half-lives of three hours or less, such as simvastatin with half-life of two hours. Exceptions are rosuvastatin and atorvastatin have longer half-lives at 19 and 14 hours respectively.

For the propose of introducing the thesis, I will focus on the pharmacokinetics of simvastatin, since majority of the relevant translational studies used simvastatin.

Simvastatin comes in a white crystalline powder insoluble in water but soluble in methylene chloride and ethanol [398]. It is administered as a prodrug and activated in the liver to the active metabolites ß-hydroxy acid and its 6'-hydroxy, 6'-hydroxymethyl and 6'-exomethylene derivatives [396]. Its absorption is close to 60%, and absolute bioavailability of ß-hydroxy acid is 5% [399]. Peak plasma concentration is reached within 1.3 to 2.4 hours post dose and decline to approximately 10% of peak by 12 hours post administration [398]. The recommended dose in human for its licensed use is 5 to 40 mg per day. Simvastatin demonstrates linear relationship between dose and area under the plasma concentration-time curve (AUC) up to 120 mg dosage.

Concerns had been raised about the safety of statins use recently, this was followed by the controversial retraction of high profile article in a leading medical journal [400]. Statins are relatively safe drugs and most serious adverse effects associated are myopathy and progression to fatal or non-fatal rhabdomyolysis. However the incidence of myopathy is low, dose related and at increased risk when used in combination with agents that share the common metabolic pathways. Molecular muscle damage (myofibers death) is observed when statins had been used for more than 5 days [401].

1.6.8. Rationale for statins in military trauma

Haemorrhagic shock and tissue injury initiate a cascade of inflammatory response orchestrated by the endothelium, which is escalated by reperfusion in resuscitation (section 1.4.3.3). This can be aggravated by the additional oxidative stress and inflammatory mediators generated, for example, in primary blast lung injury (section 1.4.3.4). Logistic constraints such as extended evacuation timeline

and limited resuscitation resources are possible challenges faced by the military, particularly at entry operations, or by civilian emergency services in mass casualty scenarios. Prolonged periods of hypotension as well as intravenous fluids administration may have inflammatory consequences (section 1.5.1.1), hence a 'bridging' adjunct to resuscitation to attenuate the inflammatory response is an attractive idea.

An even more appealing notion is to repurpose an old drug, as it would require lesser time and costs before clinical translation, compared to a novel drug [402]. Evidence from animal studies in IRI models and haemorrhagic shock suggest the restoration of endothelium function and redox balance by statins pre-treatment, there is sufficient evidence from literature reviewed above to suggest that statins might be beneficial if administrated early in trauma (section 1.6.5). However, there are physiological differences between the models reviewed and complex trauma (comprising of tissue injury, haemorrhagic shock and blast) (sections 1.2.5 and 1.3.4), hence these effects need to be tested in realistic models of trauma in conjunction with current resuscitation strategies.

Based on the current evidence, as a proof of principle it would be sensible to establish the effect of statins pre-treatment in complex trauma, prior to considering post injury administration.

1.6.9. Purpose of thesis

The aim of this thesis is to investigate, as a proof of concept, whether simvastatin given as a short treatment pre-injury, will attenuate subsequent inflammatory response and protect against endothelial damage in a relevant model of complex battlefield injuries and subsequent resuscitation.

CHAPTER 2 METHODOLOGY

2.1. Experimental Design

2.1.1. Introduction

Tissue injury and haemorrhage lead to localised and systemic hypoperfusion, and subsequent reperfusion injury during resuscitation. The inflammatory responses arising from these insults may lead to systemic and remote organ damage, which complicates the clinical management of trauma patients. The use of explosives in recent conflicts results in blast injuries (including primary blast injury to the lungs), which have been shown to interact with the physiological and inflammatory responses to trauma, posing even greater clinical challenges. In addition, the management of military trauma casualties is further complicated by long evacuation timelines and limited resuscitation strategies for example, which may escalate the inflammatory response. The use of pharmacological adjuncts to resuscitation may be a bridging solution to this latter problem. Based on the literature reviewed earlier (section 1.6.5), there is evidence to suggest that statins might attenuate the ischaemia-reperfusion injury if administered early. This chapter will briefly cover the experimental design of this proof of concept study, the aim of which is to 1) establish model severity; 2) explore feasible analysis of blood and tissue samples and 3) evaluate the potential of statins to limit the inflammatory burden in a relevant trauma and resuscitation model.

2.1.2. Model requirements

2.1.2.1. Injurious components

In the context of battlefield trauma, there are two types of injury that are of relevance (section 1.1); penetrating injury caused by bullets, or fragments in casualties a significant distance away from the centre of an explosion; and those injured close to an explosion, where the risk of primary blast injury (from the shock wave) is greater, see section 1.3.2.3. Two models of injury are therefore required; combined tissue injury and haemorrhagic shock, with and without additional primary blast injury, all with subsequent clinically relevant resuscitation. UK civilian trauma is largely comprised of blunt injury with extensive tissue damage (e.g. RTC), and this is reflected in the proposed model that includes tissue damage and haemorrhage in the absence of blast injury.

2.1.2.2. Severity of injury requirements

One of the predictors of multi-organ failure post trauma is injury severity measured using the Injury Severity Score (ISS). A high ISS is associated with development of multi-organ failure (section 1.1.4), whilst patients with mild or moderate injuries are less likely to develop remote organ injury. The population of patients that are likely to benefit from a resuscitation adjunct to modulate early inflammatory response, have severe but not unsalvageable injuries, therefore the model should reflect this.

As part of the Remote Damage Control Resuscitation strategy, a limited period of hypotensive resuscitation is currently used in the pre-hospital setting, particularly when blood products are not readily available or only a limited amount of intravenous fluids are available [403]. As prolonged hypotension is harmful [275],

the resuscitation target is revised on arrival to the hospital environment where there is access to blood products and surgical capabilities. The resuscitation regimen of the model aims to reflect the current clinical practice by having two distinct resuscitation phases. The pre-hospital phase in the model will represent the 'worst case scenario' where there are no blood products and only a limited amount of intravenous fluid is available. In the hospital phase, the animals will be resuscitated with blood to a more normotensive target. However, without a rat blood bank of unlimited blood products, the infused 'blood' for this study is mixture of shed blood (from the haemorrhage phase) supplemented with colloid (in a 3:1 ratio of blood:colloid) to boost volume. After the animals are fully resuscitated to stable conditions (shock reversed) and all the 'blood' transfused, intravenous fluid is given at a maintenance rate until the end of the experiment.

2.1.2.3. Choice of model

The ideal scenario to test the hypothesis is to conduct a clinical trial. However, there are currently no strong indications for the use of statins in trauma from the existing evidence in literature to support this (section 1.6.6). Therefore we are left the following options: a pre-clinical study in an animal model; a study in human volunteers; or a study using alternatives to 'whole body' experiments. Following the principles of the 3R's (replacement, reduction and refinement) [404] human volunteers and *in vitro* studies were considered to avoid the use of animals. The option to use healthy human volunteers is not possible because replicating the severity of injury would cause significant harm and therefore be unacceptable and unethical. *In vitro* models (established cell lines, tissues) are not sophisticated enough to represent the complex interactions of physiological and immunological

changes in trauma and resuscitation, which depend on the interaction of several body systems. Hence, the only remaining option is to use an animal model.

2.1.2.4. Choice of species

Animal models broadly classify into large and small animals, each has its advantages and disadvantages [405]. The advantages of using small animals are lower cost in comparison to large animals and in keeping with the 3Rs principles they are of lower sentience. The rat has the advantage over the mouse, as their size allows for easier instrumentation and there is a larger blood volume in comparison, which allows for greater sampling and analysis. Haemorrhage, tissue injury and blast models are well described in rats; and cardiovascular response to haemorrhage and tissue injury is similar between rats and man [406, 407]. There is already an existing body of evidence for the use of statins in IRI rat models (section 1.6.5), this helps with the selection of an approximate dosage in the experimental design. Although the rat is genetically distant to humans, sharing 90% of genome with human, some immune responses to haemorrhagic shock are similar in human [408, 409]. The main disadvantage of a small animal model in this study is the limited blood available for serial sampling, but it is possible to overcome this with the selection of analysis techniques.

2.1.2.5. Choice of outcomes

Potential study outcomes include survival, organ failure, organ and endothelial injury, inflammatory or immune response. Although clinically highly relevant, choosing survival as an outcome measure in this study would be challenging. A long observational period would be required, since their proposed pleiotropic properties

would suggest that statins are unlikely to influence mortality in the acute stages (section 1.6.2). Furthermore, although many clinical trauma research papers report 30-day mortality, this is not a robust outcome measure as this would include patients who died from causes not directly related to the initial injury [410]. Other clinically relevant outcomes such as organ failure would also require long observational period, which would also require a recovery model. A recovery model is not favoured due to costs and the ethical challenges such models present. Other outcomes could be chosen to avoid the need of a recovery model, such as markers in the acute phase that could indicate ongoing or impending inflammation or endothelial or organ injury.

2.1.3. Drug administration

Protective effects of statins in ischaemia-reperfusion injury (IRI) have been observed using different statins in a range of doses, delivered via various routes and with various durations of pre-treatment (Table 3 in section 1.6.5). Simvastatin was chosen for this study as it has the largest body of evidence suggesting efficacy in IRI or haemorrhage rat models. The normal administration route is oral, as it is a pro-drug that requires activation in the GI tract. Therefore oral administration under supervision (to ensure drug administration) was chosen, as it is least distressing for the animals. Peak absorption of simvastatin in humans is within four hours, as the rats are not fasted, the last dose of simvastatin can be administrated on the morning of the experiment.

The dose utilised in the study presented in this thesis was 5 mg/kg, which is approximately middle of the range seen in studies conducted in the rat (Table 3 in section 1.6.5). According to body surface area conversion Food and Drug

Administration (FDA) tabulation, 5 mg/kg in rat equals to 0.8 mg/kg in human, hence not an unachievable dosage for future translation. Unfortunately none of the previous studies reported the plasma levels of statins or the active metabolites for protective effects statins to be observed in IRI. In order to have proof of successful dosing, terminal samples were taken to quantify simvastatin active metabolite, ß-hydroxy acid, which remains detectable in plasma in humans 30 hours post ingestion of a dose of 80 mg [411]. The advantages of terminal sampling are that it would 1) provide evidence that systemic simvastatin active metabolite is present for the duration of the experiment, and 2) not compromise the stability of the animals.

2.1.4. The 3Rs

Replacement was discussed earlier in the chapter (section 2.1.2.3).

2.1.4.1. Reduction

In order to minimise the number of animals used in the study, longitudinal measurements of mediators were made by serial sampling of small volumes of blood, rather than culling multiple groups of animals at specific time points. In addition, tissue sampling was confined to one time point (a terminal sample 6 hours after the start of resuscitation).

2.1.4.2. Refinement

Refinement is concerned with minimising the suffering caused by experimental procedures, and as a model of severe traumatic injury was required, the animals were anaesthetised throughout the experiment to minimise suffering. In order to minimise the cardiovascular effects of anaesthesia such as cardiopulmonary

depression, alfaxalone was used. This class of anaesthetic has also been shown to preserve the haemodynamic response to injury [79, 412]. Recovery from anaesthesia was considered but for this proof of concept phase it was decided that the animals should remain anaesthetised to eliminate suffering. Prolonged anaesthesia presents its own challenges however and therefore the choice of outcome measures was very important.

2.1.5. Outcome measures

The experiment is limited to less than 12 hours for two main reasons; 1) the duration for maintenance of anaesthesia and 2) the severity requirement of the model would suggest that animals would likely to need further transfusion to maintain clinical stability beyond twelve hours, and this would require more animals to be sacrificed for blood bank facilities. On the other hand, the experiment needs to be of sufficient length for the effects of injury to manifest and thus evaluate a potential treatment effect. Six hours from injury is a good starting point, as various haemorrhage and trauma rat models have shown elevated and detectable inflammatory markers six hours from injury [250].

The ideal outcome measures should be detectable and change within the time frame of the experiment, and intervals at which the measurements are taken should capture the changes over time. Outcome measurements broadly fall into physiological state and immune response. Close monitoring of the degree of shock and oxygen debt is important as it is a crucial part of the model. Invasive arterial monitoring would be desirable as it allows continuous measurements of arterial blood pressure and allows arterial blood sampling for degree of shock to be evaluated using base excess and lactate for example.

Part of this proof of concept study is to evaluate and determine which are the most suitable outcome measures for the immune response and feasibility of assays, to overcome some of the limitations from this model. In order to correlate the immune response with the physiological state, it is desirable for measurements of immune response to be taken at identical time points. However, the changes from immune response are unlikely to change at intervals as rapidly as parameters for shock, and with the limited blood available for sampling, sampling at a few overlapping time points is acceptable.

Measurements of immune response from the domains of: cell death, inflammation, apoptosis, oxidative stress and endothelial injury are suitable, as statins have demonstrated beneficial effects in these areas (section1.6.5). Flow cytometry analysis would be desirable as it can provide data for most of these domains, however this method was not possible in this model due to the limited volume of each serial blood sample.

Methods for analysing plasma inflammatory markers or mediators include enzyme-linked immunosorbent assay (ELISA) or multiplexed bead array assays (MBBA). ELISA is the gold standard for quantitative analysis, however as each assay tests for a single analyte, the number of analytes that could be assayed using this method will be limited by the volume of blood that can be withdrawn for analysis in a small animal model. Although less reliable for absolute quantification, MBBA is able to test for more analytes on focused pathways using the least amount of blood. Choosing MBBA in this study would be appropriate, multiple analytes analysis will allow definition of the immune response in the model, and the comparison between treatment groups. DAMPS, such as HMGB1 are a marker of cell death and seen in samples from injured soldiers from Bastion [413], and are likely to be elevated within

the early phase of the experiment. HMGB1 can only be analysed by ELISA. The decision to use an inflammation focused MBBA and an ELISA for HMGB1 is reasonable starting point.

Circulating endothelial cells (CECs) are indicators of endothelial damage, they were seen in a rabbit model with localised blast to hind limb at six hours from injury [224]. The authors postulated the presence of CECs was likely from biochemical pathways leading to endothelial cells detachment rather than mechanical force, as the increased CECs was at six hours rather than at one hour. One of the methods for measuring these rare CECs is to use the imaging flow cytometry technology. A terminal blood sample from this model would allow sufficient volume for this method. There is no clear evidence to suggest sampling earlier than six hours would be necessary.

Tissue samples from various organs could be exploited for gene expression, protein and histological evaluation. Gene expression for markers of inflammation, apoptosis, and oxidative stress can signpost relevant markers for further investigation such as protein analysis. Molecular techniques for gene expression analysis range from single quantitative polymerase chain reaction (qPCR) to microarray. As each single qPCR provides information for one gene, it is suitable for validating microarray results or when the number of genes to be investigated is small. On the other hand, microarray examines thousands of genes at the same time to generate gene expression profiles, which then requires further work for validation. Areas of interests can be pre-determined (inflammation and apoptosis for example), and whilst this is potentially limiting it does have the flexibility to explore numerous markers for the purpose of signposting, therefore this middle ground

approach using pathway focused array panels for gene analysis is acceptable for this study.

As this is a proof of concept study, interim analysis is planned on some of the outcome measurements to determine 1) the potential utility of simvastatin as a resuscitation adjunct for poly-trauma and 2) ascertain the number of animals required to power the study adequately. The results from interim analysis would determine if it is appropriate to continue the *in vivo* phase.

2.2. Methods

2.2.1. Ethical approval

This prospective, randomised, double-blinded, placebo controlled study was conducted on terminally anaesthetised rats. The study was subjected to ethical review at Defence Science and Technology Laboratory (Dstl) Porton Down and conducted in accordance with the Animals (Scientific Procedures) Act 1986 (Project license PPL 30/3004).

2.2.2. Husbandry

Adult male Porton-Wistar rats (Porton Down, UK; body weight range 223 g-293 g) were used. Animals were kept in 12 hour to 12 hour light-dark cycle, fed on standard rat diet (Rat Diet, LabDiet®, USA) with access to food and water *ad libitum*. Weight measurements were taken daily and animals micro-chipped before the study commenced after attaining a minimum bodyweight of 200 g.

2.2.3. Injury and treatment groups

Two injury strands were studied (blast or sham blast) and one surgical control group (Figure 14). Animals in both injury strands underwent haemorrhage and tissue injury, whilst those in the surgical control group had no injury or haemorrhage. Animals in each injury strand were randomised into one of two treatment strands (statins and placebo). Those in the surgical control group were only given placebo[4].

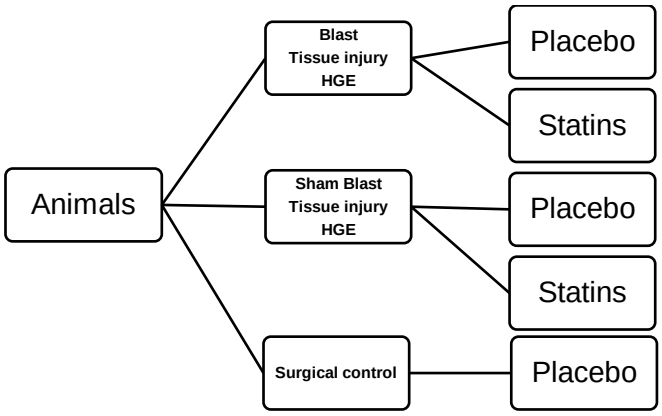

Figure 14 Study group allocation.
HGE, haemorrhage.

2.2.4. Randomisation and blinding

Animals were randomised into the 5 groups[5] shown in Figure 14 using computer generated randomisation tables (Microsoft Excel, Microsoft Office, USA). Researchers were blinded to treatment strand.

2.2.5. Drug preparation

Simvastatin (European Pharmacopoeia Reference Standard EPS0650000) was dissolved in 96% ethanol (Ph Eur, Fluka Analytical, Switzerland) to yield a 40

[4] A parallel study shared the surgical control group (414. Thomas, G.O.R., *Use of erythropoietin in trauma, blast and haemorrhage*. 2016, University of Swansea.)
[5] Randomised into 7 groups, of which 2 groups belong to a parallel study (414. ibid.

mg/ml solution. Approximately 800 mg to 900 mg of white chocolate chunks (Dr Oetker, Germany) were melted over a water bath set at a temperature of 55^{o}C. 35 µl of simvastatin solution was pipetted into the melted chocolate for rats over 240 g; 30 µl of simvastatin solution was added into chocolate for rats 240 g and below. This gave a dose range of 5 mg/kg to 6 mg/kg for rat weighing between 200 g to 240 g, and 5 mg/kg to 5.8 mg/kg for those weighing 240 g to 280 g. Placebo chocolates had ethanol but no statin. The chocolate was allowed to cool and set into discs, and stored at 4^{o}C for up to 3 months.

Plain white chocolate discs (no added simvastatin or ethanol) were given to all rats in the first two days to allow acclimatisation to the taste. Day 3 to Day 7 (five days) the rats were given either placebo chocolates, or one of the two statin chocolates depending on body weight.

2.2.6. Anaesthesia

The injury protocol was conducted on day 7 (after 5 daily doses of placebo/statin chocolates). Anaesthesia was induced using isoflurane (IsoFlo®, Abbott Laboratories Ltd, UK) in an induction chamber. Isoflurane was set initially at 2% and increased to 5% delivered by 100% oxygen at 1.5L/min (Frontline Plus 690, Blease Medical Equipment Ltd, UK).

Once anaesthetised, animals were removed from the chamber and placed supine on the operating table. Surgical anaesthesia was maintained by inhalation of isoflurane (1.5%-2.5%) delivered via a facemask with an integrated scavenging system. Target depth of surgical anaesthesia was denoted by loss of pedal withdrawal reflex and no cardiovascular response to painful stimuli.

2.2.7. Surgical preparation and intra-operative monitoring

Ocular lubricant (Lacri-Lube®, Allergan, UK) was applied to both eyes to avoid corneal desiccation. Body temperature was maintained between 38°C and 38.5 °C using a thermostatically controlled heating mat (Homeothermic blanket system with flexible probe, Harvard Apparatus, UK). A pulse oximeter sensor (FootClip™, Starr Life Sciences Corps, UK) was attached on the left hind foot for intraoperative non-invasive measurements of heart rate, respiration rate and arterial oxygen saturation (MouseOx®, Starr Life Sciences Corp, UK).

Surgical fields were prepared in the neck, tail, right groin and buttock area by shaving and cleansing with povidone-iodine (Vetasept®, Animalcare, UK). Animal was covered in sterile drape and surgery was performed under sterile conditions.

A 3Fr catheter (Rat FVC, Instech Laboratories Inc, USA) was surgically placed in the left external jugular vein. 2Fr catheter (Mouse JVC, Instech Laboratories Inc, USA) was surgically placed in the right femoral artery and secured with tissue glue (Indermil® xfine, Henkel, Ireland). Both jugular vein and femoral artery catheters were pre-flushed with heparinised saline (10IU/ml) and pin ports (PinPort™, Instech Laboratories Inc, USA) connected to the distal ends of the catheters. Both neck and groin skin incisions were closed with continuous non-absorbable sutures (5-0 Mersilk™ Ethicon, UK). The right femur was exposed by blunt dissection of the muscle bellies of biceps femoris. The tail vein was cannulated using a 22GA peripheral venous catheter (BD Instye™, USA).

After surgery, anaesthesia was converted from isoflurane to an intravenous infusion of alfaxalone (Alfaxan®, Jurox, UK) into the tail vein via a continuous syringe pump (PHD Ultra, Harvard Apparatus, UK). Isoflurane inhalation and 100% oxygen were discontinued, and the facemask was removed. Alfaxalone infusion

started at 20-25 mg/kg/hour and adjusted according to the depth of anaesthesia via monitoring reflexes such as pedal withdrawal. In the experiment phase, target response was absence of pedal withdrawal reflex and mild cardiovascular response (transient increase in heart rate and or blood pressure) to painful stimuli.

2.2.8. Experiment protocol

2.2.8.1. Injury phase

2.2.8.1.1. Blast injury

Thoracic blast injuries were produced using a compressed air blast wave generator [415]. Release of the solenoid-controlled valve discharged compressed air from the pressure reservoir onto an aluminium disc, which ruptured at high pressure to generate a blast wave. The magnitude of blast wave exposure was controlled by adjusting the distance between the rupturing disc and the target. In this experiment, the exposure distance was set at 3 cm from the end of the blast nozzle to the target marked on the right chest (mid point between right tip of scapula and point of elbow whilst rat in left lateral recumbent position). Consistency of blast load was checked prior to each experiment, using a piezoelectronic pressure transducer, amplifier and data collection system, as described by Jaffin *et al* [415]. Anaesthetic level was deepened transiently prior to blast exposure.

2.2.8.1.2. Tissue injury

Two minutes after blast or sham blast exposure, after checking the depth of anaesthesia is adequate, a single transverse fracture was created at mid-femur using surgical scissors via the incision made during the surgical preparation.

2.2.8.1.3. Haemorrhage

Five minutes after blast or sham blast, haemorrhage was initiated by controlled withdrawal of blood via a previously inserted vascular cannula at a rate of 1.2 ml/kg/min to remove 30% estimated blood volume[6]. Blood was collected in syringes preloaded with citrate phosphate dextrose (CPD)[7] to prevent coagulation, and stored at room temperature for reinfusion later in the protocol.

2.2.8.2. Resuscitation phase

After the end of haemorrhage, the resuscitation phase began. The first 90 minutes of resuscitation represented pre-hospital resuscitation, where animals remained hypotensive. A target blood pressure of approximately 45 mmHg was maintained using normal saline infusion capped at maximum volume of 14.286 µl/g[8]. Once all the saline had been administered, the target blood pressure was then maintained by infusion of a colloid solution (Gelofusine®, capped at 14.286 µl/g). Use of colloid at this stage of the protocol was rare (Table 4). Conversely, animals that showed strong auto-resuscitation (restoration of blood pressure higher than 20 mmHg above the target without need for resuscitation fluid) were subjected to further withdrawal of blood in 0.1 ml aliquots to attain the hypotensive target.

After 90 minutes, the resuscitation target was revised to reflect a more aggressive in-hospital resuscitation using blood[9] up to a volume equivalent to 40% of each rat's estimated pre-haemorrhage blood volume. A disposable 18 micron blood

[6] Total blood volume estimated as 6.06ml/100g body weight 416. Heath, D.F., *The effect of scald injury upon the distribution of glucose between red cells and plasma and upon the turnover of glucose in red cells in the rat.* Br J Exp Pathol, 1973. **54**(4): p. 359-67.
[7] CPD from blood collection bags (RCB434CCL; Pall Medical, Portsmouth, UK).
[8] Equivalent to 1L per 70kg.
[9] Whole blood with Gelofusine® ratio 3:1 to increase the volume from 30% to 40% estimated original blood volume.

filter (Hemo-nate® Filter, Utah Medical Products Ltd, USA) was used to remove any particulate debris prior to infusion. After all the blood had been administered, maintenance fluid using Gelofusine® (8 ml/kg/hour) was given until the end of the experiment (six hours from the start of resuscitation).

	Simvastatin	Placebo
Sham blast	2/16	4/15
Blast injury	2/7	0/7

Table 4 Number of animals given all the permissible saline and some colloid resuscitation/total number of animals in the group during the pre-hospital resuscitation phase.

2.2.9. Physiological monitoring

Arterial blood pressure was measured continuously using a strain gauge manometer (Senso-Nor 844, Senso-Nor, Norway), and recorded continuously using a computerised data acquisition system (MacLab/8s, ADInstruments, New Zealand) and Chart software (Chart version 4.2.3, ADInstruments, New Zealand). Oxygen saturation (SpO_2) and heart rate were displayed using pulse oximetry as previously described earlier.

2.2.10. Blood sampling

Aliquots of 0.15 ml arterial blood were collected anaerobically for blood gas monitoring (GEM3500, Instrumentation Laboratory, USA) and aliquots of 0.25 ml arterial blood were collected for inflammatory mediators and simvastatin assays (Table 5). The sample volume was replaced with normal saline after each sampling, except in the surgery control group where Gelofusine® was used.

Blood samples for inflammatory mediators and simvastatin assays were immediately transferred to citrate coated microcentrifuge tubes (Teklab, UK) and subsequently centrifuged in at 16.2 x g for 5 minutes at room temperature

(Heraeus™ Pico™, Thermo Scientific, USA). After centrifugation, the supernatant was extracted and stored in cryogenic tubes (Nalgene™, Thermo Scientific, USA) at -80^{o}C for offline batch analysis. Samples for imaging flow cytometry were collected in EDTA tubes (K2EDTA, Teklab, UK) (see section 2.2.17.1).

Time point (min)	Arterial blood gas (0.15 ml)	Inflammatory mediators assay (0.25 ml)	Imaging flow cytometry (1 ml)	Simvastatin assay (0.25 ml)	Total sample volume (ml)
Pre-blast	Yes	Yes			0.40
Pre-HGE	Yes				0.15
R0	Yes				0.15
R30	Yes				0.15
R60	Yes				0.15
R90	Yes	Yes			0.40
R120	Yes				0.15
R180		Yes			0.25
R240	Yes				0.15
R360	Yes	Yes	Yes	Yes	1.65

Table 5 Experiment blood sampling schedule.
HGE, Haemorrhage; R, Resuscitation; Rx, x minutes of resuscitation. An additional 0.1ml was taken at pre-blast and R360 and placed in PAXgene® Blood RNA tubes for alter analysis by QMUL (see Annex A).

2.2.11. Humane killing

Animals were killed humanely at the end of the experiment with an overdose of 1ml pentobarbital sodium 20%v/v (JML, UK).

2.2.12. Post-mortem examination

A *post-mortem* (PM) examination was conducted immediately after death. Macroscopic appearances of internal organs were recorded, particularly the degree of blast injury to the lungs. Samples for histology samples were fixed in 10% formalin solution (Formaldehyde 4% aqueous solution, VWR International, USA) or in Bouin's solution (Bouin's solution, Sigma-Aldrich®, USA) and stored at room temperature. In addition, tissue samples were snap frozen in liquid nitrogen. The

snap frozen samples were placed in tissue processing cassettes (Histosette® I, Simport, Canada), dropped in liquid nitrogen and stored at -80°C. Tissue samples for downstream RNA extraction were each stored in cryogenic tubes with 1 ml RNAlater® (Sigma-Aldrich®, USA) stored at 4°C overnight before being transferred to -80°C for long-term storage. The PM tissue samples are summarised in Table 6.

	Formaldehyde	**Bouin's**	**Fresh frozen tissue**	**RNA later®**
Small bowel	Yes		Yes	Yes
Kidney	Yes	Yes	Yes	Yes
Liver	Yes	Yes	Yes	Yes
Spleen			Yes	
Heart			Yes	
Lung	Yes	Yes	Yes	Yes

Table 6 Tissue sampling and fixatives in post-mortem.

2.2.13. Inflammatory mediators

Plasma levels of inflammatory mediators were assessed using a range of techniques such as multiplexed immunoassay and enzyme linked immunosorbent assay (ELISA).

2.2.13.1. ELISA

HMGB1 plasma levels were analysed using a commercially available sandwich-enzyme immunoassay (HMGB1 ELISA, IBL International, Germany). Sample preparation and storage conditions were described in section 2.2.10.

The protocol was performed in accordance with the manufacturer's instructions. In brief, all reagents were allowed to reach room temperature. 100 µl of diluent buffer (0.01% NaN_3) was added to each well on the antibody-coated (anti-HMGB1 polyclonal antibody) 96-well microtiter plates. Preparation of positive control and serial dilutions of standard were also performed in accordance with the manufacturer's instructions. 10 µl of diluent buffer, standards, positive control and

each plasma sample were pipetted in duplicate into the respective wells of the microtiter plates. The plates were covered with adhesive foil and incubated for 20-24 hours at 37^{o}C to allow specific binding of analytes to the immobilised antibodies. The incubation solution was discarded afterwards and the plates were washed five times using 400 µl wash buffer [1X; prepared in phosphate buffered saline (PBS)-Tween 20]. 100 µl enzyme conjugate (peroxidase-linked anti-HMGB1,2 monoclonal antibody) was pipetted into each well and was allowed to incubate for two hours at 25^{o}C. The incubation solution was discarded and the plates were washed as described earlier. 100 µl of colour solution (3,3', 5,5'-Tetramethylbenzidine) was added into each well for detection and incubated for 30 minutes at room temperature. The colour reaction was blocked by adding 100 µl of stop solution (0.35 M H_2SO_4) into each well, which produced a noticeable colour change from blue to yellow. Optical density measurements were read using a photometer at 450 nm (Multiskan Ascent 354 microplate reader, Thermo Labsystems, Finland) and data acquisition software (Ascent™ software version 2.6, Thermo Labsystems, Finland). The concentration of HMGB1 was determined using comparison to 4-parameter logistic standard curve (normal range 0 – 80 ng/ml). When samples had HMGB1 concentrations above the most concentrated samples, the assay was repeated on diluted (in diluent buffer) plasma samples. The limit of detection for this assay is 1 ng/ml.

2.2.13.2. Multiplexed Immunoassay

Levels of plasma cytokines and chemokines were analysed using a commercially available Luminex MAP® technology kit (Milliplex MAP Rat cytokine/chemokine magnetic bead panel, Merck Millipore, Germany). This allows

the simultaneous measurement of 27 mediators from a single sample. See Table 7 for a list of analytes and minimal detection values for this assay.

Sample preparation and storage conditions were described in section 2.2.10. The analysis protocol was performed in accordance with the manufacturer's instructions. In brief, all reagents were allowed to reach room temperature. 200 µl of assay buffer was added to each well of a 96-well plate which was subsequently agitated at room temperature for ten minutes before assay buffer was removed. Preparation of positive control, serum matrix and serial dilutions of standard were completed according to the manufacturer's instructions. 25 µl of standards and positive control were added in duplicates to the appropriate wells in duplicate. 25 µl of serum matrix was added to the standard and control wells. For the sample wells, 25 µl assay buffer and 25 µl of sample (1:2 dilution in assay buffer) were added.

Rat cytokine/chemokine antibody-immobilised premixed magnetic beads were vortexed for one minute, and 25 µl of beads were pipetted into each well. The plates were sealed in foil and incubated on a plate shaker at room temperature for two hours, to allow specific binding of the antibodies with target analytes. Plates were washed twice using 200 µl wash buffer (60 ml 10X wash buffer with 540 ml deionized water) on magnetic plate carrier (Bio-Plex™ Pro Wash Station, Bio-Rad, USA), to stop the beads (and therefore cytokines) being removed during the wash steps. 25 µl of biotin-labelled detection antibodies was added to each well, and the plates were sealed in foil and incubated on a plate shaker for one hour at room temperature. 25 µl of reporter dye (streptavidin-phycoerythrin) was added to each well, followed by a final incubation at room temperature on a plate shaker for 30 minutes. The plates were washed twice using 200 µl wash buffer on a magnetic plate carrier. The wash buffer was completely removed, and 125 µl of sheath fluid

was added to all wells. The plate was shaken for five minutes to resuspend the beads.

The plates were then read immediately (Bio-Plex™ 200 system, Bio-Rad, USA). Median fluorescent intensity was analysed using data acquisition software (Bio-Plex Manager™ Software version 6.0, Bio-Rad, USA). Analyte concentrations from sample wells were calculated using 5 parameter logistic curve fitting method.

Analyte	MinDC (pg/ml)	Analyte	MinDC (pg/ml)
G-CSF	1.8	IFNγ	6.2
Eotaxin (CCL11)	3.2	IL-5	7.4
GM-CSF	6.8	IL-17A	2.3
IL-1α	4.2	IL-18	6.2
Leptin	10.2	MCP-1 (CCL2)	9.0
MIP-1α (CCL3)	0.8	IP-10 (CXCL10)	1.4
IL-4	3.1	GRO/KC (CXCL1)	19.7
IL-1β	2.8	VEGF	2.6
IL-2	5.4	Fractalkine (CX3CL1)	0.7
IL-6	30.7	LIX (CXCL5)	20.9
EGF	0.3	MIP-2 (CXCL2)	11.3
IL-13	2.4	TNF-α	1.9
IL-10	2.7	RANTES (CCL5)	1.3
IL-12p70	3.3		

Table 7 List of analytes and their minimal detection concentration (MinDC) for Milliplex MAP Rat cytokine/chemokine magnetic bead panel[10].

2.2.14. Gene expression analysis

Tissue samples (Table 6) collected in RNAlater® were processed in batches for RNA extraction, before quantification via quantitative reverse transcription polymerase chain reaction (RT-qPCR) using commercially available pathway-specific arrays (Rat Inflammatory Responses & Autoimmunity RT^2 Profiler PCR Array and Rat Apoptosis RT^2 Profiler PCR Array, Qiagen®, USA). Each 96-well plate

[10] Available from manufacturer's protocol supporting documentation.

allowed simultaneous analysis of 84 different genes (Table 8). A further customised array panel (Qiagen®, USA) assessed 7 additional genes (HIF1a, Vcam1, Nos2, Nos3, Icam1, Pecam1, Thbd).

2.2.14.1. RNA isolation

Total RNA was extracted from tissue samples using the commercially available RNeasy® Mini kit (Qiagen®, Germany) with an additional phenol-chloroform extraction step. In brief, tissues stored in RNAlater® (see section 2.2.12 for post-harvest preparation and storage) were disrupted and homogenized (TissueRuptor®, Qiagen®, USA) in lysis reagent (QIAzol Lysis Reagent, Qiagen®, Germany). Chloroform was added to the lysate forming a biphasic emulsion, which after centrifugation at 10,000 x g for 18 minutes at 4^{o}C, separated into the upper hydrophilic component (inorganic phase containing DNA and contaminants) and the lower hydrophobic layer (organic phase). The upper aqueous phase was pipetted off carefully and kept, whilst the phenol-chloroform solid waste was discarded. An equal amount of ethanol was added to the supernatant and this was used for the standard RNeasy Mini kit protocol as per the manufacturer's instructions. On-column DNAse digestion (RNase-free DNase set, Qiagen®, Germany) removed any residual DNA contamination.

RNA purity and concentration (ng/µl) was measured using a spectrophotometer (Nanodrop® 1000, Thermo Scientific, USA) after extraction. The ratio of sample absorbance at 260 and 280 nm (260/280) and at 260 and 230 nm (260/230) gave acceptable thresholds of purity (greater than 1.8 and greater than 1.7, respectively). RNA integrity was assessed using the Agilent RNA 6000 Nano Kit and Agilent 2100 Bioanalyzer System (Agilent Technologies, USA) based on the

principles of gel electrophoresis. Using an algorithm based on the size of the rRNA bands, a RNA Integrity Number (RIN) was generated for each analysis; RIN of more than 7 was accepted.

2.2.14.2. RNA quantification

2.2.14.2.1. cDNA synthesis

The first step in mRNA quantification was cDNA synthesis using the RT^2 First Strand kit (Qiagen®, USA) according to the manufacturer's instructions. In brief, RNA (5 µg) sample was mixed with Buffer GE (2 µl) to create the genomic DNA elimination mix (total volume 10 µl) and incubated for 5 minutes at 42^{o}C (Applied Biosystems® 2720 Thermal cycler, Life Technologies, USA), followed by cooling on ice for at least one minute. This eliminated any genomic DNA present prior to reverse transcription (RT). Next the reverse-transcription mix (10 µl), containing a reverse transcriptase, random hexamers and Oligo dT primers, was added to the genomic DNA elimination mix and incubated at 42^{o}C for 15 minutes and 95^{o}C for 5 minutes to terminate the enzyme reaction. The reverse-transcription mix contained an external RNA control to check the efficiency of the RT reaction. RNase-free water (91 µl) was added to the final mixture, the cDNA synthesis reaction was stored at -20^{o}C or progressed immediately to the RT-qPCR protocol.

2.2.14.2.2. RT-qPCR protocol

RT-qPCR was performed using RT^2 profiler PCR arrays as per the manufacturer's instructions. The PCR components mix was prepared with RNase-free water (1248 µl), RT^2 SYBR Green master mix (1350 µl) (Qiagen®, USA) and cDNA synthesis reaction (102 µl). 25 µl of the PCR components mix was distributed

into each well of the RT^2 profiler PCR array using 8-channel pipette (new pipette tips were used for each column to prevent cross contamination of the wells). The array was sealed with optical strips and centrifuged at 1000 x g for 1 minute at 20^{o}C (Allegra^{TM} 21R centrifuge, Beckman Coulter, USA) to remove any bubbles. The real-time cycler (Applied Biosystems PRISM® 7000 Sequence Detection System, ThermoFisher Scientific, USA) was set as per Table 9 for the amplification process.

Threshold cycle (C_t) was calculated for each well by data acquisition software (Applied Biosystems PRISM® 7000 Sequence Detection System software version 1, ThermoFisher Scientific, USA). Baseline was manually adjusted to between cycles 6 and 10, and threshold was set at 1 Delta Rn for all arrays. Cq (C_t) values were exported via Excel. Three positive PCR controls, a genomic DNA control and three reverse-transcription controls served as quality control in each array (see Table 10). Where indicated, plates not meeting the quality control requirements were either repeated or validated using "minus RT control"[11].

Cq values were uploaded onto quantitative PCR data analysis programme (qbase+, Biogazelle, Belgium). geNorm algorithm was used to check the stability of the housekeeping genes on the panels. A global mean normalisation strategy was adopted when no three or more housekeeping genes were suitable on the panel (B De Craene 2017, personal communications). Average Cq was determined as arithmetic mean, and scaled to Group 1 (surgical control). Normalised relative quantities (NRQ) values were generated for each target gene from each sample by qbase+. NRQ were exported via excel, and since NRQ is a log-normal distribution, the geometric mean of the group was calculated for each gene. The geometric

[11] To test for genomic DNA contamination present in the extracted RNA samples, the reverse transcription step was carried out in the absence of reverse transcriptase, this was called the minus RT control.

mean is 1 for surgical control, so the geometric mean of injured groups was expressed as a ratio (fold change). Genes were down-selected from the arrays for statistical analysis if geometric mean is ≥3 or ≤ 0.33.

Genes on apoptosis panel				Genes on inflammatory response panel			
Abl1	Birc5	Cycs	Polb	Bcl6	Ccr2	Ifnγ	Lta
Aifm1	Bnip2	Dad1	Prdx2	C3	Ccr3	Il10	Ltb
Akt1	Bnip3	Dapk1	Prlr	C3ar1	Ccr4	Il10rb	Ly96
Anxa5	Bok	Dffa	Pycard	C4a	Ccr7	Il17a	Myd88
Apaf1	Card10	Dffb	Ripk2	Ccl1	Cd14	Il18	Nfkb1
Api5	Casp1	Diablo	Sphk2	Ccl11	Cd40	Il1a	Nos2
Aven	Casp12	Fadd	Tnf	Ccl12	Cd40lg	Il1b	Nr3c1
Bad	Casp14	Faim	Tnfrsf10b	Ccl17	Cebpb	Il1r1	Ptgs2
Bag1	Casp2	Fas	Tnfrsf11b	Ccl19	Crp	Il1rap	Ripk2
Bak1	Casp3	Faslg	Tnfrsf1a	Ccl2	Csf1	Il1rn	Sele
Bax	Casp4	Gadd45a	Tnfrsf1b	Ccl20	Cxcl1	Il22	Tirap
Bcl10	Casp6	Hrk	Tnfsf10	Ccl21	Cxcl10	Il23a	Tlr1
Bcl2	Casp7	Il10	Tnfsf12	Ccl22	Cxcl11	Il23r	Tlr2
Bcl2a1	Casp8	Lta	Tp53	Ccl24	Cxcl2	Il5	Tlr3
Bcl2l1	Casp8ap2	Ltbr	Tp53bp2	Ccl25	Cxcl3	Il6	Tlr4
Bcl2l11	Casp9	Mapk1	Tp63	Ccl3	Cxcl5	Il6r	Tlr5
Bcl2l2	Cd40	Mapk8ip1	Tp73	Ccl4	Cxcl9	Il7	Tlr6
Bid	Cd40lg	Mcl1	Tradd	Ccl5	Cxcr2	Cxcr1	Tlr7
Bik	Cflar	Naip6	Traf2	Ccl6	Cxcr4	Il9	Tnf
Birc2	Cidea	Nfkb1	Traf3	Ccl7	Faslg	Itgb2	Tnfsf14
Birc3	Cideb	Nol3	Xiap	Ccr1	Fos	Kng1	Tollip

Table 8 Genes analysed on real-time quantitative polymerase chain reaction (RT-qPCR) array panels.

Cycles	Duration	Temperature
1	10 minutes	95°C
40	15 s	95°C
	1 min	60°C

Table 9 Cycling conditions for amplification as per manufacturer's instructions.

Control	Accepted values
Positive PCR control (PPC)	Average C_t^{PPC} 20 ± 2 on each array
Genomic DNA control (GDC)	C_t GDC > 35
Reverse transcription control (RTC)	ΔC_t = AVG C_t^{RTC} – AVG C_t^{PPC} ΔC_t <5

Table 10 RT2 Profiler PCR Array quality control.

2.2.15. Gene expression profiling

Additional gene expression profiling analysis of the model was performed at Queen Mary University of London. Methodology can be found in the report (Annex A). The data generated from this collaboration will be used in the discussion to support the results from the analysis done in-house.

2.2.16. Protein analysis

Fresh frozen tissues (Table 6) collected from *post-mortem* were processed in batches for protein analysis. Tissue preparation and storage conditions were described in section 2.2.12.

2.2.16.1. Total protein extraction

Tissue samples were weighed prior to being homogenized (TissueRuptor®, Qiagen®, USA) at room temperature in appropriate amounts of cell lysis buffer (20 ml per 1 g, T-PER® tissue protein extraction reagent, Thermo Scientific, USA) and protease inhibitors (10 µl per 1 ml lysis buffer, Halt protease inhibitor cocktail EDTA-free, Thermo Scientific, USA). Samples were centrifuged (Centrifuge 5417R, Eppendorf, Germany) at 10,000 x g for 5 minutes at room temperature. The supernatant was extracted and stored in aliquots using Eppendorf safe-lock tubes (Eppendorf, Germany) at -80^{o}C.

2.2.16.2. Total protein quantification

Total protein concentration was determined by colorimetric detection of cuprous cation using commercially available bicinchonimic acid assay (Pierce BCA protein assay kit, Thermo Scientific, USA). In brief, the samples and reagent were

allowed to equilibrate to room temperature. Standards and working reagent were prepared according to the manufacturer's protocol. The samples were diluted with PBS in the following ratios; liver 1:10, kidney and small bowel 1:5. 25 µl of standards and samples were pipetted into duplicate wells of a 96-well microtiter plate, and 200 µl of working reagent into each well. The plate was incubated at 37^{o}C for 30 minutes, and cooled to room temperature before absorbance measurements were read using a photometer at 562 nm (Multiskan Ascent 354 microplate reader, Thermo Labsystems, Finland) and data acquisition software (Ascent™ software version 2.6, Thermo Labsystems, Finland). Total protein concentration was determined using comparison to 4-parameter logistic standard curve (range 0 – 2000 µg/ml) and multiplied by relevant dilution factor.

2.2.16.3. Tissue proteins ELISA

2.2.16.3.1. Tumour Necrosis Factor-alpha (TNF-α) and Interleukin-6 (IL-6)

Liver TNF-α and IL-6 were analysed using commercially available sandwich-enzyme immunoassay (Legend Max™ Rat TNF-α ELISA kit with pre-coated plate and Legend Max™ Rat IL-6 ELISA kit with pre-coated plate, Biolegend, USA). Sample preparation and storage conditions are described in sections 2.2.12, 2.2.16.

The assay protocol was performed in accordance with the manufacturer's instructions. In brief, all reagents were allowed to reach room temperature. All protein samples concentrations were adjusted to 7000 µg/ml, by adding an appropriate amount of cell lysis buffer and protease inhibitor solution. Preparation of positive control and serial dilutions of standard were performed according to the manufacturer's instructions. 96-well microtiter plates were washed four times using 350 µl wash buffer. 50 µl of assay buffer was added to each well that contained

either standard dilutions or samples. 50 µl of standard dilutions or protein samples were pipetted in duplicate into the respective wells of the microtiter plates. The plates were sealed and incubated for 2 hours at room temperature while shaking at 200 rpm, to allow specific binding of analytes to the immobilised antibodies. Incubation solution was discarded afterwards and plates were washed as previously described. 100 µl detection antibody solution was pipetted into each well and allowed to incubate for 1 hour at room temperature while shaking at 200 rpm. The incubation solution was discarded, and the plates were washed as described earlier.

100 µl of Avidin-HRP solution was added into each well for colorimetric detection and incubated for 30 minutes at room temperature while shaking at 200 rpm. The incubation solution was discarded and plates were washed as described earlier with the exception of soaking for 1 minute between each wash to minimise the background. 100 µl of substrate solution was added to each well and the plate was incubated in the dark for 10 minutes (IL-6) or 15 minutes (TNF-α). The colour reaction was blocked by adding 100 µl of stop solution (hydrochloric acid) into each well, which produced a noticeable colour change from blue to yellow. Optical density measurements of the samples were read using a photometer at 450 nm (Multiskan Ascent 354 microplate reader, Thermo Labsystems, Finland) and data acquisition software (Ascent™ software version 2.6, Thermo Labsystems, Finland). The concentration of IL-6 or TNF-α was determined using comparison to 5-parameter logistic standard curve (IL-6 range 0 – 1200 pg/ml, TNF-α range 0 – 500 pg/ml). The limit of quantification for IL-6 is 5.3 pg/ml and 4.2 pg/ml for TNF-α.

2.2.16.3.2. Heme oxygenase-1 (HO-1)

HO-1 in liver, small bowel and kidney were analysed by sandwich-enzyme immunoassay. Sample preparation and storage conditions were described in sections 2.2.12, 2.2.16. Protein samples were made to the following concentrations by adding an appropriate amount of cell lysis buffer and protease inhibitor solution: liver 7000 µg/ml, kidney to 3000 µg/ml and small bowel 2500 µg/ml. The protocol was optimised from Abcam matched pair antibodies protocol.

96-well microtiter plates (Immunlon® 2HB flat bottom MicroTiter® plates, Thermo Scientific, USA) were coated with 100 µl per well of 2.5 µg/ml anti-heme oxygenase-1 antibody (ab13248, Abcam, UK) in 100 mM carbonate coating buffer (3.03 g Na_2CO_3, 6.0 g NaHCO3 make up to 1000 ml with distilled water adjusted to pH 9.6). The plates were incubated overnight at 4^{o}C to allow absorption of the capture antibody. The plates were washed three times with wash buffer (PBST - 0.1% v/v Tween 20 in Phosphate Buffered Saline) 300 µl per well. 150 µl of blocking buffer (2% w/v bovine serum albumin in PBST) was added to each well and incubated at room temperature for one hour. Blocking buffer was aspirated from the wells.

Standard dilutions were prepared using recombinant human heme oxygenase 1 protein (ab85243, Abcam, UK) diluted in blocking buffer to the following concentration: 2000 ng/ml, 500 ng/ml, 125 ng/ml, 31.25 ng/ml, 7.8 ng/ml, 1.95 ng/ml and 0.4875 ng/ml. 50 µl of blocking buffer, standard dilutions and samples were pipetted into relevant wells in duplicates, and incubated for one hour at room temperature to allow target analyte binding to immobilised antibody. Protein solution was removed by washing the plates as previously described. 50 µl of detector antibody (ab13243, Abcam, UK) at 0.5 µg/ml was added to each well and incubated

for an hour at room temperature. The plates were washed to remove detection antibody solution.

100 µl of Conjugate secondary antibody (goat anti-rabbit IgG (H+L) secondary antibody HRP conjugate, ThermoFisher Scientific, USA), diluted 1:10000 in blocking buffer, was added to each well and incubated for an hour at room temperature. Detector antibody solution was removed by plate washing. 50 µl of tetramethylbenzidine peroxidase substrate (1-Step™ Ultra TMB-ELISA substrate solution, ThermoFisher Scientific, USA) was added to each well and allowed to incubate for 20-25 minutes. The reaction was stopped by adding 50 µl of 0.25M sulfuric acid to each well. Optical density measurements of the samples were read using a photometer at 450 nm (Multiskan Ascent 354 microplate reader, Thermo Labsystems, Finland) and data acquisition software (Ascent™ software version 2.6, Thermo Labsystems, Finland). The concentration of HO-1 was determined using comparison to 5-parameter logistic standard curve (range 1 – 2000 ng/ml).

2.2.17. Imaging flow cytometry

2.2.17.1. Antibodies incubation

A method for imaging flow cytometry of CECs in human blood has been described by Samsel *et al* [417] and formed the basis for development of this protocol. Antibodies were titrated on blood samples from pilot animals, spiked with commercial rat aortic endothelial cells[12] (RAOECs, ECACC, Salisbury, UK) in the case of CD146. Sample preparation for immunophenotyping started immediately once the terminal samples were taken. 1 ml of blood was pipetted into flow cytometry tube (BD Falcon™ round bottom polystyrene tube, BD Biosciences, USA).

[12] 1 x 10^5 RAOECs in 1 ml of blood.

10 µl of 0.5 mg/ml purified mouse anti-rat CD32 (BD Pharmingen™, BD Biosciences, USA) was added to the sample for 'blocking' and incubated for 5 minutes at room temperature.

The following antibodies were added to the sample (Table 11):

Antibody	Volume	Concentration	Manufacturer
CD45-FITC	80 µl	0.5 mg/ml	BD Pharmingen™, BD Biosciences, USA
CD146-PE	480 µl	neat	R&D Systems
CD3-APC	100 µl	0.2 mg/ml	BD Pharmingen™, BD Biosciences, USA

Table 11 Antibodies added during immunophenotypic staining of CECs.

240 µl of flow buffer (constituted from PBS and 0.1% w/v bovine serum albumin) was added to the sample and mixed at 4^{o}C (HulaMixer® Sample Mixer, Life Technologies™, USA) for 45 minutes. The mixture was then centrifuged at 300 x g for 10 minutes at room temperature (Heraeus™ Megafuge™ 16 Centrifuge Series, Thermo Scientific, USA). The supernatant was removed carefully using a pipette. Lysis buffer (Lysing Solution 10x Concentrate, BD FACS™, BD Biosciences) was diluted to 1:10 in water to make a final concentration of formaldehyde 1.5%. 2 ml of diluted lysis buffer was added to the pellet and incubated at room temperature with the occasional vortex (3 times). The cell pellet was then washed twice in 2 ml of flow buffer. 250 µl of flow buffer was added to re-suspend the cell pellet for storage at 4^{o}C overnight. Data was collected from single colour (e.g. CD45 only, CD3 only and CD146 only) controls and used to create a compensation matrix that was applied to all subsequent samples.

2.2.17.2. Gating strategies

Imaging flow cytometry was conducted the next day, if this was not possible then samples were left for another 24 hours such as all samples were analysed within 2 days. Images were captured using ImageStream^{X} Mark II (Amnis Corporation, USA) and data acquisition via INSPIRE® Software (Amnis Corporation, USA). Data analysis was performed using IDEAS® Software (Amnis Corporation, USA). A minimum of 500,000 nucleated events (cells) were collected for each animal. DAPI (4',6-diamidino-2-phenylindole) was used for nuclear staining at 1 µg/ml. Gating strategies for different cell types are illustrated in Figure 15 - Figure 17.

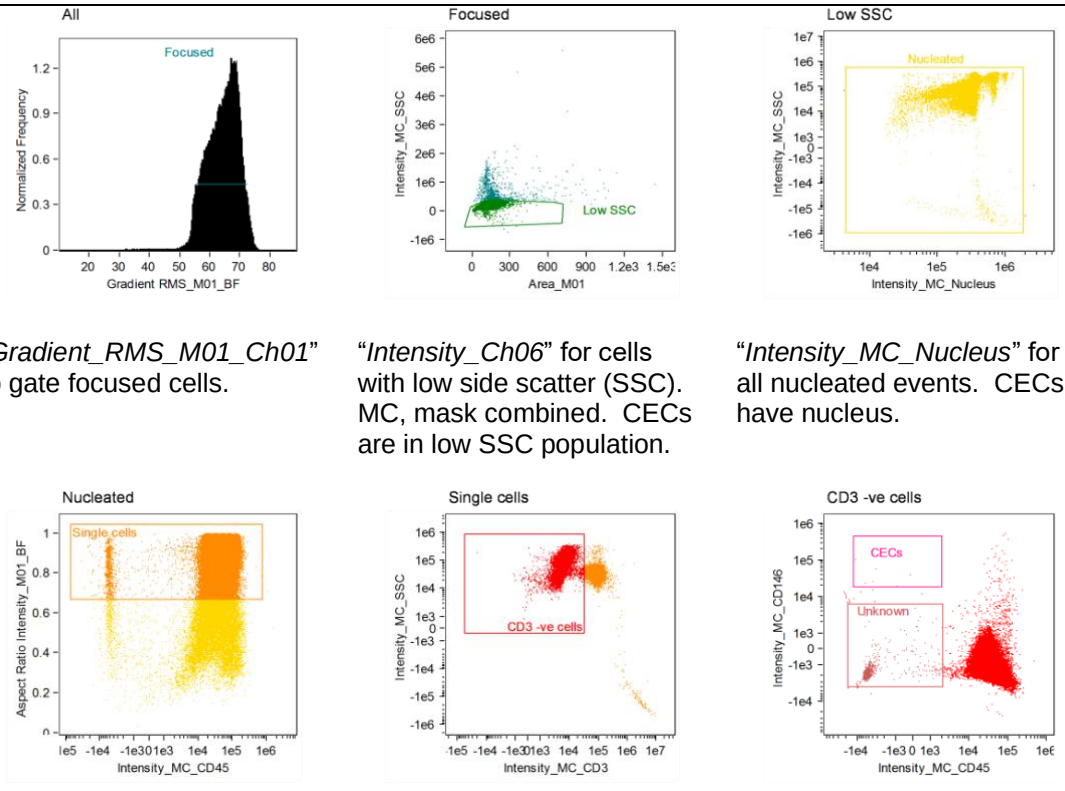

"*Gradient_RMS_M01_Ch01*" to gate focused cells.

"*Intensity_Ch06*" for cells with low side scatter (SSC). MC, mask combined. CECs are in low SSC population.

"*Intensity_MC_Nucleus*" for all nucleated events. CECs have nucleus.

"*Intensity_CD45 vs Aspect_Ratio_M01_BF*" for single cell events. BF, Brightfield.

"*Intensity_MC_CD3 vs Intensity_SSC*" to remove CD3+ cells for CD3- population. T-cells are CD3+ and are removed.

"*Intensity_CD45 vs Intensity_CD146*" to remove CD45+ events for CECs. Unknown, CD45- and CD146- population. CECs are CD45- and CD146+.

Figure 15 Gating strategy for circulating endothelial cells (CECs).

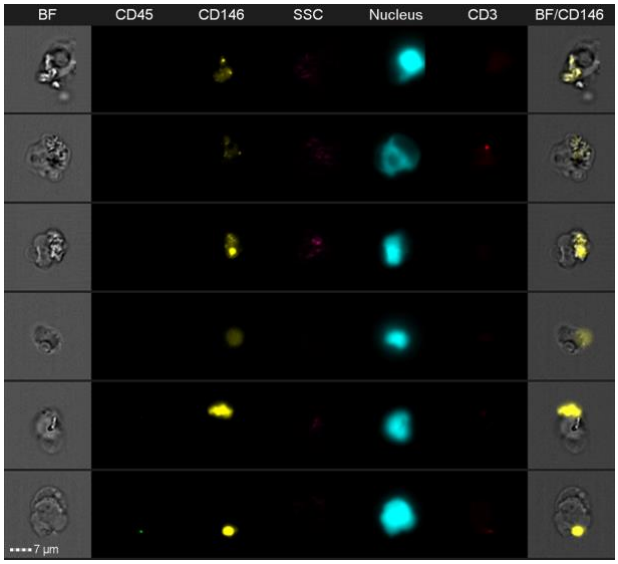

Figure 16 Circulating endothelial cells (CEC), CD3-, CD45- and CD146+.

Apoptotic cells

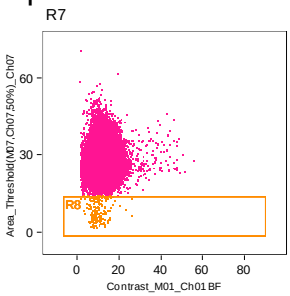

Nuclear fragmentation was measured in all nucleated events using the contrast of the BF imagery along with the area of the 50% brightest pixels in the nucleus. When apoptotic cell nucleus undergoes fragmentation, these can be seen as bright spots in the nuclear channel of the ImageStream^{x}, as well as becoming darker in the BF channel. Population of cells with low nuclear area and contrast was defined as apoptotic cells. Further breakdown of cell types amongst apoptotic events was not performed.

Granulocytes

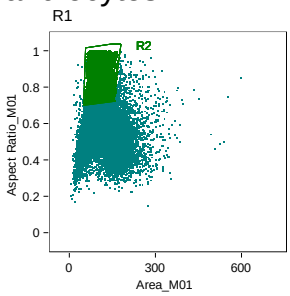

R2: Single cell events.

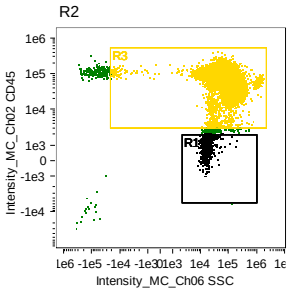

R3: CD45 positive cells.

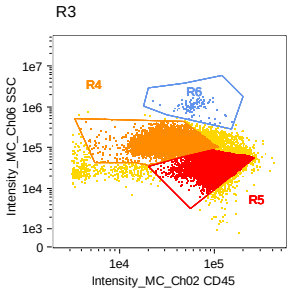

High side scatter and low CD45 expression for granulocytes (R4). Granulocytes are cells with high SCC and low CD45.

Neutrophils

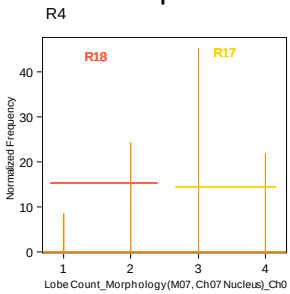

Neutrophils were identified from the granulocyte population using the lobe count feature. Any cell with 3 or 4 lobes in its nucleus is deemed to be a neutrophil (R17)

Figure 17 Gating strategies for apoptotic cells, granulocytes and neutrophils.

2.2.18. Histology

See Table 6 for sampling, fixatives and storage. Paraffin wax-embedded tissues were microtomed to thickness of 4-5 microns and stained with haematoxylin and eosin before assessment under light microscopy by Envigo CRS Ltd, Suffolk,

UK. Samples were subjectively assessed for the presence of oedema, inflammatory cell infiltration and haemorrhage. Each incidence was reported by the pathologist as mild, moderate or severe.

2.2.19. Simvastatin Assay

The plasma concentration of simvastatin and its active metabolite simvastatin hydroxy acid were measured using liquid chromatography triple quadrupole tandem mass spectrometry (LC-QQQ-MS) to quantify successful dosage of simvastatin and its bioactivity. The quantification limit of simvastatin and simvastatin hydroxy acid range from 5 ng/ml to 100 ng/ml. The analysis was developed and performed by the UKAS Analytical Chemistry Laboratory at Dstl Porton Down.

Plasma sample collection and storage is detailed in section 2.2.10. 50 µl of sample plasma was added to 50 µl methanol containing deuterated simvastatin and simvastatin hydroxy acid as internal standard, followed by vortex mixing. 200 µl Methyl-tert-butyl-ether (MTBE) was added to the mixture and centrifuged at 14300 rpm for 5 mins. The supernatant was transferred to a glass tube and dried under a stream of nitrogen at 40^{o}C. The dried samples were reconstituted in 100 µl using 50:50 methanol: water, and filtered using centrifuge filters (PVDF 0.22 µM filter).

Calibration standards of simvastatin and simvastatin hydroxy acid were added to blank rat plasma at 5 ng/ml, 7.5 ng/ml, 10 ng/ml, 50 ng/ml and 100 ng/ml. They were prepared as described above for sample preparation. Analysis was performed using Thermo Scientific Quantum Ultra QQQ with Thermo Accela 1250 HPCL system.

2.2.20. Inclusion and exclusion criteria

Animals must survive to the study endpoint, which is six hours from the onset of resuscitation, therefore any animal that does not survive to the study endpoint is excluded from final data analysis.

2.2.21. Statistical analysis

Test of normality was performed and appropriate transformation was applied if required to normalise the data distribution prior to parametric statistical analysis. Data that proved resistant to transformation to a normal distribution were analysed using appropriate non-parametric tests. Data sets are expressed as mean with standard error of mean (SEM) where the distribution is normal, otherwise as median and interquartile range (IQR). Graphs were drawn using GraphPad Prism and statistical analysis were performed using NCSS. Paired t-test (parametric) or Wilcoxon signed rank matched pair test (non-parametric) were performed as appropriate for paired observations (two time points). Independent t-test (parametric) or Mann-Whitney U test (non-parametric) were used for comparison of independent samples (single time point measurements). One way analysis of variance (ANOVA) for repeated measures over time (parametric) or Friedman's test (non-parametric) were used to compare data within the same group (four time points). Comparison between two groups over three repeated measures over time was done using analysis of co-variance (parametric). Comparison between three independent groups were performed using one-way ANOVA (parametric) or Kruskal-Wallis one-way ANOVA on ranks (non-parametric). Fisher's LSD Multiple Comparison Test or Dunn's test was used for planned *post hoc* comparisons between groups. A *p*-value of less than 0.05 was deemed statistically significant

CHAPTER 3 RESULTS

3.1. Number of animals

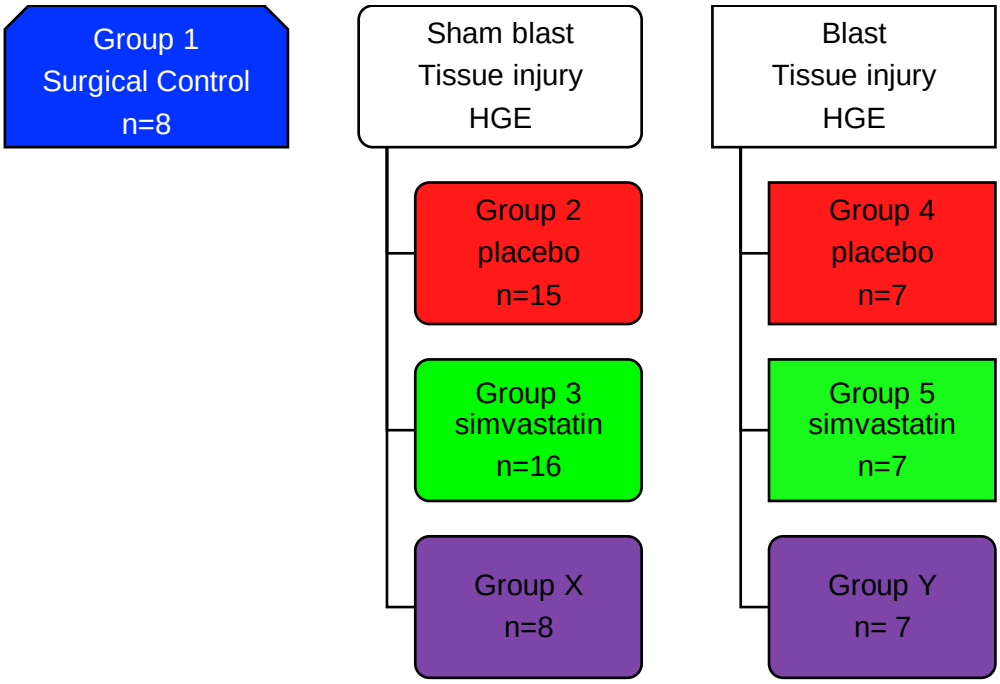

Figure 18 Animal groupings.

114 animals were initially included in the study. 36 animals were excluded from final analysis because they did not survive to the Study Endpoint. Nine animals that survived to the Study Endpoint were excluded due to medical causes that may confound the results, e.g. haematuria and three were excluded for technical reasons such as infusion pump failure. Therefore 68 animals were included in the final analysis (see Figure 18). Group X and Group Y were part of a separate study that shared the control group with this current study, and were treated identically to the placebo groups up till the end of pre-hospital (hypotensive resuscitation) phase. Their results were used in section 3.3.1 as part of the analysis.

3.2. Physiology

3.2.1. Demographics

Baseline values for a range of variables are shown in Table 12 and Table 13. There were no significant differences in baseline values between groups in either sham blast (Table 12) or the blast (Table 13) injury strands, with the exception of the body weights in the sham blast injury strand (P=0.035). *Post hoc* analysis revealed that the statistically significance difference in body weight was between Groups 1 and 2 only (P=0.027). However, this difference in body weight is relatively small and unlikely to have had any impact on the outcome of the study (i.e. it was of no physiological significance).

	Group 1 Surgical control (n=8)	Group 2 Sham blast placebo (n=15)	Group 3 Sham blast simvastatin (n=16)	*P* values
Weight (g)	259±6	244±3	249±2	*0.035*
Body Temperature (^oC)	38.3±0.1	38.3±0.1	38.4±0.0	*NS*
▲*Baseline PaO_2 (kPa)*	10.09±0.49	10.00±0.18	10.28±0.24	*NS*
▲*Baseline $PaCO_2$ (kPa)*	6.43±0.30	6.59±0.11	6.57±0.12	*NS*
▲*Baseline pH*	7.396±0.012	7.391±0.006	7.393±0.005	*NS*
▲*Baseline arterial base excess (mM)*	3.8±0.5	4.3±0.4	4.2±0.4	*NS*
▲*Baseline haematocrit (%)*	39.3±0.5	38.6±0.7	38.3±0.5	*NS*
▲*Baseline glucose (mM)*	8.3±0.2	8.1±0.2	8.3±0.2	*NS*
Baseline mean blood pressure (mmHg)	100.1±4.2	100.0±3.2	100.5±3.1	*NS*
Baseline heart rate (beats/min)	439±10	434±7	440±6	*NS*

Table 12 Baseline values for the sham blast (no blast) injury strand. Data expressed as mean±SEM. ▲1 animal missing from Group 1 for arterial blood gas analysis as it was not possible to obtain arterial samples, therefore for blood gas samples n=7 in Group 1. NS, not statistically significant (P>0.05).

	Group 1 Surgical control (n=8)	Group 4 Blast placebo (n=7)	Group 5 Blast simvastatin (n=7)	*P* values
Weight (g)	259±6	243±3	253±5	*NS*
Body Temperature (^{o}C)	38.3±0.1	38.2±0.1	38.1±0.1	*NS*
▲*Baseline PaO_2 (kPa)*	10.09±-0.49	9.54±0.29	9.62±0.25	*NS*
▲*Baseline $PaCO_2$ (kPa)*	6.43±0.30	6.78±0.17	7.05±0.11	*NS*
▲*Baseline pH*	7.396±0.012	7.384±0.012	7.373±0.008	*NS*
▲*Baseline arterial base excess (mM)*	3.8±0.5	4.4±0.4	4.4±0.6	*NS*
▲*Baseline haematocrit (%)*	39.3±0.5	39.4±0.9	40.3±0.7	*NS*
▲*Baseline glucose (mM)*	8.3±0.2	7.9±0.2	7.7±0.2	*NS*
Baseline mean blood pressure (mmHg)	100.1±4.2	96.0±1.5	110.1±5.3	*NS*
Baseline heart rate (beats/min)	439±10	417±7	440±6	*NS*

Table 13 Baseline values for the blast injury strand.
Data expressed as mean±SEM. ▲1 animal missing from Group 1 for arterial blood gas analysis as it was not possible to obtain arterial samples, therefore for blood gas samples n=7 in Group 1. NS, not statistically significant (*P*>0.05).

3.2.2. Cardiovascular response to injury phase

Sham blast exposure (no blast) did not lead to any significant changes in heart rate or blood pressure (Figure 19). Subsequent haemorrhage (approximately 30% blood volume) led to a significant fall in blood pressure and decrease in heart rate (Figure 19). There was no significant difference between the placebo and simvastatin groups in these cardiovascular parameters (Figure 19). Subsequently, each animal's MBP was maintained at an approximate target of 45mmHg by withdrawal of additional blood (supplementary haemorrhage) and/or limited infusion of saline/Gelofusine® (see sections 2.2.8) until R90. The initial reduction in heart rate from the haemorrhage phase reversed over the course of 90 minutes. The change in HR over time (baseline to R90) was statistically significant (*P*<0.001), but there was no significant difference between Groups 2 and 3 (*P*=0.691). There were

no significant differences in the resulting overall blood volume deficit[13] between Groups 2 and 3 at R90 (Group 2, 35.94±1.33%; Group 3, 38.44±1.28%; *P*=0.185).

Blast exposure led to a brief period of bradycardia (*P*<0.001) and hypotension (*P*<0.001) (Figure 20 and Figure 21), resulting in a significant change in MBP and heart rate (HR) over time. There was a significant difference in MBP between simvastatin/placebo groups (*P*=0.015) but no significant difference in HR (*P*=0.621). *Post hoc* analysis indicated the difference of MBP lay at baseline (*P*=0.031), which was not physiologically significant as the MBP is within normal range in both groups. An apnoea of 21(13) seconds [median (IQR)] was recorded in Group 4 and 22(8) seconds in Group 5 after blast exposure, and there was no significant difference between the two groups (*P*=0.805).

There was a partial recovery in MBP and HR (Figure 21) before haemorrhage commenced. Haemorrhage led to a significant fall over time in blood pressure and increase in HR over time (*P*<0.001and *P*=0.044 respectively) (Figure 21). There were no significant differences between Groups 4 and 5 in these cardiovascular parameters from start of haemorrhage to R90 (*P*=0.966 MBP, *P*=0.497 HR) (Figure 21). The overall blood volume deficit in placebo and simvastatin groups at R90 was similar (Group 4, 39.24+/-1.23%; Group 5, 39.17+/-1.54%; *P*=0.972).

In the absence of haemorrhage and injury, there were no significant changes in MBP or heart rate in Group 1 (*P*=0.383 and *P*=0.406, Figure 19 and Figure 21).

[13] The overall volume deficit was calculated as the original 30% blood volume removed during the initial haemorrhage phase, plus any additional blood taken during the period R0-R90, minus the intravascular portion of any resuscitation fluid given during this phase. For more detail see section 2.2.8.1.3.

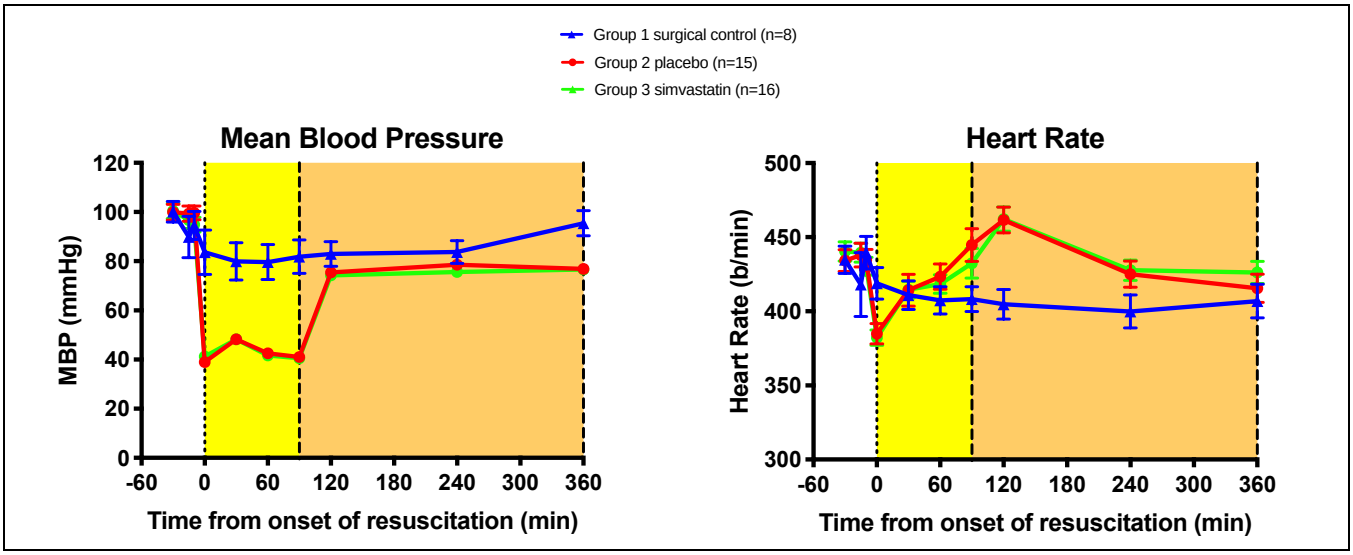

Figure 19 Mean arterial blood pressure (MBP) and heart rate in animals in the sham blast injury strand.
Data expressed as mean±SEM. First (dotted) line represents onset of resuscitation 0 min, second (dashed) line represents onset of revised resuscitation target at 90 min, third (dashed) line represents end of experiment at 360 min.

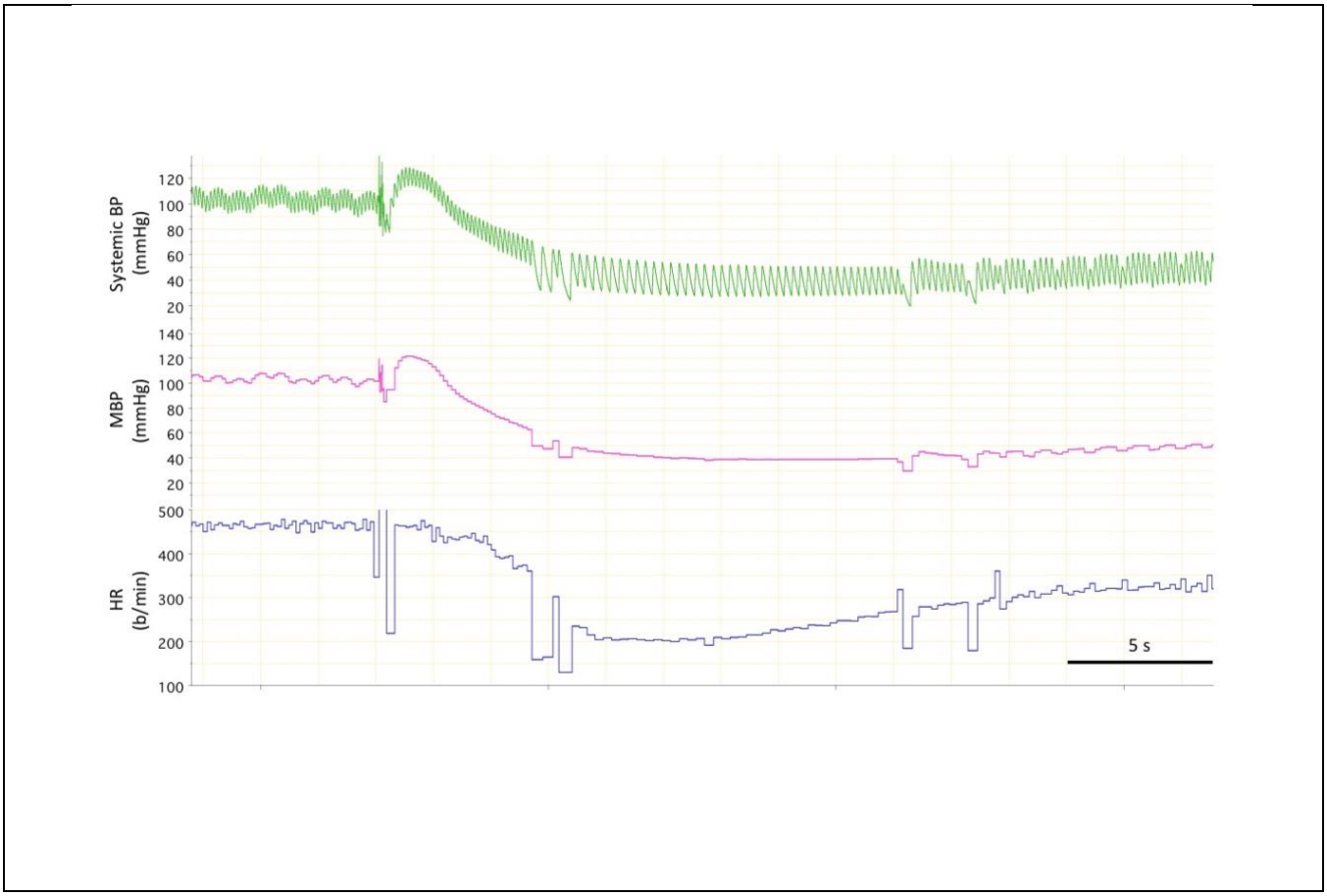

Figure 20 Representative trace demonstrating arterial BP, MBP and HR during blast exposure in one rat.

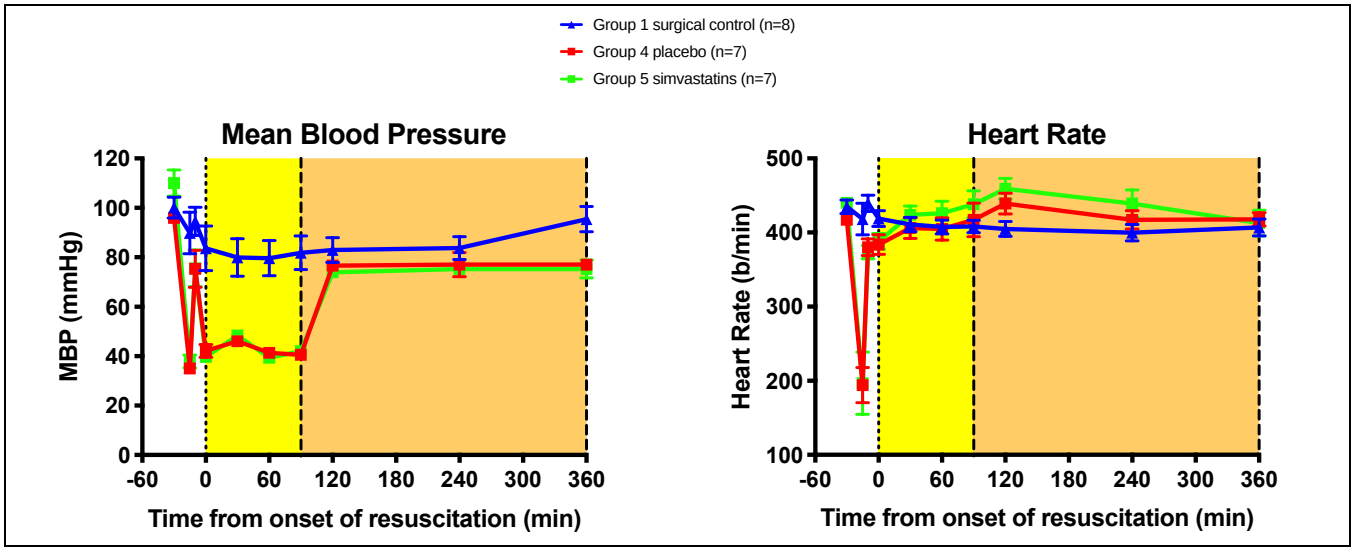

Figure 21 Mean arterial blood pressure (MBP) and heart rate in animals in the blast injury strand.
Data expressed as mean±SEM. First (dotted) line represents onset of resuscitation 0 min, second (dashed) line represents onset of revised resuscitation target at 90 min, third (dashed) line represents end of experiment at 360 min.

3.2.3. Cardiovascular response to resuscitation

In sham blast injury strand, MBP was restored to the normotensive target (approximately 70-80mmHg) with the rapid infusion of whole blood early in the 'in-hospital' resuscitation phase and remained stable for the rest of the experiment facilitated by the background infusion of Gelofusine® (Figure 19) (commenced once all blood given). There was no significant difference in MBP between Groups 2 and 3 in this period (R90 to R360) (*P*=0.327). A corresponding increase in HR was observed at the restoration of MBP, the HR returned to baseline for the rest of the experiment. There was no significant difference in HR between the two groups during this time period (*P*=0.964). The time taken to taken to initially achieve the normotensive target (*P*=0.949), and the total volume of fluid infused in the entire experiment (*P*=0.167) were similar between the two groups (Table 14).

The cardiovascular response to normotensive resuscitation was also seen in the blast injury strand. Fluid requirement and time to restore and maintain the

normotensive targets for animals in the blast injury strand are listed in Table 15. There was a statistically significant difference between Groups 4 and 5 in time taken to reach the normotensive target (*P*=0.025), but this is unlikely of physiological significance as it is very small and there was no difference between these groups in the total volume of fluid infused during the course of the experiment (*P*=0.902). In the resuscitation period, there were no significant differences between Groups 4 and 5 for MBP and HR (*P*=0.647 and *P*=0.499 respectively).

MBP and HR remained at baseline throughout the 'in-hospital' resuscitation for surgical control animals on maintenance infusion of 0.9% sodium chloride (*P*=0.102 and *P*=0.300 respectively).

	Group 2 Sham blast placebo (n=15)	Group 3 Sham blast simvastatin (n=16)	*P* values
Total volume infused from R0 to R360 (ml)	10.89±0.42	11.63±0.31	*NS*
*Time taken to reach normotensive resuscitation target (minutes)**	1.30(0.20)	1.38(0.25)	*NS*

Table 14 Time and volume required to reach and maintain target mean arterial blood pressure in sham blast injury strand.
Data expressed as mean±SEM, unless stated *median (25th – 75th quartile). NS, not statistically significant (*P*>0.05).

	Group 4 Blast placebo (n=7)	Group 5 Blast simvastatin (n=7)	*P values*
*Total volume infused from R0 to R360 (ml)**	11.84(1.53)	12.19(1.31)	*NS*
Time taken to reach normotensive resuscitation target (minutes)	2.09±0.23	1.38±0.04	0.025

Table 15 Time and volume required to reach and maintain target mean arterial blood pressure in blast injury strand.
Data expressed as mean±SEM, unless stated *median (25th – 75th quartile). NS, not statistically significant (*P*>0.05).

3.2.4. Arterial chemistry response to surgery and anaesthesia

In Group 1, arterial blood gas parameters were within the normal ranges and remained unchanged from baseline levels throughout the experiment, except for lactate (*P*<0.001), potassium (*P*<0.001), calcium (*P*=0.001) and haematocrit (*P*<0.001) (Figure 22 - Figure 24). These changes are small and not of physiological consequence, as the values are within normal ranges.

3.2.5. Arterial chemistry response to injury and resuscitation

3.2.5.1. Sham blast injury strand

There were no changes in arterial oxygen (PaO_2) and arterial carbon dioxide ($PaCO_2$) after sham blast (no blast) exposure in Groups 2 and 3 (Figure 22). After injury (femur fracture and haemorrhage), the level of PaO_2 rose above baseline (*P*<0.001), whilst the level of $PaCO_2$ fell over the duration of pre-hospital phase (R0-R90) (*P*<0.001). There were no significant differences between groups in levels of either PaO_2 and $PaCO_2$ (*P*= 0.257 and *P*= 0.825 respectively) in this phase. After R90, PaO_2 started to fall and $PaCO_2$ started to rise, both parameters stabilised by R120 but did not return to baseline for the rest of the experiment (both *P*<0.001). There were no significant differences between Groups 2 and 3 in these parameters (*P*=0.656 and *P*=0.882) in the period R90 to R360.

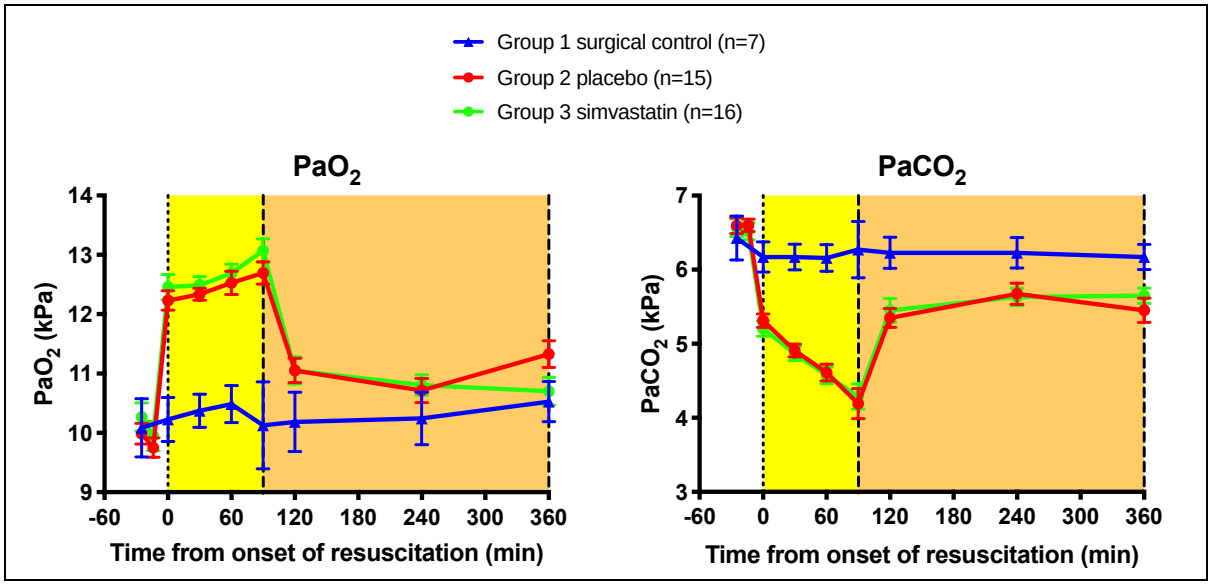

Figure 22 Arterial partial pressure of oxygen PaO_2 and carbon dioxide $PaCO_2$ of sham blast groups and surgical control.
Data expressed as mean±SEM. First (dotted) line represents onset of resuscitation 0 min, second (dashed) line represents onset of revised resuscitation target at 90 min, third (dashed) line represents end of experiment at 360 min.

The pH in Groups 2 and 3 fell modestly below baseline after injury but stayed within normal limits during the prehospital phase (*P*<0.001) (Figure 23). There was no difference in pH levels between the two groups during this initial phase of the study (*P*=0.893). By R120, pH returned to baseline levels, and remained at this level for the remainder of the experiment, again the changes were statistically significant over time (*P*<0.001) but without differences between Groups 2 and 3 (*P*=0.887).

Base excess in Groups 2 and 3 dropped rapidly and significantly from baseline immediately after injury and continued a downward trend in the pre-hospital phase (*P*<0.001, Figure 23). This decline was reversed from R90 and levels returned to just below pre-injury baseline by the end of the experiment (*P*<0.001). Lactate showed the opposite trend to base excess after injury, where there was a steep rise (*P*<0.001) after injury/haemorrhage followed by its reversal after R90 (*P*<0.001, Figure 23). There were no significant differences between the two groups in the

absolute values of either lactate or ABE over the entire time course of the study (*P*=0.209 and *P*=0.867 respectively). The shock burden (area under time curve of arterial base excess) were comparable between treatment groups throughout the course of the study (*P*=0.711).

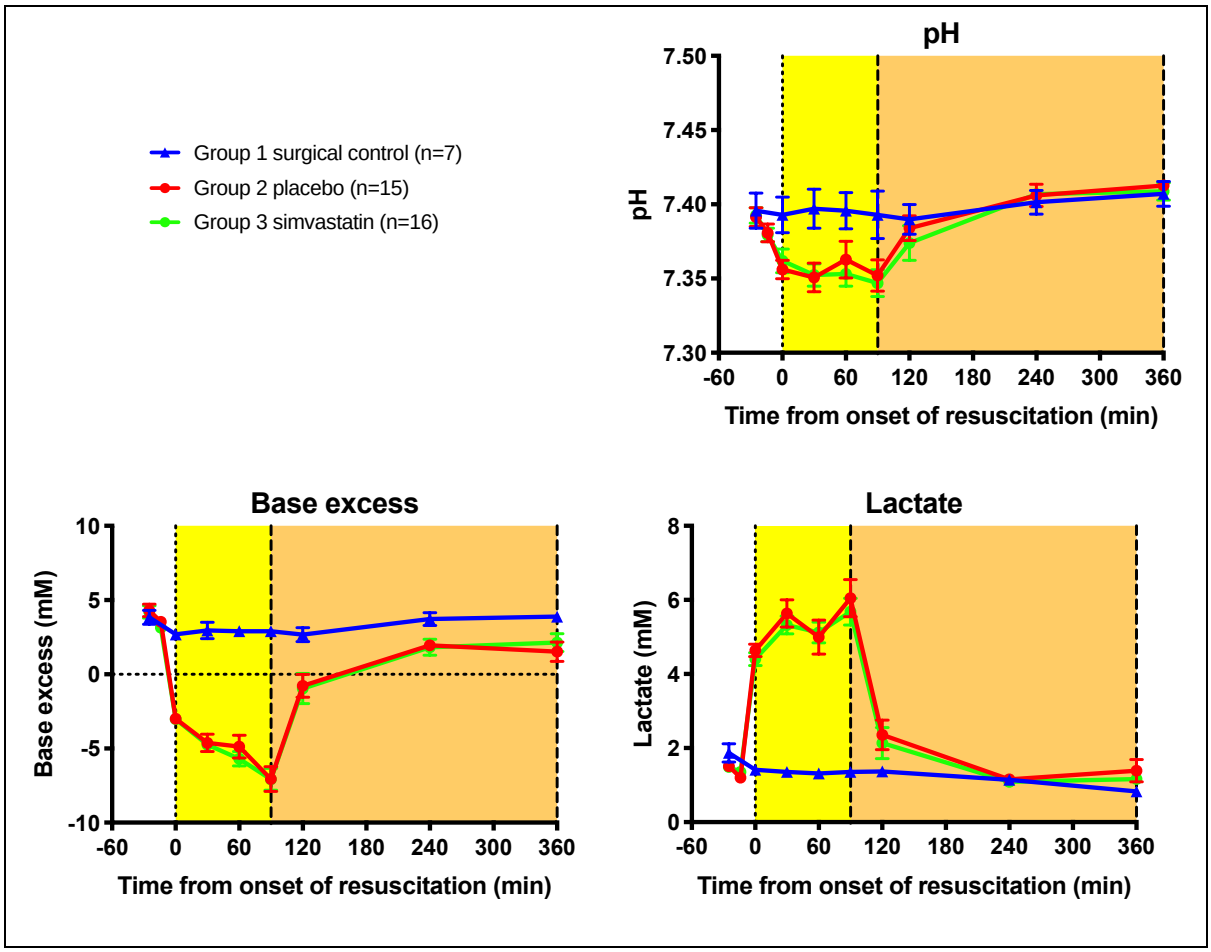

Figure 23 Serial arterial pH, base excess and lactate measurements of sham blast groups and surgical control.
Data expressed as mean±SEM. First (dotted) line represents onset of resuscitation 0 min, second (dashed) line represents onset of revised resuscitation target at 90 min, third (dashed) line represents end of experiment at 360 min.

There were statistically significant changes in arterial potassium levels over time in both Group 2 and 3 (*P*<0.001), without any significant difference between these groups (*P*=0.463). Hyperkalaemia developed as arterial potassium rose above baseline during the injury (baseline to R0) and subsequent pre-hospital

resuscitation (R0 to R90) periods (*P*<0.001), followed by a rapid return to baseline by R120, where it remained for the remainder of the study (*P*<0.001) (Figure 24).

There was a decline in ionized calcium levels from R30 onwards in the injury groups, which stabilised with in-hospital resuscitation from R120 to the rest of the experiment (*P*<0.001). The changes were not statistically different between Groups 2 and 3 (*P*=0.366).

After injury, there was a transient elevation in glucose in Groups 2 and 3, followed by a downward trend to below baseline in the pre-hospital resuscitation phase (Figure 24). These changes were statistically significant over time (*P*<0.001) but not between treatment groups (*P*=0.521). This decline was reversed at the start of in-hospital resuscitation and returned to baseline by R240 (*P*<0.001) and again without significant difference between the two groups (*P*=0.794).

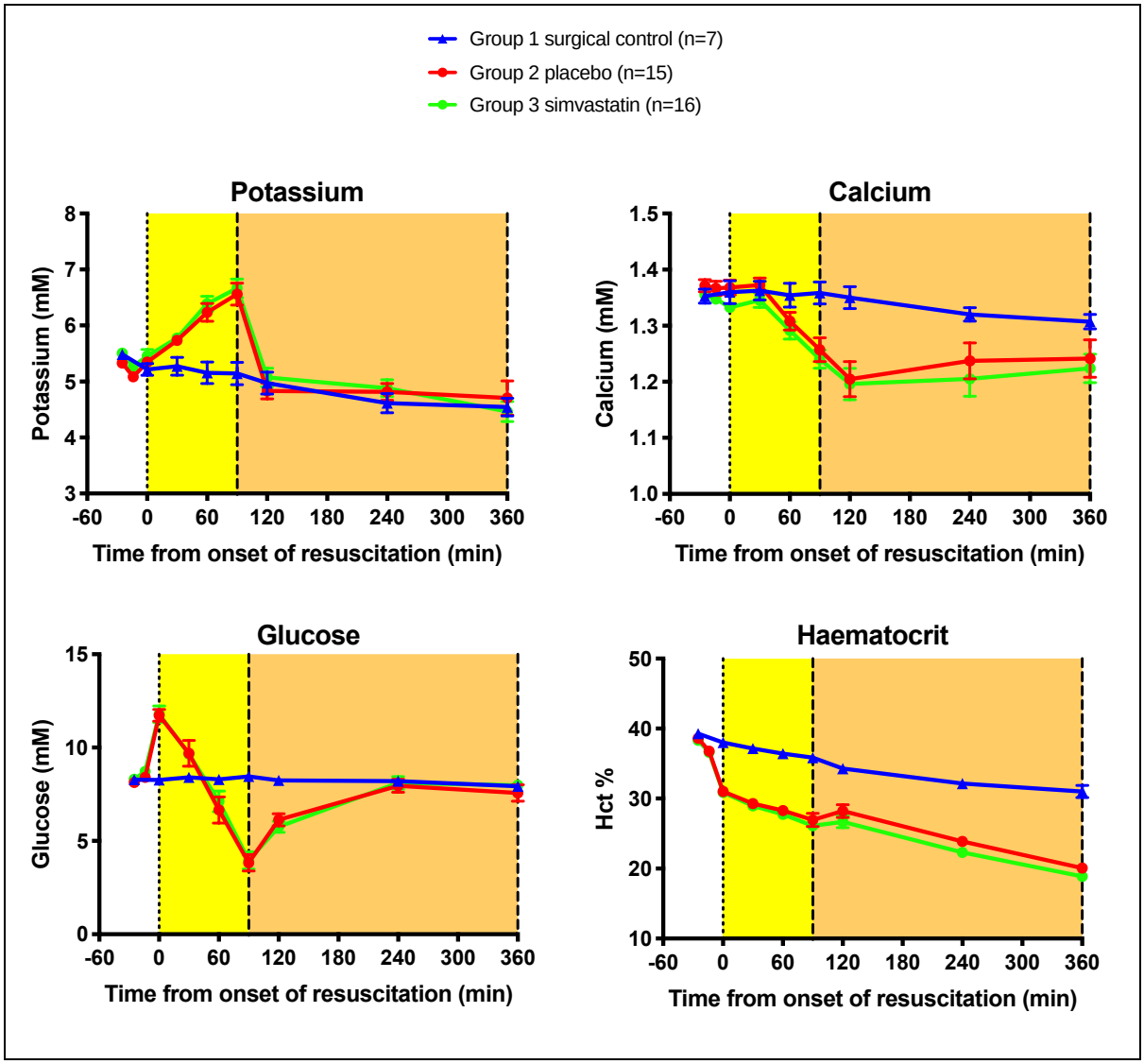

Figure 24 Serial arterial potassium, ionized calcium, glucose, haematocrit measurements of sham blast groups and surgical control.
Data expressed as mean±SEM. First (dotted) line represents onset of resuscitation 0 min, second (dashed) line represents onset of revised resuscitation target at 90 min, third (dashed) line represents end of experiment at 360 min.

Haematocrit fell after injury and continued on gradual decline over the course of the experiment in Groups 2 and 3 (P<0.001) (Figure 24). There was no significant difference in haematocrit between Groups 2 and 3 over the course of the study (P=0.309).

3.2.5.2. Blast injury strand

There was a transient fall in PaO_2 in Groups 4 and 5 immediately after blast exposure (Figure 25). By R0 (after haemorrhage and tissue injury), PaO_2 had recovered to baseline and continued to elevate in pre-hospital resuscitation phase. These changes were statistically significant over time (P<0.001) but not significantly different between treatment groups (P=0.060). By R120, PaO_2 returned to baseline levels and remained there for the rest of the study (P<0.001). There is a statistically significant difference in PaO_2 between Groups 4 and 5 (P=0.034), but this is no of biological significance at this level of oxygen tension where blood is likely to be fully saturated.

After blast exposure, there were small and variable change in $PaCO_2$ from baseline in Groups 4 and 5 (Figure 25). The level of $PaCO_2$ fell below baseline after haemorrhage and tissue injury and continued to decline in the pre-hospital phase (P<0.001). The pattern of response and absolute levels attained in Groups 4 and 5 were similar (P=0.830 and P=0.825 respectively) for this whole period (between baseline and R90). During the initial phase of in-hospital resuscitation (R90-R120), $PaCO_2$ rose and subsequently remained stable at a level below the initial baseline for the reminder of the experiment. These changes in $PaCO_2$ over time were statistically significant (P<0.001), although there was no difference in pattern of response (P=0.676) or absolute levels between Groups 4 and 5 between groups during the in-hospital phase (P=0.882). After R120, $PaCO_2$ plateaued below baseline for the remainder of the experiment.

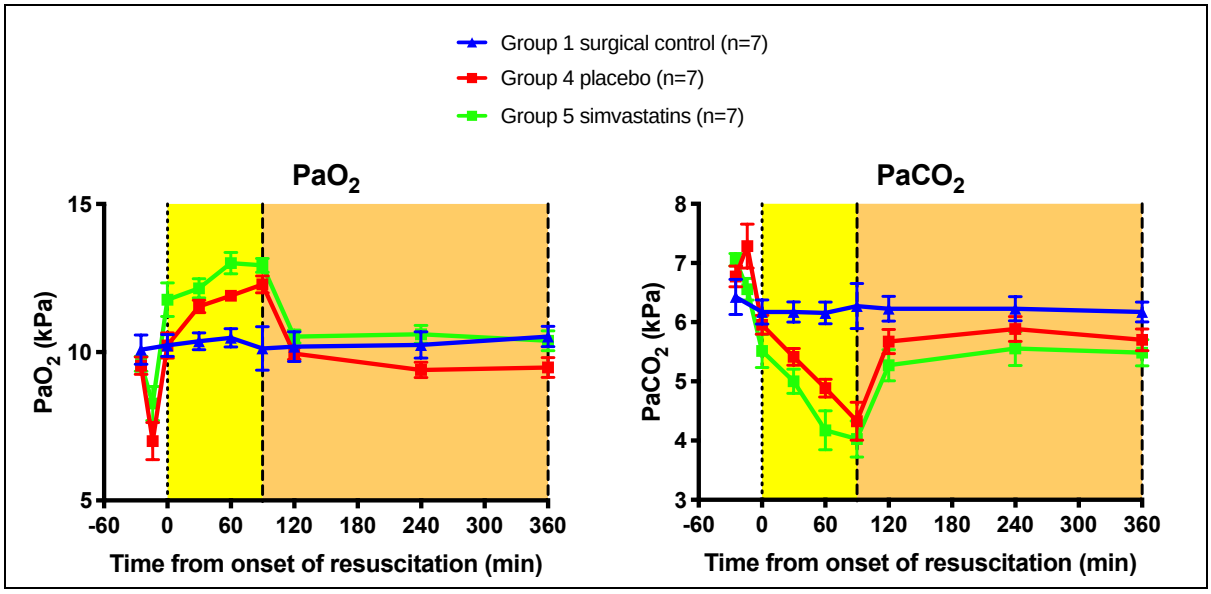

Figure 25 Arterial partial pressure of oxygen PaO_2 and carbon dioxide $PaCO_2$ of blast groups and surgical control.
Data expressed as mean±SEM. First (dotted) line represents onset of resuscitation 0 min, second (dashed) line represents onset of revised resuscitation target at 90 min, third (dashed) line represents end of experiment at 360 min.

pH declined after blast exposure and continued to fall after haemorrhage and tissue injury in Groups 4 and 5 (Figure 26). During the pre-hospital and subsequent in-hospital phases there were recovery of pH in both groups. The changes in pH over time were statistically significant (*P*=0.004) without significant difference in pattern or absolute levels between groups (*P*= 0.380 and *P*= 0.933 respectively).

Base excess started to drop from baseline immediately after blast exposure and continued to fall after haemorrhage and tissue injury (Figure 26) in Groups 4 and 5. The downward trend continued for the rest of the pre-hospital phase (*P*<0.001). This decline was reversed from R90 and measurements returned to just below pre-injury baseline levels by the end of the experiment (*P*<0.001). The changes in ABE over time were statistically significant without significant difference in pattern or absolute levels between Groups 4 and 5 (*P*= 0.810 and *P*= 0.294 respectively). Lactate was unchanged after blast exposure but then rose steeply after haemorrhage and tissue injury in Groups 4 and 5 (Figure 26). This upward trend continued in the pre-hospital resuscitation phase (*P*<0.001) and was reversed from

R90, and measurements returned to baseline by the end of the experiment (*P*<0.001). The changes in ABE were statistically significant over time (*P*<0.001) without significant difference in pattern or absolute levels between groups (*P*= 0.663 and *P*= 0.209 respectively). The shock burden over the course of the study were similar between the two groups (*P*=0.313).

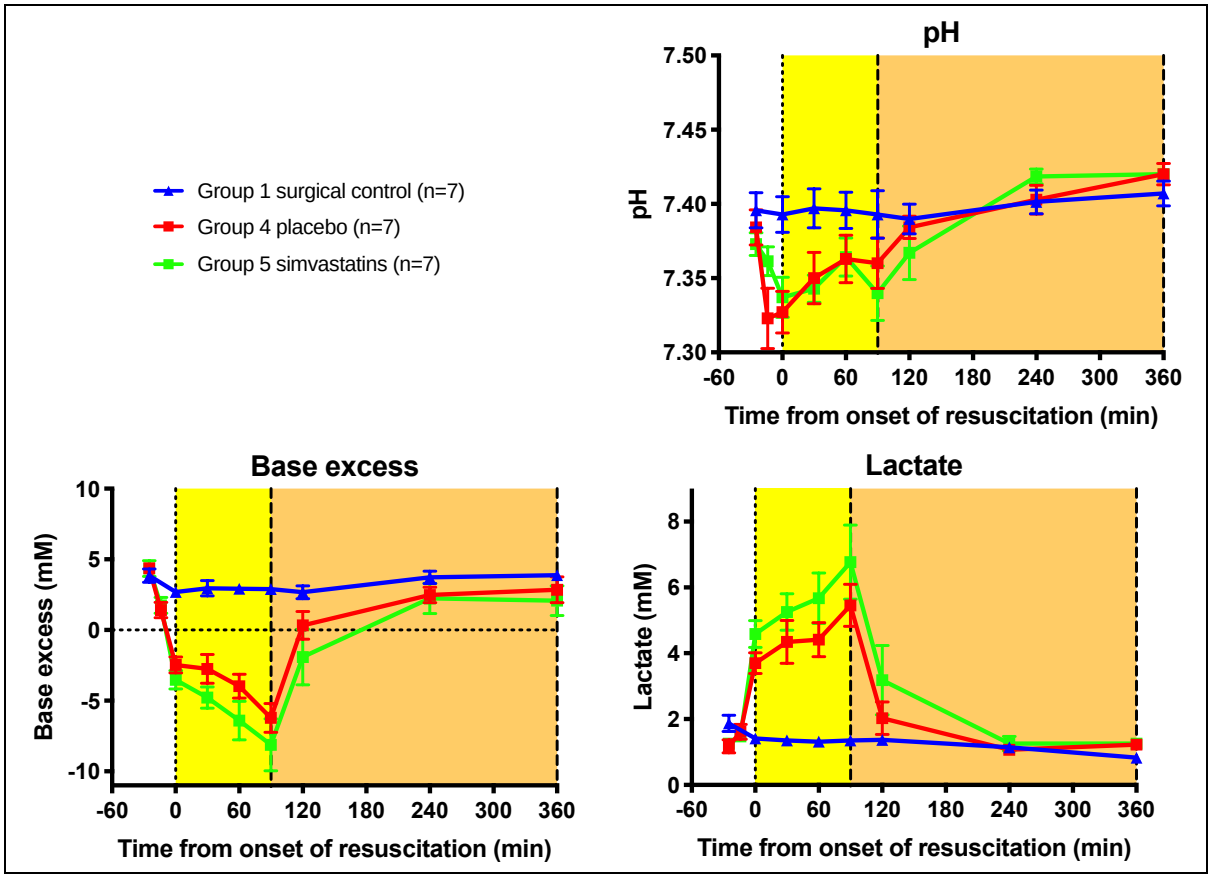

Figure 26 Serial arterial pH, base excess and lactate measurements of blast groups and surgical control.
Data expressed as mean±SEM. First (dotted) line represents onset of resuscitation 0 min, second (dashed) line represents onset of revised resuscitation target at 90 min, third (dashed) line represents end of experiment at 360 min.

For ease of description but not direct comparison, the patterns of response in potassium, calcium, glucose and haematocrit in Groups 4 and 5 were similar to those described earlier in Groups 2 and 3 (Figure 27). There were no statistically significant differences between Groups 4 and 5 in these parameters throughout the course of the experiment.

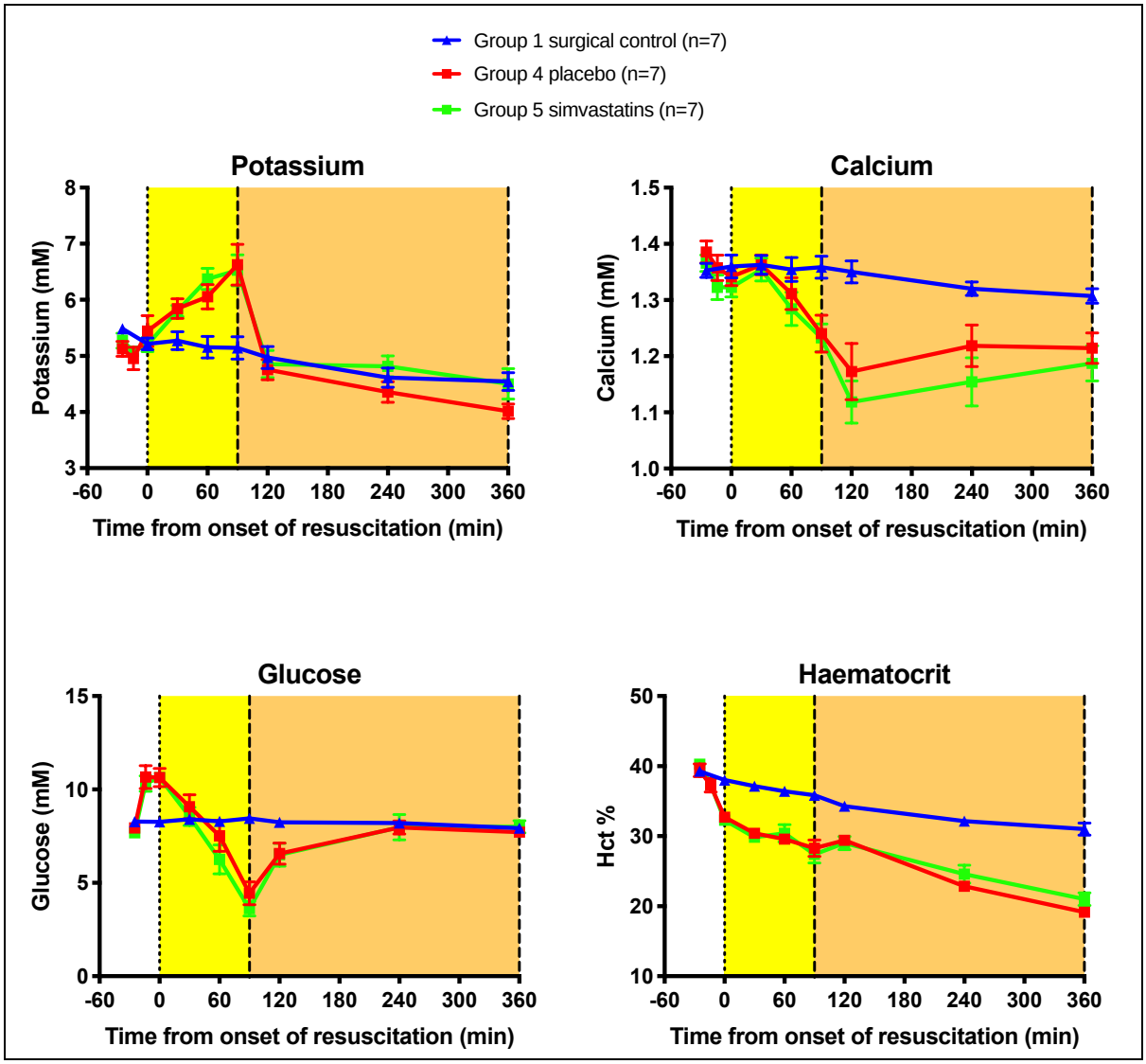

Figure 27 Serial arterial potassium, ionized calcium, glucose and haematocrit measurements of blast groups and surgical control.
Data expressed as mean±SEM. First (dotted) line represents onset of resuscitation 0 min, second (dashed) line represents onset of revised resuscitation target at 90 min, third (dashed) line represents end of experiment at 360 min.

3.3. Plasma DAMPs and inflammatory mediators

	Group 1 (n=8)	Group 2 (n=15)	Group 3 (n=16)	Group 4 (n=7)	Group 5 (n=7)	Group X (n=7)	Group Y (n=7)
Simvastatin	No	No	Yes	No	Yes	No	No
Tissue injury + HGE	No	Yes	Yes	Yes	Yes	Yes	Yes
Thoracic blast	No	No	No	Yes	Yes	No	Yes

Table 16 Injury and treatment in animals of each group.

3.3.1. Effect of simvastatin pre-treatment at baseline

To determine whether simvastatin pre-treatment affected the animals prior to the experiment, comparison was done on the 'pre-blast' plasma samples between animals that received no pre-treatment (Groups 1+ 2+ 4+ X +Y, n=44) and those that received simvastatin pre-treatment (Group 3+5, n=23) (Table 16). Groups X and Y formed a separate study (not part of this thesis), but shared the control group from this study and were treated identically up until the end of the pre-hospital resuscitation phase (R90).

Pre-injury HMGB1 levels were at or below limits of detection for most of the animals, except for one animal which is an outlier (Figure 28). This animal was excluded from further analysis in this assay. Pre-treatment with simvastatin did not affect baseline HMGB1 levels.

The 27-plex luminex assay gave results for nine chemokines, ten pro-inflammatory cytokines, three anti-inflammatory cytokines, four growth factors and leptin. Data from analytes with concentrations at the limit of detection in all groups, at all time points, (G-CSF, GM-CSF, IL-1α, IL-4, IL-6, IL-13) are not presented.

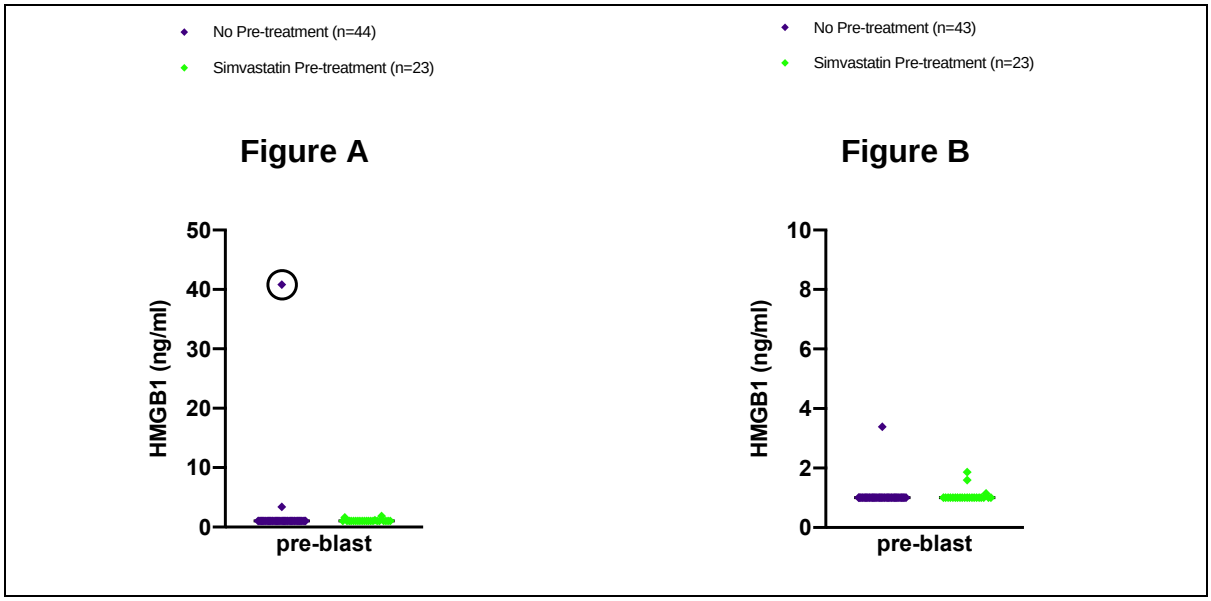

Figure 28 (A) Plasma HMGB1 concentration in animals with or without simvastatin pre-treatment. One outlier (circled) was excluded from the no pre-treatment group. (B) Outlier excluded from no pre-treatment group.
Data represented as median (25^{th} – 75^{th} percentile).

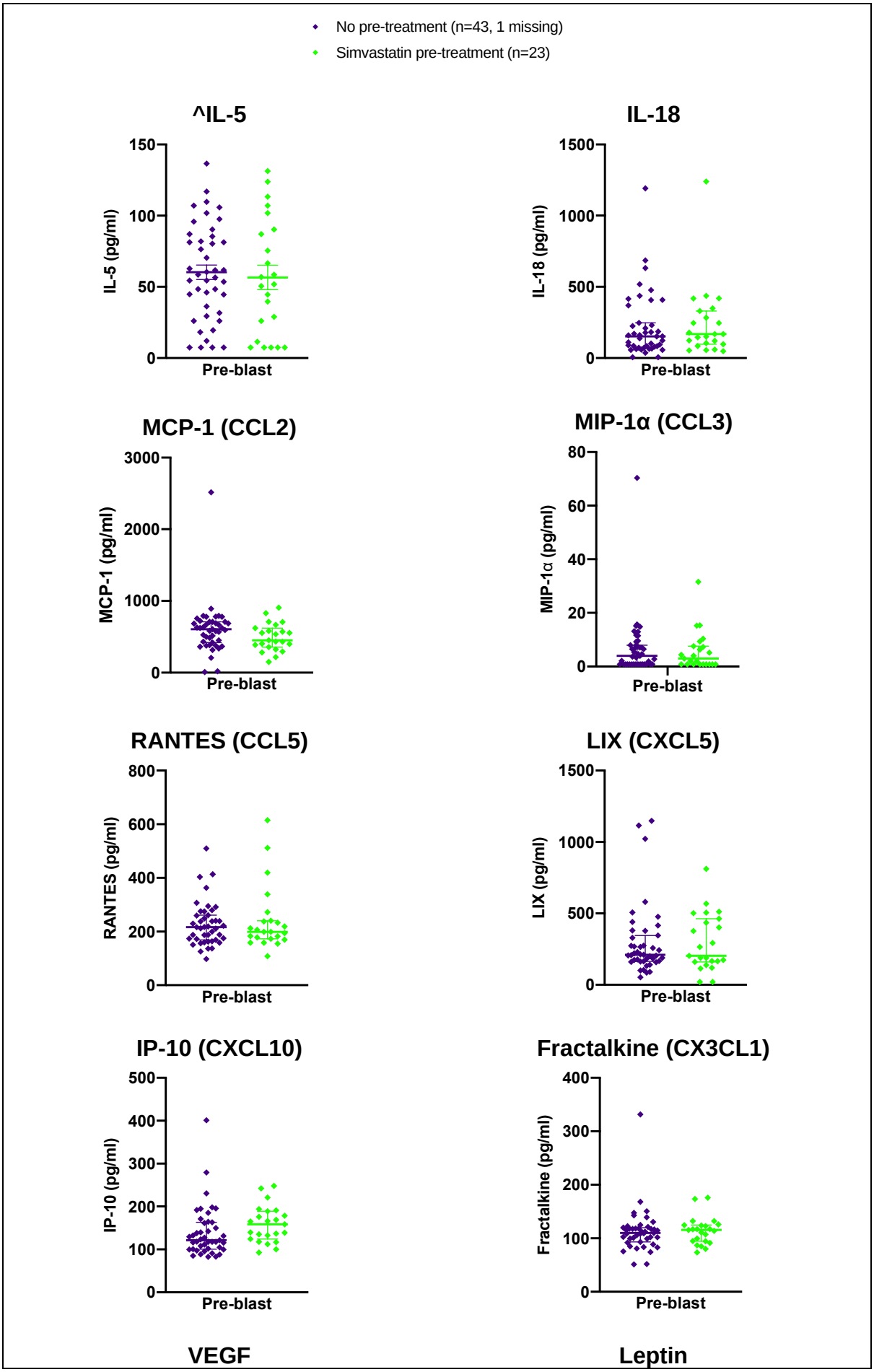
No pre-treatment (n=43, 1 missing)
Simvastatin pre-treatment (n=23)
^IL-5
IL-5 (pg/ml)
150
100
50
0
Pre-blast
IL-18
IL-18 (pg/ml)
1500
1000
500
0
Pre-blast
MCP-1 (CCL2)
MCP-1 (pg/ml)
3000
2000
1000
0
Pre-blast
MIP-1α (CCL3)
MIP-1α (pg/ml)
80
60
40
20
0
Pre-blast
RANTES (CCL5)
RANTES (pg/ml)
800
600
400
200
0
Pre-blast
LIX (CXCL5)
LIX (pg/ml)
1500
1000
500
0
Pre-blast
IP-10 (CXCL10)
IP-10 (pg/ml)
500
400
300
200
100
0
Pre-blast
Fractalkine (CX3CL1)
Fractalkine (pg/ml)
400
300
200
100
0
Pre-blast
VEGF
Leptin

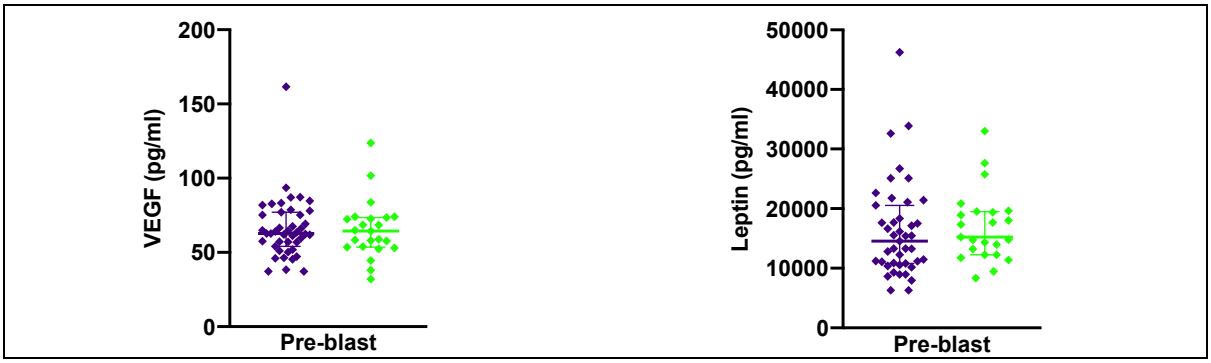

Figure 29 Plasma concentration of inflammatory mediators in animals with or without simvastatin pre-treatment.
Data represented as median (25th – 75th percentile), unless stated ^mean+/-SEM.

At pre-blast the majority of analytes were below or at the limit of detection, except for IL-5, IL-18, MIP-1α, MCP-1, IP-10, fractalkine, LIX, RANTES, VEGF and leptin (see Figure 29). This complicated the statistical analysis for outliers. Animals with outlying results at baseline in multiple markers were omitted in the analysis. Overall, there were no significant differences between animals with or without simvastatin pre-treatment after surgery and initial anaesthesia.

3.3.2. Determine the effect of injury

3.3.2.1. Effect of sham blast, haemorrhage and tissue injury

To determine the effect of sham blast, the *change* between 'pre-blast' and 'R90' was determined in the surgical control (Group 1, uninjured) and injured (Groups 2 + X) groups (Table 16). The concentrations of HMGB1 and 20 of 21 analytes were significantly elevated at R90 from baseline in the injured group (paired analysis, Figure 30, Figure 31 and Table 17). There was no significant change of analytes in surgical control over the two time points in most analytes apart from VEGF and TNF-α.

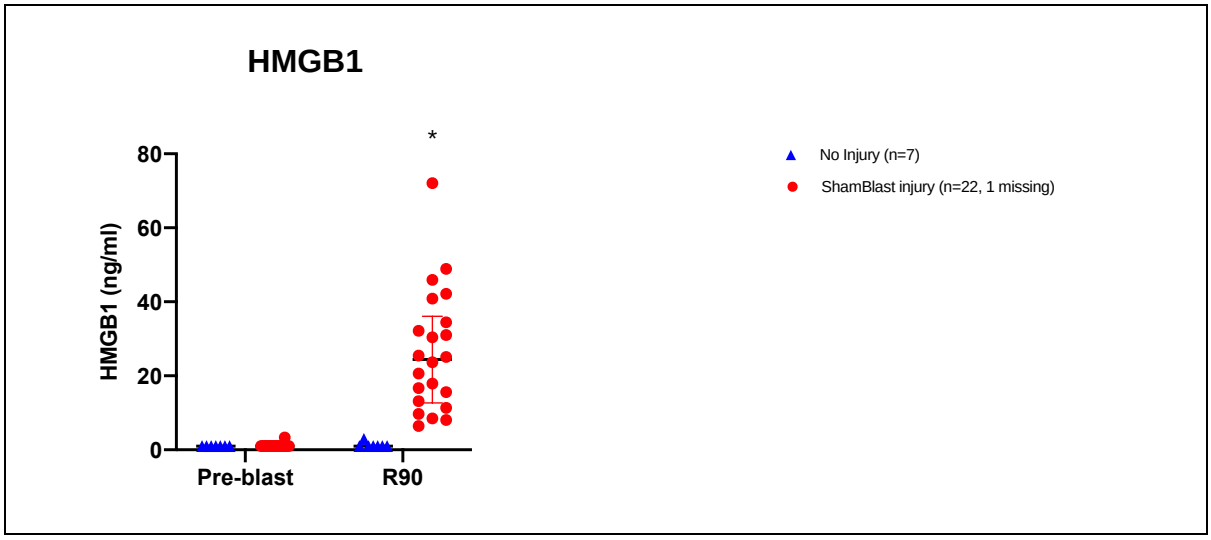

Figure 30 Plasma HMGB1 concentration in the uninjured surgical control group and the injured (sham blast) group.
Data represented as median (25th – 75th percentile). ****p<0.05* **as significant when compared to pre-blast.**

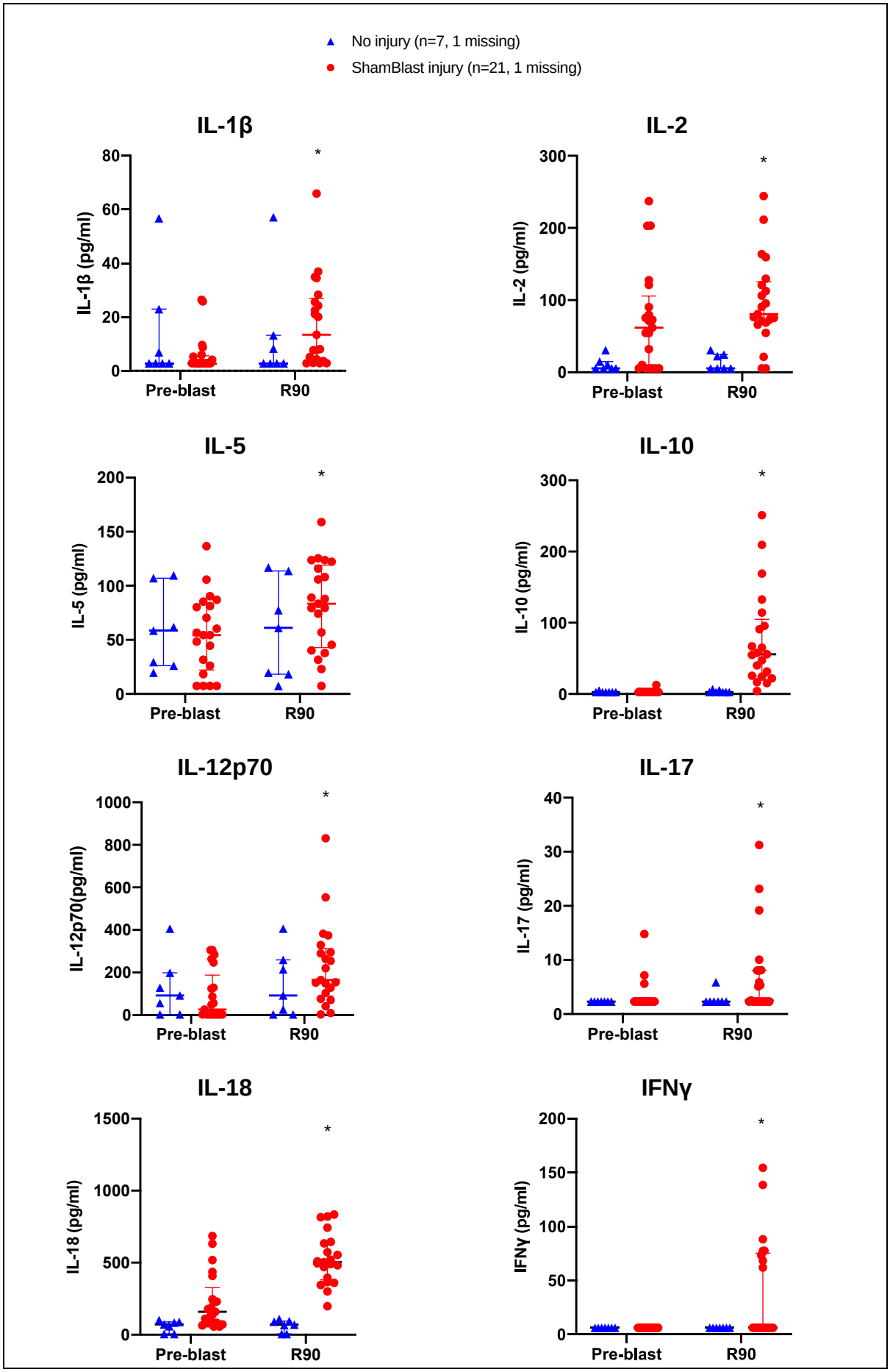
No injury (n=7, 1 missing)
ShamBlast injury (n=21, 1 missing)
IL-1β
IL-1β (pg/ml)
80
60
40
20
0
Pre-blast
R90
*
IL-2
IL-2 (pg/ml)
300
200
100
0
Pre-blast
R90
*
IL-5
IL-5 (pg/ml)
200
150
100
50
0
Pre-blast
R90
*
IL-10
IL-10 (pg/ml)
300
200
100
0
Pre-blast
R90
*
IL-12p70
IL-12p70(pg/ml)
1000
800
600
400
200
0
Pre-blast
R90
*
IL-17
IL-17 (pg/ml)
40
30
20
10
0
Pre-blast
R90
*
IL-18
IL-18 (pg/ml)
1500
1000
500
0
Pre-blast
R90
*
IFNγ
IFNγ (pg/ml)
200
150
100
50
0
Pre-blast
R90
*

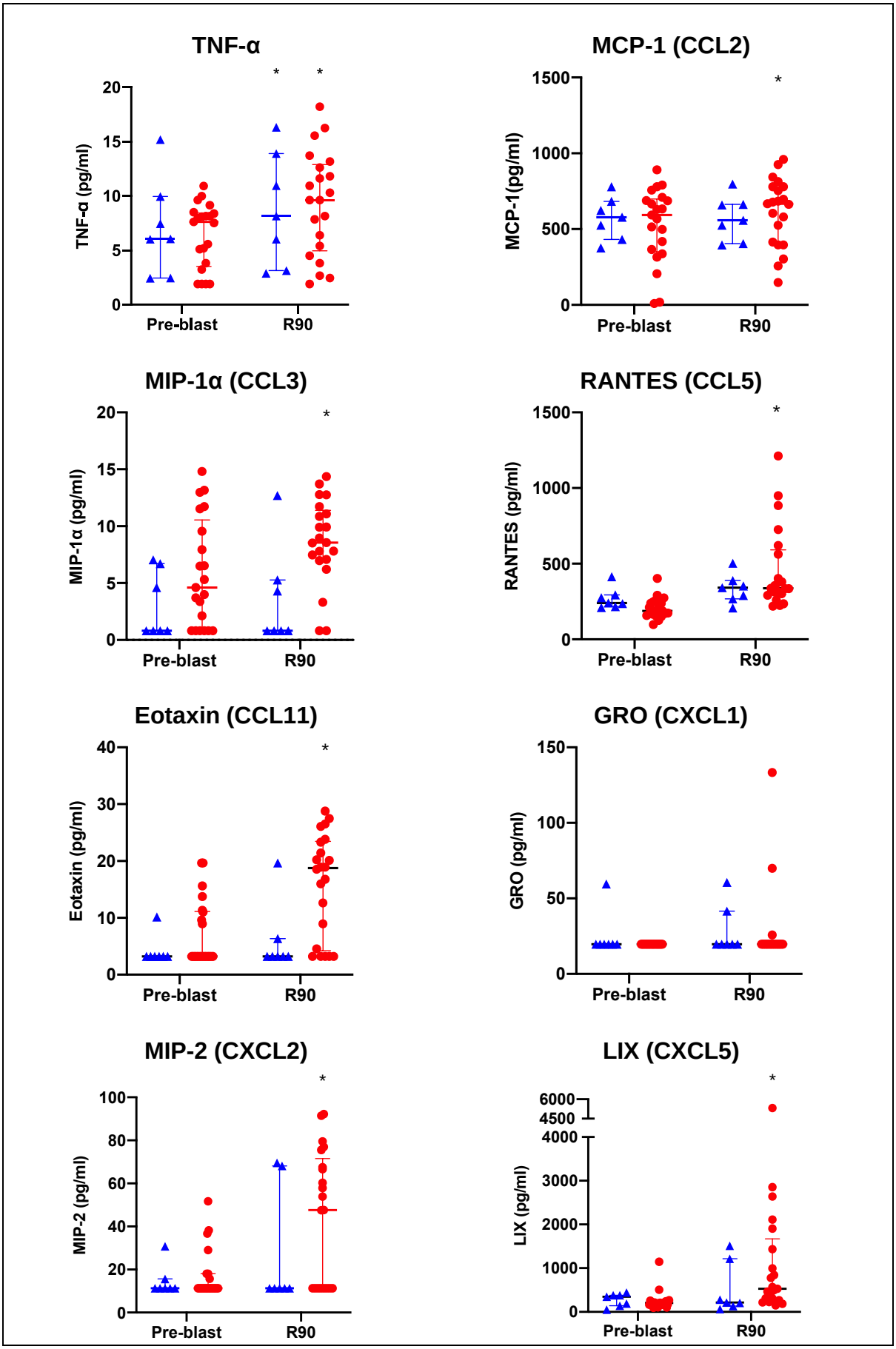
TNF-α
TNF-α (pg/ml)
20
15
10
5
0
Pre-blast
R90
MCP-1 (CCL2)
MCP-1(pg/ml)
1500
1000
500
0
Pre-blast
R90
MIP-1α (CCL3)
MIP-1α (pg/ml)
20
15
10
5
0
Pre-blast
R90
RANTES (CCL5)
RANTES (pg/ml)
1500
1000
500
0
Pre-blast
R90
Eotaxin (CCL11)
Eotaxin (pg/ml)
40
30
20
10
0
Pre-blast
R90
GRO (CXCL1)
GRO (pg/ml)
150
100
50
0
Pre-blast
R90
MIP-2 (CXCL2)
MIP-2 (pg/ml)
100
80
60
40
20
0
Pre-blast
R90
LIX (CXCL5)
LIX (pg/ml)
6000
4500
4000
3000
2000
1000
0
Pre-blast
R90

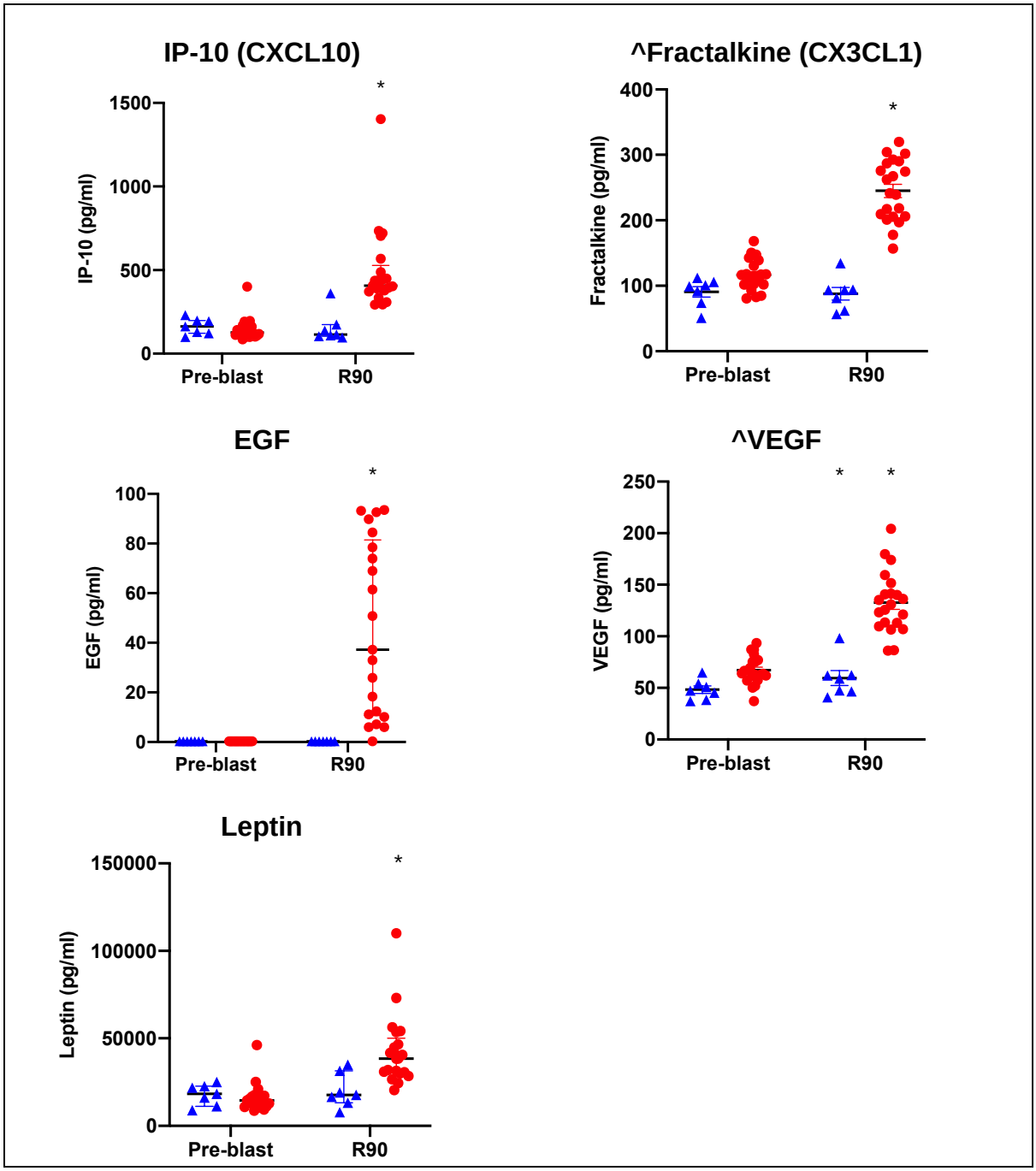

Figure 31 Plasma concentration of inflammatory mediators in the uninjured surgical control group and the injured (sham blast) group.
Data represented as median (25th – 75th percentile), unless stated ^mean+/-SEM. *$p<0.05$ as significant when compared to pre-blast.

3.3.2.2. Effect of blast, haemorrhage and tissue injury

To determine the effect of thoracic blast, haemorrhage and tissue injury, the *change* between 'pre-blast' and 'R90' was determined in the surgical control (Group 1, uninjured) and those injured (Groups 4 + Y) (Table 16). Concentration of HMGB1

and 20 of 21 analytes were significantly elevated at R90 from baseline in the injured group (Figure 32, Figure 33 and Table 17).

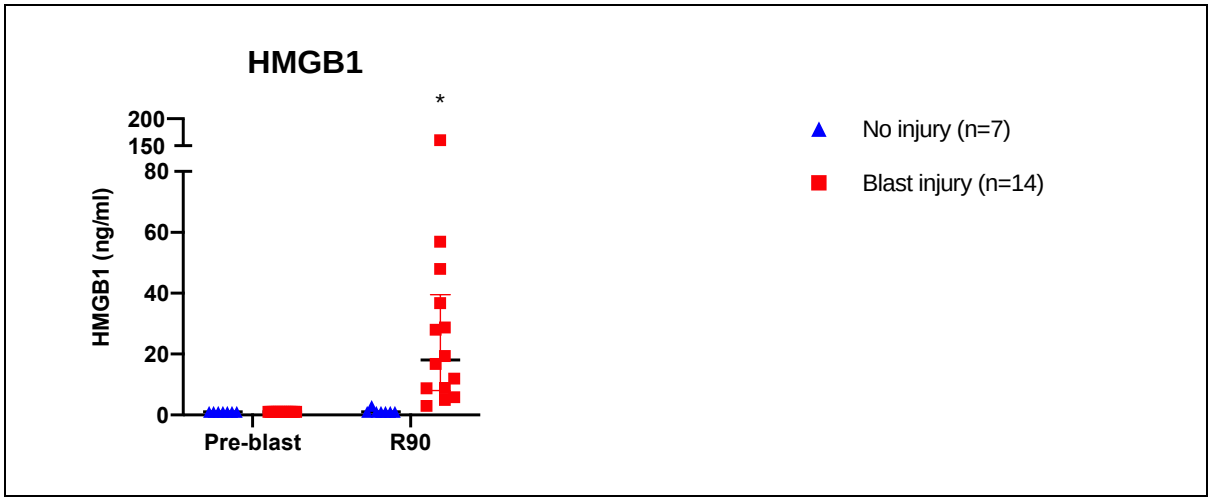

Figure 32 Plasma HMGB1 concentration in the uninjured surgical control group and the injured (blast) group.
Data represented as median (25th – 75th percentile), unless stated ^mean+/-SEM. *$p<0.05$ as significant when compared to pre-blast.

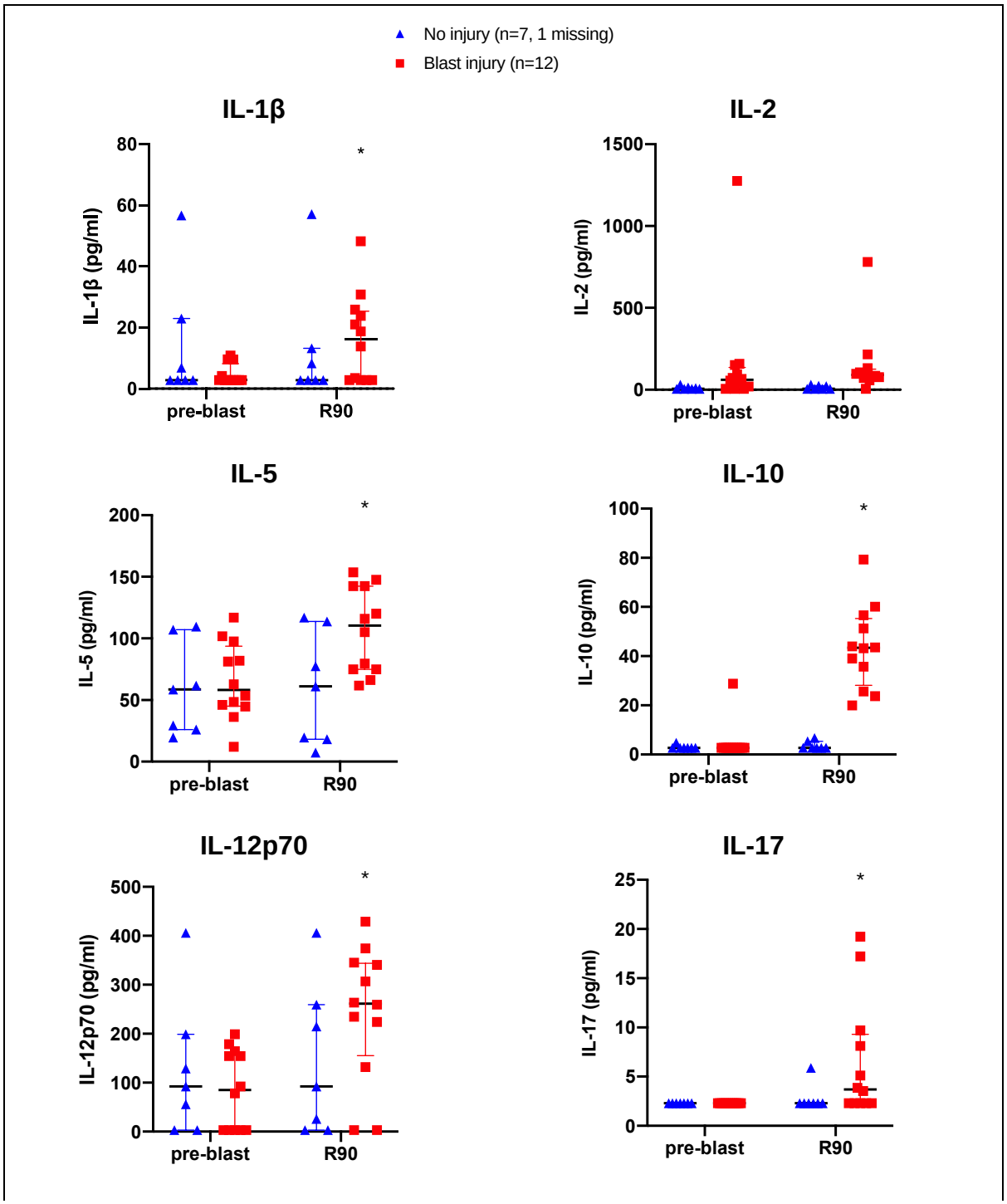
No injury (n=7, 1 missing)
Blast injury (n=12)
IL-1β
IL-1β (pg/ml)
80
60
40
20
0
*
pre-blast
R90
IL-2
IL-2 (pg/ml)
1500
1000
500
0
pre-blast
R90
IL-5
IL-5 (pg/ml)
200
150
100
50
0
*
pre-blast
R90
IL-10
IL-10 (pg/ml)
100
80
60
40
20
0
*
pre-blast
R90
IL-12p70
IL-12p70 (pg/ml)
500
400
300
200
100
0
*
pre-blast
R90
IL-17
IL-17 (pg/ml)
25
20
15
10
5
0
*
pre-blast
R90

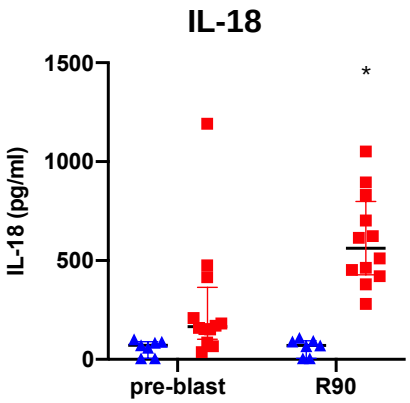
IL-18
IL-18 (pg/ml)
1500
1000
500
0
*
pre-blast
R90

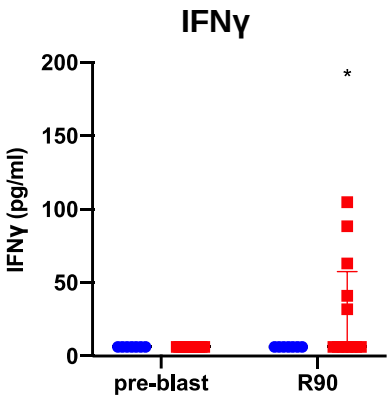
IFNγ
IFNγ (pg/ml)
200
150
100
50
0
*
pre-blast
R90

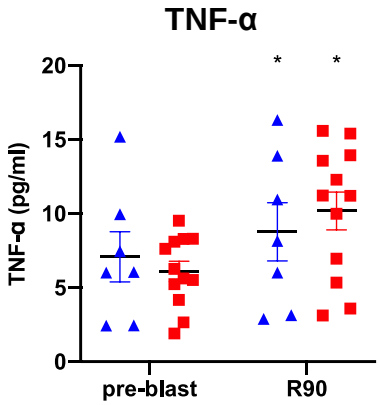
TNF-α
TNF-α (pg/ml)
20
15
10
5
0
*
*
pre-blast
R90

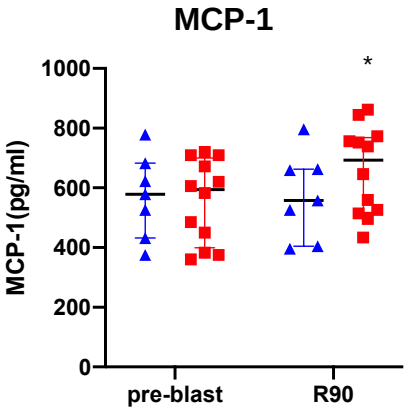
MCP-1
MCP-1(pg/ml)
1000
800
600
400
200
0
*
pre-blast
R90

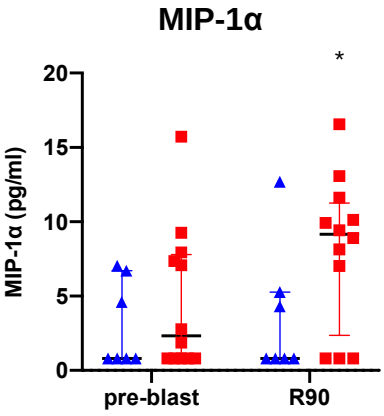
MIP-1α
MIP-1α (pg/ml)
20
15
10
5
0
*
pre-blast
R90

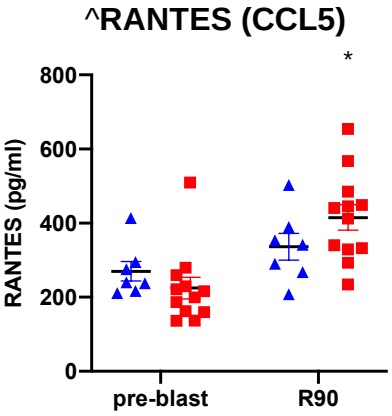
^RANTES (CCL5)
RANTES (pg/ml)
800
600
400
200
0
*
pre-blast
R90

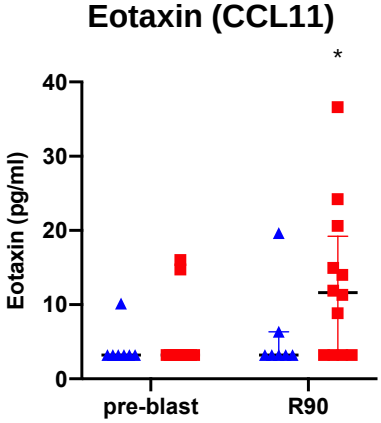
Eotaxin (CCL11)
Eotaxin (pg/ml)
40
30
20
10
0
*
pre-blast
R90

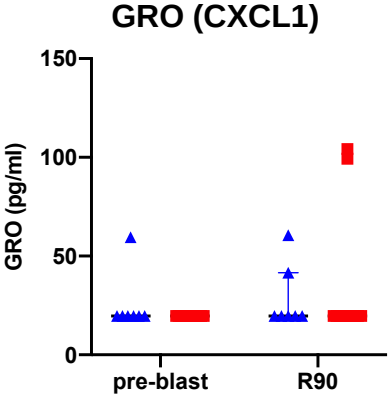
GRO (CXCL1)
GRO (pg/ml)
150
100
50
0
pre-blast
R90

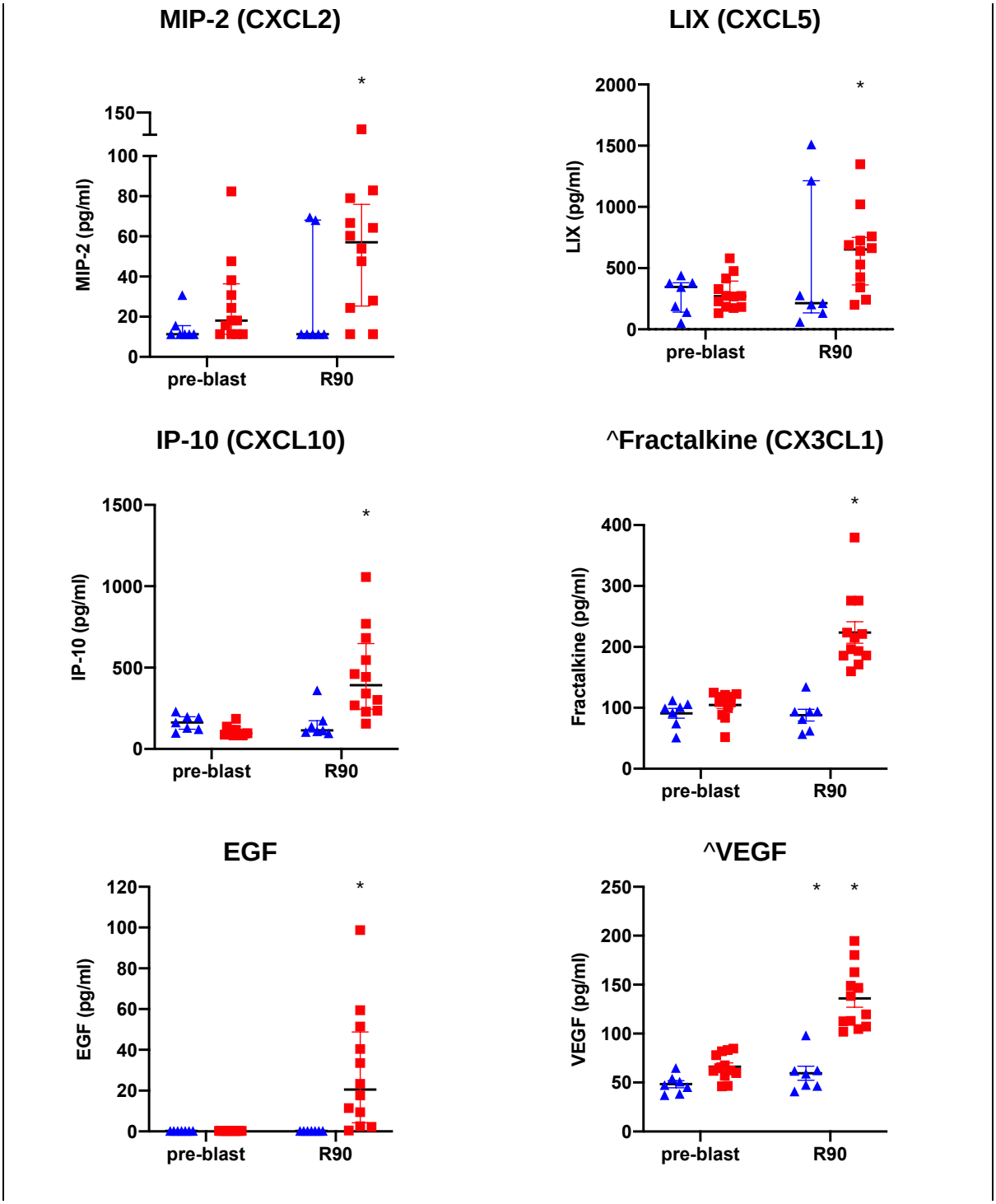
MIP-2 (CXCL2)
MIP-2 (pg/ml)
150
100
80
60
40
20
0
pre-blast
R90
*
LIX (CXCL5)
LIX (pg/ml)
2000
1500
1000
500
0
pre-blast
R90
*
IP-10 (CXCL10)
IP-10 (pg/ml)
1500
1000
500
0
pre-blast
R90
*
^Fractalkine (CX3CL1)
Fractalkine (pg/ml)
400
300
200
100
0
pre-blast
R90
*
EGF
EGF (pg/ml)
120
100
80
60
40
20
0
pre-blast
R90
*
^VEGF
VEGF (pg/ml)
250
200
150
100
50
0
pre-blast
R90
* *

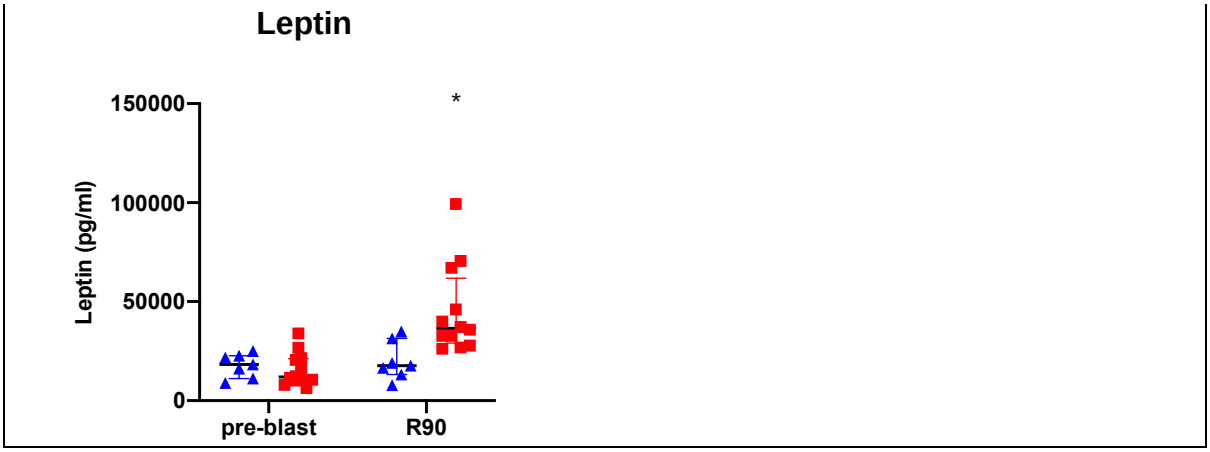

Figure 33 Plasma concentration of inflammatory mediators in the uninjured surgical control group and the injured (blast) group.
Data represented as median (25th – 75th percentile), unless stated ^mean+/-SEM. **p<0.05* as significant when compared to pre-blast.

Analyte	No injury	Sham Blast injury	Blast injury
HMGB1	*NS*	**P<0.0001*	*P=0.0025*
IL-1β	*NS*	**P=0.0001*	**P=0.0064*
IL-2	*NS*	*P=0.0046*	*NS*
IL-5	*NS*	**P<0.0001*	**P<0.0001*
IL-10	*NS*	*P<0.0001*	**P<0.0001*
IL-12p70	*NS*	**P=0.0005*	**P=0.0014*
IL-17α	*NS*	*P=0.0011*	**P=0.0329*
IL-18	*NS*	**P<0.0001*	**P=0.0018*
IFNγ	*NS*	**P=0.0048*	**P=0.0354*
TNF-α	*P=0.0274*	**P=0.0003*	**P=0.0007*
MCP-1	*NS*	**P=0.0043*	**P=0.0003*
MIP-1α	*NS*	**P=0.0009*	**P=0.0115*
Rantes	**NS*	*P<0.0001*	**P<0.0001*
Eotaxin	*NS*	**P<0.0001*	**P=0.0053*
GRO	*NS*	*NS*	*NS*
MIP-2	*NS*	**P=0.0001*	**P=0.0008*
LIX	*NS*	*P=0.0002*	**P=0.0048*
IP-10	*NS*	*P<0.0001*	**P=0.0008*
Fractalkine	**NS*	**P<0.0001*	**P<0.0001*
EGF	*NS*	*P<0.0001*	**P=0.0059*
VEGF	**p=0.0482*	**P<0.0001*	**P<0.0001*
Leptin	*NS*	*P<0.0001*	*P=0.0025*

Table 17 Effect of injury.
Wilcoxon signed rank test unless indicated (*paired t-test). NS, not significant (*P>0.05*).

3.3.3. Effect of surgery and anaesthesia

Establishing the effect of surgery and anaesthesia was required to allow correct conclusions to be drawn from the results on the effects of treatment. This

was achieved by inspecting the effect of time in surgical control on samples from the four time points (pre-blast, R90, R3h, R6h). Statistical analysis has shown significant changes over time in IL-10, MIP-1α, and Fractalkine (Table 18, Figure 34). For IL-10 there was an overall significant difference over time, however *post hoc* analysis did not reveal a significant difference between any two time-points in the pre-planned analysis. For MIP-1α, the significant difference was between comparing R6h and the other 3 time points. There was a significance difference between pre-blast and R6h in Fractalkine.

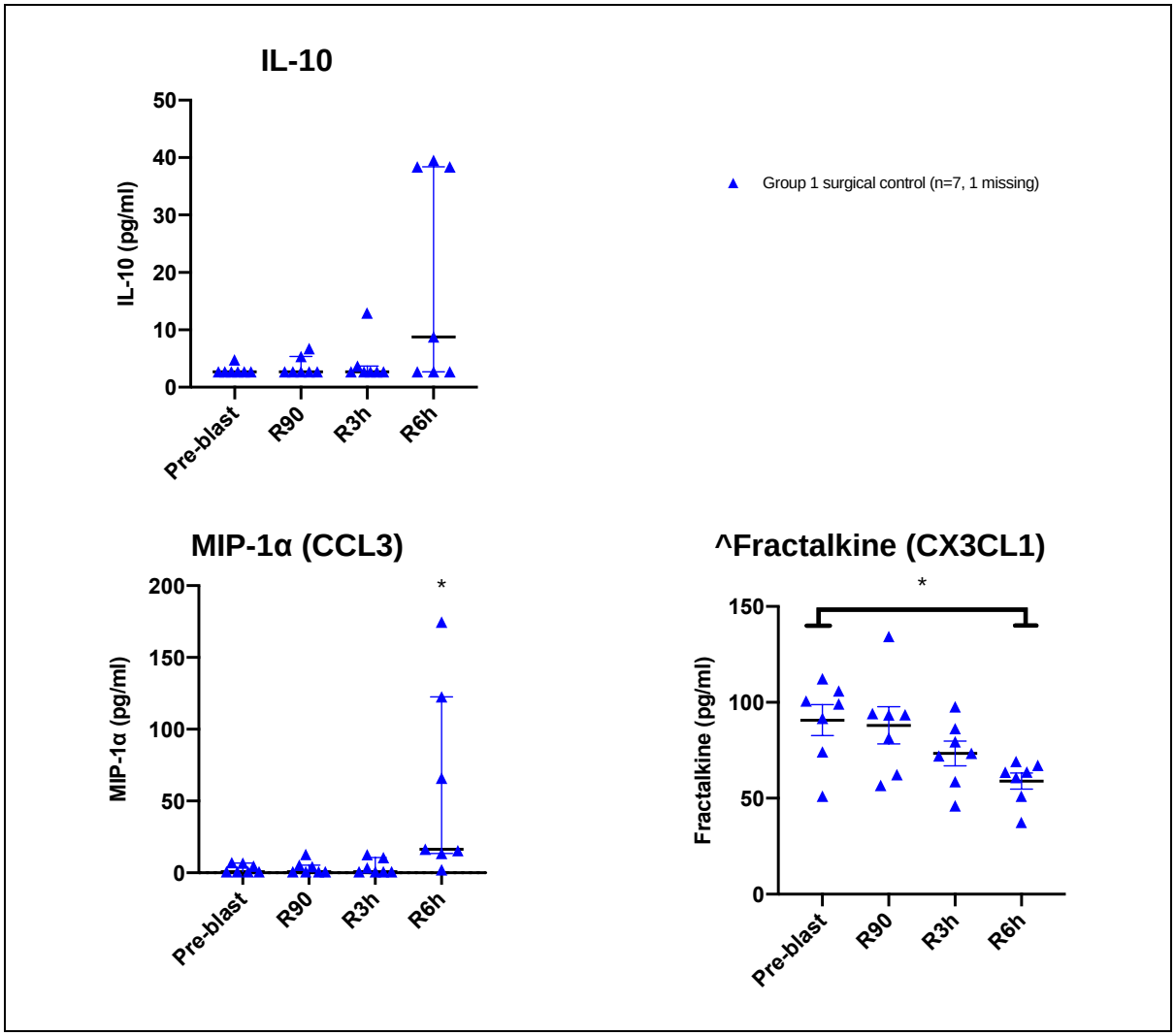

Figure 34 Effect of time on IL-10, MIP-1a and Fractalkine in the surgical control group (Group 1).
^One way ANOVA (Friedman's test). **p<0.05*.

3.3.4. Determine the effect of treatment

3.3.4.1. Effect of treatment in sham blast injury strand

To determine the effect of simvastatin pre-treatment in haemorrhage and tissue injury a comparison was made between Groups 2 and 3. Because of the distribution of data at the 'pre-blast' time-point, it was impossible to use ANOVA over time when all four (pre-blast – R360) time points were included. Instead, comparison at 'pre-blast' between Groups 2 and 3 were made using either t-test or Mann-Whitney U test, and valid analysis of covariance was performed for the remaining three time points (R90, R3h and R6h).

3.3.4.1.1. Effect of treatment on baseline values

There was no significant difference between Groups 2 and 3 at pre-blast for all of the analytes, apart from LIX ($p=0.0452$) (Table 18). The elevation from baseline observed at R90 displayed a downward trend at the subsequent time points, which was statistically significant in 7 analytes (IL-12p70, IL-18, fractalkine, LIX, EGF, RANTES, leptin) (Figure 35, Figure 36). As surgical control had significant change between pre-blast and R6h for fractalkine (Table 18, Figure 34), it is not possible to comment if the changes over time observed in the injured groups were due to the effects of injury or simply the passage of time and prolonged anaesthesia.

3.3.4.1.2. Effect of time during resuscitation

Both GRO and VEGF showed a delayed change over time, with the highest levels in the sampling regimen being seen 3 hours after the start of resuscitation. Initial analysis (Figure 36) showed that GRO was unchanged from baseline at 90 min after the start of resuscitation (R90), and the elevation in VEGF, although statistically

significant, was modest. However, by 3 hours after the start of resuscitation (R3h) both mediators (GRO and VEGF) were elevated markedly and significantly above the levels seen at R90 (Figure 36). Subsequently, by 6 hours after the start of resuscitation (R6h) GRO had returned to levels that were not significantly different to those seen at R90, whilst VEGF remained significantly above the levels seen at R90. MIP-1α showed significant elevation in injured groups at R6h in comparison to R3h, however this was also seen in Group 1, hence likely to be an effect of surgery and anaesthesia (Table 18, Figure 34). There was no effect of time at R3h or R6h when compared to R90 for the rest of the analytes (Table 18).

3.3.4.1.3. Effects of treatment: differences between simvastatin and placebo groups

There were no significant differences between simvastatin and placebo-treated groups for any analyte except for IL5, IL12p70 and IL-17 (Table 18). In the case of IL-5, although there was an overall significant difference between groups, *post hoc* analysis failed to identify any specific time point where the groups differed. For IL-12p70 and IL-17 *post hoc* analysis showed that the groups were different at R3h only, but the difference was not sustained at R6h (Figure 36). There was no difference in the pattern of response between the two treatment groups for any analyte (Table 18).

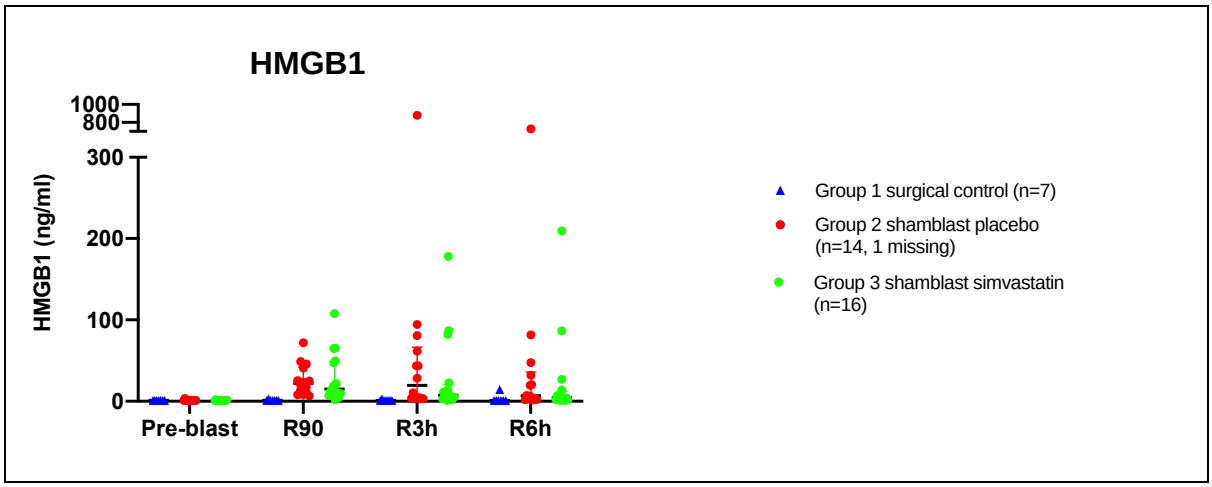

Figure 35 Plasma HMGB1 level recorded over time in the uninjured surgical control group and the two injured groups (sham blast) treated respectively with simvastatin and placebo. Data represented as median (25th – 75th percentile).

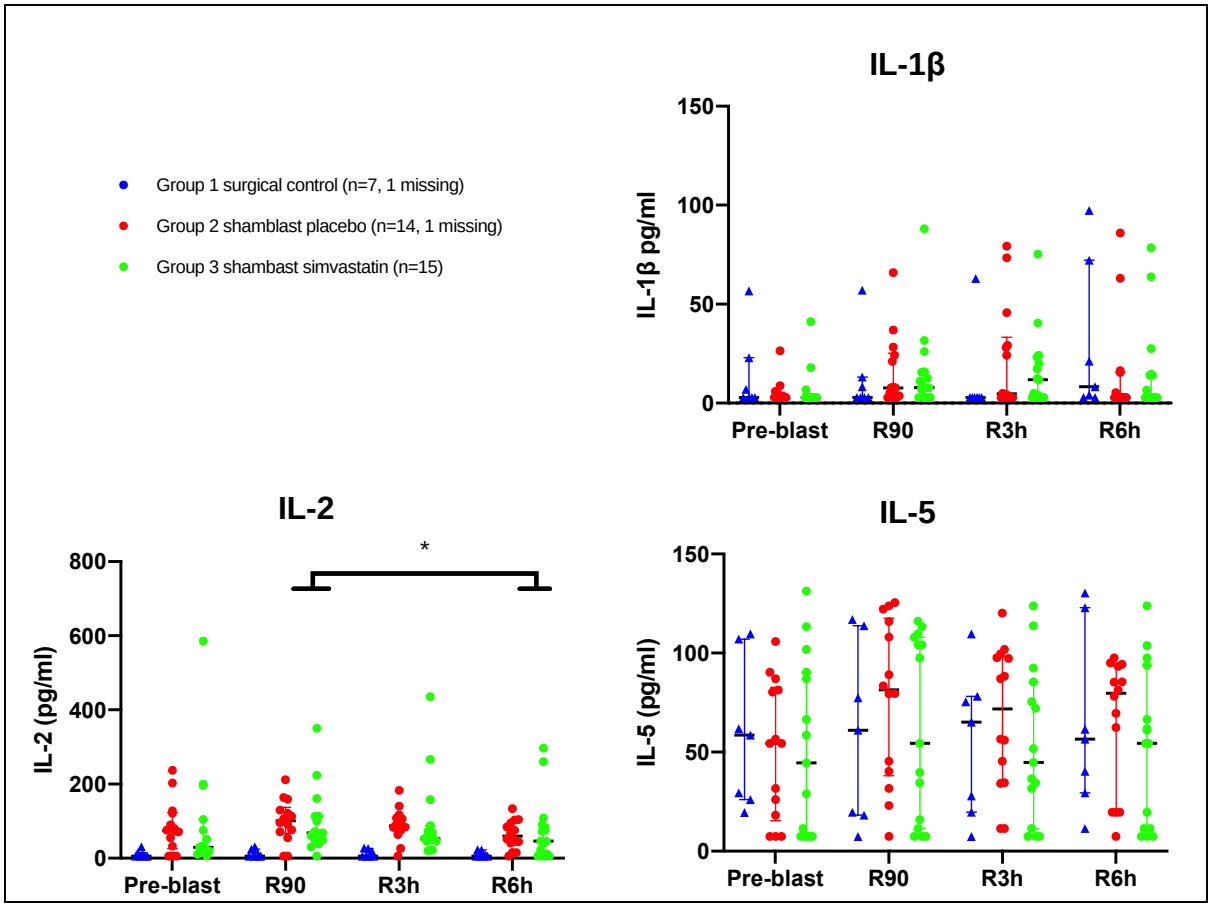

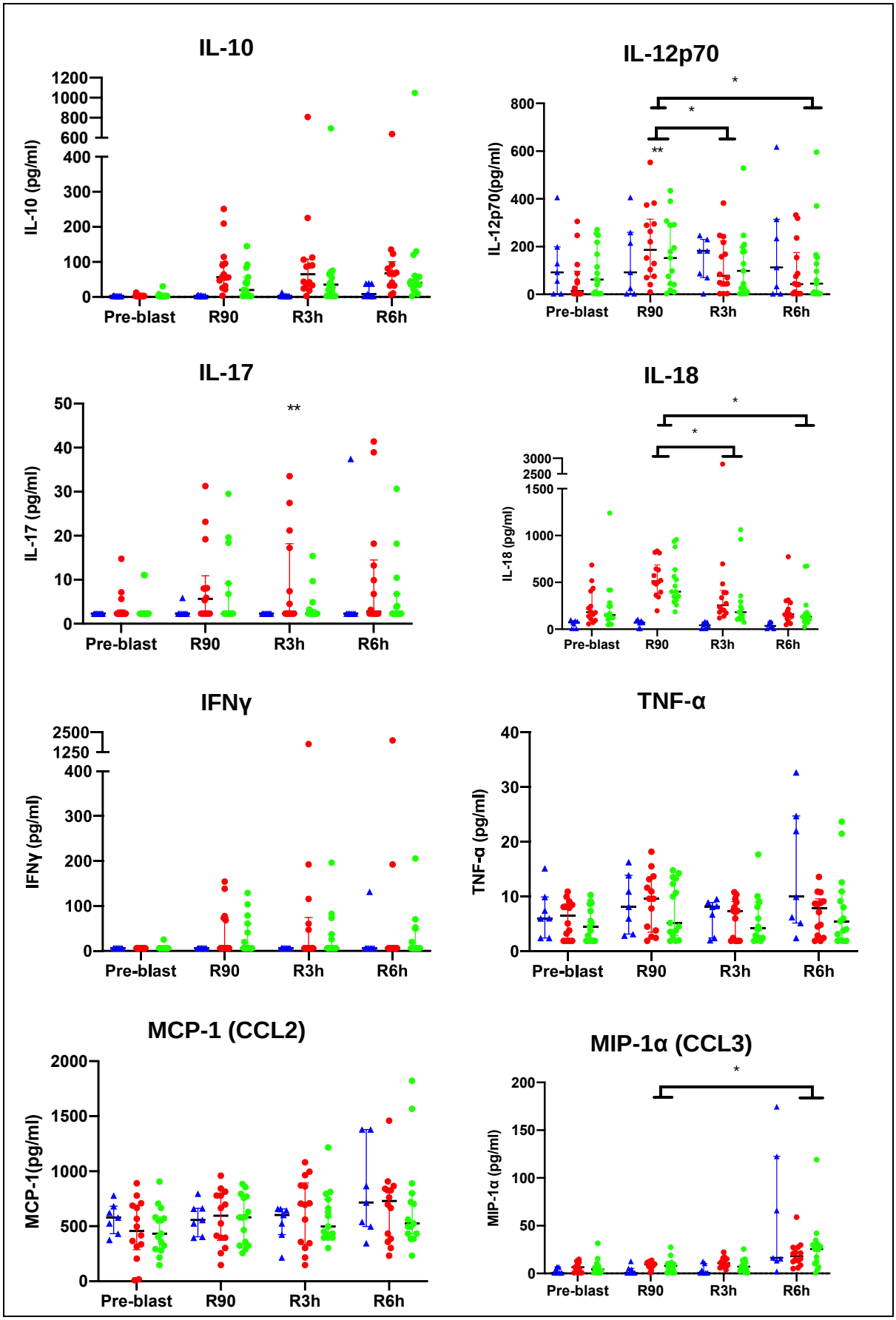
IL-10
IL-10 (pg/ml)
1200
1000
800
600
400
300
200
100
0
Pre-blast
R90
R3h
R6h
IL-12p70
IL-12p70(pg/ml)
800
600
400
200
0
*
*
**
Pre-blast
R90
R3h
R6h
IL-17
IL-17 (pg/ml)
50
40
30
20
10
0
**
Pre-blast
R90
R3h
R6h
IL-18
IL-18 (pg/ml)
3000
2500
1500
1000
500
0
*
*
Pre-blast
R90
R3h
R6h
IFNγ
IFNγ (pg/ml)
2500
1250
400
300
200
100
0
Pre-blast
R90
R3h
R6h
TNF-α
TNF-α (pg/ml)
40
30
20
10
0
Pre-blast
R90
R3h
R6h
MCP-1 (CCL2)
MCP-1(pg/ml)
2000
1500
1000
500
0
Pre-blast
R90
R3h
R6h
MIP-1α (CCL3)
MIP-1α (pg/ml)
200
150
100
50
0
*
Pre-blast
R90
R3h
R6h

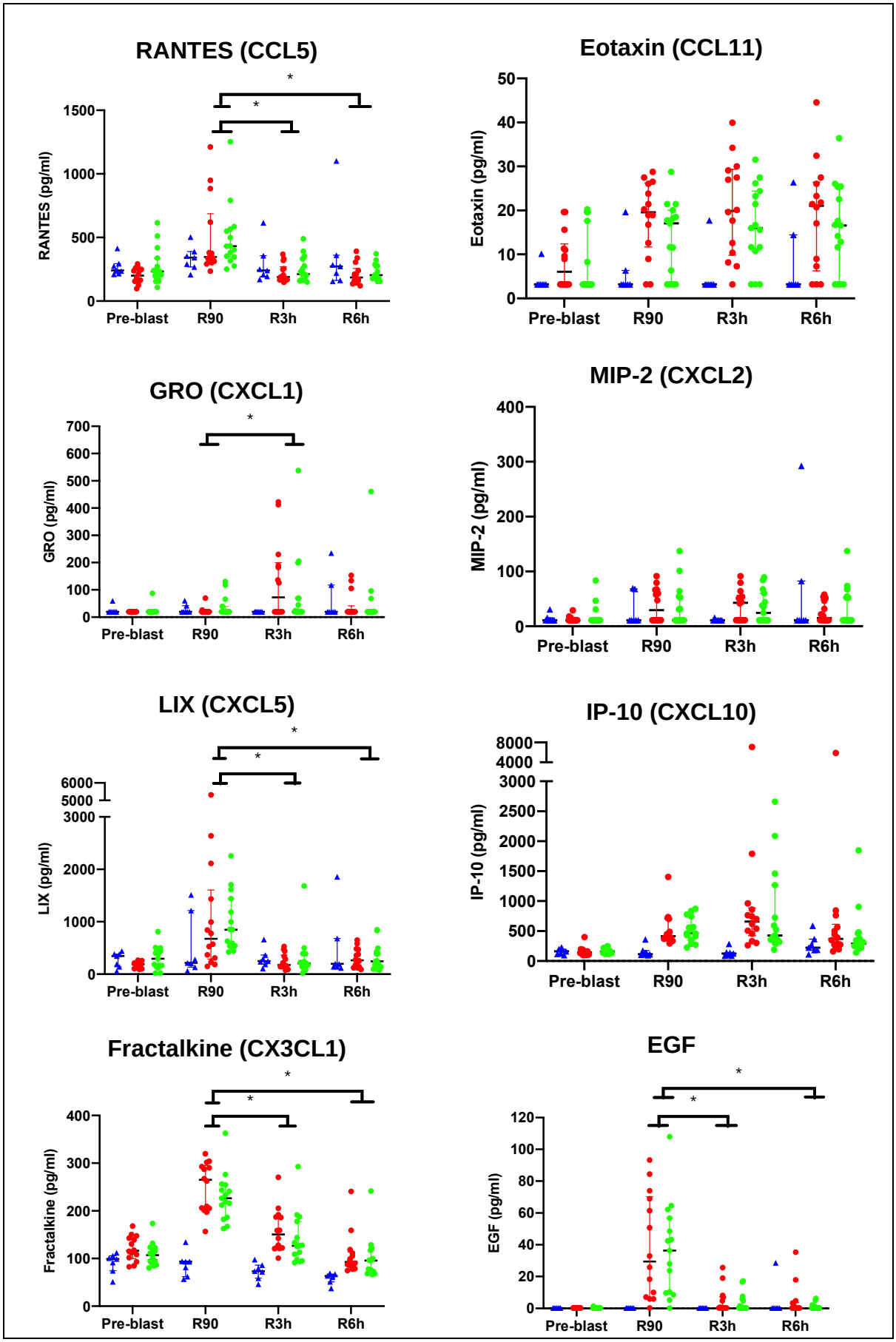
RANTES (CCL5)
RANTES (pg/ml)
1500
1000
500
0
Pre-blast
R90
R3h
R6h
*
Eotaxin (CCL11)
Eotaxin (pg/ml)
50
40
30
20
10
0
GRO (CXCL1)
GRO (pg/ml)
700
600
500
400
300
200
100
MIP-2 (CXCL2)
MIP-2 (pg/ml)
LIX (CXCL5)
LIX (pg/ml)
6000
5000
3000
2000
1000
IP-10 (CXCL10)
IP-10 (pg/ml)
8000
4000
Fractalkine (CX3CL1)
Fractalkine (pg/ml)
EGF
EGF (pg/ml)
120
100
80
60
40
20

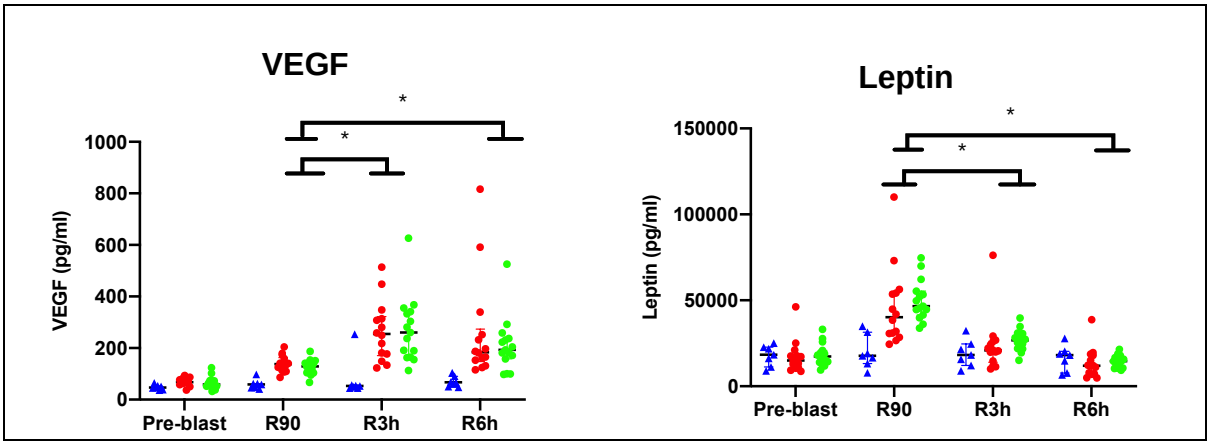

Figure 36 Plasma concentration of inflammatory mediators recorded over time in the uninjured surgical control group and the two injured groups (sham blast) treated respectively with simvastatin and placebo.
Horizontal bars represent *post hoc* comparisons between two indicated time points for the combined injured groups. * indicates P<0.05 for any particular comparison. Data represented as median (25th – 75th percentile).

Analyte	Effect of time in Gp 1	Effect of treatment (Gp 2 vs 3) at pre-blast	Effect of treatment (Gp 2 vs 3) from R90 to R6h	Effect of time [1]R90 vs R3h/ [2]R90 vs R6h	Pattern of response (Gp 2 vs 3)
HMGB1	*NS*	*NS*	*NS*	*NS*	*NS*
IL-1β	*NS*	*NS*	*NS*	*NS*	*NS*
IL-2	*NS*	**NS*	*NS*	*[2]P=0.0050*	*NS*
IL-5	*^NS*	**NS*	*P=0.0063*	*NS*	*NS*
IL-10	*P=0.0370*	*NS*	*NS*	*NS*	*NS*
IL-12p70	*^NS.*	*NS*	*P=0.0161*	*[1,2]P=0.0016*	*NS*
IL-17	*NS*	*NS*	*P=0.0453*	*NS*	*NS*
IL-18	*NS*	**NS*	*NS*	*[1,2]P=0.0015*	*NS*
IFNγ	*NS*	*NS*	*NS*	*NS*	*NS*
TNF-α	*^NS*	**NS*	*NS*	*NS*	*NS*
MCP-1	*^NS*	**NS*	*NS*	*NS*	*NS*
MIP-1α	*P=0.0009*	**NS*	*NS*	*[2]P=0.0001*	*NS*
RANTES	*^NS*	**NS*	*NS*	*[1,2]P<0.0001*	*NS*
Eotaxin	*NS*	**NS*	*NS*	*NS*	*NS*
GRO	*NS*	*NS*	*NS*	*[1]P=0.0084*	*NS*
MIP-2	*NS*	*NS*	*NS*	*NS*	*NS*
LIX	*NS*	**P=0.0452*	*NS*	*[1,2]P<0.0001*	*NS*
IP-10	*^NS*	*NS*	*NS*	*NS*	*NS*
Fractalkine	*^P=0.0203*	**NS*	*NS*	*[1,2]P<0.0001*	*NS*
EGF	*NS*	*NS*	*NS*	*[1,2]P<0.0001*	*NS*
VEGF	*^NS*	**NS*	*NS*	*[1,2]P<0.0001*	*NS*
Leptin	*^NS*	**NS*	*NS*	*[1,2]P=0.0001*	*NS*

Table 18 Effect of treatment in sham blast injury strand.
Friedman's test for effect of time in Group 1, unless stated ^one way ANOVA. Mann-Whitney U test for Group 2 and 3 comparisons unless stated *t-test. Analysis of covariance for effect of time, group and pattern for R90 to R6h. NS, not significant (*P>0.05*).

3.3.4.2. Effect of treatment in blast injury strand

To determine the effect of simvastatin pre-treatment in haemorrhage and tissue injury with concomitant thoracic blast injury, comparison was made between Groups 4 (placebo) and 5 (simvastatin). For the ease of description but not direct comparison, the significant changes in R90 with R3h and R6h comparisons noted in sham blast strand were also seen here (see section 3.3.4.1, Figure 37 and Figure 38). However, the exception is VEGF where the significance difference was only seen at R90 to R6h comparison.

There was no significant difference between Groups 4 and 5 at the four time points and in the pattern of response, to demonstrate an effect of treatment (Table 19).

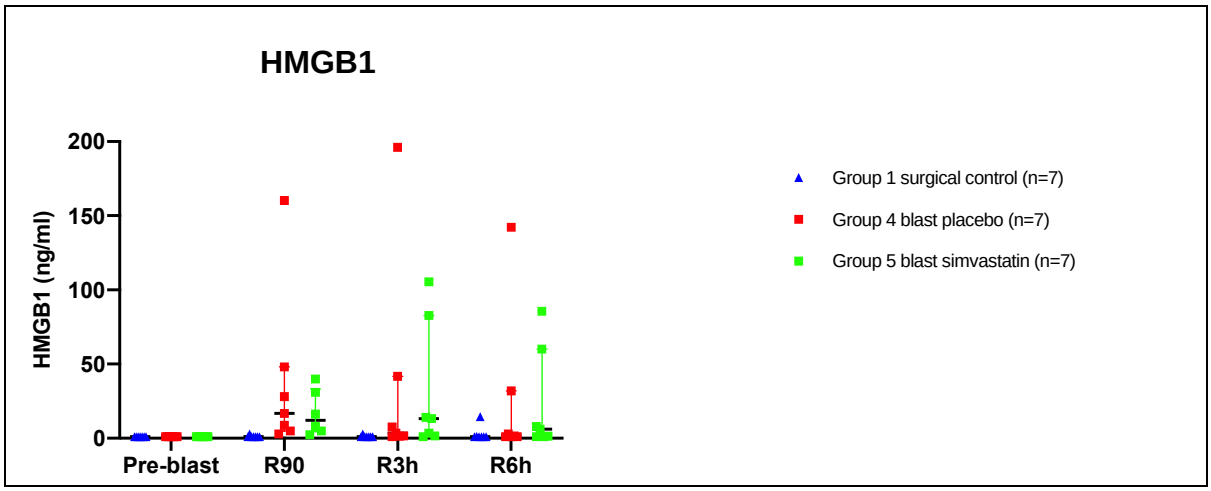

Figure 37 Plasma HMGB1 level recorded over time in the uninjured surgical control group and the two injured groups (blast) treated respectively with simvastatin and placebo. Data represented as median (25th – 75th percentile).

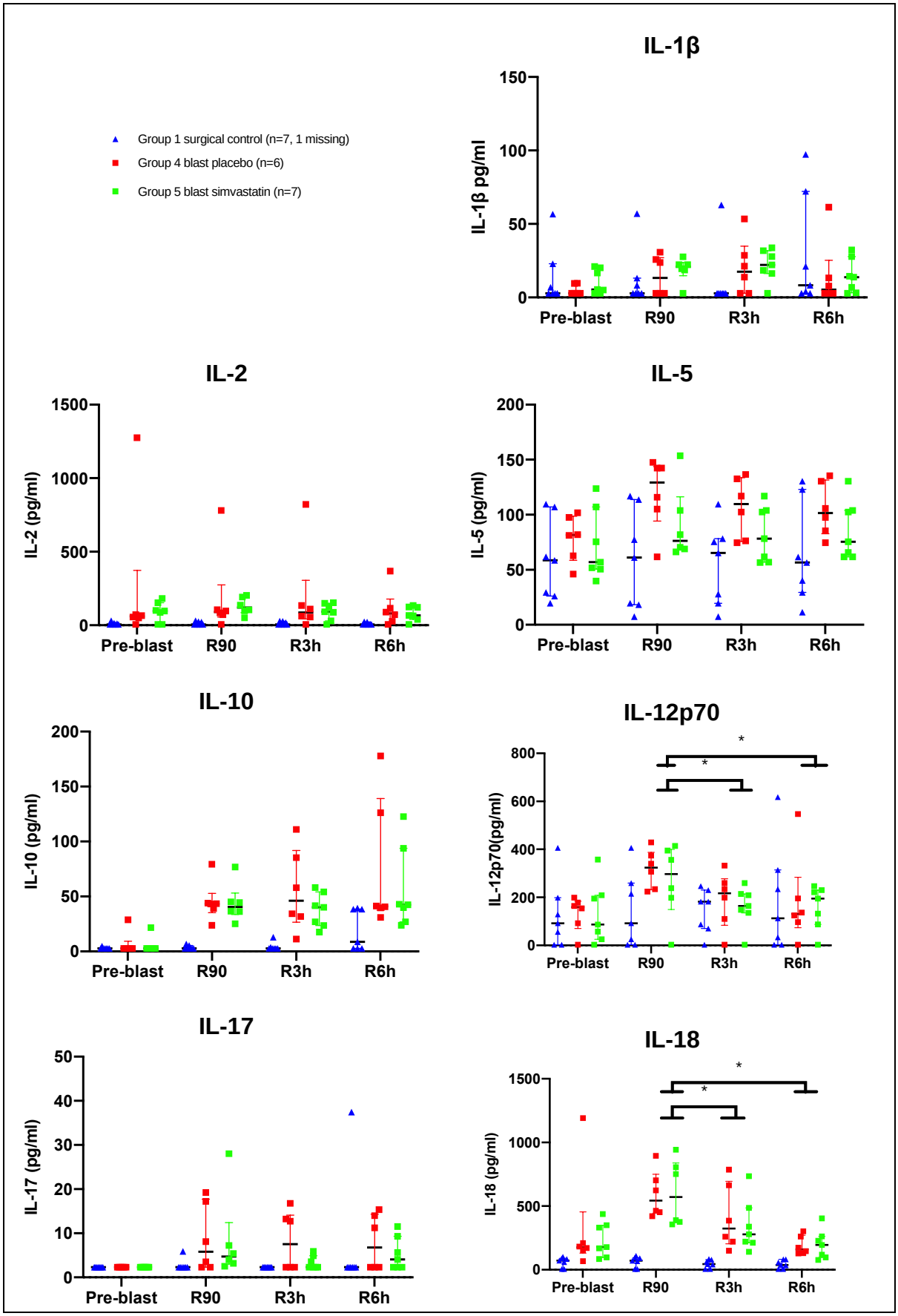
Group 1 surgical control (n=7, 1 missing)
Group 4 blast placebo (n=6)
Group 5 blast simvastatin (n=7)
IL-1β
IL-1β pg/ml
150
100
50
0
Pre-blast
R90
R3h
R6h
IL-2
IL-2 (pg/ml)
1500
1000
500
0
IL-5
IL-5 (pg/ml)
200
150
100
50
IL-10
IL-10 (pg/ml)
IL-12p70
IL-12p70(pg/ml)
800
600
400
200
*
IL-17
IL-17 (pg/ml)
50
40
30
20
10
IL-18
IL-18 (pg/ml)

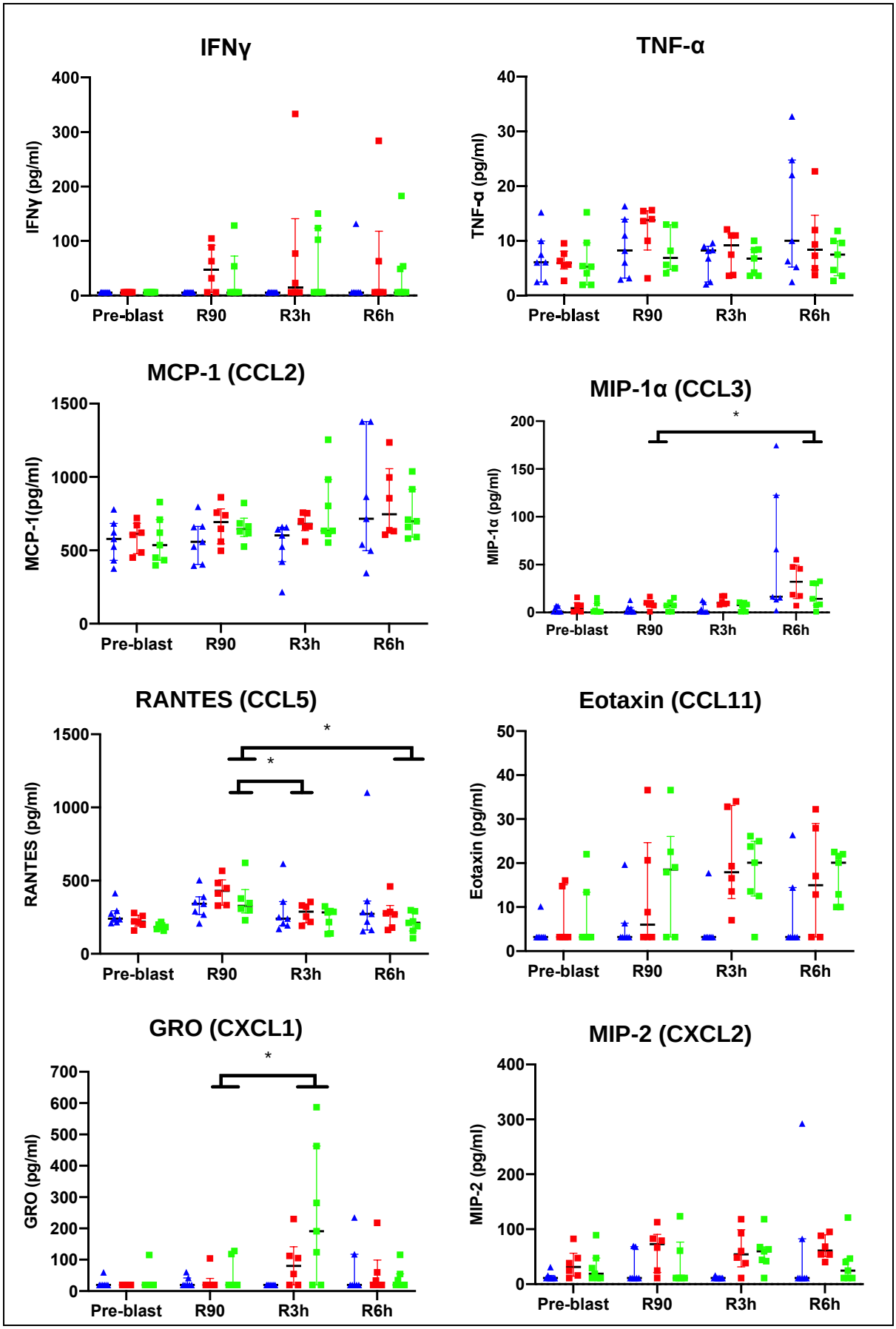
IFNγ
IFNγ (pg/ml)
400
300
200
100
0
Pre-blast
R90
R3h
R6h
TNF-α
TNF-α (pg/ml)
40
30
20
10
0
Pre-blast
R90
R3h
R6h
MCP-1 (CCL2)
MCP-1(pg/ml)
1500
1000
500
0
Pre-blast
R90
R3h
R6h
MIP-1α (CCL3)
MIP-1α (pg/ml)
200
150
100
50
0
*
Pre-blast
R90
R3h
R6h
RANTES (CCL5)
RANTES (pg/ml)
1500
1000
500
0
*
*
Pre-blast
R90
R3h
R6h
Eotaxin (CCL11)
Eotaxin (pg/ml)
50
40
30
20
10
0
Pre-blast
R90
R3h
R6h
GRO (CXCL1)
GRO (pg/ml)
700
600
500
400
300
200
100
0
*
Pre-blast
R90
R3h
R6h
MIP-2 (CXCL2)
MIP-2 (pg/ml)
400
300
200
100
0
Pre-blast
R90
R3h
R6h

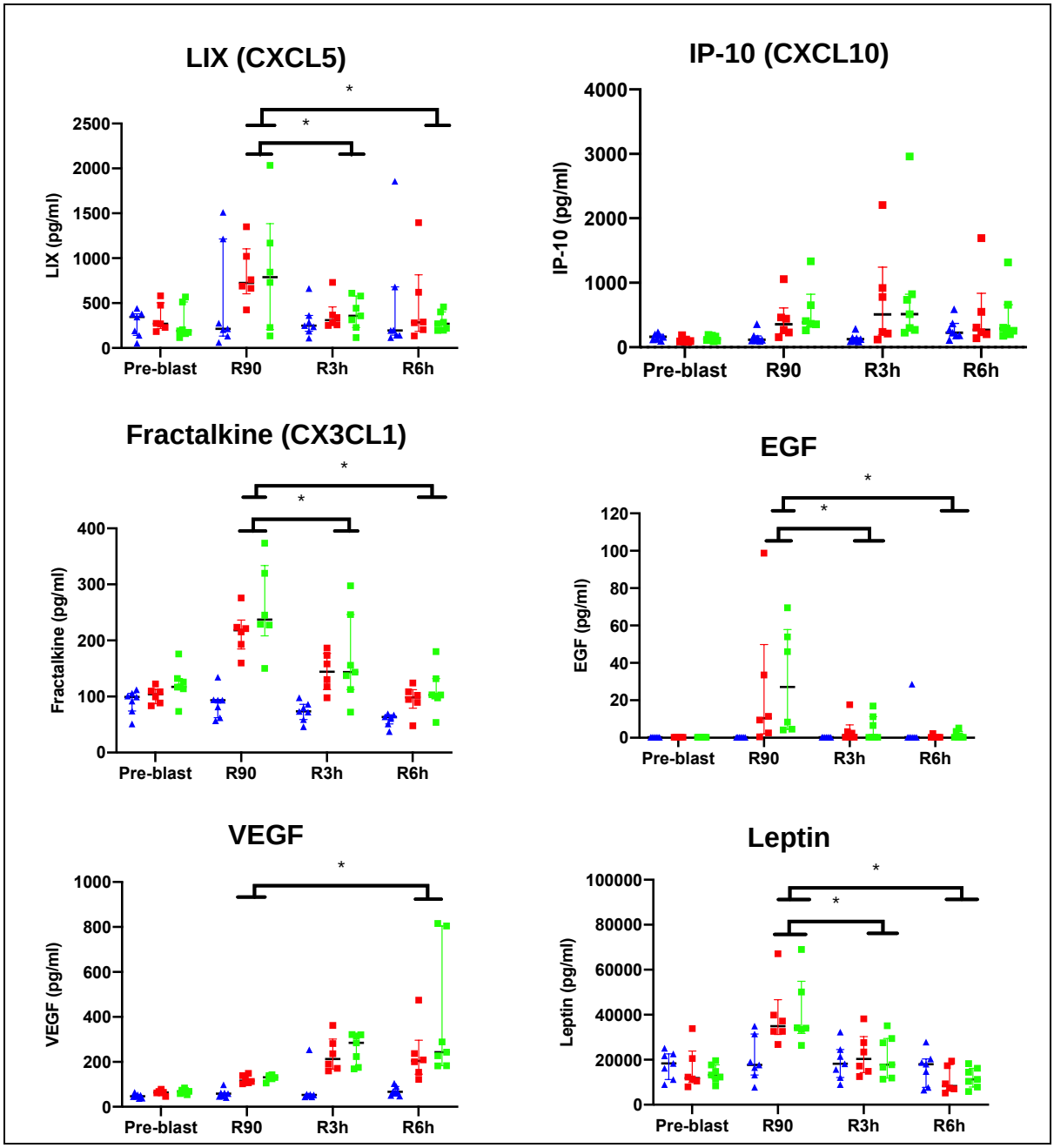

Figure 38 Plasma concentration of inflammatory mediators recorded over time in the uninjured surgical control group and the two injured groups (blast) treated respectively with simvastatin and placebo.
Horizontal bars represent *post hoc* comparisons between two indicated time points for the combined injured groups. * indicates P<0.05 for any particular comparison. Data represented as median (25th – 75th percentile).

Analyte	Effect of time in Group 1	Effect of treatment (Gp 4 vs 5) at pre-blast	Effect of treatment (Gp 4 vs 5) from R90 to R6h	Effect of time [1]R90 vs R3h/ [2]R90 vs R6h	Pattern of response (Gp 4 vs 5)
HMGB1	*NS*	*NS*	*NS*	*NS*	*NS*
IL-1β	*NS*	*NS*	*NS*	*NS*	*NS*
IL-2	*NS*	*NS*	*NS*	*NS*	*NS*
IL-5	*^NS*	*NS*	*P=0.0184*	*NS*	*NS*
IL-10	*P=0.0370*	*NS*	*NS*	*NS*	*NS*
IL-12p70	*^NS*	*NS*	*NS*	*[1,2]P=0.0079*	*NS*
IL-17	*NS*	*NS*	*NS*	*NS*	*NS*
IL-18	*NS*	*NS*	*NS*	*[1,2]P<0.0001*	*NS*
IFNγ	*NS*	*NS*	*NS*	*NS*	*NS*
TNF-α	*^NS*	*NS*	*NS*	*NS*	*NS*
MCP-1	*^NS*	*NS*	*NS*	*NS*	*NS*
MIP-1α	*P=0.0009*	*NS*	*NS*	*[2]P<0.0001*	*NS*
RANTES	*^NS*	*NS*	*NS*	*[1,2]P=0.0002*	*NS*
Eotaxin	*NS*	*NS*	*NS*	*NS*	*NS*
GRO	*NS*	*NS*	*NS*	*[1]P=0.0091*	*NS*
MIP-2	*NS*	*NS*	*NS*	*NS*	*NS*
LIX	*NS*	*NS*	*NS*	*[1,2]P=0.0065*	*NS*
IP-10	*^NS*	*NS*	*NS*	*NS*	*NS*
Fractalkine	*^P=0.0203*	*NS*	*NS*	*[1,2]P<0.0001*	*NS*
EGF	*NS*	*NS*	*NS*	*[1,2]P=0.0021*	*NS*
VEGF	*^NS*	*NS*	*NS*	*[2]P=0.0052*	*NS*
Leptin	*^NS*	*NS*	*NS*	*[1,2]P=0.0006*	*NS*

Table 19 Effect of treatment in blast injury strand.
Friedman's test for effect of time in Group 1, unless stated ^one way ANOVA. Mann-Whitney U test for Group 4 and 5 comparisons unless stated *t-test. Analysis of covariance for effect of time, group and pattern for R90 to R6h. NS, not significant (*P>0.05*).

3.4. Tissue proteins

3.4.1. Sham blast injury strand

3.4.1.1. Heme oxygenase (HO-1)

Heme oxygenase (HO-1) was detected in all liver samples taken 6 hours post resuscitation (Figure 39). One animal appeared to be an outlier in Group 1. Overall there was a significant difference between groups in liver HO-1 levels (*P*=0.0204, Kruskall-wallis), due to liver HO-1 was significantly increased in both injured groups (Groups 2 and 3) compared to the control group (Group 1). HO-1 was detected in small bowel across the groups, however there were no significant difference

(*P*=0.9214) between groups to indicate an effect of injury nor treatment. HO-1 was not detected in kidney samples from any groups (data not shown).

3.4.1.2. IL-6 and TNF-α

IL-6 was detected in liver and kidney, and TNF-α were detected in liver in all three groups (Figure 39). The same animal appeared to be an outlier in both kidney and liver IL-6. There was no significant difference between groups in liver IL-6 (*P*=0.1749) or TNF-α (*P*=0.6788), suggesting that neither injury nor drug treatment had an effect on IL-6 and TNF-α in these tissues. IL-6 was significantly different between groups (*P*=0.0018) in the kidney, the difference being between surgical control (Group 1) and injury (Groups 2 or 3). However, there was no significant difference between Groups 2 and 3 to suggest effect of treatment.

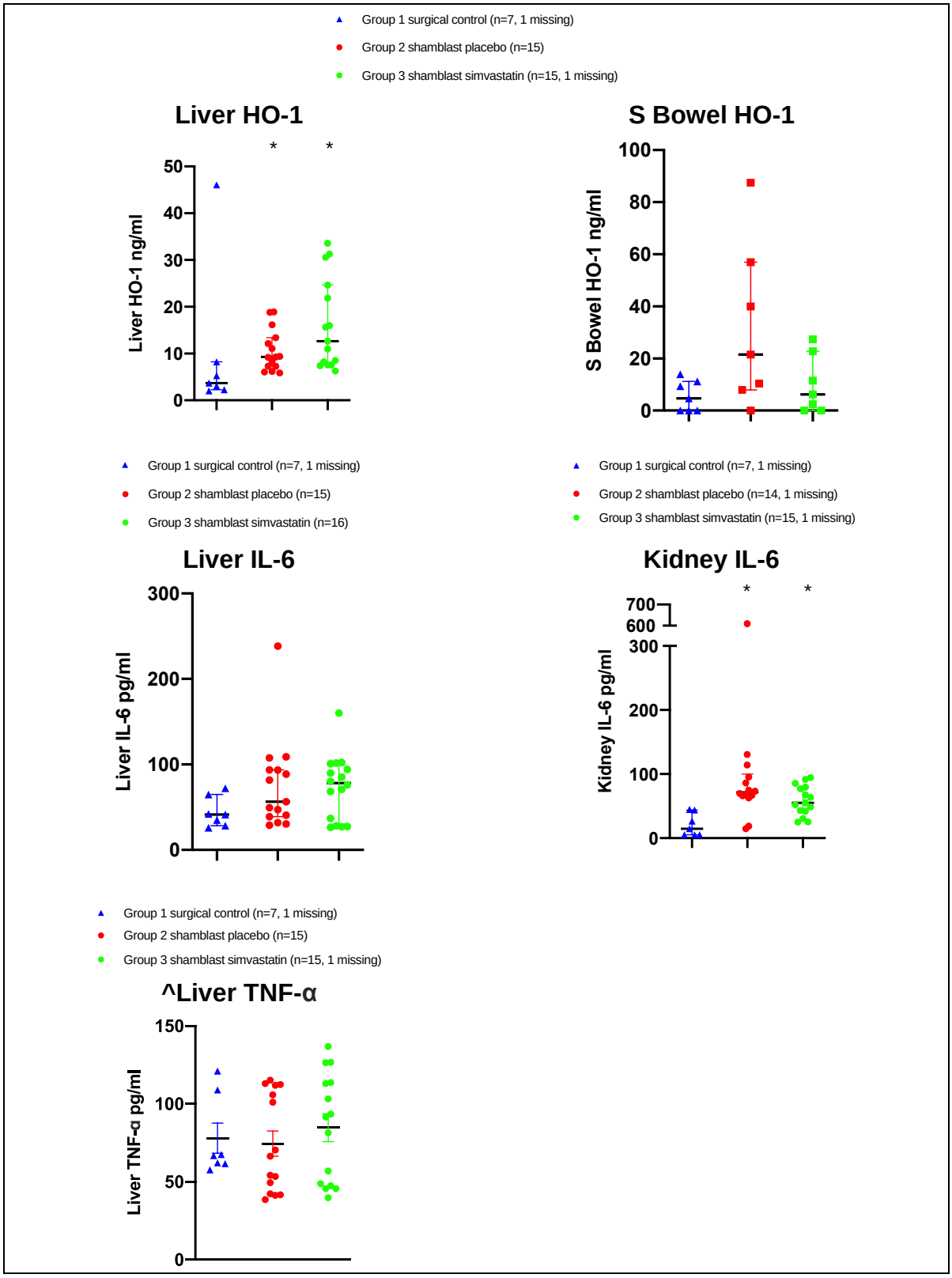

Figure 39 Protein expression in tissues for animals with or without haemorrhage and femur fracture.
Data expressed as median (25th – 75th percentile), unless stated ^mean±SEM. Kruskal-wallis one-way analysis of variance on ranks for non-parametric data and one-way ANOVA for parametric data. *P<0.05 as statistically significant when compared to surgical control Group 1.

3.4.2. Blast injury strand

3.4.2.1. Heme oxygenase (HO-1)

Similar levels of HO-1 was detected in all three groups in liver (*P*=0.0874) and small bowel (*P*=0.1483) (Figure 40).

3.4.2.2. IL-6 and TNF-α

There was no effect of injury or treatment on liver IL-6 (*P*=0.5384) or TNF-α (*P*=0.0774) (Figure 40). IL-6 was significantly different between groups (*P*=0.0011) in the kidney, the difference being between surgical control (Group 1) and injury (Groups 4 or 5). However, there was no significant difference between Groups 4 and 5 to suggest effect of treatment.

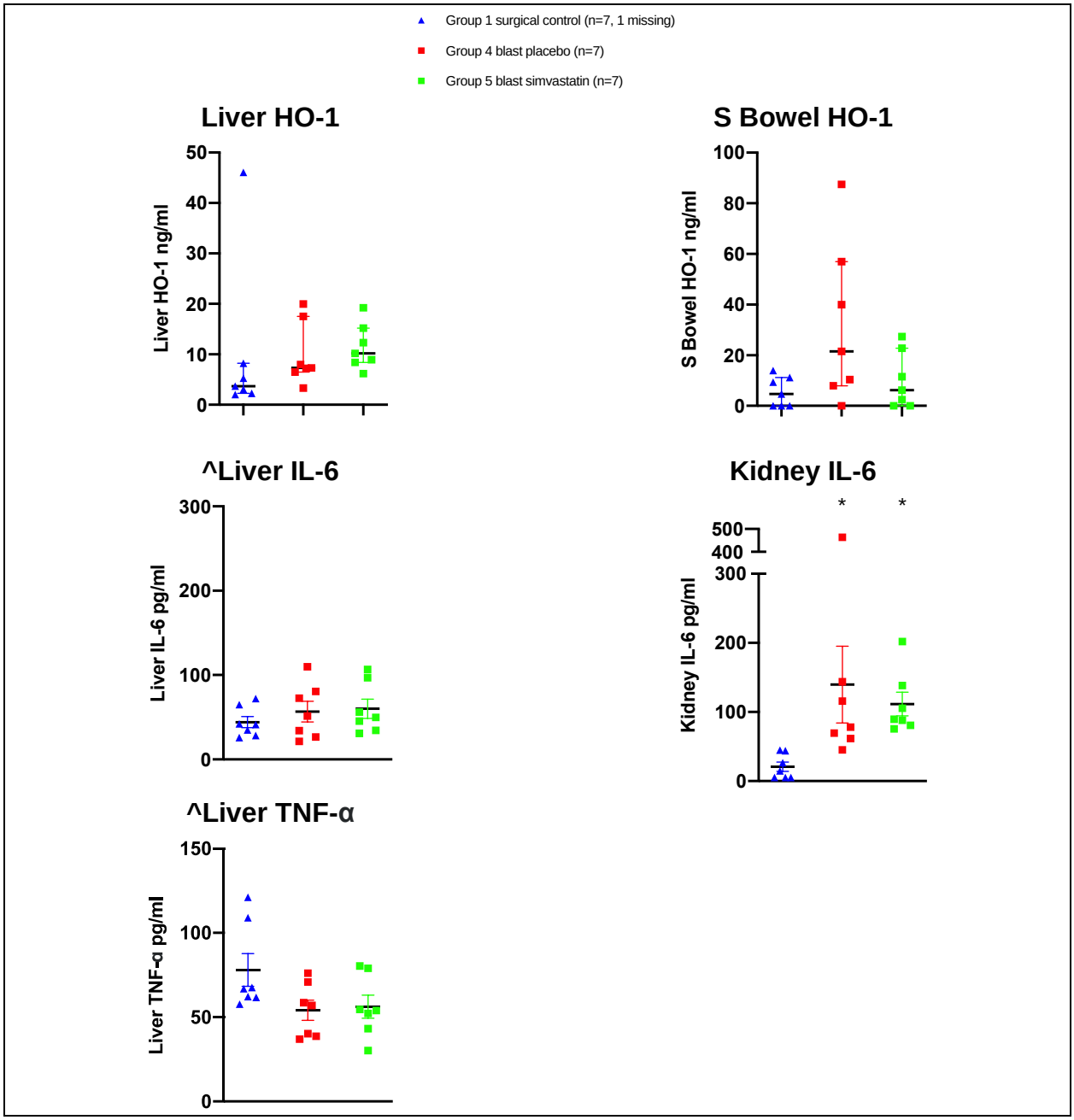

Figure 40 Protein expression in tissues for animals with or without thoracic blast, haemorrhage and femur fracture.
Data expressed as median (25th – 75th percentile), unless stated ^mean±SEM. Kruskal-wallis one way analysis of variance on ranks for non-parametric data and one-way ANOVA for parametric data. *P<0.05 as statistically significant when compared to surgical control Group 1.

3.5. Gene array analysis

3.5.1. Sham blast injury strand

Genes were down-selected from the arrays if their expression changed 3-fold, in either direction, in the placebo Group 2 compared to surgical control Group 1 (Table 20). These were then tested for statistical significance using analysis of variance to determine the effect of haemorrhage and tissue injury.

Three genes (Tp63, Cidea, Lta) from the apoptosis panel had significantly changed in the kidney and liver. Expression of Tp63 was significantly reduced (11-fold downregulated) in the kidney but significantly increased (8-fold) in the liver.

13 genes from the inflammation panel showed statistically significant changes in kidney, liver and lungs. Significant changes in Sele, Cxcl5 and IL-9 were seen in more than one organ, however IL-9 was upregulated (23-fold) in liver but downregulated in the lungs. The majority of the inflammatory genes were otherwise upregulated, particularly Fos (34-fold) and Ptgs2 (15-fold) in liver. Overall, these findings indicate that the haemorrhage and tissue injury resulted in clear evidence of modulation of genes associated with inflammation, but relatively little evidence of modulation of genes associated with apoptosis.

Comparison between Groups 2 and 3 of the fold changes in the 13 genes described above showed no statistically significant differences between groups for any of the genes. Four additional genes (cxcl2 in lung, cxcr1 in kidney, fadd in liver and trl5 in small intestine) showed a 3-fold change when compared between the simvastatin treated animals (Group 3) and the surgical controls (Group 1). However, although some of these genes also showed a statistically significant difference when comparing Groups 3 and 1, there were no significant difference between Groups 2

and 3. Overall, pre-treatment with simvastatin did not affect the transcriptional response to haemorrhage and tissue injury in the genes and organs studied here.

		Down-selected genes with 3 fold or more change Gp 2 ShB placebo vs Gp 1 surgical control				Down-selected genes with 3 fold or more change Gp 3 ShB simvastatin vs Gp 1 surgical control			
Panel	**Gene**	**SBowel**	**Kidney**	**Liver**	**Lung**	**SBowel**	**Kidney**	**Liver**	**Lung**
I	Ccl11		0.2817*						
I	Ccl19		3.8921*			0.2378			
I	Ccl20	0.2614		0.2959			3.3493		
I	Ccl7			7.9284*					
I	Ccr1			3.3237*					
A	Cidea		0.0875*						
I	Crp		0.2906		4.1932				
I	Cxcl1		4.3591*						
I	Cxcl2								4.5450*#
I	Cxcl5		12.3374*	5.3847*					
I	Cxcr1						0.3196		
A	Fadd							3.0274	
I	Fos			34.3470*					
I	IL22		0.2201*						
I	IL6		9.1186*						
I	Il9			23.3745*	0.2975*				
I	Kng1		4.3877*						
A&I	Lta	0.2845	0.3041						
A	Naip6	0.3045							
I&C	Nos2			3.5396					
I	Ptgs2			15.1180*					
I	Sele			4.9900 *	5.2307*				
I	Tlr5					0.2885#			
A	Tp63		0.0837*	8.2431*					

Table 20 Down-selected genes with 3 fold or more changes in sham blast injury strand. I, inflammatory; A, apoptosis; C, custom. Red denotes upregulation, blue downregulation. ANOVA. *P<0.05 Group 2 versus Group 1, #P<0.05 Group 3 versus Group 1, ▲Group 2 versus Group 3.

3.5.2. Blast injury strand

Genes were down-selected from the arrays if their expression changed 3-fold, in either direction, in the placebo-treated Group 4 compared to the surgical control

Group 1 (Table 21). These were then tested for statistical significance using analysis of variance to determine the effect of thoracic blast, haemorrhage and tissue injury.

Most of the genes that had the requisite 3-fold change and statistically significant differences were from the inflammatory panel, with the majority being upregulated, particularly IL-9 (20-fold), Fos (11-fold), Ptgs2 (9-fold) in the liver. Sele and Cxcl5 were upregulated in the liver and lungs. Overall, these findings indicate that the combined thoracic blast, haemorrhage and tissue injury in Group 4 resulted in clear evidence of modulation of genes associated with inflammation, but again relatively little evidence of modulation of genes associated with apoptosis.

Of the down-selected genes listed above (those that showed statistically significant 3-fold changes between placebo-treated and surgical control groups), further analysis comparing placebo (Group 4) vs simvastatin (Group 5) revealed significant difference in the expression of Tlr5 and Ccl11. A further analysis comparing the simvastatin-treated Group 5 to the surgical controls (Group 1) revealed 13 additional genes were altered 3-fold in at least one of the four organs that were assessed. Amongst these latter 13 genes, the difference in the expression of 5 of the genes was statistically significantly different between Groups 4 (placebo) and 5 (simvastatin). Therefore, from all the genes examined, a total of 7 genes showed statistically significant differences between simvastatin and placebo-treated groups (Groups 4 and 5).

		Down-selected genes with 3 fold or more change Gp 4 B placebo vs Gp 1 surgical control				Down-selected genes with 3 fold or more change Gp 5 B simvastatin vs Gp 1 surgical control			
Panel	**Gene**	**SBowel**	**Kidney**	**Liver**	**Lung**	**SBowel**	**Kidney**	**Liver**	**Lung**
A	Abl1								3.0449
A	Bnip3					**3.0555*#▲**			
I	Ccl11			0.1978*▲					
I	Ccl19						3.9849*#		
I	Ccl20		10.8044						
I	Ccl24							0.2286*#	
I	Ccl7			7.2815*					
I	Ccr1							3.3296*#	
I	Ccr3				0.3103*				
A	Cidea						0.2188		
I	CRP						0.1835		3.4704
I	Cxcl1		4.2584		5.2037*				
I	Cxcl2				4.7842*				
I	Cxcl3				4.0816*			0.3075	
I	Cxcl5		4.5884	4.5258*	4.5262*				
I	Cxcr1						0.1808		
I	Fos			11.8950*					
I	IL17a		0.3224	0.2184*					
I	IL22		0.1221*	0.2661		0.2130#			
I	IL6		15.8165*					3.1570#	
I	IL9			20.5902*					
I	Kng1						**4.1970*#▲**		
A&I	Lta			0.2625*		**0.2298#▲**			
A	Naip6	0.2677							
A&I	Nfkb1			3.8233					
I	Ptgs2			9.4173*					
I	Sele		4.2806*	4.4469	4.2475*				
I	Tlr5	0.3047*▲			0.3132			0.2108*#	
A&I	Tnf							**0.2756#▲**	
A	Tp63						0.0908#		
C	Thbd					0.3253			
C	Vcam1					**0.3073▲**			

Table 21 Down-selected genes with 3 fold change or more in blast injury strand.
I, inflammatory; A, apoptosis; C, custom. Red denotes upregulation, blue downregulation.
ANOVA. *P<0.05 Group 4 versus Group 1, #P<0.05 Group 5 versus Group 1, ▲Group 4 versus Group 5.

3.6. Imaging flow cytometry

There was no significant difference in the number of circulating endothelial cells (CECs) (*P*=0.2817), granulocytes (*P*=0.8637), neutrophils (*P*= 0.6700) or immature neutrophils (*P*=0.2578) between groups, suggesting that there was not an effect of injury nor treatment in sham blast injury strand (Figure 41). Overall, there was significant difference between groups for apoptotic cells (*P*=0.0410, Kruskall-Wallis) due to a difference between the surgical control (Group 1) and both injured groups (Groups 2 and 3). There were no significant difference between Groups 2 and 3 to suggest effect of treatment.

Similarly, in blast injury strand, there was no significant difference in CECs (*P*=0.1948), apoptotic cells (*P*=0.1215), granulocytes (*P*=0.2688), neutrophils (*P*=0.2792) and immature neutrophils (*P*=0.0770) between groups to indicate an effect of injury or treatment (Figure 42).

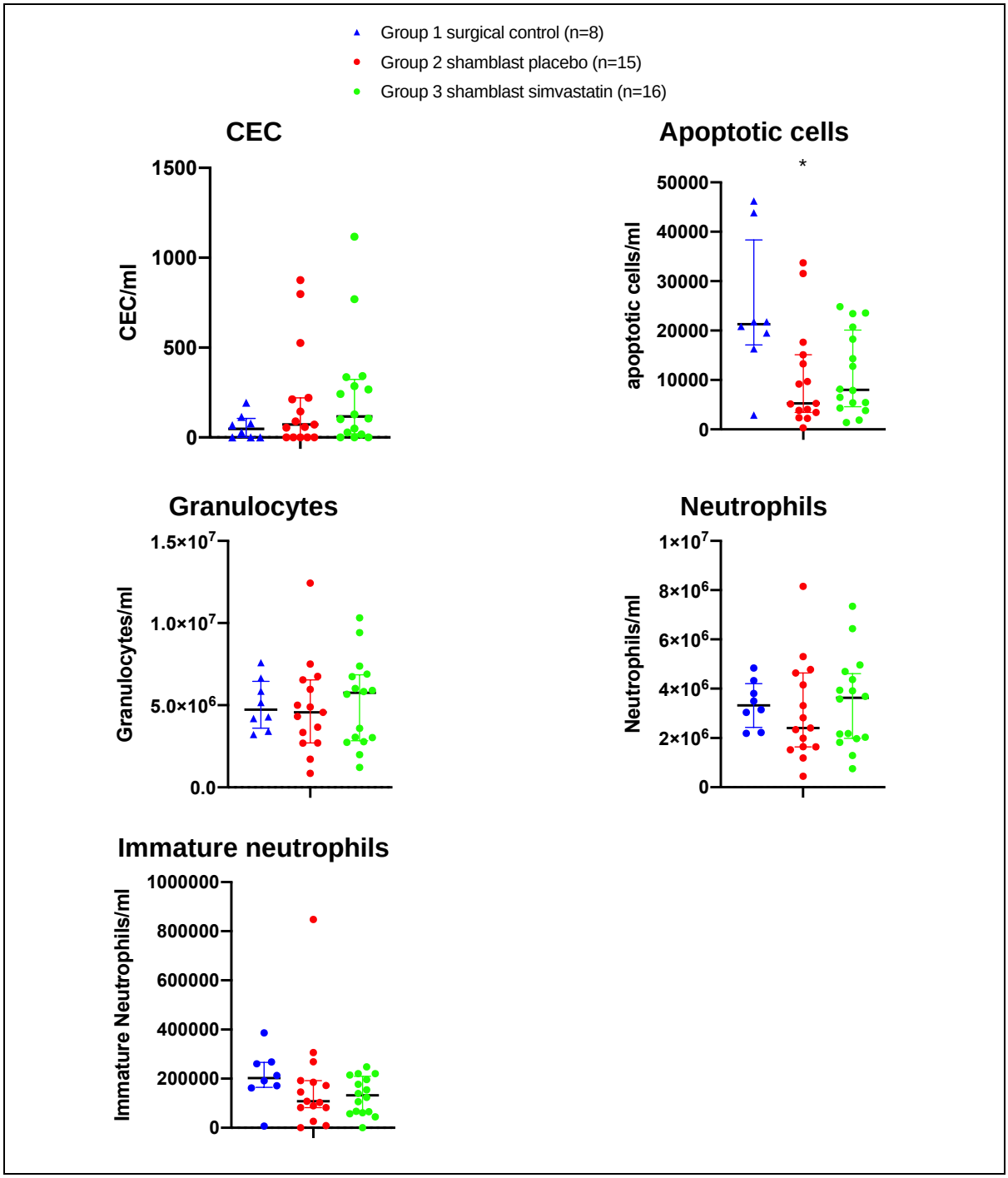

Figure 41 Imaging flow cytometry data presented in cell/ml after correction for blood volume dilution for animals with or without haemorrhage and femur fracture.
Data presented as median (25th – 75th percentile). *P<0.05 as statistically significant when compared to surgical control Group 1.

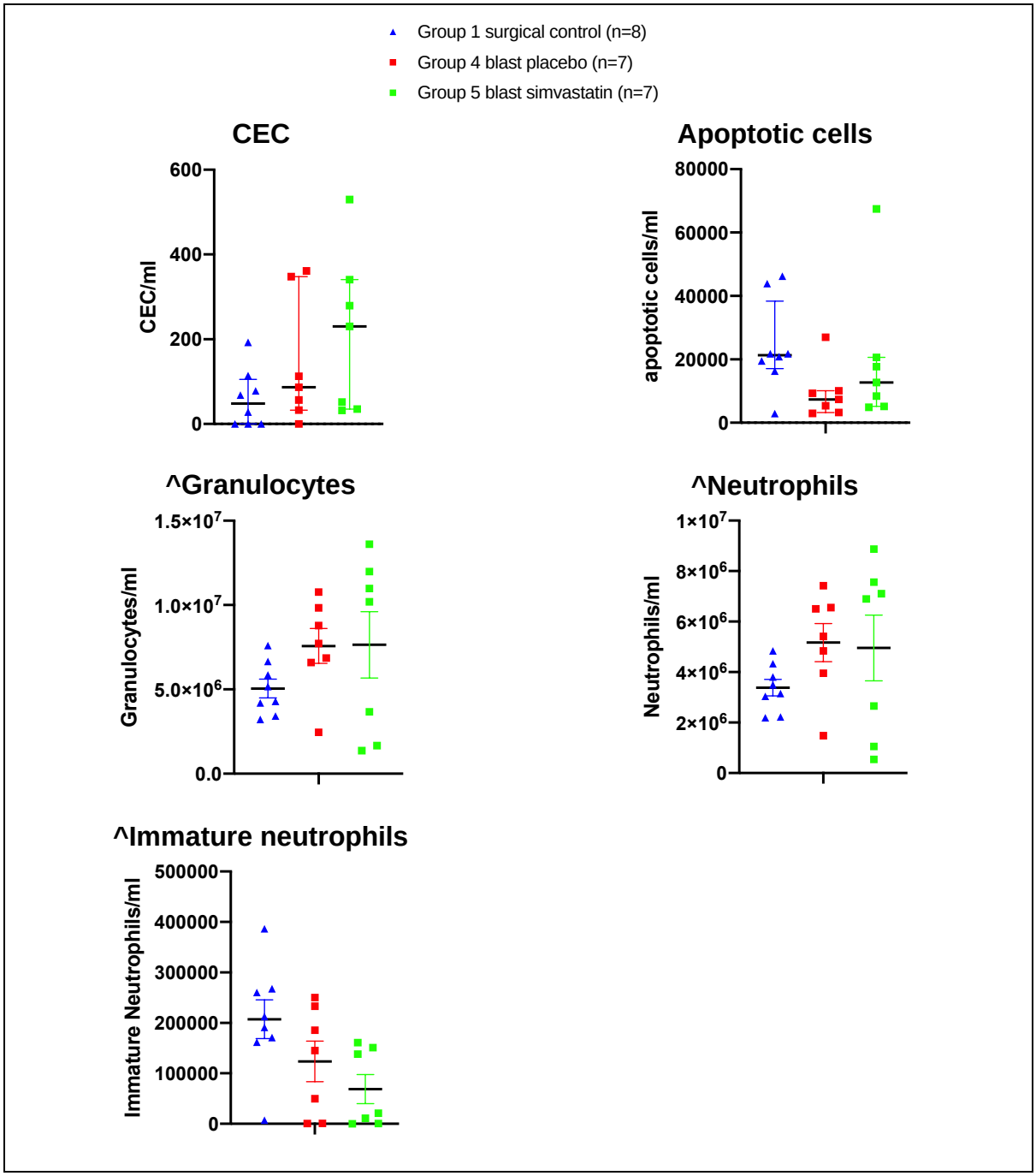

Figure 42 Imaging flow cytometry data presented in cell/ml after correction for blood volume dilution for animals with or without thoracic blast, haemorrhage and femur fracture. Data presented as median (25th – 75th percentile), unless stated ^mean±SEM.

3.7. Histology

3.7.1. Effect of surgery and anaesthesia

The histological changes in Group 1 were minimal in all tissues, except for the lungs where 50% of the animals had evidence of moderate pulmonary oedema (Figure 43A).

3.7.2. Effect of injury

Similar to the surgical control group, no histopathological findings were reported in small bowel, but moderate pulmonary oedema was observed in lungs (Figure 43B). In the liver and kidneys, more changes were noted in the sham blast injury strand (Group 2) when compared to surgical control (Group 1). In Group 2 there was a higher incidence of focal or multifocal hepatocellular necrosis and moderate vacuolation of cortical tubular epithelium.

The effect of blast was most noted in lungs (Figure 43C). 80% of animals of blast-exposed animals had alveolar haemorrhage which was not generally seen in surgical or sham blast groups. Again, there were higher incidences of moderate cortical tubular epithelium vacuolation and hepatocellular necrosis in the blast animals when compared to the surgical controls. See Table 22 - Table 24.

3.7.3. Effect of treatment

There were no consistent histopathological findings in any tissue to suggest an effect of drug (placebo vs simvastatin) treatment in either sham blast or blast injury strand. See Table 22 - Table 24.

3.7.4. Severity of histological changes in comparison to mediator levels (section 3.3)

Moderate hepatocellular necrosis (see 2.2.18) was observed in animals that had the highest concentration of DAMPS and inflammatory mediators or liver IL-6. One animal (ES149) from Group 2 consistently had the highest concentration of DAMPS and inflammatory mediators in plasma at various time points amongst the sham blast groups, as well as liver and kidney IL-6 concentrations. Moderate hepatocellular necrosis was noted in this animal, unlike the rest which had minimal to slight changes. However, there were no renal histopathological results to correlate to the kidney IL-6 expression due to missing tissue samples.

The highest concentration of DAMPS, plasma inflammatory mediators or liver IL-6 was observed in the animals (of Groups 3 and 4: ES100 and ES131, ES45) that also had moderate hepatocellular necrosis. By contrast, other animals of these groups had lower indices of damage and inflammation, and only minimal or slight histological changes.

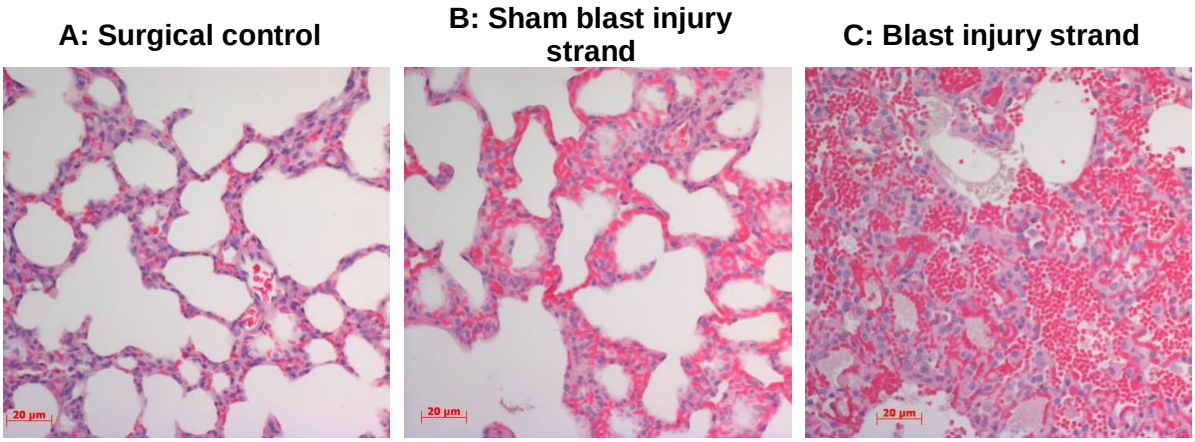

Figure 43 Histological changes in lung tissues. (A) Surgical control, (B) Sham blast injury strand, (C) Blast injury strand.

Group 1	Group 2	Group 3	Group 4	Group 5
Surgical control	***Sham Blast** + Tissue injury + HGE Placebo*	***Sham Blast** + Tissue injury + HGE Simvastatin*	***Blast** + Tissue injury + HGE Placebo*	***Blast** + Tissue injury + HGE Simvastatin*

Group	1	2	3	4	5
Necrosis, Hepatocellular, Foci					
Minimal	1	7	3	2	0
Slight	0	3	0	0	2
Moderate	0	1	2	0	1
Total (Relative %)	1 (13)	11 (79)	5 (36)	2 (33)	3 (60)
Necrosis, Hepatocellular, Centrilobular/Midzonal					
Slight	0	0	0	0	1
Moderate	0	0	0	1	0
Total (Relative %)	0 (0)	0 (0)	0 (0)	1 (17)	1 (20)
Necrosis, Hepatocellular, Centrilobular					
Minimal	0	0	0	1	0
Total (Relative %)	0 (0)	0 (0)	0 (0)	1 (17)	0 (0)
Infiltrate, Inflammatory Cell, Portal					
Minimal	1	1	2	2	0
Total (Relative %)	1 (13)	1 (7)	2 (14)	2 (33)	0 (0)
Leukocytosis, Sinusoidal					
Minimal	0	2	2	1	1
Total (Relative %)	0 (0)	2 (14)	2 (14)	1 (17)	1 (20)
Extramedullary Haemopoiesis					
Minimal	4	1	0	2	0
Total (Relative %)	4 (50)	1 (7)	0 (0)	2 (33)	0 (0)
Number of tissues examined	8	14	14	6	5

Table 22 Summary of histopathological findings in hepatic tissues taken at end of experiment.

Group	1	2	3	4	5
Vacuolation, Tubular Epithelium, Cortex					
Slight	7	3	1	1	1
Moderate	1	10	15	5	4
Total (Relative %)	8 (100)	13 (100)	16 (100)	6 (100)	5 (100)
Vacuolation, Tubular Epithelium, Medulla					
Minimal	1	8	11	4	3
Slight	1	3	4	2	2
Total (Relative %)	2 (25)	11 (85)	15 (94)	6 (100)	5 (100)
Dilatation, Tubular, Cortex					
Minimal	1	1	3	2	0
Slight	0	0	0	1	0
Total (Relative %)	1 (13)	1 (7)	3 (19)	3 (50)	0 (0)
Dilatation, Tubular, Medulla					
Minimal	0	0	0	1	0
Moderate	0	0	0	0	0
Total (Relative %)	0 (0)	0 (0)	0 (0)	1 (17)	0 (0)
Number of tissues examined	8	13	16	6	5

Table 23 Summary of histopathological findings in renal tissues taken at end of experiment.

Group	1	2	3	4	5
Pulmonary Oedema, Alveoli, Lumen					
Minimal	0	3	6	2	2
Slight	0	3	2	1	1
Moderate	4	2	2	0	2
Marked	0	0	0	1	0
Total (Relative %)	4 (50)	8 (57)	10 (71)	4 (80)	5 (100)
Pulmonary Oedema, Alveoli, Septal					
Minimal	0	3	5	2	1
Slight	4	7	6	1	3
Moderate	1	1	1	0	0
Total (Relative %)	5 (63)	11 (79)	12 (86)	3 (60)	4 (80)
Infiltrate, Inflammatory Cell, Alveoli, Septal					
Minimal	7	10	9	3	3
Slight	0	1	1	0	1
Total (Relative %)	7 (88)	11 (79)	10 (71)	3 (60)	4 (80)
Infiltrate, Inflammatory Cell, Perivascular					
Minimal	1	4	7	2	4
Slight	1	1	0	0	1
Total (Relative %)	2 (25)	5 (36)	7 (50)	2 (40)	5 (100)
Leukocytosis					
Minimal	3	2	3	1	2
Slight	1	1	0	0	1
Total (Relative %)	4 (50)	3 (21)	3 (21)	1 (20)	3 (60)
Haemorrhage, Alveoli,					
Minimal	0	0	0	0	1
Slight	1	0	0	1	0
Moderate	0	0	1	1	0
Marked	0	0	0	2	1
Total (Relative %)	1 (13)	0 (0)	1 (7)	4 (80)	2 (40)
Number of tissues examined	8	14	14	5	5

Table 24 Summary of histopathological findings in pulmonary tissues taken at end of experiment.

3.8. Simvastatin assay

Simvastatin was detected in plasma at below assay calibrated range (data not presented). Its active metabolite simvastatin hydroxy acid was detected in all the animals that received treatment, ranging from below the calibrated range of 5ng/ml to 46.2ng/ml (Figure 44).

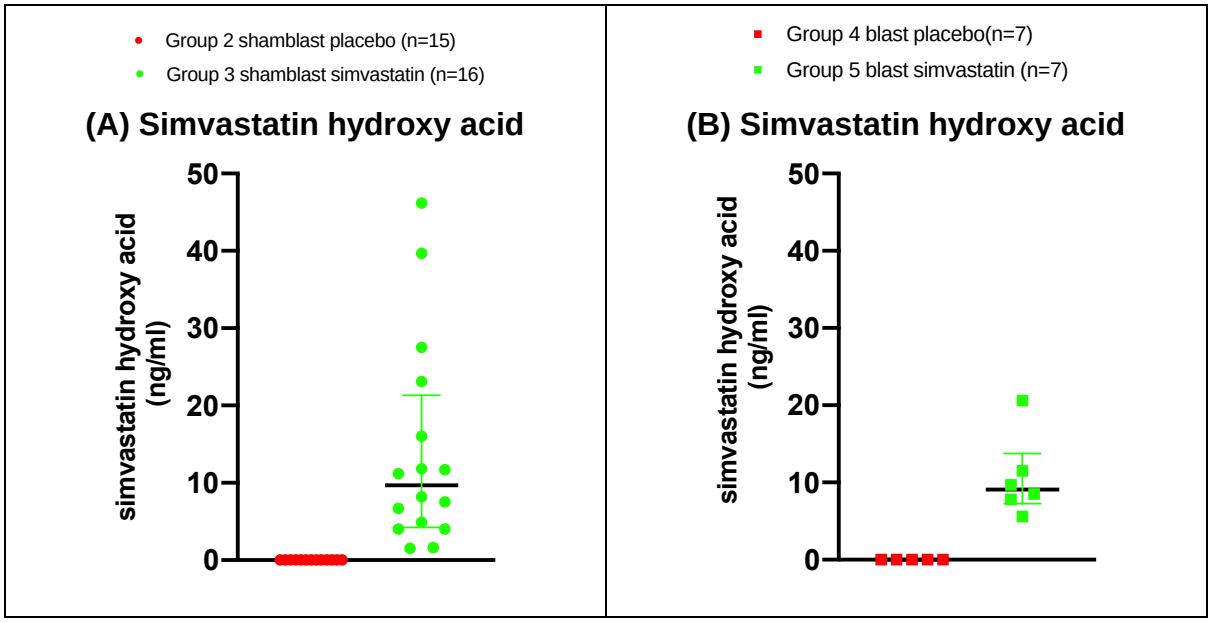

Figure 44(A) Plasma level of simvastatin hydroxy acid in sham blast injury strand (Groups 2, 3). (B) Plasma level of simvastatin hydroxy acid in blast injury strand (Groups 4, 5). Data presented as median (25^{th} – 75^{th} percentile).

CHAPTER 4 DISCUSSION

4.1. Physiology

The model comprised of tissue injury and significant blood loss, which in combination led to clinically significant shock that was evident as a fall in base excess and a rise in arterial lactate. In the pre-hospital resuscitation phase (first 90 minutes), the animals remained hypotensive, and changes in the base excess, lactate and potassium reflected the severity of the trauma burden. However, the animals were not moribund as these changes were (partially) reversible when tissue perfusion was restored with the more aggressive fluid resuscitation during the in-hospital resuscitation phase resulting in a higher blood pressure. These cardiovascular and metabolic derangements were observed in all treatment groups but not in the surgical control group, hence they are likely to be the consequences of injury.

Metabolic acidosis as a consequence of haemorrhage and tissue injury, was partially compensated by hyperventilation. Respiratory compensation was evident by the fall in carbon dioxide tension, which limited the fall of pH but within normal range (despite high lactate levels and low base excess). The increase of arterial oxygen tension seen immediately after injury in the sham blast animals (although not of clinical significance for overall oxygen transport), is the physiological consequence of the increased ventilation due to stimulation of the peripheral chemoreceptors. These peripheral chemoreceptors are likely to be stimulated initially as the consequence of a sympathetically-driven reduction in chemoreceptor blood flow (causing local hypoxia), which is later supplemented by a stimulation arising from an arterial acidosis to elicit hyperventilation [418].

A substantial amount of blood was removed from the animals, approximately 30% of estimated blood volume. The animals demonstrated an appropriate cardiovascular response to blood loss and tissue injury (fall in BP and HR) and subsequent fluid resuscitation (increase in BP and HR) [74, 419]. The fall in BP is expected from 30% volume loss. The reduced heart rate is less intuitively obvious, but is well reported in the literature as a second ('depressor') phase of the response to haemorrhage (beyond an initial tachycardic phase), and is the result of a reflex reduction in sympathetic tone and possibly increase in vagal activity (see section 1.2.3.3), likely due to activation of neural receptors in the ventricular wall during forceful contractions of the heart around chambers with reduced volume. As expected from previous reports in the literature [59], this depressor reflex was reversed by the refilling of the ventricles during resuscitation. Pre-treatment with statins did not alter the cardiovascular response to injury and fluid resuscitation, and consequently there was no difference in the blood volume deficit, the fluid volume infused nor the time taken to achieve blood pressure targets between placebo and simvastatin groups.

These findings are congruent with those reported by Relja *et a*l [369] but different to those of Lee *et al* [368] (see section 1.6.5.2). This is unsurprising since the statins (simvastatin 5mg/kg) and model used in the present study equates much more closely to that used by Relja than Lee. The model used in this study, and that reported by Relja *et al*, was conducted in anaesthetised animals with an approximate blood volume loss of 30-35% with an element of a pressure target as part of the haemorrhage model, while Lee *et al* used a 60% blood volume haemorrhage in conscious restrained rats (wholly volume driven with no pressure target). While the anaesthesia element is likely to be of lesser importance (alfaxalone was used in the

current study in an attempt to preserve the relevant cardiovascular reflexes in a state comparable to that seen in conscious animals), the other differences could well have had an impact on the haemodynamic outcome of the studies and account for the differences noted above.

The haemorrhage component of the model in this thesis is blood pressure and shock driven (assessed by changes in base excess), rather than simply a fixed volume haemorrhage. The reason for this choice is that in the literature there are indications that the degree of oxygen debt (leading to shock which can be represented as initial base deficit and rise in lactate), is predictive of subsequent reperfusion injury and downstream inflammatory events [420, 421]. Since the aim of this study is to determine whether pre-treatment with simvastatin can attenuate a trauma/shock induced inflammatory response, it was necessary to generate an inflammatory response in placebo-treated animals, which simvastatin could potentially modulate. The approach used here of attempting to standardise the insult initiating the inflammation, was therefore an appropriate choice of haemorrhage modelling. In order to demonstrate that the shock burden (duration and degree of shock) between the two treatment groups was similar, area under the curve for base excess was compared between the two groups. This would be a fairer assessment than direct comparison of the maximum levels attained, since the duration of shock is important as well as transient depth, hence the approach of calculating an aggregated burden of shock as an area under the base-deficit time curve (which takes into the account of duration as well as depth).

The initial reduction of haematocrit (Hct) was moderate, despite removal of a substantial volume of blood over a short period of time. This could be explained by the movement of interstitial fluid into the intravascular space to partly replace the

volume lost [422, 423]. Pre-hospital resuscitation with crystalloid to a hypotensive target maintained a subtle fall in Hct, likely due to only a small percentage (25%) of crystalloid fluid remaining in the intravascular space. Resuscitation with whole blood to normotensive target during the in-hospital resuscitation phase did not return Hct back to baseline, this could be the legacy dilution effect from crystalloid infusion in the pre-hospital phase. There was a gradual reduction of Hct until the end of the experiment, and this was also observed in the surgical control, and likely to be dilutional effects from the infusion of the maintenance fluid.

There was a fall in ionized calcium at 60 minutes into the pre-hospital resuscitation phase. A plausible explanation for this is the influx of extracellular calcium into cells which had lost membrane integrity from anaerobic metabolism (failure of ion transport pumps). Another contributing factor (applicable after R90) is the citrate (used in the blood collection tube to prevent coagulation) that chelated with the serum calcium when blood was transfused back into the animals in the hospital phase. Another factor that can form complexes to result in low free calcium is the bicarbonate anion, however this is unlikely here as the animals were in compensation for metabolic acidosis (bicarbonate levels likely to be low). As calcium has inotropic effect (increasing cardiac contractility), it was reassuring that no significant differences were observed in absolute levels or pattern in both treatment groups to confound the cardiovascular response. It is also noted that this fall in calcium was not sufficient to require treatment, hence unlikely to have compromised the findings.

Hyperglycaemia after injury was expected as it is part of the stress response. The fall in glucose in the latter part of the experiment is likely to be due to the depletion of relatively small glycogen store in animals with high metabolic rate, which

is a feature of the small animal species [424]. This hypoglycaemia could potentially compromise the overall response to trauma and hence survival of the animals. However, as it occurred in a similar degree in both treatment groups in this study, it did not compromise the findings in this thesis. In future studies, considerations could be given to alleviate the observed fall by using 0.9% sodium chloride with 5% glucose as maintenance fluid (when the glucose level falls below baseline), and this has clinical precedence in paediatric practice.

The animals demonstrated the triad of bradycardia, hypotension and apnoea post thoracic blast, which is a well described reflex response [114]. Unsurprisingly, pre-treatment with simvastatin did not appear to alter the cardiorespiratory response to thoracic blast exposure with concomitant haemorrhage and tissue injury. The addition of blast injury to haemorrhage and tissue injury led to a fall in the arterial oxygen tension and small variable change in arterial carbon dioxide tension, when measured 5 minutes after thoracic blast exposure. This is unlikely to be due to apnoea (vagal reflex of primary blast injury), since the duration of apnoea lasted for seconds. Shock wave damage to alveolar capillaries resulting in haemorrhagic contaminations of lung tissue (particularly the small airways), affecting ventilation/perfusion balance and creating a shunt, could be responsible for changing the systemic partial pressure of oxygen [103].

Thoracic blast exposure is known to modify the cardiovascular response to haemorrhage [120]. The further modification of cardiovascular response to haemorrhage by *tissue injury* in combination with thoracic blast injury is yet to be defined, however this study was not designed for this purpose, hence care has been taken in this thesis not to draw conclusions from direct comparison between the sham blast and blast injury strands. The overall blood volume deficit in animals

exposed to thoracic blast was not less than that of animals in sham blast strand, suggesting that tissue injury might have a dominant effect over thoracic blast in the response to haemorrhage.

The two injury strands (sham blast and blast) of the model were severe in nature, some animals died immediately post thoracic blast exposure, post haemorrhage, or during hypotensive resuscitation phase; and some animals did not survive the six hours from onset of resuscitation. The causes of these early deaths in individual animals ranged from the consequences of severe lung injury, to hyperkalaemia, hypocalcaemia and hypoglycaemia, which have been reported in other models of haemorrhagic shock [420]. These animals were excluded in the study as the timing of death was such that there was insufficient time for there to be a measurable inflammatory response. On analysing these excluded animals, there was not a preponderance for early deaths secondary to physiological response to injury in either the simvastatin or placebo treated groups and hence systemic bias was not introduced to the study.

In summary, the severity and injurious components, and the resuscitation regimen in this model generated physiological response that was expected, which met the trauma burden required to test the hypothesis of protective effects of simvastatin pre-treatment in complex battlefield trauma.

4.2. Inflammation

This section discusses the inflammatory elements of the models of trauma reported in this thesis, which provides the background upon which to test the effects of statins on the systemic inflammation associated with trauma. Discussion of the effects of simvastatin on the inflammation is given in section 4.3.

4.2.1. Inflammatory response

The inflammatory response of the model was characterised in the domains of general inflammation, apoptosis, oxidative stress, endothelial injury and organ injury. Surgical preparation for the model described in this thesis generated minimal inflammatory responses, which is not surprising since the surgical insult was minimised. By contrast, this study has demonstrated a measurable inflammatory response following haemorrhage, tissue injury and resuscitation, with and without concomitant thoracic blast injury. Recent studies that have reported simultaneous pro-inflammatory and anti-inflammatory responses in patients within an hour after injury, such as the elevation of DAMPS, pro-inflammatory and anti-inflammatory mediators, and neutrophils with impaired functions [425, 426]. Genomic pathway analysis has demonstrated the up-regulation of innate immune response and down-regulation of adaptive inflammatory pathway within two hours of injury [427]. In both [426, 427] studies, patients who later developed MODS showed differences in their inflammatory responses at the acute stages, in comparison to those who did not develop MODS subsequently. In the current study, the inflammatory response showed some similarities to the changes reported in the literature (I will elaborate in the appropriate sections).

4.2.1.1. Generic inflammatory response – DAMPs

This study has demonstrated that surgical instrumentation had a minimal, if any effect on plasma HMGB1 levels[14]. The pre-injury levels of HMGB1 in this study

[14] DAMPs such as HMGB1 are released in the early stages of trauma to initiate the innate immune response, which orchestrates the production of inflammatory cytokines and leucocyte activation (see in section 1.4.2.1).

(1 ng/ml; which is the limit of detection for assay used) are very similar to those reported in other rat studies with similar surgical instrumentation [428], and consistent with the upper limit of normal in humans (1.4 ng/ml, when measured with the ELISA used in this study). This is reassuring because the minimal inflammatory consequence of the surgery provides scope for the trauma element of the model to produce a measurable inflammatory response. In contrast, both injury models (with and without blast) resulted in a significant and sustained elevation in plasma HMGB1 (see section 3.3). HMGB1 is either actively secreted by immune cells through intracellular signalling (which can take up to eight hours to complete); or via passive instantaneous release through cellular integrity damage [429]. In this thesis, release of HMGB1 was likely to be due to direct damage of the cells and or necrosis rather than apoptosis, as evidenced by the few changes in the expression of genes associated with apoptosis in the organs assessed (liver, kidney and small bowel). In addition, the release of HMGB1 during apoptosis is contested in the literature [430, 431].

The early detection of HMGB1 after injury (haemorrhagic shock, tissue injury and reperfusion) reported here is congruent with other reports in the literature [413, 432, 433]. Foster *et al* found HMGB1 levels in the range 3.9 to 10.1 ng/ml in admission samples of the severely injured at Camp Bastion [413]; Peltz *et al* reported HMGB1 levels 30 fold above healthy control levels in 23 severely injured patients within the first 1 to 6 hours [432]; and Cohen *et al* reported elevated levels as early as 30 minutes post injury [433], suggesting that the findings from the rat model used in this thesis are consistent with human clinical data.

It is not possible to determine the peak of HMGB1 release in this study due to the intermittent nature of the sampling. A single HMGB1 assay uses 20μl of plasma,

which limit the number of samples that could be taken. However, a clear elevation was observed at the earliest sampling time point, demonstrating one facet of an early inflammatory response. For some animals, the elevation is less pronounced at the final sampling point after period of 'hospital resuscitation', suggesting an early response that is starting to resolve by 6 hours from the start of resuscitation. In a separate murine haemorrhage model of 30% blood volume, plasma HMBG1 was elevated only at the 24-hour time point, but not at the earlier 4-hour time point [207]. The timing of sampling at 4 hours may have missed any early peak, and the relatively late elevation at 24 hours could be due to a mechanism such as active secretion. By contrast, a closed bilateral femur fracture murine model showed plasma HMGB1 levels elevated at one hour but not six hours post injury [129]. However, these models differ in species, severity, injury components and fluid resuscitation. In the current model, there is a trend for declining levels of HMGB1 (but still elevated from baseline) at 6 hours, however It is not possible to predict whether there would be a late peak with a longer experiment.

Plasma levels of HMGB1 in humans, have been found to have positive correlation with arterial base deficit, ISS, plasma IL-6, development of renal and lung injury, and mortality [433]. In a porcine model, haemorrhagic shock, intensity and duration also correlated with the magnitude of HMGB1 release [434]. These results are in contrast to a smaller study where no relationship was found between plasma HMGB1 level and ISS or base deficit, but this could be due to the small cohort of patients studied [432]. In the present study, the animal with the highest HMGB1 levels (Figure 35) in sham blast injury placebo (Group 2) had indicators of the worst shock in the group, for example the highest potassium and worse base excess. In addition, we have also found plasma HMGB1 levels to be much higher in animals

that died early in the experiment due to profound shock (data not shown). Together these results suggest that there may be a relationship between shock and HMGB1 levels similar to that reported by others [433] and [434]. In support of this, a multiple correlation analysis revealed a trend suggestive of an association between HMGB1[15] and both ABE (negative relationship, R-squared 0.1073, P=0.0828) and plasma potassium levels (positive relationship, R-squared 0.1047, P=0.0869), although this did not attain statistical significance.

The function and activity of HMGB1 is dependent on its post-translational modification and oxidation, as detailed in the review by Deng M *et al* [435]. For example, extracellular disulphide HMGB1 binds to receptors such as TLR4 and RAGE to trigger immune cascades via signalling pathways such as Nf-kB [436]. Although it is not possible to differentiate between the various forms of HMGB1 using the methods (ELISA) utilised in this study, a corresponding rise in chemokines and cytokines was observed in both injury strands in this model. This may suggest that HMBG1 released following injury orchestrated a downstream inflammatory response (as described in section 1.4.2.1) by activating PRRs such as those from the TLR family.

Extracellular HMGB1 may form complexes with pro-inflammatory cytokines such as IL-1β to exert inflammatory responses [437]. The formation of immune complexes is thought to be independent of the redox state of HMGB1, unlike other HMGB1 signalling functions [438]. This may be relevant in this current study as markers of oxidative stress were only elevated significantly in one organ (see discussion later section 4.2.1.7). In an *in vitro* study using synovial fibroblasts,

[15] To allow this analysis the data was transformed by correlating the square root of the HMGB1 data against ABE and plasma potassium. This was only possible for the non-blast injury data, while the blast data was resistant to transformation that allowed the analysis.

HMGB1/IL-1β complex promoted prostaglandin production [438]. This is of interest for two reasons: firstly, IL-1β was elevated post injury in this experiment. Secondly, prostaglandin-endoperoxide synthase 2 (ptgs2) gene expression was markedly upregulated in livers from injured groups in this study (see section 3.5). I made attempts to develop a protocol to co-immunoprecipitate HMGB1/IL-1β complexes from plasma to confirm complex formation, but was unsuccessful during the period of the PhD studies.

In summary, the early post-injury detection of HMGB1 observed in the model is congruent with most data from trauma patients and animal models. HMGB1 release following trauma is known to trigger the innate immune response such as the production of inflammatory cytokines and leucocyte activation. It would be interesting to investigate any post-translational modification or complex formation of the HMGB1 detected here to learn more about its precise function in this study. As these complexes may also affect the detection of HMGB1 by ELISA it is possible the circulating protein may be even higher than measured here.

4.2.1.2. Generic inflammatory response – inflammatory mediators

4.2.1.2.1. Surgery and anaesthesia

It is clear from the results that the preparatory surgery *per se* had not itself produce a maximal inflammatory response, since injury produced an elevation in several inflammatory cytokines above baseline level. Indeed, in many cases, e.g. IL-10, IL-17, IFNγ, the levels seen at baseline were below the limits of detection of the assay, although for others e.g. IL-5, IL-18, IP-10, measurable levels were found. Attempts to identify the normal range for each analyte from the peer reviewed literature proved unsuccessful. However, normal sample ranges were obtained from

the manufacturer (Annex B). The baseline values from the current study were within manufacturer's normal range except for IL-5. It is clear from the evidence here (plus those from HMGB1 and physiological parameters), that surgery has not produced a marked inflammatory response at baseline to confound the results presented in this thesis.

Data from the surgical control group indicated that there was some degree of inflammation from the prolonged anaesthesia (more than six hours) over the entire course of the protocol, but this is not unexpected. However, compared to the injury groups, the inflammation in the surgical control group is small. Indeed, most of the markers from the multiplex assay did not change significantly over time in surgical control group, with the exceptions of IL-10, MIP-1α and fractalkine. Again, as with the HMGB1 and the stable physiological parameters, this is unlikely to be of clinical significance.

4.2.1.2.2. Effect of injury

The elevation of plasma inflammatory mediators (pro- and anti-inflammatory cytokines, chemokines from C-C, CXC, CX3C subgroups, growth factors and leptin hormone) from baseline, were notable after 90 minutes of hypotensive resuscitation. This was generally maintained over the course of the study, although the degree of elevation at subsequent time points was not as marked. There was subsequent increased expression of CXC chemokine family genes in liver (GRO, LIX) and kidney (LIX) (6 hour time point). However, CXCR2 gene (the receptor for the above chemokines) did not change significantly.

Similar changes were observed when thoracic blast injury was added to haemorrhage and tissue injury, except for the notable addition of increased gene

expression of CXC family (CXC 1,2,3,5) in lungs. Primary blast lung injury leads to release of inflammatory mediators independent of haemorrhagic shock [214]. The increased CXC gene expression in blast lungs would indicate a local inflammatory response, probably due to haemorrhage from the initial rupture of alveolar capillaries, which is consistent with the earlier reports of pulmonary inflammation after blast exposure [213]. Where the trends in mediators between blast and non-blast injured animals are similar, it is possible that those mediators are not produced specifically as part of the response in blast, but as part of the generic innate response to injury. It may also be possible that the release of these mediators are already maximal with the combined haemorrhagic shock and tissue injury, hence additional thoracic blast injury did not add to the production of mediators.

Concomitant pro-inflammatory and anti-inflammatory responses have been reported in the acute period after trauma [426, 427]. Some of the plasma inflammatory mediators that were elevated or upregulated in the studies reported by Hazeldine *et al* [426] and Cabrera *et a*l [427], such as MCP-1, IL-10, IL-17, were also elevated from baseline 90 minutes after injury in this model. Other plasma chemokines and cytokines that were raised in this study, such as IL-1β, IL-12p70, IFNγ, RANTES, GRO, were elevated from baseline in other haemorrhage or polytrauma rat models [240, 439]. The comparison of the inflammatory response in this study with the literature, has not been straightforward, due to the different assays used in various studies. For example, the multiplex assay panels used in other studies comprised of different chemokine and cytokines, or ELISAs were utilised, and hence only a few analytes were tested and reported.

4.2.1.3. Pro-inflammatory response

Pro-inflammatory responses were observed in injured animals, which was expected from the literature [125]. There are numerous clinical studies that have correlated early cytokine detection with poor prognosis [440]. However, the differences between pre-clinical experimental protocols make direct comparison of cytokine/chemokine profiles (such as in terms of timing, magnitude) difficult. This point was illustrated in a study by Pfeifer *et al*, where a comparison of inflammatory responses in established haemorrhage protocols, found different results in the various haemorrhage protocols [441]. Perhaps presenting the data as fold change (from control or baseline) could facilitate the comparison between studies, by giving a sense of the magnitude of change regardless of the baseline figures (instead of absolute values), which could be very different with different models and assays.

The release of DAMPs from the initial trauma can trigger activation of the inflammasome (caspase-1 activating multiprotein complexes) to release IL-18, IL-1β and HMBG1 [442]. In this study, IL-18 was increased 90 minutes post-injury, then the levels fell at subsequent time points although it remained elevated compared to baseline. It is not possible to distinguish the source of IL-18 in this experiment, as tissue gene expression of caspase-1 was not changed significantly, however there are alternative caspase-1 independent pathways for IL-18 secretion [443]. Plasma concentration of IL-18 and timings of detection post trauma vary in the literature. One cohort study reported trauma patients with ISS score over 16 had detectable IL-18 around 60 pg/ml on admission (within 6 hours of injury) [444], others presented values in the region of 320 pg/ml on the second day after trauma [445], and 20 to 180 pg/ml in the first week post trauma [446]. Systemic IL-18 elevation post

traumatic injuries have been associated with complications such as MODS and sepsis [444].

IL-18 has pro-inflammatory properties such as the induction of IFNγ production from T-cells and natural killer (NK) cells (IL-12 dependent), NO synthesis, chemokine production, increase in cell adhesion molecules and the promotion of apoptosis through FasL [447]. Although there were no changes in FasL RNA expression in tissues, or clear evidence of apoptosis detected in this model (see later section 4.2.1.6), there were increased circulating levels of IFNγ, IL-12p70 (active heterodimer of IL-12), and chemokines from CC, CXC, CX3C family after injury. It is plausible that some of these findings were a consequence of the elevation in IL-18, although it is not possible to determine for certain in this study. One explanation for any lack of IL-18 downstream effects, could be the presence of IL-18 binding protein (IL-18bp), which was not measured in this study, which stops IL-18 binding to its receptor and affecting its bioactivity.

Chemokines are secondary pro-inflammatory mediators induced by primary pro-inflammatory mediators. Chemokines such as fractalkine, IP-10, GRO and RANTES are known to be induced by IFNγ [448], which was also elevated systemically in this model. Elevation of serum chemokines such as MCP-1, RANTES, Eotaxin, GRO and IP-10 have been observed in trauma patients and trauma-haemorrhage animal models [449, 450]. Statistical analysis in a clinical observational study suggested that circulatory IP-10 and eotaxin were predictors of MOF [449]. Species and protocol differences aside, the concentrations of plasma chemokines attained in the model in this current study appeared to be lower than that reported in the literature [240]. However it is not possible to make a true

comparison due to differences between the two studies, such as no resuscitation fluid was given and different sampling intervals in the study by Darlington *et al*.

In general, CC chemokines are mainly chemotactic for monocytes and CXC chemokines for neutrophils [451]. Fractalkine, the only member identified from the CX3C family, is a leucocyte chemoattractant and acts as an adhesion molecule [8]. However, despite the systemic chemokines elevation and increased gene expression of chemokines in liver, kidney and blast lungs, the histology results did not suggest marked inflammatory cell infiltration into tissue. There are several possibilities to account for this. The first explanation is that the cytokine levels were not elevated sufficiently (many of the circulatory chemokines appeared to be on a downward trend at the later time points) to cause changes that could be detected by histology. Although there is clear evidence of shock (presumably due to tissue hypoperfusion) during hypotensive resuscitation phase, this was reversed during the subsequent aggressive fluid resuscitation 90 minutes later, and may have contributed to a dampened response. However, a counter to this argument is that the later improved perfusion could lead to reperfusion injury, which in theory could augment a transient inflammatory response. An alternative explanation is that it was too early within the time course of the present study for the mRNA signals to be translated to histological changes.

Leptin, a satiety hormone, not commonly studied in trauma research, was elevated above baseline by the end of the pre-hospital phase. The degree of leptin elevation was significantly reduced in the period of aggressive resuscitation. Leptin is known as an inflammatory molecule that triggers multiple signalling pathways, with downstream effects such as neutrophil chemotaxis and infiltration [452]. However, the role of leptin in the inflammatory response is unclear: with some studies reporting

high leptin levels to be associated with survival from sepsis [453]. Results from focal organ ischaemia animal models (hepatic and renal) reported protective effects on organs when leptin was administrated [454, 455]. In a different study, serum leptin was reduced after an initial period of intestinal ischaemia-reperfusion (IR) in comparison to its baseline values, which the authors (based on the literature of negative correlation of leptin and IL-6 in critically unwell patients [456], and further *in vitro* work) suggest to be due to an early temporary leptin downregulation as part of the recovery process [457]. The elevation of circulatory leptin after injury and a period of relative ischaemia observed in this current study would suggest it to be a marker of an inflammatory process, however with its potential protective effect in IRI, it would be difficult to interpret the significance any changes in relation to the efficacy of treatment with statins.

Surprisingly the elevation of many of the cytokines in the present study was found to be very modest, or even non-existent. There are two possibilities that may account for this, which are not mutually exclusive. Firstly the sampling protocol may, with hindsight (see below), have missed the peak or even the whole response. Secondly, an effective resuscitation strategy may have attenuated the magnitude and duration of response. With regard to the sampling protocol, the relatively short half-life of some of the cytokines in relation to the sampling protocol may have impacted on the observed response. Had the elevations been large, or more importantly prolonged, as has been anticipated from the literature then the sampling protocol would have been adequate. However, if the elevations were modest and abbreviated then the sampling protocol would almost certainly miss the peak level and possibly miss the elevation altogether. This effect would be compounded by the impact of effective resuscitation that may have limited the magnitude, and more

importantly the duration, of cytokine release. To provide specific examples, plasma IL-6, which is commonly reported to be elevated after trauma [133] was at the limits of detection in this study. Although ***circulator***y IL-6 was not elevated after injury, there was evidence of increased ***local*** production in kidneys (RNA expression and protein levels). Marked elevation of plasma IL-6 after haemorrhage and tissue injury was reported around 45 mins into haemorrhage [133], so clearly the animals did mount an inflammatory response although this was not apparent from circulatory measurements. It may be possible that the IL-6 produced in kidneys (detected at 6 hours post injury in this study) has yet to reach the circulation or produced in insufficient quantity to have systemic effects.

Another explanation for the plasma IL-6 results, is the formation of IL-6 complexes with binding proteins or soluble receptors, such as α_2-macroglobulin [458], to render it undetectable using current assays [459, 460]. On the other hand, the absence of IL-6 might indicate that the animals were likely to survive, as IL-6 is seen as a predictor of mortality after trauma [440]. It would have been interesting to evaluate IL-6 levels in those animals that did not survive to the 6-hour time point in an attempt to verify this finding in the model, however the additional analysis was not possible.

TNFα, another commonly reported cytokine in trauma (see section 1.4.3.3.3), also appeared not to be elevated (liver tissue and plasma) in comparison to surgical control in this model. A detailed examination of the literature relating to comparable models of trauma shows a lack of agreement, such that the findings of this thesis are consistent with some, but not all reports. One study reported an elevation of TNFα from baseline (detected by ELISA) as early as ten minutes after haemorrhage, which became undetectable at 60 minutes [189]. By contrast, in a polytrauma model in rats

(40% loss of blood volume with multiple crush injuries), TNFα (detection via multiplexed bead array) was significantly raised from baseline at 30 minutes up to four hours, with its maximum elevation at 60 minutes [240]. However, another report based on a rat model (40% volume blood loss) did not find a modulation of plasma TNFα (multiplex electrochemiluminescence assay) [439]. Possible explanations for the findings in our study were discussed earlier (see IL-6), it is plausible that the initial elevation of TNF in particular in the current study was missed (particularly if the elevation was modest) due to the timing of samples, as TNF has a short half-life of less than 10 mins. Given this scenario (of IL-6 and TNFα), the multiplex approach was employed to get a representative spread of inflammatory mediators rather than selecting a few specific inflammatory markers (limited by sample volume) at this proof of concept stage.

The detection of DAMPs by PPR initiates the immune response, which generates inflammatory mediators that signal and recruit neutrophils to site of injury. In patients who sustained traumatic injuries, marked leucocytosis was noted within minutes of injuries: there was a significant increase in circulating neutrophils in patients compared to healthy controls, which remained elevated at 72 hours [426]. These findings were also echoed by Cabrera *et al* [427]. However, in contrast, there was no difference in the number of circulating neutrophils between surgical control (uninjured) and the injured groups at the 6 hour time point in both injury strands of this study. Since the comparison is made between the surgical control and injured groups (not between the baseline and later time points *within* injured groups), one may argue that preparatory surgery, anaesthesia and the passage of time may have produced maximal leukocytosis, hence no difference was seen from the imaging flow cytometry analysis. This scenario is unlikely in view of the evidence presented so far

(see section 4.2.1.2.1) indicate that surgery did not generate a marked inflammatory response. It is possible that the sample timings could have missed the initial increase in circulating neutrophil numbers, as the plasma chemokines and cytokines were elevated from baseline mainly at the earlier time points and were on a downward trend by 6 hours, hence the recruitment of neutrophils was not continued. However, the histology results (samples taken at 6 hours) did not suggest marked leukocytosis in tissue to support the notion for an historical increase in circulatory neutrophils which have since moved from the circulation to the tissue at the time of sampling. The final possibility is that the ischaemia-reperfusion injury in this model was not sufficient to generate a systemic increase in neutrophils.

4.2.1.4. Anti-inflammatory response

There was also concomitant anti-inflammatory response from the model in both injury stands, evident from the elevation of plasma IL-10 known for its anti-inflammatory actions [461]. This early immune suppression is well documented in the literature, a recent study reported a significant rise in IL-10 in patients within an hour post traumatic injury in comparison to healthy controls [426]. However, other anti-inflammatory cytokines (IL-4 and IL-13) on the multiplex array panel, were at the limits of detection at all time points. Increased IL-10 in circulation (max 20 pg/ml) was reported at 2 hours and returned to baseline by 4 hours in a murine trauma haemorrhage model [462]. In the current model, accepting differences in species and protocol, the IL-10 levels attained were much higher and remained elevated at 6 hours after resuscitation. The role of IL-10 post injury is deemed controversial, with divided opinion whether it acts an immunosuppressive mediator or regulates the pro-inflammatory response; and it is unclear if its presence post trauma indicates poor

prognosis or confers protection [463]. It is possible that the low levels of plasma TNFα and IL-6 in the current models were because of the suppressive actions of IL-10. There is evidence in literature to suggest that neutralisation of IL-10 via antibody appeared to increase the production of TNFα and IL-6 [462].

Ptgs2 (COX-2) is a key enzyme in the synthesis of prostaglandin (PG) E_2 which has suppressive effects on acute inflammatory mediators [464]. Increased Ptgs2 RNA expression in liver of the injured groups was observed 6 hours after resuscitation in this study, in comparison to surgical control. These findings are consistent with other reports in the literature, for example in a haemorrhagic shock and resuscitation rat model treatment with a COX-2 inhibitor treatment exacerbated the hepatic injury [465]. Hence the authors suggested COX-2 derived PG have protective effects in remote organ injury for haemorrhagic shock. However, the interpretation of the finding is difficult because in the current study there was no PGE_2 tissue expression to confirm translation of the gene into protein (COX-2) either directly or indirectly.

4.2.1.5. Correlation with severity of injury

Systemic elevation of some cytokines and chemokines (such as IL-6, TNFα, IL-18, IP-10 and eotaxin) has been associated with poor prognosis in clinical studies as mentioned in section 4.2.1.3. It has been noticed that the concentrations of plasma cytokines and chemokines for one animal (ES149) from the sham blast placebo group, appeared higher than the rest of the group during the hospital resuscitation phase. Unlike most of the animals in the study, IL-6 in this animal was elevated during the aggressive resuscitation phase (data not shown). There were also corresponding outlying results in the liver and kidney proteins, and moderate

necrosis in liver on histology examination. This animal appeared to display a more severe inflammatory response despite the same physiological response to injury. Perhaps there are some preceding predispositions, such as genetics, for a variant response to the same physical insult [427].

4.2.1.6. Apoptosis

Programmed cell death in remote organs has been observed in various haemorrhagic resuscitation models [369, 466]. In the present study, the majority of the genes from the apoptosis panel on the qPCR array did not show a significant fold change (3 fold from surgical control either direction and statistically significant) in the injured group, apart from Cidea gene (Cell Death Inducing DFFA Like Effector A, activates apoptosis) and Tp63 gene (Tumour protein 63). Direction of Tp63 gene expression was inconsistent between organs: it was markedly downregulated in kidney but upregulated in liver, and the significance of this is unclear. Tp63 protein functions include cell proliferation, survival and apoptosis, and it is possible that the organs were at different stages of the inflammatory response or perfusion state to explain the differences in transcriptional expression.

c-Fos which codes for transcription factor complex AP-1, is an immediate early gene which responds rapidly and transiently to various stimuli such as stress or cytokines, and also has links to apoptosis. A study postulated that the overexpression of c-Fos was correlated with programmed cell death [467]. Local c-Fos mRNA expression was increased after 15 minutes of reperfusion in a small intestinal IRI rat model, c-Fos protein and apoptotic cells were detected immunohistochemically. In the current study, c-Fos RNA expression was markedly elevated in liver from both sham blast and blast injury groups. However, most of the

apoptotic genes (see section 3.5) on the array panel did not show sufficient fold change at the time of sampling to warrant further statistical analysis. The results from this qPCR panel only provides information on the relative levels of apoptotic related genes but not their protein expression or their activation status. It could therefore be possible that apoptosis may still have occurred in this model. However, there was a lack of circulating apoptotic cells (see section 3.6), and features of apoptosis were not reported in the histology findings (see section 3.7). The limited evidence presented in this thesis did not give a clear indication that apoptosis is a feature of the model.

It is impossible to tell if this overexpression of c-FOS in liver, was the legacy of IRI, or the lead up to programmed cell death which would become apparent later. On the other hand, in a cDNA microarray study on a rat model of haemorrhage and resuscitation, the authors conclude that the lack of fold change in c-FOS would suggest an attempt in cellular recovery [468]. Therefore, the lack of c-FOS expression in kidneys, lungs and small bowel in this present study may suggest the degree of ischaemic insult was lower than anticipated and therefore these organs recovered from the insult. However, there was overexpression of c-FOS in the liver indicating a more significant injury.

There could be a few plausible explanations to explain the apoptosis findings. The samples for apoptosis qPCR array, imaging flow cytometry, and histological examination all stemmed from single sampling time point. It was possible that by the time of sampling (at the end of the experiment), aggressive resuscitation would have reversed the initial IRI injury and any apoptotic events (or signals for) would have completed. To elaborate, that the signals for programmed cell death might have been and gone, or the cells that were supposed to die, have died. Perhaps, by using

methods that could detect apoptosis at its various stages; an assay for the detection of early apoptosis event (e.g. detection of caspases) and a different method to confirm later apoptotic event (e.g. crytomorphological alterations, DNA fragmentations), may somewhat overcome some limitations of a single sampling time point. Another possibility could be the suppression of apoptosis by IL-9 (markedly increased RNA expression in liver), however there was no confirmation from plasma or tissue expression of IL-9 in this study. Consequently it is not possible to provide a definitive reason for the relative lack of apoptosis in this study compared to others in the published literature.

4.2.1.7. Oxidative stress

The evidence for oxidative stress in this injury model was mixed. Firstly, growth factors associated with angiogenesis (VEGF and EGF) were elevated from baseline after injury. This could be induced in response to hypoxia and reactive oxygen species (ROS) [469]. However, there were no significant changes found in HIF-1α, iNOS or eNOS RNA expression in liver, kidney, small bowel or lungs in either of the injury strands. Heme oxygenase (HO-1) protein expression was detected in the liver and small bowel, however a statistically significant increase in injured animals over surgical control was only seen in liver from the sham blast strand. Therefore, the mixed results made interpretation of oxidative stress exposure in this model challenging.

Tissues were examined for HO-1 protein expression because there are reports in the literature of increased HO-1 mRNA expression in liver and kidney in a rat haemorrhagic shock model [470]. Pilot results from this study also showed increased fold change in HO-1 mRNA in liver and small bowel. HO-1 is known to be

induced by stimuli that cause cellular stress, such as hypoxia and ischaemia-reperfusion (see section 1.6.5.1). Its expression is regulated by various transcription factors such as erythroid-2 related factor 2 (Nrf2) and MAPK [471]. The upregulation of HO-1 may have a protective role in oxidative stress injury [472] (see sections 1.4.3.4 and 1.6.5.1). It is unclear how increased HO-1 confers protection against reperfusion injury: suggested mechanisms include the degradation of free heme (a pro-oxidant and tissue inflammation activator) by HO-1, which produces carbon monoxide and bilirubin to mediate anti-oxidative, anti-inflammatory and anti-apoptotic activities [472]. Although it was a useful marker to indicate hypoxic exposure and oxidative stress, perhaps it was not the best marker to indicate effect of treatment given the protective effects. Its elevation could be interpreted as either the animal was coping better with the insult, or needing to compensate harder to cope with the injury, hence difficult to deduce from the changes if the treatment had been beneficial. Statins have been shown to increase HO-1 expression in various IRI models (see section 1.6.5.1). However, it was a fairly stable protein (does not required immediate processing) for downstream analysis, compared to ROS or glutathione for example, that require tissues to be processed immediately. Unsuccessful attempts were made to optimise a commercially available assay to detect myeloperoxidase (MPO) activity, which possibly would work better with fresh or short-term storage samples.

It was possible that by the time of tissue sampling (as with apoptosis), any directional changes of HIF-1α, iNOS or eNOS RNA expression from the ischaemia period would have reversed or corrected with the aggressive resuscitation. Hence tissue expression of HO-1 was not changed in some tissues. Another explanation is that the degree of (global) shock the animals experienced did not generate oxidative

stress in the some of the organs sampled, however this is less likely due to the severity of the model.

4.2.1.8. Endothelial and organ injury

Injury to the endothelium results in the loss of barrier function, with the increase in permeability allowing movement of fluid and inflammatory mediators into interstitial space. This activation of the endothelium generates more inflammatory mediators, escalating the inflammatory response to develop MODS. There are suggestions in the literature that the presence of CECs may indicate endothelial damage [473]. However, in the present study, there were no significant difference in CECs between surgical control and either of the injury strands as anticipated.

The extent of endothelial injury (indicated by CECs) in this study was less than previously reported [224]. Direct high blast exposure to the hindlimb in a rabbit model generated CECs (mean >2000 cells/ml) at six hours post injury, which were significantly elevated in comparison to one hour after injury, and to sham animals at that time point. The authors postulated that the appearance of CECs in their model was likely to be due to detachment via biochemical processes rather than from the mechanical force generated by the blast, as the peak of CECs was seen at six hours instead of one hour post injury [224]. Their study differs from the current study in terms of injury mechanism, species and methodology used to enumerate CECs (modified CD146-based immunomagnetic separation). It is possible that the shedding of endothelial cells from the endothelial wall into the circulation in the current study was due to damage to the cells or the vessel wall, for example inflammation of the endothelium. HMGB1, a marker of cell death, was elevated at 90 minutes from baseline after hypotensive resuscitation. There was also a

corresponding rise in VEGF, a mediator of endothelial activation indicating endothelial disruption, from the end of the ischaemic period to the end of experiment. Like the apoptosis and oxidative stress markers, the CECs may have already been shed and cleared from circulation by the end of the experiment (point of sampling). Perhaps, if there were baseline or serial measurements for CECs, observable differences might be found. However, this was not possible due to the limited blood volume of the rat.

By contrast, there was other evidence of local endothelial activation/injury; a significant increase in E-selectin RNA expression in liver and lungs for sham blast injury strand, kidney and lungs in blast injury. The increased gene expression of E-selectin at the end of the resuscitation period could be a signal for repair mechanism [474], or to prepare for the movement of neutrophils from circulation to site of injury. However, there were no significant changes in the tissue RNA expression of other adhesion molecules (PECAM, ICAM, VCAM) at the six-hour time point to suggest the latter and minimal leucocytosis was reported in the lung and liver histology. The other possibility is that the signals and the neutrophil migration had occurred earlier, and fluid resuscitation had reduced further inflammatory effects. Evidence from several animal studies suggest that some blood components offer protection against endothelial injury from haemorrhagic shock (see section 1.5.1.2.2). It was not possible to confirm the presence or absence of adhesion molecules tissue expression without immunohistochemistry results.

With regards to broader organ injury, there were no histopathological changes seen in small bowel, which concurred with the qPCR array results. This is unexpected, as blood redistributes to muscles during haemorrhagic shock and tissue injury at the expense of splanchnic circulation. There are a few possible

explanations for these findings: 1) perhaps the period of ischaemia (90 minutes) was not extensive enough to produce marked microscopic necrotic changes in the small bowel, or 2) the animals were well resuscitated such that no further cellular damage occurred, or 3) any pathology was not extensive and therefore was perhaps missed during sampling, and finally like the other analysis mentioned earlier, 4) the timing of the sampling might have missed the changes. Histological changes were modest in livers and kidneys and therefore unlikely to be clinically significant.

Pulmonary oedema was present in surgical control samples. This could be due to the effect of gravity, as the animals were lying in the lateral decubitus position for the duration of the experiment, similar to the patients developing atelectasis post-operatively. The lack of artificial ventilation for these animals whilst under anaesthesia may also contribute to this. Physiology data did not indicate reduction in gas exchange, hence the oedema seen was probably not of clinical significance. Alveolar haemorrhage was present in the blast groups, this was likely extravasated blood from the ruptured alveolar capillaries. This was consistent with the literature [213], together with the physiological reflex of apnoea, hypotension and bradycardia, indicating that the thoracic blast exposure had achieved the intended effect.

4.2.2. Inflammation summary

Taken together, there was a measurable inflammatory response in both injury strands. The early detection of some inflammatory mediators is congruent with other trauma studies, whilst the lack of detection of IL-6 and TNFα was at odds with the literature. The inflammatory response was more pronounced at the end of the pre-hospital (ischaemic) phase, and less obvious in the various outcomes measured at the end of the hospital resuscitation. This does not mean that the model is not

relevant, as this model has been shown to have a similar gene profile to patients who later developed MODS, during the hyperacute phase post injury [16](Annex A). However, although the gene profile of this rat model is similar to the patient group from Cabrera et al, the degree of transcriptional changes between the two could be different as it has been argued that the degree of ***transcriptional*** changes may be modest in the milder responses [241].

The less than expected changes in the injured groups compared to surgical control, may be explained by 1) the timing of the sample (too early or late for the changes/makers measured), 2) the choice of markers and methods of detection, 3) the possible reversal of metabolic derangements with the hospital resuscitation regimen, leading to less cell death and a reduced inflammatory response subsequently. The effect of anaesthesia over time may have contributed to the results seen in the inflammatory outcomes, which were only measured at the end of the experiment. However this was unlikely as the systemic concentration for the majority of the inflammatory mediators remained unchanged throughout the course of the experiment in the control group. The absence of baseline data for some of the modalities added to the challenge in interpreting the results. In summary, the injurious components and the resuscitation regimen in this model generated a measurable inflammatory response required to test the hypothesis of protective effects of simvastatin pre-treatment in complex battlefield trauma.

4.3. Effect of treatment

Simvastatin pre-treatment had no statistically significant effect on the inflammatory response to injury in either of the injury strands in this study.

[16] Collaborative study with QMUL.

Successful dosing was confirmed via direct supervision of chocolate consumption by the animals, and via the measurement of simvastatin hydroxy acid (active metabolite) in plasma. The range of simvastatin hydroxy acid concentration was sizable, despite the same dosage administered. This subject-dependent yield of simvastatin hydroxy acid is consistent with human studies, and believed to be due to different sites of hydrolysis (plasma/hepatic or tissue esterase activity by gastrointestinal tract) [411].

It is unclear whether the variation in the concentration of active metabolite would result in variable HMG-CoA reductase pathway inhibition, thereby producing different degrees of clinical effect. Animals with the least simvastatin hydroxy acid concentration did not display any trend for different results from the rest of their group. There were no significant differences in the blood volume deficit between placebo or treatment groups in either injury strand, to suggest a protective or detrimental effect of simvastatin pre-treatment in the response to haemorrhage. Therefore, even if the range of plasma simvastatin hydroxy acid is wide, it is apparent that all of the concentrations were comparable in terms of biological effect on the response to trauma. Hence the variation in plasma simvastatin levels is unlikely to have influenced the outcome of the study.

The negative findings from this present study echoes the results from RCTs which investigated the use of statins in sepsis or ARDS [386, 393, 394]. It was possible that patients in those studies were already critically unwell with an established inflammatory process prior to statins treatment, hence perhaps beyond the scope of statins intervention. The current study differs in this aspect since the animals received pre-treatment with simvastatin *before* haemorrhagic shock and trauma. One explanation for a lack of efficacy of statins in the current study could be

that the magnitude of the inflammatory response, resulting from the degree of shock, was too high for any treatment to have any inflammatory modulation. However, the markers of shock were reversible (by resuscitation) in the latter phase of the experiment, and the histology results did not show overwhelming evidence of organ damage, which renders this explanation unlikely.

Another suggestion for the lack of efficacy of statins could be that the animals were well resuscitated with the current hospital resuscitation regimen, with maximum benefits achieved already, such that statins had little scope to further improve outcome. This notion is supported by the less apparent inflammatory changes at the later stages of the experiment. In the subgroup analysis of the HARP-2 trial, simvastatin treatment increased survival in patients with hyper-inflammatory subphenotype ARDS (e.g. higher values of sTNF-1, IL-6 and lower platelets), but not those with the hypo-inflammatory subphenotype [475]. Hence, it is possible that statins may have an effect in scenarios where pre-hospital phase is prolonged or resuscitation is without blood products, where the magnitude of inflammation could be higher.

The third explanation could be the mevalonate pathway was already suppressed by illness or injury, hence further inhibition of HMG-CoA reductase by statins would not produce beneficial effects. This has been proposed as an explanation for the negative findings in a simvastatin ARDS trial, that hypocholesterolaemia in critically unwell patients suggest existing inhibition of HMG-CoA reductase [393]. This may be a plausible explanation when treatment was given after the initial insult. However, the animals in the current study had treatment before injury, mevalonate pathway suppression would have been inhibited by statins prior to injury, making this suggestion less conceivable. Because this study found a

negative effect of statins (i.e. little or no effect), demonstration of adequacy of dosing has increased importance. Although I have shown that statins were present in blood, with hindsight a more comprehensive demonstration of efficacy of dosing would have been beneficial, for example by demonstrating successful HMG-CoA reductase inhibition by statins in this model prior to injury, such as the measurements of downstream products melavonate pathway (such as cholesterol or ubiquinone see Figure 13). To further the discussion that hypocholesterolaemia is a mechanism for lack of efficacy, lower than expected values of serum cholesterol were reported in critically injured (trauma) patients on admission, the mechanisms for this was unclear [476]. However, there are contrary results in rabbit models of ischaemia and tissue injury, that indicated increased serum cholesterol after injury [477, 478]. Finally, the reasons for hypocholesterolaemia in critically unwell patients are likely to be multifactorial, rather than just HMG-CoA inhibition.

The negative results for the effects of simvastatin in the sham blast strand is clear, as the study was powered correctly with additional animals based on the power calculations at interim analysis. The effect size seen at interim analysis for the blast strand was smaller, and would require a large number of additional animals to determine a statistically significant effect. This suggests that the clinical effect of simvastatin (if any) in blast injury was likely to be small, hence it was decided that it was inappropriate to undertake additional *in vivo* experiments in the blast groups.

In summary, despite confirmed successful dosing, simvastatin pre-treatment appeared not to have an effect in this model, which concurred with some clinical trials in critically unwell patients.

4.4. Limitations

The study presented in this thesis utilised a small animal model of traumatic injury and inevitably limitations exist, and some of the disadvantages of using a small animal model were briefly addressed in the experimental design chapter. The main limitation in the study was the limited amount of blood available for downstream analysis. The blood volume in these rats was approximately 16ml, multiplex bead array analysis plus one ELISA assay required 0.25ml and imaging flow cytometry required 1 ml. Therefore, in addition to the haemorrhage injurious component of the model, it was not possible to have samples for all analyses at multiple time points throughout the study without the samples inducing a significant haemorrhage on their own.

The model reflected the 'best case' scenario of a matured operation (the later years of Op Herrick [33] for example), in which the patient was evacuated to hospital facilities within 90 minutes of injury [479], where ischaemia was reversed with blood products resuscitation. The results of this study suggest that statins may have little role to play under these circumstances (where aggressive early resuscitation limits the inflammatory response). This study did not explore the situation where blood products are unavailable, or when the evacuation timelines are significantly longer due to tactical constraints. In those circumstances, with less efficient resuscitation and longer evacuation times, tissue protection may be more important. Assessment of this, though, would require a different model where the inflammatory response develops to a greater degree e.g. when crystalloids are predominantly used for resuscitation and simulated 'pre-hospital' times are longer, consistent with the subgroup analysis reported by Calfee *et al* (HARP-2 trial)[475].

In this (my) study, some animals succumbed to their injuries prior to reaching experiment end point due to the severe nature of the injury model, and the impact was an increased length of time to reach the required sample size. There was no preponderance for early deaths in the groups pre-treated with simvastatin, hence no bias was introduced to the study. If a more severe model was used in order to generate an inflammatory response of larger magnitude, such as a longer ischaemic period for example, this would need to be balanced against the possibility of more animals succumbing to their injuries prior to the end of the experiment. Similarly, animals with the same injurious components but without blood products resuscitation, would also be more likely to die. It is likely that the injuries would have to be moderated to allow the animal to survive for a sufficient period of time for the experiment. This balance of a milder injurious insult could dampen the inflammatory response and make the assessment of drug effect equally as difficult as in the current study. Finally, the observational period after injury was curtailed at six hours in this study, which may be too early for markers of complicated outcomes (such as MOF) to be apparent.

The use of multiplex bead array assay in the study makes comparison of absolute values to results from existing literature difficult, as ELISA was often used in the earlier publications. The choice of inflammatory biomarkers on the multiplex panel was limited by the species (for example more markers are available for humans) and the compatibility between antibodies to avoid multiplexing artefacts (such as cross reaction of antibodies) [480]. Tissue samples were snap frozen immediately after harvest due to logistical practicalities, however this limited the options for downstream analysis, such as oxidative stress detection. The detection of reactive oxygen species (ROS), for example, would require immediate processing

of samples, which is not practical in addition to the immediate processing required for imaging flow cytometry. The decision was made to focus on imaging flow cytometry for direct evidence of endothelial damage, rather than endothelial activation, since in the context of this study the damage is highly likely to be the cumulative effect of the inflammatory response.

Tissue cytokine analysis was only performed for two pro-inflammatory cytokines in trauma using ELISA. Perhaps in addition, the multiplex bead array assay could be used to detect local protein expression in tissue especially if the bead array could be customised to those markers of greatest interest. This may help to interpret the results for the plasma inflammatory proteins that showed less elevation from baseline at the end of the experiment. Although the additional data could possibly help to define the inflammatory response of the model (by indicating whether a local inflammatory response exists in the tissues), it is unlikely to change the overall conclusion on the effects of simvastatin pre-treatment on injury, hence it was felt that the costs of the additional analysis could not be justified.

In the pathway focused real-time qpcr array, no technical replicates of the target genes were performed. Normalisation of the gene expression levels would remove experimentally induced non-biological variation. In our study, upon testing the stability of the housekeeping (reference) genes using GeNorm, it was not feasible to use three or more of the existing housekeeping genes on the panel to normalise the data, as the stability criteria was not consistently met. This was overcome by using global mean normalisation, after seeking expert advice from q base+ (B De Craene 2017, personal communications). Pathway focused gene array was used in the anticipation that it would signpost relevant biomarkers for downstream confirmation, without the costs and extensive bioinformatics analysis

required for genome-wide gene arrays results interpretation. However, the magnitude of changes (fold change) in tissue protein genes expression in either direction and the number of genes implicated by the 3-fold cut off did not lead to any clear targets for confirmation.

Terminal tissue samples were taken at a single time-point (six hours after resuscitation) at the end of the experiment. The comparison of injured animals to surgical control at this single time point removed the confounding effects of surgery and anaesthesia, such that any changes seen were the effect of injury. This experimental design ensures that the least number of animals was used to achieve the study objectives in accordance to the 3R principles. The downside of this, is the lack of baseline and serial comparison for the results generated from these samples, potentially missing some changes from inflammatory results due to the sample timing. However, this is somewhat compensated by the serial sampling of systemic inflammatory markers. In addition, the results from tissue analysis were used as an adjunct to support the plasma data.

Although histological data from the terminal tissue samples would give an indication of organ injury, it does not reflect organ function. In this model, invasive arterial monitoring gave some information on respiratory and cardiac function. Liver function tests (LFTs), urea and electrolytes (U&Es) measurements, as well as urine output via urinary catheter could give assessment on hepatic and renal function. However due to the limited blood volume, only terminal sampling is possible for this model. One way to address this problem in the future studies would be to utilise a model of a larger animal where increased blood sampling was possible to facilitate a more comprehensive, and repeated, assessment of organ function.

The simvastatin dose used in this study was 5mg/kg, this was selected from a range of doses used in other published studies (Table 3). It may be possible that an effect could be seen at higher doses such as 10mg/kg. However, 10mg/kg in rat would equate to 1.6mg/kg in human according to body surface area conversion FDA tabulation, which is higher than recommended dosage for humans, and therefore unlikely to be translatable to clinical practice (restricted human dosing simvastatin 80mg).

Successful dosing of simvastatin was demonstrated in this study but not the pharmacological effect of HMG Co-A reductase activity. The negative findings in this study are different to the other single organ IRI and HS/R models in the literature. Therefore, the study could be improved by demonstrating reduced HMG Co-A reductase inhibition by simvastatin, by measuring plasma cholesterol or ubiquinone from the pre-injury sample (see section 4.3). A commercially available cholesterol quantitation kit (Sigma-Aldrich, MAK043) requires a minimum of 0.1ml plasma, therefore due to the small blood volume available in the rat for sampling, this has to be rationalised. A pre-injury plasma sample for cholesterol testing, would be at the expense of other analyte analysis but should be considered if future work was undertaken.

If the findings for the effect of simvastatin had been positive, the translation of these results to clinical application would be limited by the notion of giving pre-treatment to healthy soldiers, and whether the immunomodulation response seen at molecular level would have positive clinical outcomes. This would require further investigations to establish if these positive effects could be seen with post injury dosing, and whether there are potential benefits in the longer term (beyond 6 hours).

Despite the limitations presented, the objectives of the study were achieved, in that there was a measurable inflammatory response post injury, such that an effect of simvastatin pre-treatment could have been demonstrated in the model. The study therefore yielded a clear outcome; simvastatin does not provide a measurable protective effect on the post trauma inflammatory response, in the context of a relevant injury and pre-hospital resuscitation that has been used in recent mature operations for military casualties. Whether statins might be of benefit in future operations in more austere circumstances that include limitations in access to blood products and prolonged evacuation times remain to be seen.

4.5. Future directions

It was disappointing that the pre-injury administration of simvastatin had no measurable effect in this model of poly-trauma as there would be a number of avenues that could be taken if a positive effect had been demonstrated.

Firstly, it would be essential to demonstrate whether these positive effects are seen with a post-injury dosing regimen. Post-injury simvastatin dosing is possible using intravenous (i.v.) route, by either preparing simvastatin in 10% v/v dimethyl sulfoxide (DMSO) [354], or dissolving simvastatin in a solution containing ethanol/1,2-Propanediol/sterile water 10/60/30, v/v% [481]. Since pleiotropic properties of statins are class effects, the other option is to use a different statin which can be administrated in hydroxy acid form. I would consider administrating the drug as a far forward resuscitation adjunct at the end of the pre-hospital phase (in transit to hospital), or immediately on arrival to hospital at the latest.

Secondly, the long-term effects (beyond 6 hours) would need to be proven for the treatment to be accepted clinically. In order to assess benefits beyond 6 hours,

an option is to maintain the current model for up to 24 hours after resuscitation. Ethical considerations need to be taken for prolonged anaesthesia or recovery. Perhaps the post injury dosing experiments should be undertaken first, as that would utilise less animals. If benefits are not seen in the post-injury dosing experiments, unless it is acceptable by the military command to give a prophylactic short course of simvastatin to soldiers prior to high risk military operations, it would be pointless to pursue further with the 24-hour model.

Regardless of the lack of drug effect in this study, an important element of the study was to explore a range of outcome measures for the acute inflammatory response in a poly-trauma model that includes blast injury. The conclusion of this exploration would be to make recommendations for future studies not only for the methodologies to be used but also the direction of future work.

Results generated from the inflammatory response raised several questions that need to be addressed. Post-translational modification or complex formation of HMGB1 can affect its detection using standard ELISA, such that the measured HMGB1 levels using standard ELISA might be lower than the actual levels (or even give a false negative), which will confound the assessment of its downstream effects. Alternative methods to overcome this include: Western blotting, electrophopretic mobility shift assay (EMSA), liquid chromatography-tandem mass spectrometry (LC/MS) and PCA-ELISA. Western blotting is labour intensive and provides semi-quantitative data, which is not ideal for quantitative comparison required here. EMSA relies on the detection of DNA-protein complexes between HMGB1 and radiolabelled hcDNA by electrophoresis. The perchloric acid (PCA) precipitation step in EMSA dissociates the HMGB1-protein complexes, hence has the advantage of measuring total HMGB1 concentration [482]. LC/MS has been reported to

successfully quantify total and acetylated HMGB1, however there is an expression of concern for this publication, as the results appeared not to be repeatable using the methods described [483, 484]. The use of PCA to dissociate protein-protein complex prior to ELISA have been shown to improve HMGB1 measurements [485]. Amongst the methods listed, the use of PCA prior to standard ELISA appears to be the most feasible for future work.

The literature suggests that HMBG1/IL-1β promote prostaglandin production, and the results from this current study suggests these complexes may be present. Confirmation of these complexes would strengthen the notion that HMGB1 exerts downstream inflammatory effects in this model, furthermore, HMBG1/IL-1β complexes have not been demonstrated in a haemorrhage polytrauma model. The presence of these complexes could be established by co-immunoprecipitation (Co-IP), followed by Western blotting (WB) of the eluate. I would start by optimising the protocol of commercially available Co-IP kit, such as trying various combinations and concentrations of antibodies, on commercial rat plasma incubated with HMGB1 and IL-1β to begin with, prior to utilising the limited study samples. However, it is possible that HMGB1/IL-1β complex concentration is below the limits of detection for WB in the study samples.

Moving onto another pro-inflammatory analyte, IL-18, which was elevated from baseline after injury. The presence of IL-18 binding protein (IL-18bp) can affect its bioactivity by binding to the IL-18 receptor. Therefore, appropriate inference of the IL-18 results depends on the presence of IL-18bp, which was not investigated in this study. Although there is no commercially available IL-18bp ELISA kit for rat, the successful development of IL-18bp ELISA for rat has been described, and could be considered for future methodology [486].

Gene expression of Ptgs2 and IL-9 was markedly increased in injured animals compared to surgical control at the end of experiment. Direct confirmation of PGE_2 and IL-9 in tissues, using ELISA for example, is necessary prior to any speculation of their downstream actions in this model. Other proteins of interest in tissue samples include stable markers of oxidative stress, such as 4-hydroxynonenal (4-HNE), protein carbonyl and 8-Oxo-2'-deoxyguanosine (8-OHdG). These are stable markers that could be assessed by ELISA, stable in the storage conditions used in this study, to provide information in addition to the HO-1 analysis.

Next questions to be addressed are those raised from the effect of simvastatin pre-treatment. One of the possible explanations for the lack of effect from simvastatin pre-treatment in this model, was that maximum benefits were already achieved by the robust hospital resuscitation regimen, and statins or any resuscitation adjuncts would not be able to further improve outcome. It may be possible for statins to provide protective effects in situations under military tactical constraints, or mass casualty scenarios, where pre-hospital phase is prolonged or blood products are unavailable. Although the resuscitation protocol used in the current study would serve as an excellent positive control for future studies, a more severe model comprising of a longer period of permissive hypotension, or minus blood resuscitation, would be required to test this hypothesis. However, it is likely that some animals will succumb to injuries before the end of the experiment, meaning more animals would be used and it would take longer to achieve the numbers required for adequate power. Perhaps a different choice of outcome measures and earlier experimental end points might overcome these potential problems. However, it would be important for such a study to be undertaken under terminal anaesthesia to minimise suffering.

Although not proven, it is suggested HMG-CoA reductase is already substantially inhibited in ARDS patients, hence the lack of beneficial effects from simvastatin in the trial. It would be interesting to establish whether HMG-CoA reductase is inhibited in trauma, which if it is, would theoretically remove statins as a post injury adjunct.

For future studies of resuscitation adjunct in trauma, changes could be made to the current model and outcome measures. Firstly, in the context of the magnitude of the inflammatory response there is little to be gained by the addition of blast injury in the first instance when evaluating further resuscitation adjuncts. The multiplex array could be customised to the markers of interest (from the current results) and use the same array used for both plasma and tissue protein analysis. The lack of changes between surgical control and injured animals in terminal samples (gene expression, tissue protein and circulating cells), could be addressed by adjusting the duration of the experiment. The timing of the sampling could be too early or too late to detect the changes in these particular modalities. If the same outcome measures are used, it would be sensible to move the end of experiment to the right, for example terminating the study at eight hours post resuscitation. Terminating the study early to capture the early changes does not fit with the eventual aim of establishing effects in the later time course, unless using reliable early markers for late inflammatory changes.

Alternatively, a model in a different species could be considered. As one of the main limitations of this study was the small blood volume available for downstream analysis, the larger animals could be considered if costs permitted, such as a porcine model. This would allow serial blood sampling at close intervals, and

expand the available techniques for downstream analysis such as flow cytometry or imaging flow cytometry (although analysis is limited by available antibodies).

4.6. In conclusion

I am of the opinion that resuscitation adjuncts to modulate inflammatory response would be of benefit, not only to the military in treating patients with complex battlefield injuries, but also in severe civilian trauma. From the research presented in this thesis, I recommend the following for future resuscitation adjunct (pre-treatment or at point of injury) studies in a terminally anaesthetised rat poly-trauma model:

- Blood samples should be taken at the following time points: pre-injury, 45, 90, 120, 240, 360, 480 minutes post injury.
- This blood sampling regimen would necessitate timed culls at 120 minutes and 480minutes.
- Serial blood samples should be analysed for arterial blood gas, HMGB1, customised multiplex panel of inflammatory mediators. Additionally, blood samples taken terminally at 120 minutes and 480 minutes for imaging flow cytometry, LFTs and U&Es.
- Tissue samples should be collected and fresh frozen for downstream gene expression (inflammatory, apoptosis, oxidative stress array panels) analysis, histology and protein (inflammatory, oxidative stress markers) analysis. Fresh tissue samples could be taken from the pilot animals for immediate processing to assay for ROS, before deciding if this were to be included in the main phase.
- Regular bladder emptying every 2 hours or insertion of an urinary catheter for free drainage and urine output measurements.

- Use of 0.9% sodium chloride with 5% glucose as maintenance fluid to alleviate hypoglycaemia (small animal depletion of glycogen stores).

References

1. *National Confidential Enquiry into Patient Outcome and Death. Trauma: Who Cares?* 2007.
2. *National Audit office. Major Trauma care in England*. 2010.
3. Pfeifer, R., et al., *Patterns of mortality and causes of death in polytrauma patients--has anything changed?* Injury, 2009. **40**(9): p. 907-11.
4. Polinder, S., et al., *Assessing the burden of injury in six European countries.* Bull World Health Organ, 2007. **85**(1): p. 27-34.
5. *Trauma and Audit Research Network. Modelling trauma workload: A project for the Department of Health*. 2009, National Audit Office.
6. Sauaia, A., et al., *Epidemiology of trauma deaths: a reassessment.* J Trauma, 1995. **38**(2): p. 185-93.
7. Baker, S.P., et al., *The injury severity score: a method for describing patients with multiple injuries and evaluating emergency care.* J Trauma, 1974. **14**(3): p. 187-96.
8. *Ministry of Defence. British fatalities Operations in Afghanistan*. Available from: https://www.gov.uk/government/fields-of-operation/Afghanistan#fatalities.
9. *OP HERRICK casaulty and fatality table*. 2013; Available from: https://www.gov.uk/government/publications/op-herrick-casualty-and-fatality-tables.
10. *MInstry of Defence. Defence Statistics (Health). Bi-Annual tracking Afghanistan VSI/SI Operational casualties: 8 Oct 2007 to 30 September 2013*, D.S. (Health), Editor. 2014.
11. Kelly, J.F., et al., *Injury severity and causes of death from Operation Iraqi Freedom and Operation Enduring Freedom: 2003-2004 versus 2006.* J Trauma, 2008. **64**(2 Suppl): p. S21-6; discussion S26-7.
12. Owens, B.D., et al., *Combat wounds in operation Iraqi Freedom and operation Enduring Freedom.* J Trauma, 2008. **64**(2): p. 295-9.
13. Frykberg, E.R. and J.J. Tepas, 3rd, *Terrorist bombings. Lessons learned from Belfast to Beirut.* Ann Surg, 1988. **208**(5): p. 569-76.
14. Ryan, J. and H. Montgomery, *The London attacks--preparedness: Terrorism and the medical response.* N Engl J Med, 2005. **353**(6): p. 543-5.
15. Turegano-Fuentes, F., et al., *Injury patterns from major urban terrorist bombings in trains: the Madrid experience.* World J Surg, 2008. **32**(6): p. 1168-75.
16. Craigie, R.J., et al., *Manchester Arena bombing: lessons learnt from a mass casualty incident.* J R Army Med Corps, 2018.
17. Ramasamy, A., et al., *Injuries from roadside improvised explosive devices.* J Trauma, 2008. **65**(4): p. 910-4.
18. *Defence Statistics (Health) Ministry of Defence. Quarterly Afghanistan and Iraq Ampuation Statistics 7 October 2001 to 30 September 2013*. 2013: Bristol.
19. Morrison, J.J., et al., *Associated injuries in casualties with traumatic lower extremity amputations caused by improvised explosive devices.* Br J Surg, 2012. **99**(3): p. 362-6.
20. Andersen, R.C., et al., *Dismounted Complex Blast Injury.* J Surg Orthop Adv, 2012. **21**(1): p. 2-7.
21. Champion, H.R., et al., *A profile of combat injury.* J Trauma, 2003. **54**(5 Suppl): p. S13-9.

22. Hodgetts, T.J., et al., *ABC to <C>ABC: redefining the military trauma paradigm.* Emerg Med J, 2006. **23**(10): p. 745-6.
23. Alam, H.B., et al., *Application of a zeolite hemostatic agent achieves 100% survival in a lethal model of complex groin injury in Swine.* J Trauma, 2004. **56**(5): p. 974-83.
24. Pusateri, A.E., et al., *Effect of a chitosan-based hemostatic dressing on blood loss and survival in a model of severe venous hemorrhage and hepatic injury in swine.* J Trauma, 2003. **54**(1): p. 177-82.
25. Walters, T.J., et al., *Effectiveness of self-applied tourniquets in human volunteers.* Prehosp Emerg Care, 2005. **9**(4): p. 416-22.
26. Wedmore, I., et al., *A special report on the chitosan-based hemostatic dressing: experience in current combat operations.* J Trauma, 2006. **60**(3): p. 655-8.
27. Tien, H.C., et al., *An evaluation of tactical combat casualty care interventions in a combat environment.* J Am Coll Surg, 2008. **207**(2): p. 174-8.
28. *Army Medical Services Core Doctrine. AC 62202. March 2012*. 2012.
29. Bricknell, M.C., *The evolution of casualty evacuation in the British Army in the 20th century (Part 3)--1945 to present.* J R Army Med Corps, 2003. **149**(1): p. 85-95.
30. Bricknell, M., *For debate: the Operaional Patient Care Pathway.* J R Army Med Corps, 2014. **160**: p. 64-69.
31. *Ministry of Defence. Joint Doctrine Publication 4-03. Joint Medical Doctrine. Chapter 2 part 1 section 1*. 2014.
32. Davis, P.R., A.C. Rickards, and J.E. Ollerton, *Determining the composition and benefit of the pre-hospital medical response team in the conflict setting.* J R Army Med Corps, 2007. **153**(4): p. 269-73.
33. Morrison, J.J., et al., *En-route care capability from point of injury impacts mortality after severe wartime injury.* Ann Surg, 2013. **257**(2): p. 330-4.
34. Parker, P.J., *Casualty evaciation timelines: an evidence-based review.* J R Army Med Corps, 2007. **153**(4): p. 274-277.
35. Mcleod, J., T. Hodgetts, and P. Mahoney, *Combat "Category A" calls: evaluating the prehospital timelines in a military trauma system.* J R Army Med Corps, 2007. **153**(4): p. 266-268.
36. Trunkey, D.D., *Trauma. Accidental and intentional injuries account for more years of life lost in the U.S. than cancer and heart disease. Among the prescribed remedies are improved preventive efforts, speedier surgery and further research.* Sci Am, 1983. **249**(2): p. 28-35.
37. Demetriades, D., et al., *Trauma deaths in a mature urban trauma system: is "trimodal" distribution a valid concept?* J Am Coll Surg, 2005. **201**(3): p. 343-8.
38. Gofrit, O.N., et al., *The trimodal death distribution of trauma victims: military experience from the Lebanon War.* Mil Med, 1997. **162**(1): p. 24-6.
39. Keene, D.D., et al., *Died of wounds: a mortality review.* J R Army Med Corps, 2016. **162**(5): p. 355-360.
40. Wafaisade, A., et al., *Epidemiology and risk factors of sepsis after multiple trauma: an analysis of 29,829 patients from the Trauma Registry of the German Society for Trauma Surgery.* Crit Care Med, 2011. **39**(4): p. 621-8.
41. Frohlich, M., et al., *Epidemiology and risk factors of multiple-organ failure after multiple trauma: an analysis of 31,154 patients from the TraumaRegister DGU.* J Trauma Acute Care Surg, 2014. **76**(4): p. 921-7; discussion 927-8.

42. Ulvik, A., et al., *Multiple organ failure after trauma affects even long-term survival and functional status.* Crit Care, 2007. **11**(5): p. R95.
43. Moore, F.A., et al., *Postinjury multiple organ failure: a bimodal phenomenon.* J Trauma, 1996. **40**(4): p. 501-10; discussion 510-2.
44. Sluys, K., T. Haggmark, and L. Iselius, *Outcome and quality of life 5 years after major trauma.* J Trauma, 2005. **59**(1): p. 223-32.
45. Barcroft, H., et al., *Post-haemorrhagic fainting. Study by cardiac output and forearm flow.* Lancet, 1944(1): p. 489-491.
46. Patterson, S.W. and E.H. Starling, *On the mechanical factors which determine the output of the ventricles.* J Physiol, 1914. **48**(5): p. 357-79.
47. Little, R.A., et al., *Preventable deaths after injury: why are the traditional 'vital' signs poor indicators of blood loss?* J Accid Emerg Med, 1995. **12**(1): p. 1-14.
48. Angell James, J.E., *The effects of changes of extramural, 'intrathoracic', pressure on aortic arch baroreceptors.* J Physiol, 1971. **214**(1): p. 89-103.
49. Cowley, A.W., Jr., J.F. Liard, and A.C. Guyton, *Role of baroreceptor reflex in daily control of arterial blood pressure and other variables in dogs.* Circ Res, 1973. **32**(5): p. 564-76.
50. Angell James, J.E., *The effects of altering mean pressure, pulse pressure and pulse frequency on the impulse activity in baroreceptor fibres from the aortic arch and right subclavian artery in the rabbit.* J Physiol, 1971. **214**(1): p. 65-88.
51. Warner, H.R. and A. Cox, *A mathematical model of heart rate control by sympathetic and vagus efferent information.* J Appl Physiol, 1962. **17**: p. 349-355.
52. Oberg, B. and S. White, *Circulatory effects of interruption and stimulation of cardiac vagal afferents.* Acta Physiol Scand, 1970. **80**(3): p. 383-94.
53. Kirchheim, H.R., *Systemic arterial baroreceptor reflexes.* Physiol Rev, 1976. **56**(1): p. 100-77.
54. Sharma, A.C., G. Singh, and A. Gulati, *Decompensation characterized by decreased perfusion of the heart and brain during hemorrhagic shock: role of endothelin-1.* J Trauma, 2002. **53**(3): p. 531-6.
55. Evans, R.G., et al., *Neural mechanisms in the cardiovascular responses to acute central hypovolaemia.* Clin Exp Pharmacol Physiol, 2001. **28**(5-6): p. 479-87.
56. Oberg, B. and P. Thoren, *Increased activity in left ventricular receptors during hemorrhage or occlusion of caval veins in the cat. A possible cause of the vaso-vagal reaction.* Acta Physiol Scand, 1972. **85**(2): p. 164-73.
57. de Burgh Daly, M., E. Kirkman, and L.M. Wood, *Cardiovascular responses to stimulation of cardiac receptors in the cat and their modification by changes in respiration.* J Physiol, 1988. **407**: p. 349-62.
58. Oberg, B. and P. Thoren, *Circulatory responses to stimulation of left ventricular receptors in the cat.* Acta Physiol Scand, 1973. **88**(1): p. 8-22.
59. Barriot, P. and B. Riou, *Hemorrhagic shock with paradoxical bradycardia.* Intensive Care Med, 1987. **13**(3): p. 203-7.
60. De Burgh Daly, M., C.J. Lambertsen, and A. Schweitzer, *Observations on the volume of blood flow and oxygen utilization of the carotid body in the cat.* J Physiol, 1954. **125**(1): p. 67-89.
61. Biscoe, T.J., M.J. Purves, and S.R. Sampson, *The frequency of nerve impulses in single carotid body chemoreceptor afferent fibres recorded in vivo with intact circulation.* J Physiol, 1970. **208**(1): p. 121-31.

62. D'Silva, J.L., D. Gill, and D. Mendel, *The effects of acute haemorrhage on respiration in the cat.* J Physiol, 1966. **187**(2): p. 369-77.
63. Kenney, R.A. and E. Neil, *The contribution of aortic chemoceptor mechanisms to the maintenance of arterial blood pressure of cats and dogs after haemorrhage.* J Physiol, 1951. **112**(1-2): p. 223-238.
64. Jacobsen, J. and N.H. Secher, *Heart rate during haemorrhagic shock.* Clin Physiol, 1992. **12**(6): p. 659-666.
65. Koyama, S., et al., *Role of central nervous system in renal nerve activity during prolonged hemorrhagic shock in dogs.* Am J Physiol, 1988. **254**(5 Pt 2): p. R761-9.
66. Alam, M. and F.H. Smirk, *Observations in man upon a blood pressure raising reflex arising from the voluntary muscles.* J Physiol, 1937. **89**(4): p. 372-83.
67. Alam, M. and F.H. Smirk, *Observations in man on a pulse-accelerating reflex from the voluntary muscles of the legs.* J Physiol, 1938. **92**(2): p. 167-77.
68. Howard, J.M., C.P. Artz, and R. Stahl, *The hypertensive response to injury.* Ann Surg, 1955. **141**(3): p. 327-336.
69. Redfern, W.S., et al., *Effect of limb ischaemia on blood pressure and the blood pressure-heart rate reflex in the rat.* Q J Exp Physiol, 1984. **69**(4): p. 763-779.
70. Anderson, I.D., R.A. Little, and M.H. Irving, *An effect of trauma on human cardiovascular control: baroreflex suppression.* J Trauma, 1990. **30**(8): p. 974-81; discussion 981-2.
71. Coote, J.H., S.M. Hilton, and J.F. Perez-Gonzalez, *Inhibition of the baroreceptor reflex on stimulation in the brain stem defence centre.* J Physiol, 1979. **288**: p. 549-60.
72. Quest, J.A. and G.L. Gebber, *Modulation of baroreceptor reflexes by somatic afferent nerve stimulation.* Am J Physiol, 1972. **222**(5): p. 1251-1259.
73. Little, R.A. and E. Kirkman, *Cardiovascular control after injury*, in *Scientific foundations of trauma*, G.J. Cooper, et al., Editors. 1997, Butterworth-Heinemann. p. 551-563.
74. Little, R.A., H.W. Marshall, and E. Kirkman, *Attenuation of the acute cardiovascular resposnes to haemorrhage by tissue injury in the conscious rat.* Q J Exp Physiol, 1989. **74**(6): p. 825-833.
75. Wang, S.C. and R.R. Overman, *The relation of blood volume reduction to mortality rate in hemorrhagic and traumatic shock in dogs.* Am J Physiol, 1947. **148**(1): p. 164-173.
76. Rady, M.Y., et al., *The effect of nociceptive stimulation on the changes in hemodynamics and oxygen transport induced by hemorrhage in anesthetized pigs.* J Trauma, 1991. **31**(5): p. 617-21; discussion 621-2.
77. Rady, M.Y., et al., *A comparison of the effects of skeletal muscle injury and somatic afferent nerve stimulation on the response to hemorrhage in anesthetized pigs.* J Trauma, 1993. **35**(5): p. 756-61.
78. Kirkman, E., et al., *Effects of afferent neural stimulation on critical oxygen delivery: a hemodynamic explanation.* Am J Physiol, 1995. **269**(6 Pt 2): p. R1448-54.
79. Mackway-Jones, K., et al., *Modification of the cardiovascular response to hemorrhage by somatic afferent nerve stimulation with speical reference to gut and skeletal muscle blood flow.* J Trauma, 1999. **47**(3): p. 481-5.
80. Foex, B., E. Kirkman, and R.A. Little, *Injury (nociceptive afferent nerve stimulation) modifies the hemodynamic and metabolic responses to heomrrhage in immature swine.* Crit Care Med, 2004. **32**(3): p. 740-6.

81. Wilmore, D.W., et al., *The gut: a central organ after surgical stress.* Surgery, 1988. **104**(5): p. 917-23.
82. Watts, S. 2014.
83. Maynard, R.L., G.J. Cooper, and R. Scott, *Mechanisms of injury in bomb blasts and explosions*, in *Trauma: pathogenesis and treatment*, S. Westaby, Editor. 1989, Butterworth-Heinemann. p. 30-41.
84. Cullis, I.G., *Blast waves and how they interact with structures.* J R Army Med Corps, 2001. **147**(1): p. 16-26.
85. Zuckerman, S., *The Problem of Blast Injuries: (Sections of Surgery and Pathology).* Proc R Soc Med, 1941. **34**(3): p. 171-92.
86. *Medical research for prevention, mitigation, and treatment of blast injuries*, D.o.D. Directive, Editor. 2006.
87. Stuhmiller, J.H., Y. Phillips, and D. Richmond, *The physics and mechanisms of primary blast injury.*, in *Textbook of military medicine: conventional warfare: blast and burn injuries*, R.F. Bellamy and R. Zajtchuk, Editors. 1991, US Government Printing Office, Washington DC. p. 241-270.
88. Phillips, Y.Y., *Primary blast injuries.* Ann Emerg Med, 1986. **15**(12): p. 1446-50.
89. Cooper, G.J. and D.E. Taylor, *Biophysics of impact injury to the chest and abdomen.* J R Army Med Corps, 1989. **135**(2): p. 58-67.
90. DePalma, R.G., et al., *Blast injuries.* N Engl J Med, 2005. **352**(13): p. 1335-42.
91. Ritenour, A.E., et al., *Incidence of primary blast injury in US military overseas contingency operations: a retrospective study.* Ann Surg, 2010. **251**(6): p. 1140-4.
92. Cooper, G.J., et al., *Casualties from terrorist bombings.* J Trauma, 1983. **23**(11): p. 955-67.
93. Kluger, Y., et al., *The quinary pattern of blast injury.* Am J Disaster Med, 2007. **2**(1): p. 21-5.
94. Mellor, S.G. and G.J. Cooper, *Analysis of 828 servicemen killed or injured by explosion in Northern Ireland 1970-84: the Hostile Action Casualty System.* Br J Surg, 1989. **76**(10): p. 1006-10.
95. *Boston Marathon bombing: FBI reveals pressure cooker clues*, in *BBC*. 2013.
96. Dearden, P., *New blast weapons.* J R Army Med Corps, 2001. **147**(1): p. 80-6.
97. Leibovici, D., et al., *Blast injuries: bus versus open-air bombings--a comparative study of injuries in survivors of open-air versus confined-space explosions.* J Trauma, 1996. **41**(6): p. 1030-5.
98. Iremonger, M.J., *Physics of detonations and blast waves.*, in *Scientific foundations of trauma*, G.J. Cooper, et al., Editors. 1997, Butterworth-Heinemann. p. 189-199.
99. Singleton, J.A., et al., *Primary blast lung injury prevalence and fatal injuries from explosions: insights from postmortem computed tomographic analysis of 121 improvised explosive device fatalities.* J Trauma Acute Care Surg, 2013. **75**(2 Suppl 2): p. S269-74.
100. de Ceballos, J.P., et al., *11 March 2004: The terrorist bomb explosions in Madrid, Spain--an analysis of the logistics, injuries sustained and clinical management of casualties treated at the closest hospital.* Crit Care, 2005. **9**(1): p. 104-11.
101. *Centers for Disease Control and Prevention. Explosions and Blast Injuries: A Primer for Clinicians*. 08/07/2014]; Available from: http://www.bt.cdc.gov/masscasualties/explosions.asp.

102. Brown, R.F., G.J. Cooper, and R.L. Maynard, *The ultrastructure of rat lung following acute primary blast injury.* Int J Exp Pathol, 1993. **74**(2): p. 151-62.
103. Maynard, R.L., D.L. Coppel, and K.G. Lowry, *Blast injury of the lung*, in *Scientific foundations of trauma*, G.J. Cooper, et al., Editors. 1997, CRC Press. p. 214-224.
104. Elsayed, N.M. and N.V. Gorbunov, *Interplay between high energy impulse noise (blast) and antioxidants in the lung.* Toxicology, 2003. **189**(1-2): p. 63-74.
105. Kirkman, E. and S. Watts, *Characterization of the response to primary blast injury.* Philos Trans R Soc Lond B Biol Sci, 2011. **366**(1562): p. 286-90.
106. Argyros, G.J., *Management of primary blast injury.* Toxicology, 1997. **121**(1): p. 105-15.
107. Clemedson, C.J. and H.I. Hultman, *Air embolism and the cause of death in blast injury.* Mil Surg, 1954. **114**(6): p. 424-37.
108. Chiffelle, T.L., *Pathology of direct airblast injury. Technical Progress Report*. 1966, Lovelace Foundation for Medical Education and Research, Albuquerque, N. Mex.
109. Barrow, D.W. and H.T. Rhoads, *Blast concussion injury.* JAMA, 1944. **125**(13): p. 900-902.
110. Krohn, P.L., D. Whitteridge, and S. Zuckerman, *Physiological effects of blast.* The Lancet, 1942. **239**(6183).
111. Ruskin, A., O.W. Beard, and R.L. Schaffer, *Blast hypertension; elevated arterial pressures in the victims of the Texas City disaster.* Am J Med, 1948. **4**(2): p. 228-36.
112. Irwin, R.J., et al., *Cardiopulmonary physiology of primary blast injury.* J Trauma, 1997. **43**(4): p. 650-5.
113. Guy, R.J., et al., *Physiologic responses to primary blast.* J Trauma, 1998. **45**(6): p. 983-7.
114. Ohnishi, M., et al., *Reflex nature of the cardiorespiratory response to primary thoracic blast injury in the anaesthetised rat.* Exp Physiol, 2001. **86**(3): p. 357-64.
115. Irwin, R.J., et al., *Shock after blast wave injury is caused by a vagally mediated reflex.* J Trauma, 1999. **47**(1): p. 105-10.
116. Harban, F.M.J., et al., *Primary thoracic blast injury causes acute reduction in cardiac function in the anaesthetised pig.* J Physiol, 2001. **533**: p. 81P.
117. Zunic, G., et al., *Pulmonary blast injury increases nitric oxide production, disturbs arginine metabolism, and alters the plasma free amino acid pool in rabbits during the early posttraumatic period.* Nitric Oxide, 2000. **4**(2): p. 123-8.
118. Paintal, A.S., *Mechanism of stimulation of type J pulmonary receptors.* J Physiol, 1969. **203**(3): p. 511-32.
119. Kirkman, E., et al., *Effects of blast injury on the autonomic nervous system and the response to resuscitation*, in *Explosions and blast-related injuries. Effects of explosions and blast from military operations and acts of terrorism.*, N.M. Elsayed and J.L. Atkins, Editors. 2008, Elsevier. p. 105-142.
120. Sawdon, M., et al., *The effects of primary thoracic blast injury and morphine on the response to haemorrhage in the anaesthetised rat.* Exp Physiol, 2002. **87**(6): p. 683-9.
121. Ohnishi, M., et al., *Morphine blocks the bradycardia associated with severe hemorrhage in the anesthetized rat.* Brain Res, 1997. **763**(1): p. 39-46.
122. Burnet, F.M. *Immunological recognition of self. Nobel Lecture, December 12, 1960*. 1960; Available from: www.nobelprize.org/nobel_prizes/medicine/.../1960/burnet-lecture.pdf.

123. Medzhitov, R. and C.A. Janeway, Jr., *Decoding the patterns of self and nonself by the innate immune system.* Science, 2002. **296**(5566): p. 298-300.
124. Matzinger, P., *The danger model: a renewed sense of self.* Science, 2002. **296**(5566): p. 301-5.
125. Lord, J.M., et al., *The systemic immune response to trauma: an overview of pathophysiology and treatment.* Lancet, 2014. **384**(9952): p. 1455-65.
126. Pugin, J., *How tissue injury alarms the immune system and causes a systemic inflammatory response syndrome.* Ann Intensive Care, 2012. **2**(1): p. 27.
127. Hazeldine, J., P. Hampson, and J.M. Lord, *The impact of trauma on neutrophil function.* Injury, 2014. **45**(12): p. 1824-1833.
128. Zhang, Q., et al., *Circulating mitochondrial DAMPs cause inflammatory responses to injury.* Nature, 2010. **464**(7285): p. 104-7.
129. Levy, R.M., et al., *Systemic inflammation and remote organ injury following trauma require HMGB1.* Am J Physiol Regul Integr Comp Physiol, 2007. **293**(4): p. R1538-44.
130. Takeuchi, O. and S. Akira, *Pattern recognition receptors and inflammation.* Cell, 2010. **140**(6): p. 805-20.
131. Manson, J., C. Thiemermann, and K. Brohi, *Trauma alarmins as activators of damage-induced inflammation.* Br J Surg, 2012. **99 Suppl 1**: p. 12-20.
132. Medzhitov, R., *Origin and physiological roles of inflammation.* Nature, 2008. **454**(7203): p. 428-35.
133. Ayala, A., et al., *Differential alterations in plasma IL-6 and TNF levels after trauma and hemorrhage.* Am J Physiol, 1991. **260**(1 Pt 2): p. R167-71.
134. Weckbach, S., et al., *A new experimental polytrauma model in rats: molecular characterization of the early inflammatory response.* Mediators Inflamm, 2012. **2012**: p. 890816.
135. Di Padova, F., et al., *Selective and early increase of IL-1 inhibitors, IL-6 and cortisol after elective surgery.* Clin Exp Immunol, 1991. **85**(1): p. 137-42.
136. Glaser, F., et al., *General stress response to conventional and laparoscopic cholecystectomy.* Ann Surg, 1995. **221**(4): p. 372-80.
137. Svoboda, P., I. Kantorova, and J. Ochmann, *Dynamics of interleukin 1, 2, and 6 and tumor necrosis factor alpha in multiple trauma patients.* J Trauma, 1994. **36**(3): p. 336-40.
138. Huber-Lang, M., et al., *Generation of C5a in the absence of C3: a new complement activation pathway.* Nat Med, 2006. **12**(6): p. 682-7.
139. Hecke, F., et al., *Circulating complement proteins in multiple trauma patients--correlation with injury severity, development of sepsis, and outcome.* Crit Care Med, 1997. **25**(12): p. 2015-24.
140. Stahel, P.F., W.R. Smith, and E.E. Moore, *Role of biological modifiers regulating the immune response after trauma.* Injury, 2007. **38**(12): p. 1409-22.
141. Kapur, M.M., P. Jain, and M. Gidh, *The effect of trauma on serum C3 activation and its correlation with injury severity score in man.* J Trauma, 1986. **26**(5): p. 464-6.
142. Sharma, D.K., et al., *The effect of recent trauma on serum complement activation and serum C3 levels correlated with the injury severity score.* Indian J Med Microbiol, 2004. **22**(3): p. 147-52.
143. Burk, A.M., et al., *Early complementopathy after multiple injuries in humans.* Shock, 2012. **37**(4): p. 348-54.

144. Zilow, G., et al., *Complement activation and the prognostic value of C3a in patients at risk of adult respiratory distress syndrome.* Clin Exp Immunol, 1990. **79**(2): p. 151-7.
145. Ganter, M.T., et al., *Role of the alternative pathway in the early complement activation following major trauma.* Shock, 2007. **28**(1): p. 29-34.
146. Springer, T.A., *Traffic signals for lymphocyte recirculation and leukocyte emigration: the multistep paradigm.* Cell, 1994. **76**(2): p. 301-14.
147. Pries, A.R., T.W. Secomb, and P. Gaehtgens, *The endothelial surface layer.* Pflugers Arch, 2000. **440**(5): p. 653-66.
148. Ghitescu, L. and M. Robert, *Diversity in unity: the biochemical composition of the endothelial cell surface varies between the vascular beds.* Microsc Res Tech, 2002. **57**(5): p. 381-9.
149. Vestweber, D. and J.E. Blanks, *Mechanisms that regulate the function of the selectins and their ligands.* Physiol Rev, 1999. **79**(1): p. 181-213.
150. Konstantopoulos, K. and L.V. McIntire, *Effects of fluid dynamic forces on vascular cell adhesion.* J Clin Invest, 1996. **98**(12): p. 2661-5.
151. Bevilacqua, M.P., *Endothelial-leukocyte adhesion molecules.* Annu Rev Immunol, 1993. **11**: p. 767-804.
152. Williams, M.R., et al., *Emerging mechanisms of neutrophil recruitment across endothelium.* Trends Immunol, 2011. **32**(10): p. 461-9.
153. Dejana, E., *Endothelial cell-cell junctions: happy together.* Nat Rev Mol Cell Biol, 2004. **5**(4): p. 261-70.
154. Tsukamoto, T., R.S. Chanthaphavong, and H.C. Pape, *Current theories on the pathophysiology of multiple organ failure after trauma.* Injury, 2010. **41**(1): p. 21-6.
155. Saffarzadeh, M., et al., *Neutrophil extracellular traps directly induce epithelial and endothelial cell death: a predominant role of histones.* PLoS One, 2012. **7**(2): p. e32366.
156. Fuchs, T.A., et al., *Extracellular DNA traps promote thrombosis.* Proc Natl Acad Sci U S A, 2010. **107**(36): p. 15880-5.
157. Mesri, M. and D.C. Altieri, *Endothelial cell activation by leukocyte microparticles.* J Immunol, 1998. **161**(8): p. 4382-7.
158. Balvers, K., et al., *Endogenous microparticles drive the proinflammatory host immune response in severely injured trauma patients.* Shock, 2015. **43**(4): p. 317-21.
159. Paunel-Gorgulu, A., et al., *Mcl-1-mediated impairment of the intrinsic apoptosis pathway in circulating neutrophils from critically ill patients can be overcome by Fas stimulation.* J Immunol, 2009. **183**(10): p. 6198-206.
160. Akgul, C., D.A. Moulding, and S.W. Edwards, *Molecular control of neutrophil apoptosis.* FEBS Lett, 2001. **487**(3): p. 318-22.
161. Liles, W.C., et al., *Differential expression of Fas (CD95) and Fas ligand on normal human phagocytes: implications for the regulation of apoptosis in neutrophils.* J Exp Med, 1996. **184**(2): p. 429-40.
162. Paunel-Gorgulu, A., et al., *Molecular mechanisms underlying delayed apoptosis in neutrophils from multiple trauma patients with and without sepsis.* Mol Med, 2012. **18**: p. 325-35.
163. Botha, A.J., et al., *Early neutrophil sequestration after injury: a pathogenic mechanism for multiple organ failure.* J Trauma, 1995. **39**(3): p. 411-7.

164. Brundage, S.I., et al., *Amplification of the proinflammatory transcription factor cascade increases with severity of uncontrolled hemorrhage in swine.* J Surg Res, 2003. **113**(1): p. 74-80.
165. Ehrnthaller, C., et al., *Alteration of complement hemolytic activity in different trauma and sepsis models.* J Inflamm Res, 2012. **5**: p. 59-66.
166. Altavilla, D., et al., *Oxidative stress causes nuclear factor-kappaB activation in acute hypovolemic hemorrhagic shock.* Free Radic Biol Med, 2001. **30**(10): p. 1055-66.
167. Roumen, R.M., et al., *Cytokine patterns in patients after major vascular surgery, hemorrhagic shock, and severe blunt trauma. Relation with subsequent adult respiratory distress syndrome and multiple organ failure.* Ann Surg, 1993. **218**(6): p. 769-76.
168. Fink, M.P., *Reactive oxygen species as mediators of organ dysfunction caused by sepsis, acute respiratory distress syndrome, or hemorrhagic shock: potential benefits of resuscitation with Ringer's ethyl pyruvate solution.* Curr Opin Clin Nutr Metab Care, 2002. **5**(2): p. 167-74.
169. Jaeschke, H. and A. Farhood, *Kupffer cell activation after no-flow ischemia versus hemorrhagic shock.* Free Radic Biol Med, 2002. **33**(2): p. 210-9.
170. Granger, D.N. and P.R. Kvietys, *Reperfusion injury and reactive oxygen species: The evolution of a concept.* Redox Biol, 2015. **6**: p. 524-551.
171. Keel, M. and O. Trentz, *Pathophysiology of polytrauma.* Injury, 2005. **36**(6): p. 691-709.
172. Circu, M.L. and T.Y. Aw, *Reactive oxygen species, cellular redox systems, and apoptosis.* Free Radic Biol Med, 2010. **48**(6): p. 749-62.
173. Childs, E.W., et al., *In vivo visualization of reactive oxidants and leukocyte-endothelial adherence following hemorrhagic shock.* Shock, 2002. **18**(5): p. 423-7.
174. Powers, K.A., et al., *Oxidative stress generated by hemorrhagic shock recruits Toll-like receptor 4 to the plasma membrane in macrophages.* J Exp Med, 2006. **203**(8): p. 1951-61.
175. Laplace, C., et al., *Endothelial oxidative stress induced by serum from patients with severe trauma hemorrhage.* Intensive Care Med, 2005. **31**(9): p. 1174-80.
176. Szabo, C. and T.R. Billiar, *Novel roles of nitric oxide in hemorrhagic shock.* Shock, 1999. **12**(1): p. 1-9.
177. Hierholzer, C., et al., *Essential role of induced nitric oxide in the initiation of the inflammatory response after hemorrhagic shock.* J Exp Med, 1998. **187**(6): p. 917-28.
178. Anaya-Prado, R., et al., *The attenuation of hemorrhage-induced liver injury by exogenous nitric oxide, L-arginine, and inhibition of inducible nitric oxide synthase.* J Invest Surg, 2003. **16**(5): p. 247-61.
179. Md, S., et al., *The role of selective nitric oxide synthase inhibitor on nitric oxide and PGE2 levels in refractory hemorrhagic-shocked rats.* J Surg Res, 2005. **123**(2): p. 206-14.
180. Johnson, R.A., et al., *Vascular arginase contributes to arteriolar endothelial dysfunction in a rat model of hemorrhagic shock.* J Trauma, 2010. **69**(2): p. 384-91.
181. Szabo, C. and C. Thiemermann, *Invited opinion: role of nitric oxide in hemorrhagic, traumatic, and anaphylactic shock and thermal injury.* Shock, 1994. **2**(2): p. 145-55.
182. Beckman, J.S., et al., *Apparent hydroxyl radical production by peroxynitrite: implications for endothelial injury from nitric oxide and superoxide.* Proc Natl Acad Sci U S A, 1990. **87**(4): p. 1620-4.

183. Forstermann, U. and W.C. Sessa, *Nitric oxide synthases: regulation and function.* Eur Heart J, 2012. **33**(7): p. 829-37, 837a-837d.
184. Xia, Y., *Superoxide generation from nitric oxide synthases.* Antioxid Redox Signal, 2007. **9**(10): p. 1773-8.
185. Shu, X., et al., *Endothelial nitric oxide synthase in the microcirculation.* Cell Mol Life Sci, 2015. **72**(23): p. 4561-75.
186. de Perrot, M., et al., *Ischemia-reperfusion-induced lung injury.* Am J Respir Crit Care Med, 2003. **167**(4): p. 490-511.
187. Perry, B.C., et al., *Tumor necrosis factor-alpha in liver ischemia/reperfusion injury.* J Invest Surg, 2011. **24**(4): p. 178-88.
188. Deb, S., et al., *Resuscitation with lactated Ringer's solution in rats with hemorrhagic shock induces immediate apoptosis.* J Trauma, 1999. **46**(4): p. 582-8; discussion 588-9.
189. Rhee, P., et al., *Tumor necrosis factor and monocytes are released during hemorrhagic shock.* Resuscitation, 1993. **25**(3): p. 249-55.
190. Yao, Y.M., et al., *The inflammatory basis of trauma/shock-associated multiple organ failure.* Inflamm Res, 1998. **47**(5): p. 201-10.
191. Baker, T.A., et al., *Systemic release of cytokines and heat shock proteins in porcine models of polytrauma and hemorrhage*.* Crit Care Med, 2012. **40**(3): p. 876-85.
192. Hierholzer, C., et al., *Interleukin-6 production in hemorrhagic shock is accompanied by neutrophil recruitment and lung injury.* Am J Physiol, 1998. **275**(3 Pt 1): p. L611-21.
193. Diepenhorst, G.M., T.M. van Gulik, and C.E. Hack, *Complement-mediated ischemia-reperfusion injury: lessons learned from animal and clinical studies.* Ann Surg, 2009. **249**(6): p. 889-99.
194. Weiser, M.R., et al., *Reperfusion injury of ischemic skeletal muscle is mediated by natural antibody and complement.* J Exp Med, 1996. **183**(5): p. 2343-8.
195. Younger, J.G., et al., *Detrimental effects of complement activation in hemorrhagic shock.* J Appl Physiol (1985), 2001. **90**(2): p. 441-6.
196. Harkin, D.W., et al., *C5 complement inhibition attenuates shock and acute lung injury in an experimental model of ruptured abdominal aortic aneurysm.* Br J Surg, 2005. **92**(10): p. 1227-34.
197. Scalia, R., et al., *Essential role of P-selectin in the initiation of the inflammatory response induced by hemorrhage and reinfusion.* J Exp Med, 1999. **189**(6): p. 931-8.
198. Sun, L.L., et al., *Early up-regulation of intercellular adhesion molecule-1 and vascular cell adhesion molecule-1 expression in rats with hemorrhagic shock and resuscitation.* Shock, 1999. **11**(6): p. 416-22.
199. Schofield, Z.V., et al., *Neutrophils--a key component of ischemia-reperfusion injury.* Shock, 2013. **40**(6): p. 463-70.
200. Hierholzer, C. and T.R. Billiar, *Molecular mechanisms in the early phase of hemorrhagic shock.* Langenbecks Arch Surg, 2001. **386**(4): p. 302-8.
201. Wang, Q.M., et al., *Inhibition of Rho-kinase attenuates endothelial-leukocyte interaction during ischemia-reperfusion injury.* Vasc Med, 2012. **17**(6): p. 379-85.
202. Childs, E.W., et al., *Leukocyte adherence and sequestration following hemorrhagic shock and total ischemia in rats.* Shock, 1999. **11**(4): p. 248-52.

203. Kyriakides, C., et al., *Neutrophil mediated remote organ injury after lower torso ischemia and reperfusion is selectin and complement dependent.* J Trauma, 2000. **48**(1): p. 32-8.
204. Vedder, N.B., et al., *Role of neutrophils in generalized reperfusion injury associated with resuscitation from shock.* Surgery, 1989. **106**(3): p. 509-16.
205. Wang, P., Z.F. Ba, and I.H. Chaudry, *Endothelial cell dysfunction occurs very early following trauma-hemorrhage and persists despite fluid resuscitation.* Am J Physiol, 1993. **265**(3 Pt 2): p. H973-9.
206. Chang, N.J., et al., *Genome-wide gene expression profiling of ischemia-reperfusion injury in rat kidney, intestine and skeletal muscle implicate a common involvement of MAPK signaling pathway.* Mol Med Rep, 2015. **11**(5): p. 3786-93.
207. Kim, J.Y., et al., *HMGB1 contributes to the development of acute lung injury after hemorrhage.* Am J Physiol Lung Cell Mol Physiol, 2005. **288**(5): p. L958-65.
208. Woodfin, A., et al., *The junctional adhesion molecule JAM-C regulates polarized transendothelial migration of neutrophils in vivo.* Nat Immunol, 2011. **12**(8): p. 761-9.
209. Deitch, E.A., *Bacterial translocation or lymphatic drainage of toxic products from the gut: what is important in human beings?* Surgery, 2002. **131**(3): p. 241-4.
210. Moore, F.A., et al., *Gut bacterial translocation via the portal vein: a clinical perspective with major torso trauma.* J Trauma, 1991. **31**(5): p. 629-36; discussion 636-8.
211. Senthil, M., et al., *Gut-lymph hypothesis of systemic inflammatory response syndrome/multiple-organ dysfunction syndrome: validating studies in a porcine model.* J Trauma, 2006. **60**(5): p. 958-65; discussion 965-7.
212. Tiesi, G., et al., *Early trauma-hemorrhage-induced splenic and thymic apoptosis is gut-mediated and toll-like receptor 4-dependent.* Shock, 2013. **39**(6): p. 507-13.
213. Gorbunov, N.V., et al., *Air blast-induced pulmonary oxidative stress: interplay among hemoglobin, antioxidants, and lipid peroxidation.* Am J Physiol, 1997. **272**(2 Pt 1): p. L320-34.
214. Gorbunov, N.V., et al., *Pro-inflammatory alterations and status of blood plasma iron in a model of blast-induced lung trauma.* Int J Immunopathol Pharmacol, 2005. **18**(3): p. 547-56.
215. Gorbunov, N.V., et al., *Assessment of inflammatory response and sequestration of blood iron transferrin complexes in a rat model of lung injury resulting from exposure to low-frequency shock waves.* Crit Care Med, 2004. **32**(4): p. 1028-34.
216. Gorbunov, N.V., et al., *Inflammatory leukocytes and iron turnover in experimental hemorrhagic lung trauma.* Exp Mol Pathol, 2006. **80**(1): p. 11-25.
217. Chavko, M., W.K. Prusaczyk, and R.M. McCarron, *Lung injury and recovery after exposure to blast overpressure.* J Trauma, 2006. **61**(4): p. 933-42.
218. Zunic, G., et al., *Very early increase in nitric oxide formation and oxidative cell damage associated with the reduction of tissue oxygenation is a trait of blast casualties.* Vojnosanit Pregl, 2005. **62**(4): p. 273-80.
219. Elsayed, N.M., et al., *Antioxidant loading reduces oxidative stress induced by high-energy impulse noise (blast) exposure.* Toxicology, 2000. **155**(1-3): p. 91-9.
220. Chavko, M., et al., *Attenuation of pulmonary inflammation after exposure to blast overpressure by N-acetylcysteine amide.* Shock, 2009. **32**(3): p. 325-31.
221. Chavko, M., W.K. Prusaczyk, and R.M. McCarron, *Protection against blast-induced mortality in rats by hemin.* J Trauma, 2008. **65**(5): p. 1140-5; discussion 1145.

222. Cernak, I., et al., *Involvement of the central nervous system in the general response to pulmonary blast injury.* J Trauma, 1996. **40**(3 Suppl): p. S100-4.
223. Cernak, I., *The importance of systemic response in the pathobiology of blast-induced neurotrauma.* Front Neurol, 2010. **1**: p. 151.
224. Spear, A.M., et al., *Blast Wave Exposure to the Extremities Causes Endothelial Activation and Damage.* Shock, 2015. **44**(5): p. 470-8.
225. Ning, J.L., et al., *Lung injury following lower extremity blast trauma in rats.* J Trauma Acute Care Surg, 2012. **73**(6): p. 1537-44.
226. Margetic, S., *Inflammation and haemostasis.* Biochem Med (Zagreb), 2012. **22**(1): p. 49-62.
227. Esmon, C.T., *The interactions between inflammation and coagulation.* Br J Haematol, 2005. **131**(4): p. 417-30.
228. Engelmann, B. and S. Massberg, *Thrombosis as an intravascular effector of innate immunity.* Nat Rev Immunol, 2013. **13**(1): p. 34-45.
229. Brohi, K., et al., *Acute traumatic coagulopathy.* J Trauma, 2003. **54**(6): p. 1127-30.
230. Davenport, R., et al., *Functional definition and characterization of acute traumatic coagulopathy.* Crit Care Med, 2011. **39**(12): p. 2652-8.
231. Frith, D., et al., *Definition and drivers of acute traumatic coagulopathy: clinical and experimental investigations.* J Thromb Haemost, 2010. **8**(9): p. 1919-25.
232. Peltan, I.D., et al., *An International Normalized Ratio-Based Definition of Acute Traumatic Coagulopathy Is Associated With Mortality, Venous Thromboembolism, and Multiple Organ Failure After Injury.* Crit Care Med, 2015. **43**(7): p. 1429-38.
233. Kutcher, M.E., et al., *Evolving beyond the vicious triad: Differential mediation of traumatic coagulopathy by injury, shock, and resuscitation.* J Trauma Acute Care Surg, 2015. **78**(3): p. 516-23.
234. Cohen, M.J., et al., *Critical role of activated protein C in early coagulopathy and later organ failure, infection and death in trauma patients.* Ann Surg, 2012. **255**(2): p. 379-85.
235. Johansson, P.I., et al., *A high admission syndecan-1 level, a marker of endothelial glycocalyx degradation, is associated with inflammation, protein C depletion, fibrinolysis, and increased mortality in trauma patients.* Ann Surg, 2011. **254**(2): p. 194-200.
236. Biemond, B.J., et al., *Plasminogen activator and plasminogen activator inhibitor I release during experimental endotoxaemia in chimpanzees: effect of interventions in the cytokine and coagulation cascades.* Clin Sci (Lond), 1995. **88**(5): p. 587-94.
237. Taylor, F.B., Jr., et al., *Protein C prevents the coagulopathic and lethal effects of Escherichia coli infusion in the baboon.* J Clin Invest, 1987. **79**(3): p. 918-25.
238. Cohen, M.J., et al., *Protein C depletion early after trauma increases the risk of ventilator-associated pneumonia.* J Trauma, 2009. **67**(6): p. 1176-81.
239. Cole, E., et al., *Coagulation system changes associated with susceptibility to infection in trauma patients.* J Trauma Acute Care Surg, 2013. **74**(1): p. 51-7; discussion 57-8.
240. Darlington, D.N., et al., *Trauma-Induced Coagulopathy Is Associated with a Complex Inflammatory Response in the Rat.* Shock, 2015. **44 Suppl 1**: p. 129-37.
241. Xiao, W., et al., *A genomic storm in critically injured humans.* J Exp Med, 2011. **208**(13): p. 2581-90.

242. Gothner, M., et al., *Use of extracorporeal membrane oxygenation in combination with high-frequency oscillatory ventilation in post-traumatic ARDS.* Acta Anaesthesiol Scand, 2013. **57**(3): p. 391-4.
243. Peek, G.J., et al., *Efficacy and economic assessment of conventional ventilatory support versus extracorporeal membrane oxygenation for severe adult respiratory failure (CESAR): a multicentre randomised controlled trial.* Lancet, 2009. **374**(9698): p. 1351-63.
244. Alam, H.B., et al., *Effect of different resuscitation strategies on neutrophil activation in a swine model of hemorrhagic shock.* Resuscitation, 2004. **60**(1): p. 91-9.
245. Angle, N., et al., *Hypertonic saline resuscitation reduces neutrophil margination by suppressing neutrophil L selectin expression.* J Trauma, 1998. **45**(1): p. 7-12; discussion 12-3.
246. Chen, G., et al., *Effects of synthetic colloids on oxidative stress and inflammatory response in hemorrhagic shock: comparison of hydroxyethyl starch 130/0.4, hydroxyethyl starch 200/0.5, and succinylated gelatin.* Crit Care, 2013. **17**(4): p. R141.
247. Corso, C.O., et al., *Resuscitation with hypertonic saline dextran reduces endothelial cell swelling and improves hepatic microvascular perfusion and function after hemorrhagic shock.* J Surg Res, 1998. **80**(2): p. 210-20.
248. Corso, C.O., et al., *Hypertonic saline dextran attenuates leukocyte accumulation in the liver after hemorrhagic shock and resuscitation.* J Trauma, 1999. **46**(3): p. 417-23.
249. Deitch, E.A., et al., *Hypertonic saline resuscitation limits neutrophil activation after trauma-hemorrhagic shock.* Shock, 2003. **19**(4): p. 328-33.
250. Lee, C.C., et al., *Effect of different resuscitation fluids on cytokine response in a rat model of hemorrhagic shock.* Shock, 2005. **24**(2): p. 177-81.
251. Murao, Y., et al., *Hypertonic saline resuscitation reduces apoptosis and tissue damage of the small intestine in a mouse model of hemorrhagic shock.* Shock, 2003. **20**(1): p. 23-8.
252. Rhee, P., et al., *Lactated Ringer's solution resuscitation causes neutrophil activation after hemorrhagic shock.* J Trauma, 1998. **44**(2): p. 313-9.
253. Rizoli, S.B., et al., *The immunomodulatory effects of hypertonic saline resuscitation in patients sustaining traumatic hemorrhagic shock: a randomized, controlled, double-blinded trial.* Ann Surg, 2006. **243**(1): p. 47-57.
254. Savage, S.A., et al., *Endothelial dysfunction after lactated Ringer's solution resuscitation for hemorrhagic shock.* J Trauma, 2005. **59**(2): p. 284-90.
255. Shi, H.P., et al., *Hypertonic saline improves intestinal mucosa barrier function and lung injury after trauma-hemorrhagic shock.* Shock, 2002. **17**(6): p. 496-501.
256. Vega, D., et al., *The influence of the type of resuscitation fluid on gut injury and distant organ injury in a rat model of trauma/hemorrhagic shock.* J Trauma, 2008. **65**(2): p. 409-14; discussion 414-5.
257. Cai, B., et al., *Anti-inflammatory resuscitation improves survival in hemorrhage with trauma.* J Trauma, 2009. **66**(6): p. 1632-9; discussion 1639-40.
258. Cotoia, A., et al., *p-Hydroxyphenylpyruvate, an intermediate of the Phe/Tyr catabolism, improves mitochondrial oxidative metabolism under stressing conditions and prolongs survival in rats subjected to profound hemorrhagic shock.* PLoS One, 2014. **9**(3): p. e90917.
259. Dong, W., et al., *Ethyl pyruvate prevents inflammatory responses and organ damage during resuscitation in porcine hemorrhage.* Shock, 2010. **34**(2): p. 205-13.

260. Gonzales, E., et al., *Valproic acid prevents hemorrhage-associated lethality and affects the acetylation pattern of cardiac histones.* Shock, 2006. **25**(4): p. 395-401.
261. Lin, T., et al., *Cardiac histones are substrates of histone deacetylase activity in hemorrhagic shock and resuscitation.* Surgery, 2006. **139**(3): p. 365-76.
262. Kwan, I., et al., *Timing and volume of fluid administration for patients with bleeding.* Cochrane Database Syst Rev, 2014(3): p. CD002245.
263. Wright, C., et al., *Fluid resuscitation: a Defence Medical Services Delphi study into current practice.* J R Army Med Corps, 2009. **155**(2): p. 99-104.
264. Champion, H.R., *Combat fluid resuscitation: introduction and overview of conferences.* J Trauma, 2003. **54**(5 Suppl): p. S7-12.
265. Shires, T., et al., *Fluid Therapy in Hemorrhagic Shock.* Arch Surg, 1964. **88**: p. 688-93.
266. Bickell, W.H., et al., *The detrimental effects of intravenous crystalloid after aortotomy in swine.* Surgery, 1991. **110**(3): p. 529-36.
267. Stern, S.A., et al., *Effect of blood pressure on hemorrhage volume and survival in a near-fatal hemorrhage model incorporating a vascular injury.* Ann Emerg Med, 1993. **22**(2): p. 155-63.
268. Bickell, W.H., et al., *Immediate versus delayed fluid resuscitation for hypotensive patients with penetrating torso injuries.* N Engl J Med, 1994. **331**(17): p. 1105-9.
269. Butler, F.K., et al., *Fluid Resuscitation for Hemorrhagic Shock in Tactical Combat Casualty Care: TCCC Guidelines Change 14-01 - 2 June 2014.* J Spec Oper Med, 2014. **14**(3): p. 13-38.
270. Sondeen, J.L., V.G. Coppes, and J.B. Holcomb, *Blood pressure at which rebleeding occurs after resuscitation in swine with aortic injury.* J Trauma, 2003. **54**(5 Suppl): p. S110-7.
271. Mapstone, J., I. Roberts, and P. Evans, *Fluid resuscitation strategies: a systematic review of animal trials.* J Trauma, 2003. **55**(3): p. 571-89.
272. Kirkman, E., S. Watts, and G. Cooper, *Blast injury research models.* Philos Trans R Soc Lond B Biol Sci, 2011. **366**(1562): p. 144-59.
273. Kowalenko, T., et al., *Improved outcome with hypotensive resuscitation of uncontrolled hemorrhagic shock in a swine model.* J Trauma, 1992. **33**(3): p. 349-53; discussion 361-2.
274. Bickell, W.H., S.P. Bruttig, and C.E. Wade, *Hemodynamic response to abdominal aortotomy in the anesthetized swine.* Circ Shock, 1989. **28**(4): p. 321-32.
275. Garner, J., et al., *Prolonged permissive hypotensive resuscitation is associated with poor outcome in primary blast injury with controlled hemorrhage.* Ann Surg, 2010. **251**(6): p. 1131-9.
276. Doran, C.M., et al., *Targeted resuscitation improves coagulation and outcome.* J Trauma Acute Care Surg, 2012. **72**(4): p. 835-43.
277. *Battlefield Advanced Trauma Life Support hand book*. 2014.
278. Holcomb, J.B., et al., *Damage control resuscitation: directly addressing the early coagulopathy of trauma.* J Trauma, 2007. **62**(2): p. 307-10.
279. Nessen, S.C., et al., *Fresh whole blood use by forward surgical teams in Afghanistan is associated with improved survival compared to component therapy without platelets.* Transfusion, 2013. **53 Suppl 1**: p. 107S-113S.
280. Jenkins, D.H., et al., *Trauma hemostasis and oxygenation research position paper on remote damage control resuscitation: definitions, current practice, and knowledge gaps.* Shock, 2014. **41 Suppl 1**: p. 3-12.

281. Hodgetts, T.J., P.F. Mahoney, and E. Kirkman, *Damage control resuscitation.* J R Army Med Corps, 2007. **153**(4): p. 299-300.
282. Dretzke, J., et al., *Protocol for a systematic review of the clinical effectiveness of pre-hospital blood components compared to other resuscitative fluids in patients with major traumatic haemorrhage.* Syst Rev, 2014. **3**: p. 123.
283. Cap, A.P., et al., *Blood far forward: Time to get moving!* J Trauma Acute Care Surg, 2015. **78**(6 Suppl 1): p. S2-6.
284. *RePHILL*. Available from: http://www.birmingham.ac.uk/research/activity/mds/trials/bctu/trials/portfolio-v/Rephill/index.aspx.
285. Brown, J.B., et al., *Taking the Blood Bank to the Field: The Design and Rationale of the Prehospital Air Medical Plasma (PAMPer) Trial.* Prehosp Emerg Care, 2015. **19**(3): p. 343-50.
286. Reynolds, P.S., et al., *Prehospital use of plasma in traumatic hemorrhage (The PUPTH Trial): study protocol for a randomised controlled trial.* Trials, 2015. **16**: p. 321.
287. Belizaire, R.M., et al., *Microparticles from stored red blood cells activate neutrophils and cause lung injury after hemorrhage and resuscitation.* J Am Coll Surg, 2012. **214**(4): p. 648-55; discussion 656-7.
288. Belizaire, R.M., et al., *Resuscitation with washed aged packed red blood cell units decreases the proinflammatory response in mice after hemorrhage.* J Trauma Acute Care Surg, 2012. **73**(2 Suppl 1): p. S128-33.
289. Land, W.G., *Transfusion-Related Acute Lung Injury: The Work of DAMPs.* Transfus Med Hemother, 2013. **40**(1): p. 3-13.
290. Kleinman, S., et al., *Toward an understanding of transfusion-related acute lung injury: statement of a consensus panel.* Transfusion, 2004. **44**(12): p. 1774-89.
291. Shanwell, A., et al., *Generation of cytokines in red cell concentrates during storage is prevented by prestorage white cell reduction.* Transfusion, 1997. **37**(7): p. 678-84.
292. Silliman, C.C., et al., *Identification of lipids that accumulate during the routine storage of prestorage leukoreduced red blood cells and cause acute lung injury.* Transfusion, 2011. **51**(12): p. 2549-54.
293. Dzieciatkowska, M., et al., *Proteomic analysis of the supernatant of red blood cell units: the effects of storage and leucoreduction.* Vox Sang, 2013. **105**(3): p. 210-8.
294. Fisher, M., et al., *Alloimmunisation to HLA antigens following transfusion with leucocyte-poor and purified platelet suspensions.* Vox Sang, 1985. **49**(5): p. 331-5.
295. Hebert, P.C., et al., *Clinical outcomes following institution of the Canadian universal leukoreduction program for red blood cell transfusions.* JAMA, 2003. **289**(15): p. 1941-9.
296. Blumberg, N., et al., *An association between decreased cardiopulmonary complications (transfusion-related acute lung injury and transfusion-associated circulatory overload) and implementation of universal leukoreduction of blood transfusions.* Transfusion, 2010. **50**(12): p. 2738-44.
297. *National Blood Service. Guidelines for the blood transfusion services*. 2013, The Stationery Office.
298. Beckman, N., et al., *Review of the quality monitoring methods used by countries using or implementing universal leukoreduction.* Transfus Med Rev, 2004. **18**(1): p. 25-35.

299. *U.S. Department of Health and Human Services Food and Drug Admininstration. Guidance for industry: Pre-storage leukocyte reduction of whole blood and blood components intended for transfusion*, C.f.B.E.a. Research, Editor. 2012.
300. Starkey, K., et al., *Impact of high ratios of plasma-to-red cell concentrate on the incidence of acute respiratory distress syndrome in UK transfused combat casualties.* Shock, 2013. **40**(1): p. 15-20.
301. Kozar, R.A., et al., *Plasma restoration of endothelial glycocalyx in a rodent model of hemorrhagic shock.* Anesth Analg, 2011. **112**(6): p. 1289-95.
302. Peng, Z., et al., *Fresh frozen plasma lessens pulmonary endothelial inflammation and hyperpermeability after hemorrhagic shock and is associated with loss of syndecan 1.* Shock, 2013. **40**(3): p. 195-202.
303. Makley, A.T., et al., *Damage control resuscitation decreases systemic inflammation after hemorrhage.* J Surg Res, 2012. **175**(2): p. e75-82.
304. Apodaca, A., et al., *Performance improvement evaluation of forward aeromedical evacuation platforms in Operation Enduring Freedom.* J Trauma Acute Care Surg, 2013. **75**(2 Suppl 2): p. S157-63.
305. Paudyal, P., et al., *Tranexamic acid in major trauma: implementation and evaluation across South West England.* Eur J Emerg Med, 2015.
306. Jimenez, J.J., et al., *Tranexamic acid attenuates inflammatory response in cardiopulmonary bypass surgery through blockade of fibrinolysis: a case control study followed by a randomized double-blind controlled trial.* Crit Care, 2007. **11**(6): p. R117.
307. Spinella, P.C. *Tranexamic acid mechanisms and pharmacokinetics in traumatic injury (TAMPITI)*. Available from: https://clinicaltrials.gov/ct2/show/NCT02535949.
308. Rhee, P., et al., *Recombinant humanized monoclonal antibody against CD18 (rhuMAb CD18) in traumatic hemorrhagic shock: results of a phase II clinical trial. Traumatic Shock Group.* J Trauma, 2000. **49**(4): p. 611-9; discussion 619-20.
309. Seekamp, A., et al., *The effect of anti-L-selectin (aselizumab) in multiple traumatized patients--results of a phase II clinical trial.* Crit Care Med, 2004. **32**(10): p. 2021-8.
310. Cotton, B.A., *Alternative fluids for prehospital resuscitation: "pharmacological" resuscitation fluids.* J Trauma, 2011. **70**(5 Suppl): p. S30-1.
311. Bennett-Guerrero, E., et al., *A phase II multicenter double-blind placebo-controlled study of ethyl pyruvate in high-risk patients undergoing cardiac surgery with cardiopulmonary bypass.* J Cardiothorac Vasc Anesth, 2009. **23**(3): p. 324-9.
312. Gottlicher, M., et al., *Valproic acid defines a novel class of HDAC inhibitors inducing differentiation of transformed cells.* EMBO J, 2001. **20**(24): p. 6969-78.
313. Gallinari, P., et al., *HDACs, histone deacetylation and gene transcription: from molecular biology to cancer therapeutics.* Cell Res, 2007. **17**(3): p. 195-211.
314. Shults, C., et al., *Surviving blood loss without fluid resuscitation.* J Trauma, 2008. **64**(3): p. 629-38; discussion 638-40.
315. Alam, H.B., et al., *Surviving blood loss without blood transfusion in a swine poly-trauma model.* Surgery, 2009. **146**(2): p. 325-33.
316. Fukudome, E.Y., et al., *Pharmacologic resuscitation promotes survival and attenuates hemorrhage-induced activation of extracellular signal-regulated kinase 1/2.* J Surg Res, 2010. **163**(1): p. 118-26.
317. Butt, M.U., et al., *Pharmacologic resuscitation: cell protective mechanisms of histone deacetylase inhibition in lethal hemorrhagic shock.* J Surg Res, 2009. **156**(2): p. 290-6.

318. Li, R., et al., *Histone Deacetylase Inhibition and IkappaB Kinase/Nuclear Factor-kappaB Blockade Ameliorate Microvascular Proinflammatory Responses Associated With Hemorrhagic Shock/Resuscitation in Mice.* Crit Care Med, 2015. **43**(12): p. e567-80.
319. Alam, H.B. *A study to evaulate the safety and tolerability of valporic acid in healthy volunteers or trauma patients*. Available from: https://clinicaltrials.gov/ct2/show/NCT01951560.
320. Chaudry, I.H., et al., *Endocrine targets in experimental shock.* J Trauma, 2003. **54**(5 Suppl): p. S118-25.
321. Bullard, M.K., et al., *Women rule.* Surgery, 2010. **147**(1): p. 134-7.
322. Choudhry, M.A. and I.H. Chaudry, *17beta-Estradiol: a novel hormone for improving immune and cardiovascular responses following trauma-hemorrhage.* J Leukoc Biol, 2008. **83**(3): p. 518-22.
323. Jarrar, D., et al., *Mechanisms of the salutary effects of dehydroepiandrosterone after trauma-hemorrhage: direct or indirect effects on cardiac and hepatocellular functions?* Arch Surg, 2000. **135**(4): p. 416-22; discussion 422-3.
324. Lichte, P., et al., *Dehydroepiandrosterone modulates the inflammatory response in a bilateral femoral shaft fracture model.* Eur J Med Res, 2014. **19**: p. 27.
325. Shimizu, T., et al., *Mechanism of salutary effects of androstenediol on hepatic function after trauma-hemorrhage: role of endothelial and inducible nitric oxide synthase.* Am J Physiol Gastrointest Liver Physiol, 2005. **288**(2): p. G244-50.
326. Raju, R., K.I. Bland, and I.H. Chaudry, *Estrogen: a novel therapeutic adjunct for the treatment of trauma-hemorrhage-induced immunological alterations.* Mol Med, 2008. **14**(3-4): p. 213-21.
327. *Resuscitative endocrinology: Single-dose clincial uses for estrogen - traumatic hemorrhagic shock (RESCUE-Shock)*. Available from: https://clinicaltrials.gov/ct2/show/NCT00973102.
328. Sacks, F.M., et al., *The effect of pravastatin on coronary events after myocardial infarction in patients with average cholesterol levels. Cholesterol and Recurrent Events Trial investigators.* N Engl J Med, 1996. **335**(14): p. 1001-9.
329. Jukema, J.W., et al., *Effects of lipid lowering by pravastatin on progression and regression of coronary artery disease in symptomatic men with normal to moderately elevated serum cholesterol levels. The Regression Growth Evaluation Statin Study (REGRESS).* Circulation, 1995. **91**(10): p. 2528-40.
330. Kinlay, S., et al., *Effect of atorvastatin on risk of recurrent cardiovascular events after an acute coronary syndrome associated with high soluble CD40 ligand in the Myocardial Ischemia Reduction with Aggressive Cholesterol Lowering (MIRACL) Study.* Circulation, 2004. **110**(4): p. 386-91.
331. Ridker, P.M., et al., *C-reactive protein levels and outcomes after statin therapy.* N Engl J Med, 2005. **352**(1): p. 20-8.
332. Takemoto, M. and J.K. Liao, *Pleiotropic effects of 3-hydroxy-3-methylglutaryl coenzyme a reductase inhibitors.* Arterioscler Thromb Vasc Biol, 2001. **21**(11): p. 1712-9.
333. Weitz-Schmidt, G., et al., *Statins selectively inhibit leukocyte function antigen-1 by binding to a novel regulatory integrin site.* Nat Med, 2001. **7**(6): p. 687-92.
334. Frenette, P.S., *Locking a leukocyte integrin with statins.* N Engl J Med, 2001. **345**(19): p. 1419-21.

335. Lahera, V., et al., *Endothelial dysfunction, oxidative stress and inflammation in atherosclerosis: beneficial effects of statins.* Curr Med Chem, 2007. **14**(2): p. 243-8.
336. Casey, P.J., *Protein lipidation in cell signaling.* Science, 1995. **268**(5208): p. 221-5.
337. Zhang, F.L. and P.J. Casey, *Protein prenylation: molecular mechanisms and functional consequences.* Annu Rev Biochem, 1996. **65**: p. 241-69.
338. Rao, R., et al., *Lipid rafts in cytokine signaling.* Cytokine Growth Factor Rev, 2004. **15**(2-3): p. 103-10.
339. Varshney, P., V. Yadav, and N. Saini, *Lipid rafts in immune signalling: current progress and future perspective.* Immunology, 2016. **149**(1): p. 13-24.
340. Gu, M.X., et al., *Proteomic analysis of endothelial lipid rafts reveals a novel role of statins in antioxidation.* J Proteome Res, 2012. **11**(4): p. 2365-73.
341. Laufs, U., *Beyond lipid-lowering: effects of statins on endothelial nitric oxide.* Eur J Clin Pharmacol, 2003. **58**(11): p. 719-31.
342. Laufs, U. and J.K. Liao, *Post-transcriptional regulation of endothelial nitric oxide synthase mRNA stability by Rho GTPase.* J Biol Chem, 1998. **273**(37): p. 24266-71.
343. Wagner, A.H., O. Schwabe, and M. Hecker, *Atorvastatin inhibition of cytokine-inducible nitric oxide synthase expression in native endothelial cells in situ.* Br J Pharmacol, 2002. **136**(1): p. 143-9.
344. Wassmann, S., et al., *Cellular antioxidant effects of atorvastatin in vitro and in vivo.* Arterioscler Thromb Vasc Biol, 2002. **22**(2): p. 300-5.
345. Dimmeler, S., et al., *HMG-CoA reductase inhibitors (statins) increase endothelial progenitor cells via the PI 3-kinase/Akt pathway.* J Clin Invest, 2001. **108**(3): p. 391-7.
346. Dichtl, W., et al., *HMG-CoA reductase inhibitors regulate inflammatory transcription factors in human endothelial and vascular smooth muscle cells.* Arterioscler Thromb Vasc Biol, 2003. **23**(1): p. 58-63.
347. Laws, P.E., et al., *The role of statins in vascular disease.* Eur J Vasc Endovasc Surg, 2004. **27**(1): p. 6-16.
348. Eccles, K.A., et al., *Simvastatin alters human endothelial cell adhesion molecule expression and inhibits leukocyte adhesion under flow.* Atherosclerosis, 2008. **200**(1): p. 69-79.
349. Margaritis, M., K.M. Channon, and C. Antoniades, *Statins as regulators of redox state in the vascular endothelium: beyond lipid lowering.* Antioxid Redox Signal, 2014. **20**(8): p. 1198-215.
350. Maher, B.M., et al., *Statins alter neutrophil migration by modulating cellular Rho activity--a potential mechanism for statins-mediated pleotropic effects?* J Leukoc Biol, 2009. **85**(1): p. 186-93.
351. Wayman, N.S., B.L. Ellis, and C. Thiemermann, *Simvastatin reduces infarct size in a model of acute myocardial ischemia and reperfusion in the rat.* Med Sci Monit, 2003. **9**(5): p. BR155-9.
352. Naidu, B.V., et al., *Simvastatin ameliorates injury in an experimental model of lung ischemia-reperfusion.* J Thorac Cardiovasc Surg, 2003. **126**(2): p. 482-9.
353. Joyce, M., et al., *Pravastatin, a 3-hydroxy-3-methylglutaryl coenzyme A reductase inhibitor, attenuates renal injury in an experimental model of ischemia-reperfusion.* J Surg Res, 2001. **101**(1): p. 79-84.
354. Nesic, Z., et al., *Single-dose intravenous simvastatin treatment attenuates renal injury in an experimental model of ischemia-reperfusion in the rat.* J Pharmacol Sci, 2006. **102**(4): p. 413-7.

355. Hajipour, B., et al., *Simvastatin attenuates intestinal ischemia/reperfusion induced injury in rat.* Folia Morphol (Warsz), 2009. **68**(3): p. 156-62.
356. Dibazar, F., et al., *Simvastatin decreases hepatic ischaemia/reperfusion-induced liver and lung injury in rats.* Folia Morphol (Warsz), 2008. **67**(4): p. 231-5.
357. Lai, I.R., et al., *Pharmacological preconditioning with simvastatin protects liver from ischemia-reperfusion injury by heme oxygenase-1 induction.* Transplantation, 2008. **85**(5): p. 732-8.
358. Ma, M., et al., *Pretreatment with rosuvastatin protects against focal cerebral ischemia/reperfusion injury in rats through attenuation of oxidative stress and inflammation.* Brain Res, 2013. **1519**: p. 87-94.
359. Tu, Y.P., et al., *Simvastatin induces the expression of hemeoxygenase-1 against ischemia-reperfusion injury on the testes in rats.* Toxicol Lett, 2011. **207**(3): p. 242-50.
360. Saito, T., et al., *Reduction of spinal cord ischemia/reperfusion injury with simvastatin in rats.* Anesth Analg, 2011. **113**(3): p. 565-71.
361. Gholami, M.R., et al., *The effects of simvastatin on ischemia-reperfusion injury of sciatic nerve in adult rats.* Eur J Pharmacol, 2008. **590**(1-3): p. 111-4.
362. Cowled, P.A., et al., *Statins inhibit neutrophil infiltration in skeletal muscle reperfusion injury.* J Surg Res, 2007. **141**(2): p. 267-76.
363. Dillon, J.P., et al., *Pravastatin attenuates tourniquet-induced skeletal muscle ischemia reperfusion injury.* Acta Orthop, 2006. **77**(1): p. 27-32.
364. Joyce, M., et al., *Pravastatin attenuates lower torso ischaemia-reperfusion-induced lung injury by upregulating constitutive endothelial nitric oxide synthase.* Eur J Vasc Endovasc Surg, 2001. **21**(4): p. 295-300.
365. Sun, X.F., et al., *[Effects of simvastatin on pulmonary nuclear factor-kappaB and intercellular adhesion molecule-1 in rats with lung injury induced by ischemia-reperfusion of the hind limbs].* Nan Fang Yi Ke Da Xue Xue Bao, 2011. **31**(7): p. 1150-3.
366. Sun, X.F., et al., *Effects of simvastatin on lung injury induced by ischaemia-reperfusion of the hind limbs in rats.* J Int Med Res, 2007. **35**(4): p. 523-33.
367. Cowled, P.A., et al., *Simvastatin plus nitric oxide synthase inhibition modulates remote organ damage following skeletal muscle ischemia-reperfusion injury.* J Invest Surg, 2008. **21**(3): p. 119-26.
368. Lee, C.C., et al., *Fluvastatin attenuates severe hemorrhagic shock-induced organ damage in rats.* Resuscitation, 2009. **80**(3): p. 372-8.
369. Relja, B., et al., *Simvastatin reduces mortality and hepatic injury after hemorrhage/resuscitation in rats.* Shock, 2010. **34**(1): p. 46-54.
370. Schneider, E.B., et al., *Premorbid statin use is associated with improved survival and functional outcomes in older head-injured individuals.* J Trauma, 2011. **71**(4): p. 815-9.
371. Fogerty, M.D., et al., *Effect of preinjury statin use on mortality and septic shock in elderly burn patients.* J Trauma, 2010. **69**(1): p. 99-103.
372. Feeney, J.M., et al., *Prehospital HMG Co-A reductase inhibitor use and reduced mortality in ruptured abdominal aortic aneurysm.* J Am Coll Surg, 2009. **209**(1): p. 41-6.
373. Wemmelund, H., et al., *Statin use and rupture of abdominal aortic aneurysm.* Br J Surg, 2014. **101**(8): p. 966-75.

374. Raphael, J., et al., *Perioperative statin use is associated with decreased incidence of primary graft dysfunction after lung transplantation.* J Heart Lung Transplant, 2017. **36**(9): p. 948-956.
375. Efron, D.T., et al., *Preinjury statin use is associated with improved in-hospital survival in elderly trauma patients.* J Trauma, 2008. **64**(1): p. 66-73; discussion 73-4.
376. Feeney, J., et al., *Prehospital HMG Co-A reductase inhibitor use and reduced mortality in hemorrhagic shock due to trauma.* Eur J Trauma Emerg Surg, 2012. **38**: p. 171-176.
377. Neal, M.D., et al., *Preinjury statin use is associated with a higher risk of multiple organ failure after injury: a propensity score adjusted analysis.* J Trauma, 2009. **67**(3): p. 476-82; discussion 482-4.
378. Dormuth, C.R., et al., *Statin adherence and risk of accidents: a cautionary tale.* Circulation, 2009. **119**(15): p. 2051-7.
379. Schouten, O., et al., *Effect of statin withdrawal on frequency of cardiac events after vascular surgery.* Am J Cardiol, 2007. **100**(2): p. 316-20.
380. Liuni, A., et al., *Loss of the preconditioning effect of rosuvastatin during sustained therapy: a human in vivo study.* Am J Physiol Heart Circ Physiol, 2012. **302**(1): p. H153-8.
381. Akcay, M.N., et al., *The effect of short-term treatment with atorvastatin on E-selectin levels in severely burned patients.* Int J Clin Pharmacol Res, 2005. **25**(2): p. 65-9.
382. Patil, S., et al., *Prospective, double blind, randomized, controlled trial of simvastatin in human fracture healing.* J Orthop Res, 2009. **27**(3): p. 281-5.
383. Sanchez-Aguilar, M., et al., *Effect of rosuvastatin on cytokines after traumatic head injury.* J Neurosurg, 2013. **118**(3): p. 669-75.
384. Fogerty, M.D. *Pilot Trial of statins use in burns patients (BURNSTAT)*. 05/01/2016]; Available from: https://clinicaltrials.gov/ct2/show/NCT00978419.
385. Jansen, J.O., et al., *Clinical review: Statins and trauma--a systematic review.* Crit Care, 2013. **17**(3): p. 227.
386. Pasin, L., et al., *The effect of statins on mortality in septic patients: a meta-analysis of randomized controlled trials.* PLoS One, 2013. **8**(12): p. e82775.
387. Kruger, P., et al., *A multicenter randomized trial of atorvastatin therapy in intensive care patients with severe sepsis.* Am J Respir Crit Care Med, 2013. **187**(7): p. 743-50.
388. *Simvastatin and severe sepsis: a randomised controlled trial*. 09/01/2016]; Available from: http://www.controlled-trials.com/ISRCTN92093279.
389. *Statins for the early treatment of sepsis (SETS)*. 09/01/2016]; Available from: https://clinicaltrials.gov/ct2/show/NCT00528580.
390. *Statin therapy in the treatment of sepsis*. 09/01/2016]; Available from: https://clinicaltrials.gov/ct2/show/NCT00676897.
391. *Simvastatin in patients with septic shock*. [cited 09/01/2016; Available from: https://clinicaltrials.gov/ct2/show/NCT00450840.
392. Craig, T.R., et al., *A randomized clinical trial of hydroxymethylglutaryl- coenzyme a reductase inhibition for acute lung injury (The HARP Study).* Am J Respir Crit Care Med, 2011. **183**(5): p. 620-6.
393. McAuley, D.F., et al., *Simvastatin in the acute respiratory distress syndrome.* N Engl J Med, 2014. **371**(18): p. 1695-703.
394. National Heart, L., et al., *Rosuvastatin for sepsis-associated acute respiratory distress syndrome.* N Engl J Med, 2014. **370**(23): p. 2191-200.

395. *Statins and selective cyclooxygenase-2 receptor inhibitors in blunt chest trauma*. Available from: https://clinicaltrials.gov/ct2/show/NCT01623921.
396. Schachter, M., *Chemical, pharmacokinetic and pharmacodynamic properties of statins: an update.* Fundam Clin Pharmacol, 2005. **19**(1): p. 117-25.
397. Gazzerro, P., et al., *Pharmacological actions of statins: a critical appraisal in the management of cancer.* Pharmacol Rev, 2012. **64**(1): p. 102-46.
398. [cited 2019; Available from: http://www.mhra.gov.uk/home/groups/par/documents/websiteresources/con2033974.pdf.
399. Desager, J.P. and Y. Horsmans, *Clinical pharmacokinetics of 3-hydroxy-3-methylglutaryl-coenzyme A reductase inhibitors.* Clin Pharmacokinet, 1996. **31**(5): p. 348-71.
400. Godlee, F., *Adverse effects of statins.* BMJ, 2014. **348**: p. g3306.
401. Sakamoto, K. and J. Kimura, *Mechanism of statin-induced rhabdomyolysis.* J Pharmacol Sci, 2013. **123**(4): p. 289-94.
402. Oprea, T.I. and J. Mestres, *Drug repurposing: far beyond new targets for old drugs.* AAPS J, 2012. **14**(4): p. 759-63.
403. Woolley, T., et al., *Trauma Hemostasis and Oxygenation Research Network position paper on the role of hypotensive resuscitation as part of remote damage control resuscitation.* J Trauma Acute Care Surg, 2018. **84**(6S Suppl 1): p. S3-S13.
404. Russell, W.M.S.B., R.L., *The principles of humane experimental technique*. 1959, London: Methuen.
405. Lomas-Niera, J.L., et al., *Shock and hemorrhage: an overview of animal models.* Shock, 2005. **24 Suppl 1**: p. 33-9.
406. Little, R.A., H.W. Marshall, and E. Kirkman, *Attenuation of the acute cardiovascular responses to haemorrhage by tissue injury in the conscious rat.* Q J Exp Physiol, 1989. **74**(6): p. 825-33.
407. Little, R.A., et al., *Components of injury (haemorrhage and tissue ischaemia) affecting cardiovascular reflexes in man and rat.* Q J Exp Physiol, 1984. **69**(4): p. 753-62.
408. Frink, M., et al., *Experimental trauma models: an update.* J Biomed Biotechnol, 2011. **2011**: p. 797383.
409. Hauser, C.J., *Preclinical models of traumatic, hemorrhagic shock.* Shock, 2005. **24 Suppl 1**: p. 24-32.
410. Ghorbani, P., et al., *Clinical review is essential to evaluate 30-day mortality after trauma.* Scand J Trauma Resusc Emerg Med, 2014. **22**: p. 18.
411. Vree, T.B.D., E.; Ulc, I.; Horkovics-Kovats, S.; Ryska, M.; Merkx, I., *Variable plasma/liver and tissue esterase hydrolysis of simvastatin in healthy volunteers after a single oral dose.* Clin Drug Invest, 2001. **21**(9): p. 643-652.
412. Timms, R.J., *A study of the amygdaloid defence reaction showing the value of Althesin anaesthesia in studies of the functions of the fore-brain in cats.* Pflugers Arch, 1981. **391**(1): p. 49-56.
413. Foster, M.A., *Steroids and immunity from injury through to rehabilitation*, in *School of Immunity and Infection*. 2015, University of Birmingham.
414. Thomas, G.O.R., *Use of erythropoietin in trauma, blast and haemorrhage*. 2016, University of Swansea.
415. Jaffin, J.H., et al., *A laboratory model for studying blast overpressure injury.* J Trauma, 1987. **27**(4): p. 349-56.

416. Heath, D.F., *The effect of scald injury upon the distribution of glucose between red cells and plasma and upon the turnover of glucose in red cells in the rat.* Br J Exp Pathol, 1973. **54**(4): p. 359-67.
417. Samsel, L., et al., *Imaging flow cytometry for morphologic and phenotypic characterization of rare circulating endothelial cells.* Cytometry B Clin Cytom, 2013. **84**(6): p. 379-89.
418. Acker, H. and R.G. O'Regan, *The effects of stimulation of autonomic nerves on carotid body blood flow in the cat.* J Physiol, 1981. **315**: p. 99-110.
419. Sordi, R., et al., *Neuronal Nitric Oxide Synthase is Involved in Vascular Hyporeactivity and Multiple Organ Dysfunction Associated with Hemorrhagic Shock.* Shock, 2016. **45**(5): p. 525-33.
420. Torres, L.N., et al., *Systemic responses to prolonged hemorrhagic hypotension.* Am J Physiol Heart Circ Physiol, 2004. **286**(5): p. H1811-20.
421. Rixen, D. and J.H. Siegel, *Metabolic correlates of oxygen debt predict posttrauma early acute respiratory distress syndrome and the related cytokine response.* J Trauma, 2000. **49**(3): p. 392-403.
422. Jacobs, R.G., W.S. Howland, and A.H. Goulet, *Serial microhematocrit determinations in evaluating blood replacement.* Anesthesiology, 1961. **22**: p. 342-7.
423. Ryan, M.L., et al., *Initial hematocrit in trauma: a paradigm shift?* J Trauma Acute Care Surg, 2012. **72**(1): p. 54-9; discussion 59-60.
424. Kleiber, M., *Body size and metabolic rate.* Physiol Rev, 1947. **27**(4): p. 511-41.
425. Hazeldine, J., et al., *Traumatic Injury and Exposure to Mitochondrial-Derived Damage Associated Molecular Patterns Suppresses Neutrophil Extracellular Trap Formation.* Front Immunol, 2019. **10**: p. 685.
426. Hazeldine, J., et al., *Prehospital immune responses and development of multiple organ dysfunction syndrome following traumatic injury: A prospective cohort study.* PLoS Med, 2017. **14**(7): p. e1002338.
427. Cabrera, C.P., et al., *Signatures of inflammation and impending multiple organ dysfunction in the hyperacute phase of trauma: A prospective cohort study.* PLoS Med, 2017. **14**(7): p. e1002352.
428. Yang, Z., et al., *TLR4 as receptor for HMGB1-mediated acute lung injury after liver ischemia/reperfusion injury.* Lab Invest, 2013. **93**(7): p. 792-800.
429. Andersson, U. and K.J. Tracey, *HMGB1 is a therapeutic target for sterile inflammation and infection.* Annu Rev Immunol, 2011. **29**: p. 139-62.
430. Bell, C.W., et al., *The extracellular release of HMGB1 during apoptotic cell death.* Am J Physiol Cell Physiol, 2006. **291**(6): p. C1318-25.
431. Scaffidi, P., T. Misteli, and M.E. Bianchi, *Release of chromatin protein HMGB1 by necrotic cells triggers inflammation.* Nature, 2002. **418**(6894): p. 191-5.
432. Peltz, E.D., et al., *HMGB1 is markedly elevated within 6 hours of mechanical trauma in humans.* Shock, 2009. **32**(1): p. 17-22.
433. Cohen, M.J., et al., *Early release of high mobility group box nuclear protein 1 after severe trauma in humans: role of injury severity and tissue hypoperfusion.* Crit Care, 2009. **13**(6): p. R174.
434. Horst, K., et al., *Impact of haemorrhagic shock intensity on the dynamic of alarmins release in porcine poly-trauma animal model.* Eur J Trauma Emerg Surg, 2016. **42**(1): p. 67-75.

435. Deng, M., et al., *Location is the key to function: HMGB1 in sepsis and trauma-induced inflammation.* J Leukoc Biol, 2019.
436. Yang, H., et al., *MD-2 is required for disulfide HMGB1-dependent TLR4 signaling.* J Exp Med, 2015. **212**(1): p. 5-14.
437. Sha, Y., et al., *HMGB1 develops enhanced proinflammatory activity by binding to cytokines.* J Immunol, 2008. **180**(4): p. 2531-7.
438. Leclerc, P., et al., *IL-1beta/HMGB1 complexes promote The PGE2 biosynthesis pathway in synovial fibroblasts.* Scand J Immunol, 2013. **77**(5): p. 350-60.
439. Fukudome, E.Y., et al., *Pharmacologic resuscitation decreases circulating cytokine-induced neutrophil chemoattractant-1 levels and attenuates hemorrhage-induced acute lung injury.* Surgery, 2012. **152**(2): p. 254-61.
440. Hranjec, T., et al., *Diagnosis-dependent relationships between cytokine levels and survival in patients admitted for surgical critical care.* J Am Coll Surg, 2010. **210**(5): p. 833-44, 845-6.
441. Pfeifer, R., et al., *Models of hemorrhagic shock: differences in the physiological and inflammatory response.* Cytokine, 2013. **61**(2): p. 585-90.
442. Bortolotti, P., E. Faure, and E. Kipnis, *Inflammasomes in Tissue Damages and Immune Disorders After Trauma.* Front Immunol, 2018. **9**: p. 1900.
443. Nakanishi, K., et al., *Interleukin-18 regulates both Th1 and Th2 responses.* Annu Rev Immunol, 2001. **19**: p. 423-74.
444. Mommsen, P., et al., *Elevated systemic IL-18 and neopterin levels are associated with posttraumatic complications among patients with multiple injuries: a prospective cohort study.* Injury, 2009. **40**(5): p. 528-34.
445. Heizmann, O., et al., *Th1- and Th2-type cytokines in plasma after major trauma.* J Trauma, 2008. **65**(6): p. 1374-8.
446. Roetman, B., et al., *Elevated systemic interleukin-18 in multiple injured patients is not related to clinical outcome.* J Interferon Cytokine Res, 2008. **28**(12): p. 741-7.
447. Dinarello, C.A., et al., *Interleukin-18 and IL-18 binding protein.* Front Immunol, 2013. **4**: p. 289.
448. Schroder, K., et al., *Interferon-gamma: an overview of signals, mechanisms and functions.* J Leukoc Biol, 2004. **75**(2): p. 163-89.
449. Jastrow, K.M., 3rd, et al., *Early cytokine production risk stratifies trauma patients for multiple organ failure.* J Am Coll Surg, 2009. **209**(3): p. 320-31.
450. Frink, M., et al., *Monocyte chemoattractant protein-1 influences trauma-hemorrhage-induced distal organ damage via regulation of keratinocyte-derived chemokine production.* Am J Physiol Regul Integr Comp Physiol, 2007. **292**(3): p. R1110-6.
451. Graves, D.T. and Y. Jiang, *Chemokines, a family of chemotactic cytokines.* Crit Rev Oral Biol Med, 1995. **6**(2): p. 109-18.
452. Naylor, C. and W.A. Petri, Jr., *Leptin Regulation of Immune Responses.* Trends Mol Med, 2016. **22**(2): p. 88-98.
453. Bracho-Riquelme, R.L. and M.A. Reyes-Romero, *Leptin in sepsis: a well-suited biomarker in critically ill patients?* Crit Care, 2010. **14**(2): p. 138.
454. Carbone, M., et al., *Leptin attenuates ischemia-reperfusion injury in the rat liver.* Transpl Int, 2012. **25**(12): p. 1282-8.
455. Sagiroglu, T., et al., *Effects of apelin and leptin on renal functions following renal ischemia/reperfusion: An experimental study.* Exp Ther Med, 2012. **3**(5): p. 908-914.

456. Torpy, D.J., S.R. Bornstein, and G.P. Chrousos, *Leptin and interleukin-6 in sepsis.* Horm Metab Res, 1998. **30**(12): p. 726-9.
457. Shi, Y., G.T. Yan, and J. Lin, *Intestinal ischemia-reperfusion injury made leptin decreased.* Regul Pept, 2006. **133**(1-3): p. 27-31.
458. Matsuda, T., et al., *Identification of alpha 2-macroglobulin as a carrier protein for IL-6.* J Immunol, 1989. **142**(1): p. 148-52.
459. Bienvenu, J., et al., *The clinical usefulness of the measurement of cytokines.* Clin Chem Lab Med, 2000. **38**(4): p. 267-85.
460. Scheller, J., et al., *The pro- and anti-inflammatory properties of the cytokine interleukin-6.* Biochim Biophys Acta, 2011. **1813**(5): p. 878-88.
461. Saraiva, M. and A. O'Garra, *The regulation of IL-10 production by immune cells.* Nat Rev Immunol, 2010. **10**(3): p. 170-81.
462. Schneider, C.P., M.G. Schwacha, and I.H. Chaudry, *The role of interleukin-10 in the regulation of the systemic inflammatory response following trauma-hemorrhage.* Biochim Biophys Acta, 2004. **1689**(1): p. 22-32.
463. Neidhardt, R., et al., *Relationship of interleukin-10 plasma levels to severity of injury and clinical outcome in injured patients.* J Trauma, 1997. **42**(5): p. 863-70; discussion 870-1.
464. Kalinski, P., *Regulation of immune responses by prostaglandin E2.* J Immunol, 2012. **188**(1): p. 21-8.
465. Tsukada, K., et al., *Roles of cyclooxygenase-2 in tissue injury during hemorrhagic shock.* Shock, 2000. **13**(5): p. 392-6.
466. Shires, G.T., et al., *The effect of shock resuscitation fluids on apoptosis.* Am J Surg, 2005. **189**(1): p. 85-91.
467. Itoh, H., et al., *Activation of immediate early gene, c-fos, and c-jun in the rat small intestine after ischemia/reperfusion.* Transplantation, 2000. **69**(4): p. 598-604.
468. Alam, H.B., et al., *cDNA array analysis of gene expression following hemorrhagic shock and resuscitation in rats.* Resuscitation, 2002. **54**(2): p. 195-206.
469. Maulik, N., *Redox signaling of angiogenesis.* Antioxid Redox Signal, 2002. **4**(5): p. 805-15.
470. Maeshima, K., et al., *Prevention of hemorrhagic shock-induced lung injury by heme arginate treatment in rats.* Biochem Pharmacol, 2005. **69**(11): p. 1667-80.
471. Waza, A.A., et al., *A review on heme oxygenase-1 induction: is it a necessary evil.* Inflamm Res, 2018. **67**(7): p. 579-588.
472. Arimori, Y., et al., *Role of heme oxygenase-1 in protection of the kidney after hemorrhagic shock.* Int J Mol Med, 2010. **26**(1): p. 27-32.
473. Goon, P.K., C.J. Boos, and G.Y. Lip, *Circulating endothelial cells: markers of vascular dysfunction.* Clin Lab, 2005. **51**(9-10): p. 531-8.
474. Koch, A.E., et al., *Angiogenesis mediated by soluble forms of E-selectin and vascular cell adhesion molecule-1.* Nature, 1995. **376**(6540): p. 517-9.
475. Calfee, C.S., et al., *Acute respiratory distress syndrome subphenotypes and differential response to simvastatin: secondary analysis of a randomised controlled trial.* Lancet Respir Med, 2018. **6**(9): p. 691-698.
476. Dunham, C.M., M.H. Fealk, and W.E. Sever, 3rd, *Following severe injury, hypocholesterolemia improves with convalescence but persists with organ failure or onset of infection.* Crit Care, 2003. **7**(6): p. R145-53.

477. Chansouria, J.P., et al., *Alterations in lipid metabolism following trauma in rabbits.* Experientia, 1973. **29**(4): p. 393-5.
478. Johnson, S.R. and A. Svanborg, *Investigations with regard to the pathogenesis of so-called fat embolism; serum lipids and tissue esterase activity and the frequency of so-called fat embolism in soft tissue trauma and fractures.* Ann Surg, 1956. **144**(2): p. 145-51.
479. Bricknell, M.J., A., *Forward medical evacuation.* J R Army Med Corps, 2011. **157**: p. S444-448.
480. Elshal, M.F. and J.P. McCoy, *Multiplex bead array assays: performance evaluation and comparison of sensitivity to ELISA.* Methods, 2006. **38**(4): p. 317-23.
481. Mountney, A., et al., *Intravenous Administration of Simvastatin Improves Cognitive Outcome following Severe Traumatic Brain Injury in Rats.* J Neurotrauma, 2016. **33**(16): p. 1492-500.
482. Gaillard, C., et al., *A high-sensitivity method for detection and measurement of HMGB1 protein concentration by high-affinity binding to DNA hemicatenanes.* PLoS One, 2008. **3**(8): p. e2855.
483. Antoine, D.J., et al., *Molecular forms of HMGB1 and keratin-18 as mechanistic biomarkers for mode of cell death and prognosis during clinical acetaminophen hepatotoxicity.* J Hepatol, 2012. **56**(5): p. 1070-9.
484. *Expression of Concern.* J Hepatol, 2018. **69**(6): p. 1402.
485. Barnay-Verdier, S., et al., *PCA-ELISA: a sensitive method to quantify free and masked forms of HMGB1.* Cytokine, 2011. **55**(1): p. 4-7.
486. Maiti, P.K., et al., *A monoclonal antibody specific for rat IL-18BP and its application in determining serum IL-18BP.* Immunol Lett, 2003. **85**(1): p. 65-70.

Gene Expression Profiling after Trauma

Batch 1 & 2

FINAL STUDY REPORT – January 2019

Professor Karim Brohi FRCS FRCA
Tom Simpson
Centre for Trauma Sciences
Barts and The London School of Medicine & Dentistry
Queen Mary University of London

Dr Michael Barnes
Dr Claudia Cabrera
William Harvey Research Institute
Barts and The London School of Medicine and Dentistry
Queen Mary University of London

Contents

Executive Summary

Sequencing of mRNA libraries generated from two batches of paired rat model samples was successfully completed on a total of 78 samples (42 in batch 1, 36 in batch 2). High quality & consistent RNA-seq data was generated across both batches. Exploratory data analysis identified five samples as experimental outliers (ES86-SURG; ES72-SURG; ES120-SURG; ES86-PM; ES149-PM), these were excluded from further analysis (note that their paired samples were also excluded when analysing data overtime ES72-PM; ES120-PM; ES149-SURG). Key findings from the analysis were as follows

- *Effects of injury and injury + blast on transcriptome expression were similar but could be differentiated and were most strongly detected in time course analyses*
- *Very few significant treatment effects on the transcriptome were seen within time points*
- *Time course analysis showed evidence for larger differential expression in the treatment group compared to placebo*
- *Pathway analysis identified a number of trauma injury relevant pathways*
- *Putative treatment effects were identified, relating to cell death and survival processes*
- *Statin responsive genes were identified*
- *Comparison with Human trauma expression data, also showed high correlation at a pathway level*

In conclusion, available data indicates that the DSTL Rat trauma study was a technical success. Increased sample numbers from the preliminary analysis, give more confidence that sufficient power is available to detect biological effects within time point, and time course analysis also enabled the detection of both trauma injury and blast effects and putative treatment effects.

1. Introduction

1.1 Background

Understanding the molecular basis of trauma injury is essential to allow better treatment strategies to be developed and evaluated to reduce both mortality and morbidity in both civilian and military trauma. Gene expression profiling following civilian trauma injury has been now been quite widely performed by our group (Cabrera et al 2017) and others (Xiao et al 2011). Data from animal models of traumatic injury also exists (Sordi et al, 2017), and offer promise if they can be shown to correlate with human trauma studies, including prediction of therapeutic response.

Gene expression profiling of trauma injury in humans and animal models has allowed determination of specific characteristics which correlate with trauma outcomes. Gene expression profiling of our animal models (currently rat and pig) will demonstrate the strengths and weakness of the models in terms of replicating the human condition (comparing data to existing human datasets). Gene profiling in our animal models will help understand the strengths and weaknesses of these animal models and allow us to focus our research most effectively.

1.2 Summary of Requirements

The Authority (i.e. Dstl) wishes to evaluate the mechanism of military traumatic injury as well as identifying and evaluating treatment strategies. One tool for undertaking this task is using animal models of injury. It is very important to be able to characterise the animal models particularly with reference to the human condition.

The Authority has a requirement to undertake gene expression profiling in its animal models of trauma by differential gene expression in a manner that can be compared between animal models and also between animal and human. This will ensure that it can better translate its models to the human condition.

The Authority requires RNA sequencing of the blood samples provided by the Authority from animal models of traumatic injury. The Contractor (i.e. QMUL) will interpret the data using bioinformatics and provide comparison of the Authority's models response to injury with that of the Contractor's own animal and human (i.e. civilian trauma patient) data.

1.3 Contractor Deliverables

Reports to be submitted to The Authority will include:

- Success of RNA extraction and sequencing from small volume Paxgene tubes with a decision point as to whether these small volume tubes are suitable for this type of analysis.
- Raw data of samples to be provided by the Contractor
- Interpretation of data by the Contractor to include comparative analysis of data from the Authority's models and the Contractor's human trauma studies to provide

information so that Dstl can understand the similarities / differences between the model and humans.

2 Methodology

2.1 Sample transfer and processing

Samples were provided frozen, in the form of small volume PAXgene tubes labelled in a deidentified manner (i.e. bearing a unique sample ID that can be linked to sample list held by the Authority). RNA was extracted from the samples, with each analysed for nucleotide quantification (i.e. micro volume UV-Vis spectrophotometry) and quality (i.e. RNA Integrity Number). These raw data shall be provided to the Authority and a decision made whether to proceed at this stage (Milestone 1). A full description of the samples is described on *Appendix 1* Sample identifiers.

2.2 RNA sequencing

Strand specific mRNA sequence library preparation was undertaken by the Barts and the London Genome Centre (*Appendix 2* Sample RNA extraction). Next Generation Sequencing Technology was conducted to approximately 20 million reads per sample. Summary data was provided to the Authority and a joint decision was made to proceed beyond this stage (Milestone 2)

2.3 RNA abundance measurement

The reference transcript index to quantify the abundance was created with kallisto index [version 0.44.0] using Rattus_norvegicus.Rnor_6.0.cdna.all from ensembl (ftp://ftp.ensembl.org/pub/release-92/fasta/rattus_norvegicus/cdna/). Transcripts abundance was then quantified using kallisto quant [version 0.44.0 (BRAY *et al.* 2016)](see *Appendix 3* NGS transcript abundance quantification commands). The raw counts of mRNA transcript abundance calculated by kallisto were exported to R 3.5.0 for exploratory and differential expression analysis using DESeq2 [DESeq2_1.20.0](LOVE *et al.* 2014). The analysis pipeline is summarised in figure 2.1.

Figure 2.1 Summary of RNAseq analysis pipeline

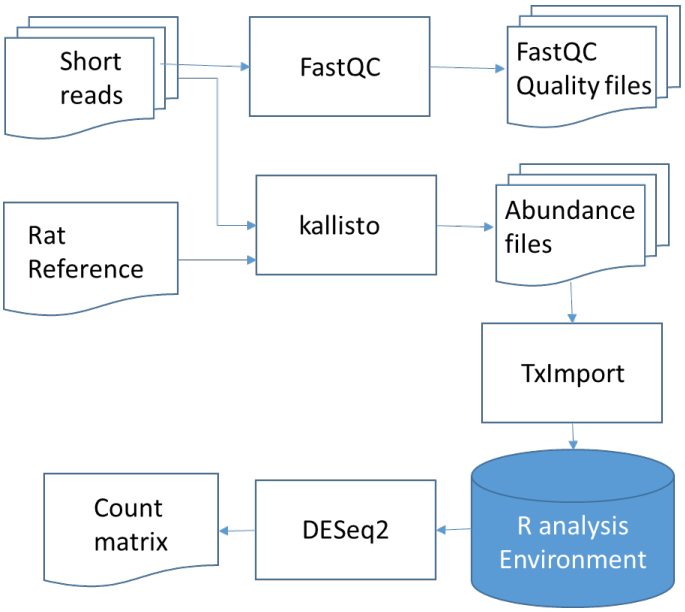

2.4 Power calculation based on pilot study

We used information gained from a pilot study using DSTL's rat model to estimate power for further analysis. The pilot study employed ~5 animals per treatment group, differential expression (DE) in direct response to simvastatin (Treatment C) treatment was not detected at a 5% FDR threshold, although differential expression was detected in 3 transcripts at 10% FDR threshold in the injury model (Table 1). Differential expression in response to trauma injury was seen with between 7-23% transcriptome DE at 5% FDR. Differential expression in response to trauma injury and blast ranged between 8-32% transcriptome DE at 5% FDR. Stronger differential expression was seen in the placebo group compared to the simvastatin group, although it is not possible to determine if this is related to treatment effect.

Table 1. Summary of differentially expressed genes in pilot study comparisons DE1-DE9.

analysis code	Longname	Investigation	p<0.05	q<0.05
DE1	DE1_SURG_TAvsTC	treatment effect in baseline samples (pre-injury)	307	0
DE2	DE2_PM_TreatAvsTreatC_NoBlast	Treatment effects in injury no-blast	648	0*
DE3	DE3_PM_TreatAvsTreatC_Blast	Treatment effects in injury + blast	250	0
DE4	DE4_PM_BlastVsNoBlast_TA	Blast effects in Treatment A	569	0
DE5	DE5_PM_BlastVsNoBlast_TC	Blast effects in Treatment C	316	0
DE6	DE6_PMvsSURG_InjuryTreatA	Changes overtime from Injury with treatment A	2152	1041
DE7	DE7_PMvsSURG_InjuryBlastTreatA	Changes overtime from Injury + blast with treatment A	2163	1205
DE8	DE8_PMvsSURG_InjuryTreatC	Changes overtime from Injury with treatment C	4395	3199
DE9	DE9_PMvsSURG_InjuryBlastTreatC	Changes overtime from Injury + blast with treatment C	5506	4445

(* 3 transcripts show DE at 10% FDR)

2.4.1 Power calculations

Using the method of Guo et al. (2014) and parameters derived from the DSTL rat pilot study, we calculated the requisite sample sizes to achieve 90% power (dotted line in figure 2.2) to detect

differential expression in different experimental conditions. We presume that 17,000 genes will pass a reasonable expression filter, and that 1-25% of these genes will prove prognostic in a sufficiently large sample depending on the condition studied. The top 5% of genes in our trauma injury analysis had an average read count of about 100 prior to normalisation; a minimum log fold change of approximately 1 after modelling; and a mean dispersion of 0.24. Results are presented in figure 1 across a range of scenarios that might be expected in the proposed study. Combination of new rat data with the existing pilot data would create a total sample size of ~10 per treatment, totalling 20 animals per comparison.

Power to detect a treatment effect: Using the Guo et al. algorithm at a 5% false discovery rate (FDR) threshold, we find that a study with 1% DE (as expected for treatment response) would require 25 animals (including both comparison groups) to identify biomarkers with a log fold change (LogFC) 2, biomarkers with more modest fold changes would require more animals. This suggests that combination of pilot data with the new rat data would be slightly underpowered to detect treatment effects, however data generated could indicate treatment trends and might identify biomarkers with a LogFC greater than 2.

Power to detect a trauma injury or blast effect: In a scenario where 25% DE is observed (as expected in trauma or blast injury), 12, 24 or 40 animals would be required to achieve 90% power to detect biomarkers with LogFC 2, 1.75 or 1.5 respectively (figure 1c). This suggests that combination of pilot data with the new rat data would be adequately powered to detect injury and blast effects for biomarkers of LogFC 2. The study would be slightly underpowered for lower LogFC, however data generated would certainly indicate trends and could be fully analysed.

Figure 2.2 Power calculations

Comparison of power across different log fold change ratios to detect different thresholds of differential expression at 5% FDR (1% DE; 5% DE; 25% DE)

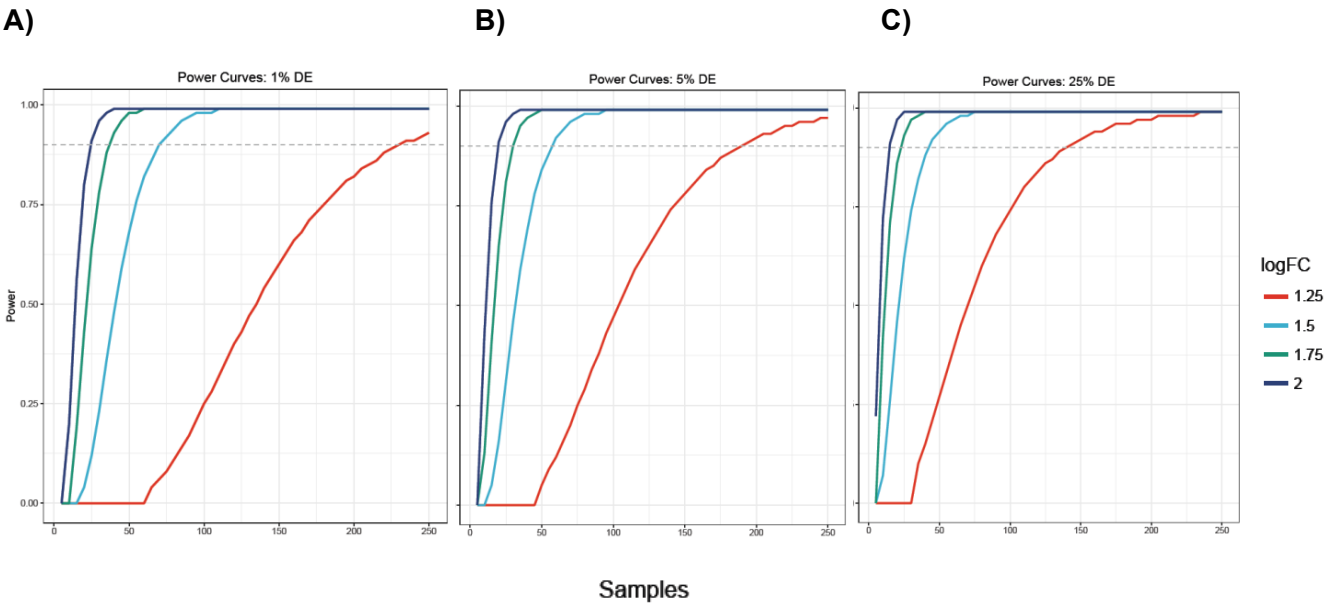

2.5 Exploratory Data Analyses

Exploratory analyses were performed using R 3.5.0. The R environment was setup using the following packages (DESeq2, data.table, tximport, rhdf5, pheatmap, vsn, RColorBrewer, ggplot2, gridExtra). Exploratory analysis was performed across all 78 samples. Genes with less than 10 counts across samples were removed from further analysis (*Appendix 4.1* R environment setup).

The variance stabilizing transformation (vsd) and the regularized log transformation (rld) were applied to the raw counts for exploratory analysis. The analyses included the assessment and visualization of the mean counts distribution, standard deviation from the mean, principal component analysis (PCA), and sample to sample distance matrix heatmaps (*Appendix 4.2*. exploratory analysis R code)

2.6 Differential Expression analysis

Differential expression analysis was performed under the R environment. The R environment was setup for analyses as described in appendix 4.1. Five outlier samples detected through the exploratory analyses were removed from the data (ES86-SURG; ES72-SURG; ES120-SURG; ES86-PM; ES149-PM). The paired samples of the outliers (i.e. ES72-PM; ES120-PM and ES149-SURG) were only removed from the differential expression analysis where a paired design was required, such as overtime comparisons. Genes with less than 10 counts across samples were removed from the data, note that more strict filtering is applied at a later stage. Differential expression analysis between SURG samples (testing for differences among all SURG samples) was performed using the "DESeq" function from DESeq2_1.20.0. The DESeq function estimates library size factors, gene dispersions and applies a negative binomial generalize linear model to fit the data. The LRT test was used to calculate the significance and differences between all SURG samples (*Appendix 4.3* LRT test). Tests between experimental groups (e.g SURG Gp2 vs SURG Gp3) were performed applying the DESeq function as described above. Due to the differences in gene dispersions between groups observed on the exploratory analyses, the library size factor estimates and gene dispersions were calculated using only the groups being tested. Significance between experimental groups was calculated using the Wald test. Batch correction and paired individual were included in the model as fixed effects when present in the comparison groups. Individuals which had samples identified as outlier were removed from the paired individual comparisons (i.e. comparing SURG Gp2 vs PM Gp2 where sample SURG-120 was identified as an outlier; both samples SURG and PM from individual 120 were removed from further analysis). Results were extracted using the "results" function from DESeq2, which calculates the false discovery rate (FDR) to adjust for multiple testing (adjusted p-values) (BENJAMINI and HOCHBERG 1995). Due to the exploratory nature of the study, test results with raw $p<0.05$ are also reported as suggestive associations. Exemplar code for the between group comparisons is included in *Appendix 4.4*.

2.7 Pathway analysis

Ingenuity pathway analysis software (IPA) (Qiagen, inc) was used to identify biological mechanisms enriched in the differentially expressed genes. This software analyses transcriptomic data in the context of known pathways and regulatory networks, identifying biological functions and/or pathways that are significantly enriched in the results. Genes from the data set that met a $q < 0.05$ cutoff and were associated with biological functions in the

Ingenuity Pathways Knowledge Base were analysed. Significance of the biofunctions and the canonical pathways were tested by a Fisher Exact test p-value, to exclude the probability of enrichment by chance alone. Pathways were grouped by the ratio value (number of significant molecules in each pathway, divided by total number of molecules that make up that pathway). To assist mechanistic interpretation and also to reflect the tendency for genes to form co-expression networks, gene expression results were partitioned into up and down regulated responses prior to pathway analysis. The objectives of the systems biological analysis were as follows:

1) To compare results generated with existing associations in literature and public data

2) To evaluate evidence of pathway and network level enrichment of differential expression

3. Results

3.1 Sample transfer

A total of 78 samples were transferred for analysis (*Appendix 1*).

The paired samples were provided having been derived from 39 animals and were either:

- 'Baseline' samples taken post experimental surgery (SURG) but immediately prior to injury:
    - Femur fracture / Haemorrhage Shock
    - Femur fracture / Haemorrhage Shock + Blast
- 'Pre mortem' (PM) samples taken 6 hours from the onset of resuscitation at experiment end (and while the animal was still alive)

The samples arose from a control group and one of 2 different treatment groups receiving either Simvastatin (5day pre-treatment) or Placebo (90mins post injury).

The samples were classified in groups:

- Group 1 = Control (surgery only no injury)
- Group 2 = Injury (femur fracture + haemorrhage) placebo
- Group 3 = Injury (femur fracture + haemorrhage) simvastatin
- Group 4 = Injury (blast + femur fracture + haemorrhage) placebo
- Group 5 = Injury (blast + femur fracture + haemorrhage) simvastatin

3.2 Sample processing

RNA was extracted from the samples, with each analysed for nucleotide quantification and quality. The analyses data (*Appendix 2*) confirmed that generally the resulting RNA samples were acceptable to support sequencing. It was noted that the yield is lower on the PM compared to SURG samples, most likely due to haemodilution. The data suggest that no change in sample collection at experiment end was required to accommodate this lower RNA recovery.

3.3 RNA sequencing

Strand specific mRNA sequence library preparation was undertaken to enable the application of Next Generation Sequencing Technology to approximately 20 million reads per sample (*Appendix 3*). This 'depth' of read had been pre-determined as suitable to provide adequate transcriptome coverage for this research objective.

3.4 Sequence Quality Assessment

Trimmed files were QC assessed and generally the data was confirmed to be high quality. A QC output example is presented in figure 3.1.

Figure 3.1 Sequence QC assessment

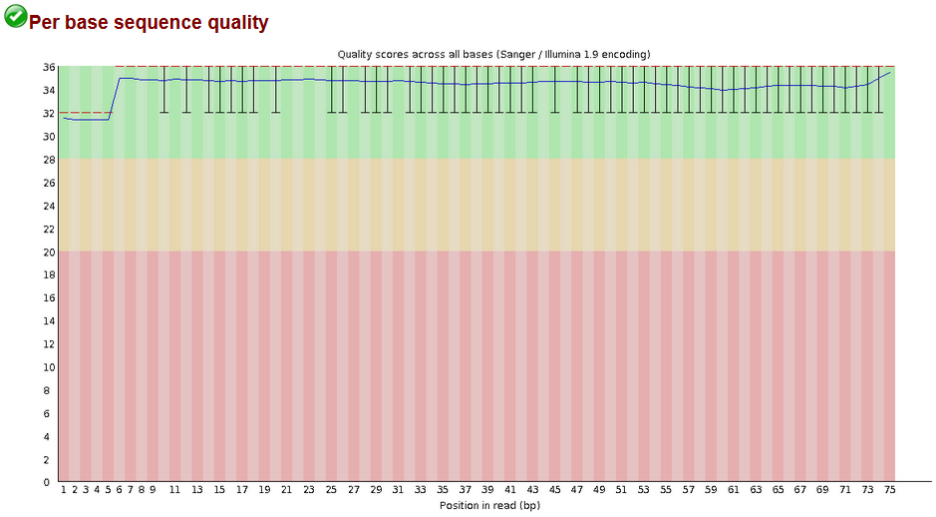

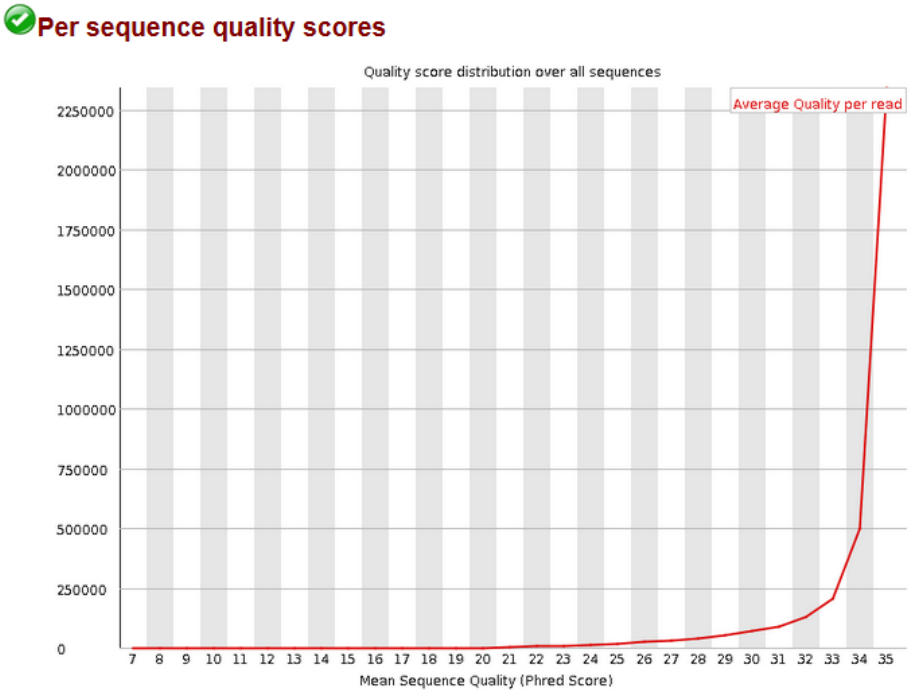

3.5 Sequence Alignment and generation of transcript abundance counts

Kallisto [version 0.44.0] was used to pseudoalign short reads to the Rat reference transcript index to quantify transcript abundance. Transcripts abundance was then quantified using kallisto quant. The concordant pair alignment rate average was 90%. Sample 1 (1-ES72-SURG_S4) was the only sample with a low concordance of 72%. The raw counts of mRNA transcript abundance calculated by kallisto were imported to R 3.5.0 using the TxImport package. Exploratory and differential expression analysis was performed using DESeq2 (*Appendix 4*).

3.6 Exploratory Data Analysis

VSD and RLD data transformations were applied to the raw counts to perform exploratory analyses. These transformations are useful to detect outliers. The variance stabilizing transformation estimates the dispersion trend and takes into consideration the experimental design. The rld transforms the count data into a log2 scale minimizing the differences between samples and normalizes data for library size. The rld transform is similar to the vst transform however is more robust when library sizes vary significantly.

The mean counts distribution, standard deviation from the mean, principal component analysis (PCA) and distance matrix heatmaps methods were used to assess the quality and variance of the samples. These methods allow us to identify possible outliers that may have bias introduced by variation in either extraction of total RNA, sequencing of individual samples or batch effects due to the sequencing at different time points.

The mean counts distribution of the transformed data using the regularized log transformation and the variance stabilizing transformation (Fig. 3.2 RLD and VSD boxplots) identified four possible outliers (i.e. ES86-SURG; ES72-SURG; ES120-SURG; ES86-PM). The evaluation of the standard deviation of the transformed data across samples against the mean, allows us to assess and visualize the variance across the count ranges and their dependence on the mean (Fig 3.3 Mean standard deviation). Principal component analysis (PCA) was applied to evaluate the overall batch effect and evaluate the variance explained by experimental groups. Heatmaps of sample to sample distances (clustering of the samples) were created to aid the assessment and visualization of similarities across samples, highlighting differences within groups/categories of samples, and identifying possible outliers.

An evaluation of the mean counts distribution was performed to ascertain the potential for bias introduced by variation in either extraction of total RNA or sequencing of individual samples. The data demonstrated a uniformity across all study samples (Figure 3.2) rejecting this possibility.

Figure 3.2 RNA read count distribution across study samples

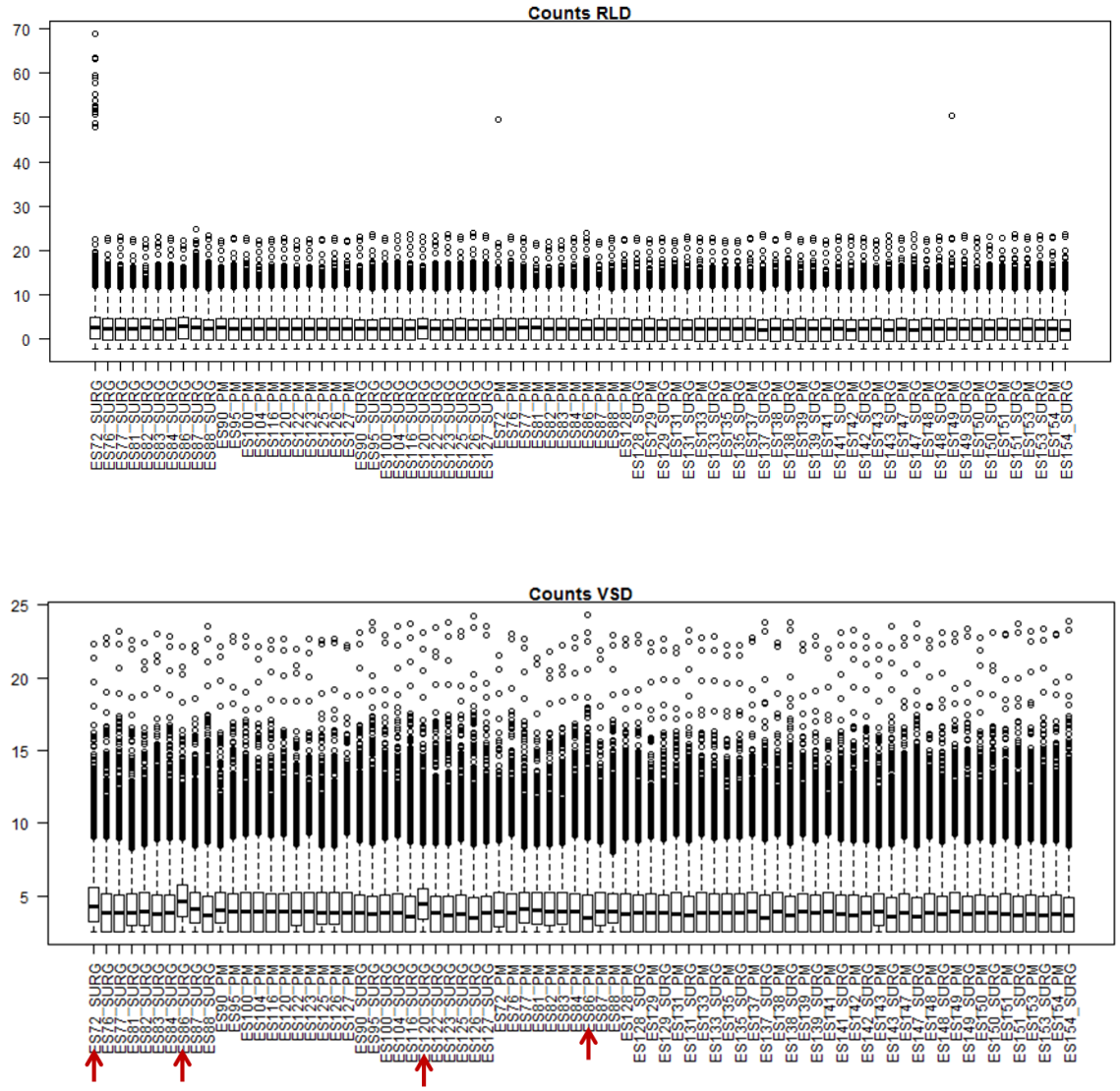

Figure 3.3 Mean standard deviation

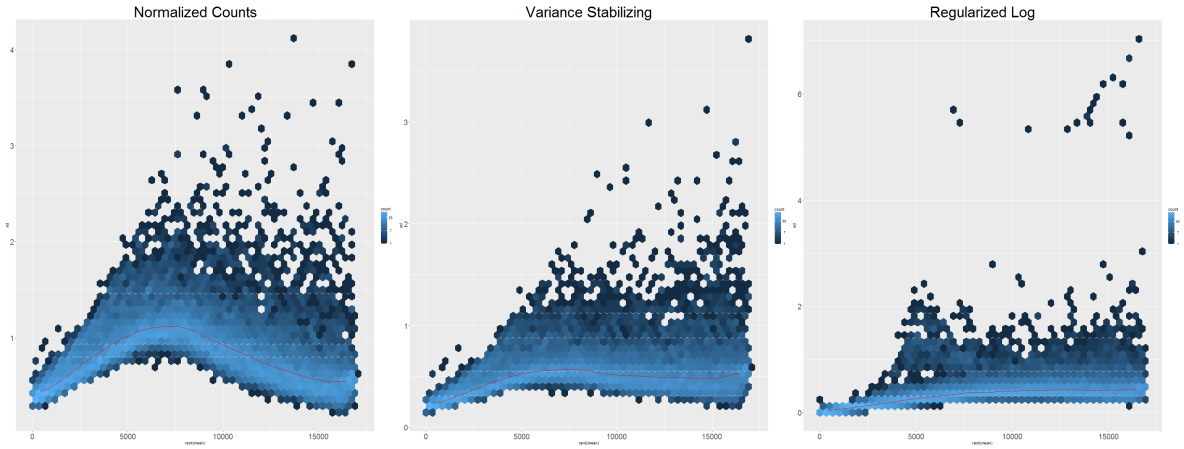

3.6.1 Principal Component Analysis

Principal component analysis (PCA) is a statistical procedure that uses an orthogonal transformation to convert a set of observations of possibly correlated variables (in this case whole transcriptome expression) into a set of values of linearly uncorrelated variables called principal components. The number of principal components is less than or equal to the number of original variables. This transformation is defined in such a way that the first principal component has the largest possible variance (that is, accounts for as much of the variability in the data as possible), and each succeeding component in turn has the highest variance possible under the constraint that it is orthogonal to the preceding components. The resulting vectors are an uncorrelated orthogonal basis set. The principal components are orthogonal because they are the eigenvectors of the covariance matrix, which is symmetric. PCA is sensitive to the relative scaling of the original variables.

We used PCA to evaluate the overall effect of experimental covariates and possible batch effects on transcriptome expression in Figure 3.4. A clear separation was seen by sample treatment status with two clusters, which were concordant with the pre-injury (SURG) and the end of experiment (PM) sample labels. Two samples were outliers on the PCA plot, suggesting a possible batch effect.

In conclusion, exploratory data analysis indicated that the RNA-seq data generated on the DSTL samples was technically of consistently high quality (based on sequence read quality and even sequence coverage across all samples); Dispersion plots and PCA revealed no major QC concerns, although two outlier samples were identified, separation was seen between samples on the basis of treatment status. To investigate this further known gene and mRNA isoform read-counts were normalised and investigated by differential expression analysis using both DESeq2 (Anders and Huber 2010). Two possible outliers (Subject 8 (Surg, ES86) and subject 27(Surg, ES120) were detected in the PCA plots. These samples were excluded from further analysis.

Figure 3.4. Principal component analysis of whole transcriptomes.

A) PCA of all samples using VSD transformation: a clear separation of samples is observed between batches. B) VSD PCA corrected for batch effects yields two clusters corresponding with the baseline (SURG) and 6-hour post resuscitation (PM) samples, possible outliers are observed in the PC-2 axis; C) VSD PCA corrected for batch effects and possible outliers removed. Further analysis was performed to detect the outliers samples. .

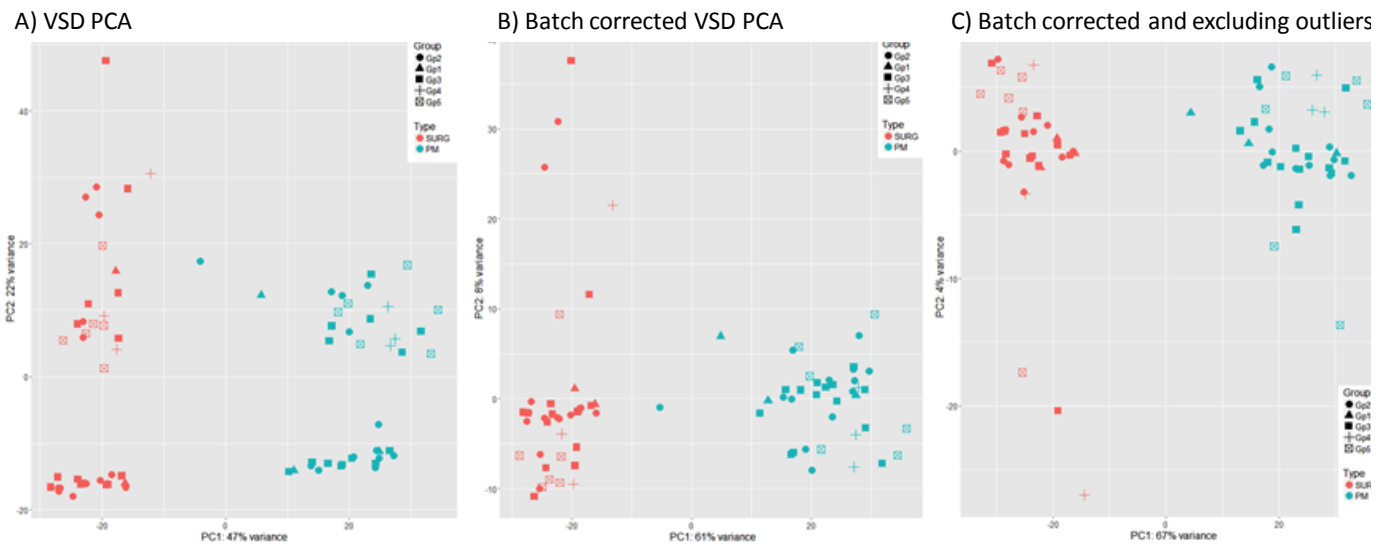

Figure 3.5. PCA - RLD all samples

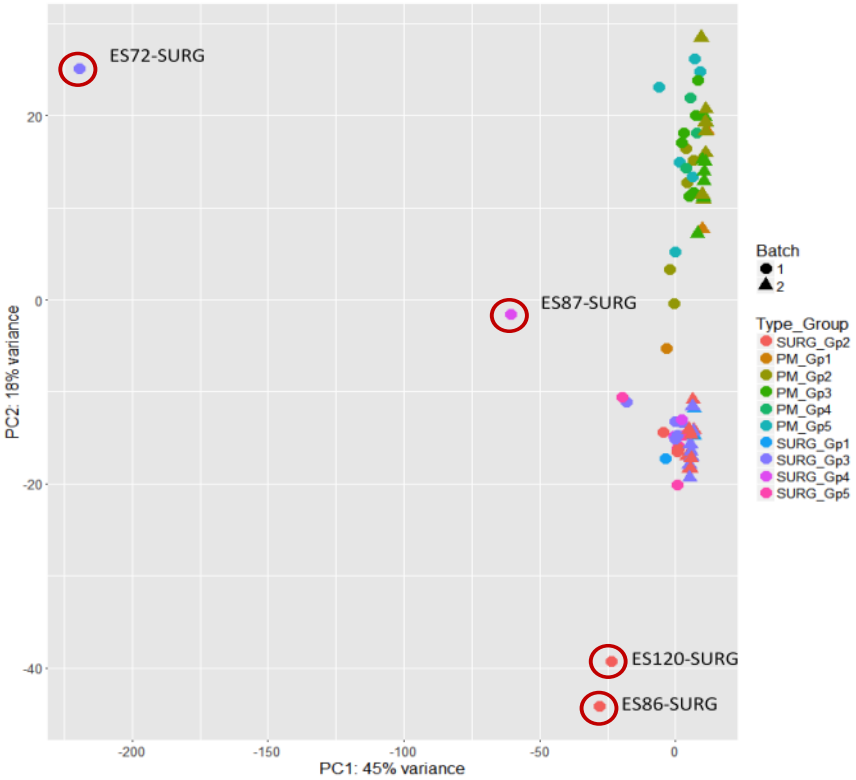

PCA yields two clusters corresponding with the baseline (SURG) and 6-hour post resuscitation (PM) samples, with four possible outliers.

Figure 3.6. PCA - VSD all samples

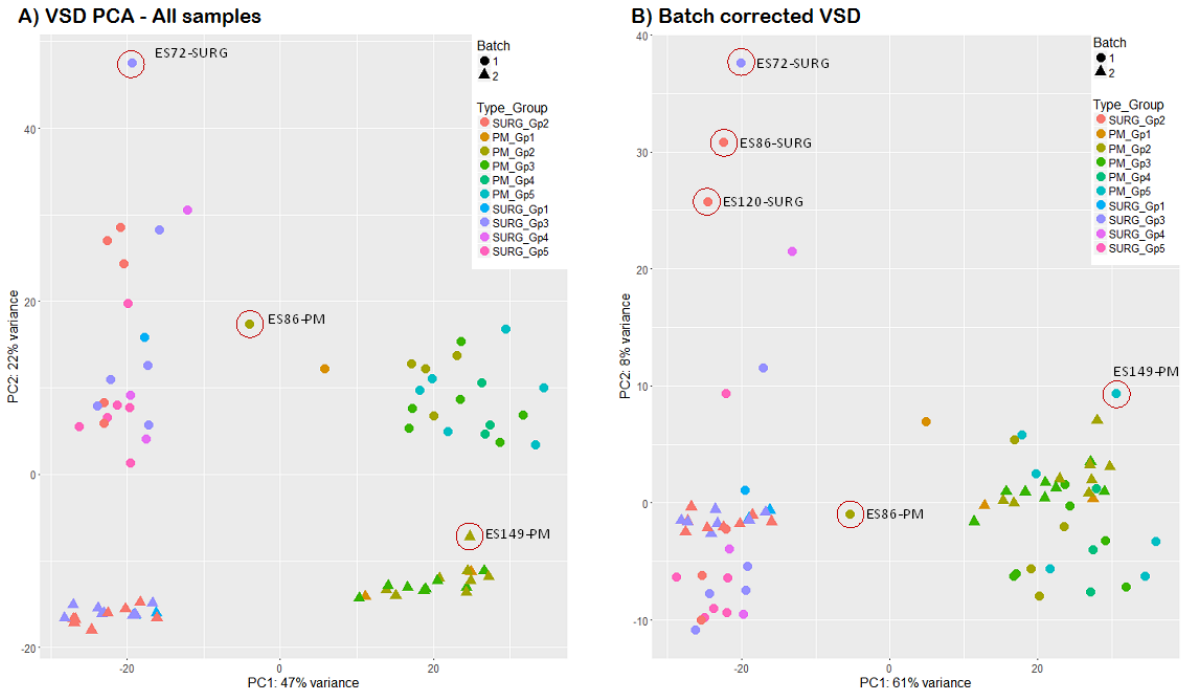

PCA analysis highlights the presence of a batch effect, which will need to be corrected for in the differential expression analysis. It also confirms the presence of outliers identified by the means counts distribution analysis and identifies an additional sample as a possible outlier (i.e. ES149-PM).

3.6.2 Gene Expression Heatmaps

The R function “dist” was used to calculate the Euclidean distance between samples. These functions avoid domination of the distance measure by a few highly variable genes, and have a roughly equal contribution from all genes. The functions were used on the rlog-transformed data.

The “PoissonDistance” command was also used, which measures dissimilarity also taking the variance structure of counts into consideration when calculating the distances between samples. The PoissonDistance function takes the original count matrix. Analyses of the sample sequence counts enabled the hierarchical clustering by sample-sample distance, to investigate the extent of differential gene expression between the baseline and end of experiment sample groups (figures 3.7a and 3.7b.). As with the principal component analysis, this analysis yielded two distinct clusters which were concordant with the pre-injury (SURG) and the end of experiment (PM) sample labels.

Figure 3.7a Hierarchical Clustered Heatmap of gene expression (Euclidean Distance)

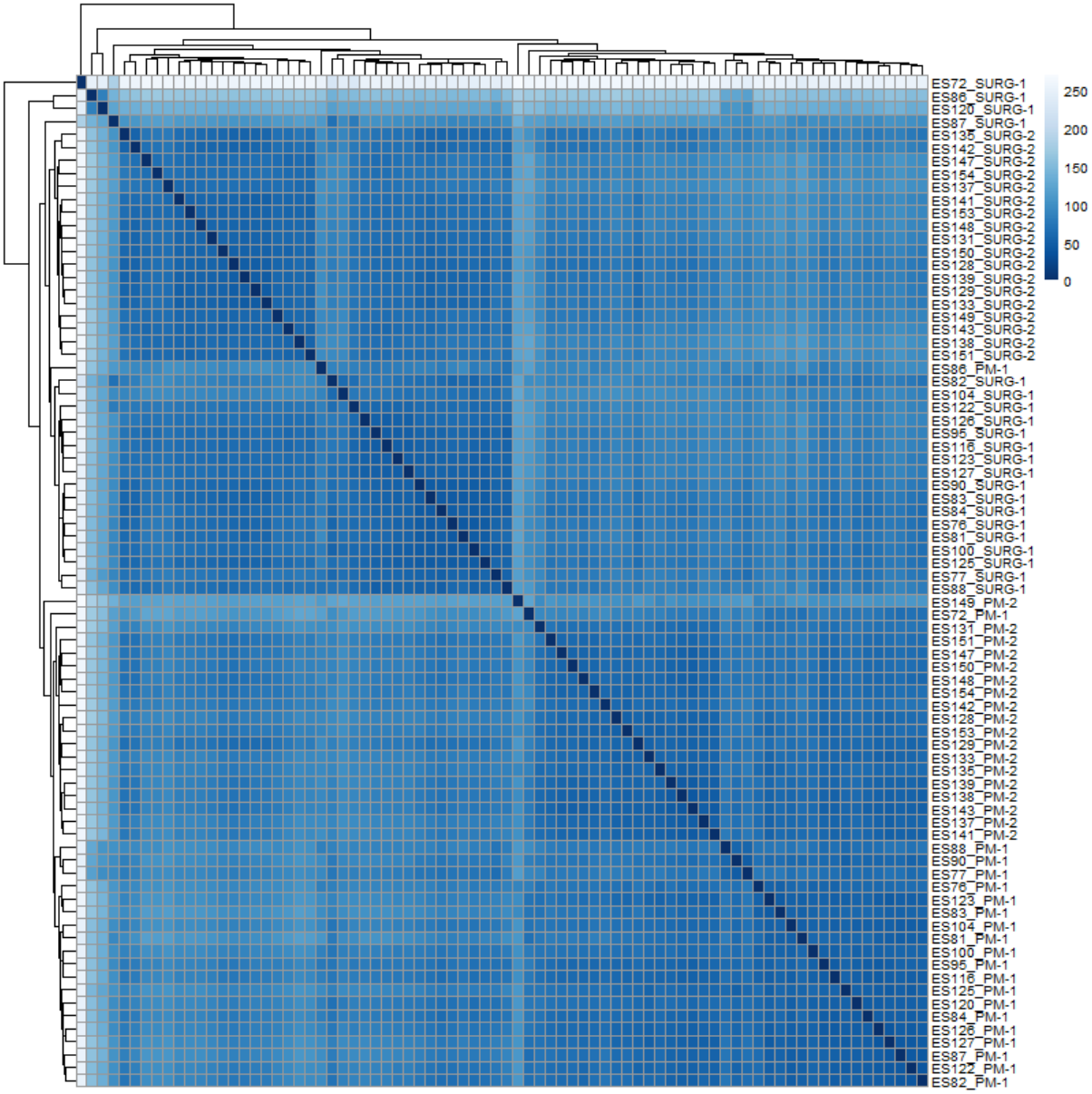

Figure 3.7b Hierarchical Clustered Heatmap of gene expression (Poisson Distance)

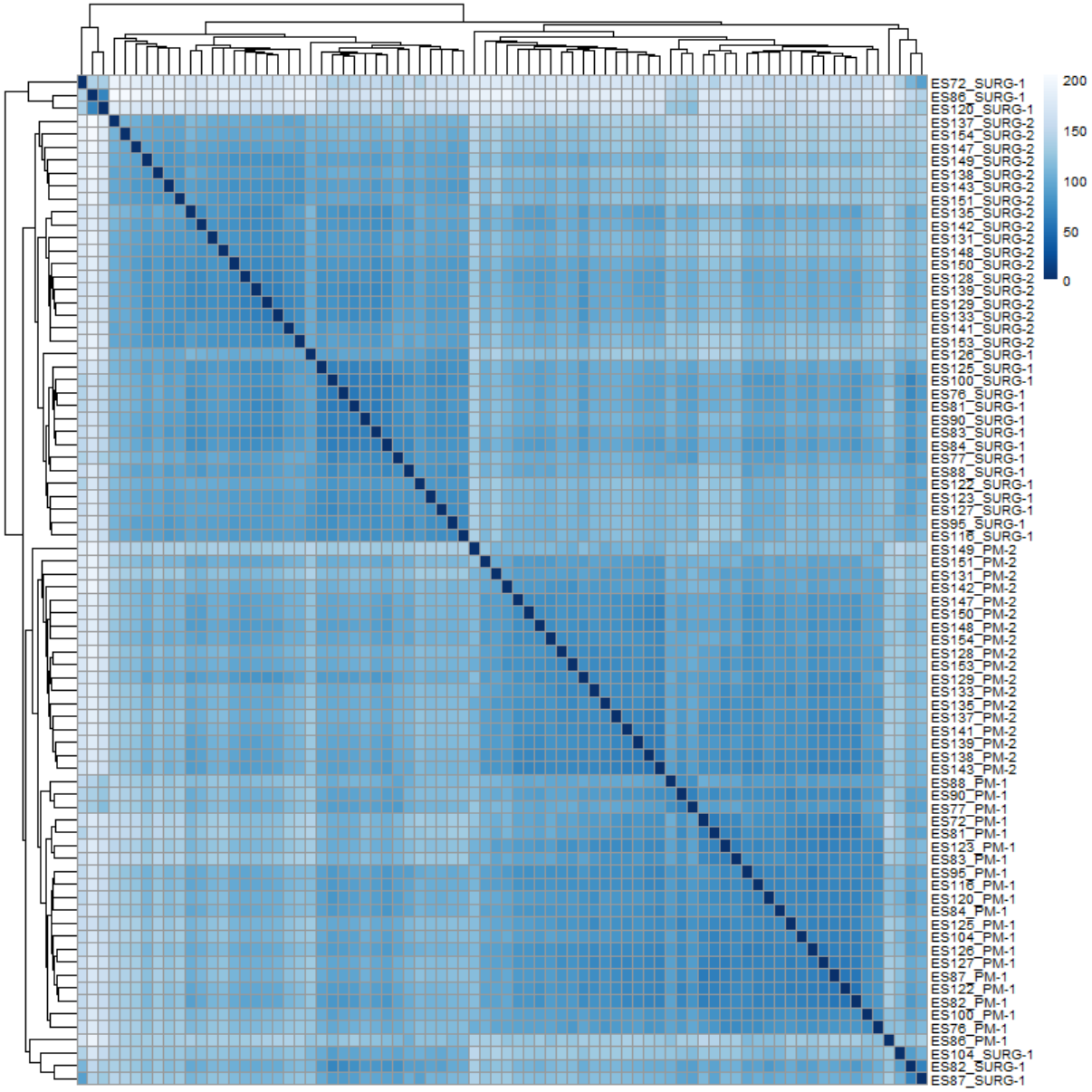

3.6.3 Analysis of sample-wide trancriptome dispersion

The heatmaps, measuring the distance between samples, confirmed the outliers highlighted by the PCA analysis. The possible outliers were investigated further by assessing the dispersion of the samples, using the DESeq2 “estimateDispersions” function (Figure 3.8). This is an estimate of variance within the data set. Dispersion estimates are the sum of two components: 1) sample-to-sample variation. 2) The uncertainty in measuring expression (shot noise), which is dominated by lowly expressed genes. The sum of both, shot noise and sample to sample variance, is considered in the differential expression inference.

Two scenarios were tested *i*) including all SURG samples, and *ii*) excluding SURG samples ES86 and ES120. The dispersion trend could not be captured using the parametric fit for the test where all samples were included. Therefore, a local regression was applied to this test.

The exploratory analysis detected the presence of five samples that might introduce undesired variation in the analyses. The PCA and heatmap plots highlighted the possible outliers. Moreover, the parametric fit could not be used when all samples were included, indicating the impact of the outliers on the gene counts. Thus, samples ES86-SURG; ES72-SURG; ES120-SURG; ES86-PM; ES149-PM were removed from further analysis.

Figure 3.8. Dispersion analysis

A) **SURG Dispersion of all samples** **B) SURG Dispersion when excluding outliers**

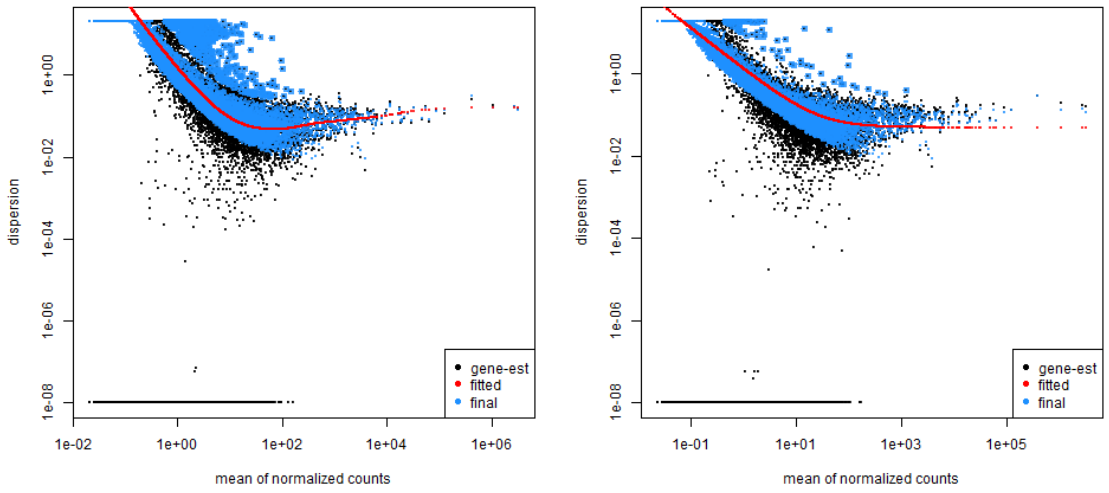

3.7 Differential expression analysis

Pre-injury (SURG) and the end of experiment (PM) samples were analysed with respect to treatment and injury. Differential expression analysis between experimental groups was performed using DESeq2. False discovery rate (FDR) q-values were calculated (Benjamini and Hochberg, 1995). Associations with FDR $q<0.05$ should be considered preliminary associations. Due to the exploratory nature of the study, test results with raw $p<0.05$ are also reported. R code used for all analyses is available in appendix 4.

The following conditions were evaluated in differential expression analysis

- *Treatment effects*
- *Injury effects*
- *Blast effects with Treatments*
- *Effects over time (Statin Treatment)*
- *Effects over time (Placebo Treatment)*

The conditions above were investigated in the following analyses

3.7.1 Summary of differential expression analysis

The results of the differential expression analyses are summarised in Table 3.1. There is very limited differential expression after FDR correction identified within time-points (T1-T15). Time course analyses identified many differentially expressed genes (T16-T20), including a large number of genes that were unique to treatment and placebo.

Table 3.1. Summary of differential expression across analyses T1-T20

Name	Sample 1	Sample no	Sample 2	Sample no	Test	DF (<=.05)
T1	SURG gp1	3	SURG gp2	11	Placebo effect	2
T2	SURG gp1	3	SURG gp3	13	Treatment effect baseline	1
T3	SURG gp2	11	SURG gp3	13	Treatment effect baseline	0
T4	PM gp1	3	PM gp2	11	Injury effect	2
T5	PM gp1	3	PM gp3	14	Treatment and Injury effect	3
T6	PM gp2	11	PM gp3	14	Treatment effect end of expriment	0
T7	SURG gp1	3	SURG gp4	3	Blast ? and Placebo effect	5
T8	SURG gp1	3	SURG gp5	6	Blast ? and Treatment effect	2
T9	SURG gp2	11	SURG gp5	6	Blast? and Placebo effect	0
T10	SURG gp4	3	SURG gp5	6	Treatment effect in (Blast?) baseline	1
T11	PM gp1	3	PM gp4	3	Injury and Blast effect in placebo	44
T12	PM gp1	3	PM gp5	6	Injury and Blast effect in treatment	41
T13	PM gp2	11	PM gp4	3	Blast effect (in placebo)	2
T14	PM gp2	11	PM gp5	6	Blast and treatment effects	3
T15	PM gp4	3	PM gp5	6	Treatment effects (in blast)	1
T16	SURG gp1	3	PM gp1	3	Surgery effect	479
T17	SURG gp2	10	PM gp2	10	Injury effect overtime in placebo samles	3706
T18	SURG gp3	13	PM gp3	13	Injury effect overtime in treated samples	4118
T19	SURG gp4	3	PM gp4	3	Injury and blast overtime in placebo samples	733
T20	SURG gp5	6	PM gp5	6	Injury and blast overtime in treated samples	3537

3.7.2 Evaluation of differential expression within time-points (T1-T15)

A range of analyses were performed in an attempt to detect differential expression within time-point across treatments. Generally very little differential expression was detected and a decision was to take focus on time course analyses, which maximise the power of the study. Full results for analyses T1-T15 are available on request.

3.7.3 Evaluation of differential expression across treatments over time (T16-T20)

T16: Surgery effect

The surgery effect was investigated by comparing all SURG samples in group 1 (3 samples) vs all PM samples in group 1 (3 samples). This comparison showed 479 significant genes ($q<0.05$) between the two groups. The top twenty associated genes are reported in table 3.1, all associations are reported in supplementary file 3.1 (**T16**).

T17: Injury effect overtime in placebo samples

The effect of injury overtime in placebo treated samples was investigated by comparing all SURG samples in group 2 (10 samples) vs all PM samples in group 2 (10 samples). This comparison showed 3706 significant genes (q<0.05) between the two groups. The top twenty associated genes are reported in table 3.2, all associations are reported in supplementary file 3.1 (**T17**).

Table 3.2. Top 20 differentially expressed genes in comparison T16 (Surgery Effect)

Gene	Gene Description	Druggable	Drugged	base mean expression	log2 FC	p	q
Csf3r	colony stimulating factor 3 receptor (granulocyte)	Y	Y	907	-3.33	1.27E-50	8.52E-47
S100a9	S100 calcium binding protein A9	Y	.	6129	-3.38	2.41E-49	8.09E-46
S100a8	S100 calcium binding protein A8	Y	Y	2772	-3.51	7.45E-43	1.67E-39
Mmp8	matrix metallopeptidase 8 (neutrophil collagenase)	Y	Y	964	-3.69	2.77E-40	4.65E-37
Mcemp1	mast cell expressed membrane protein 1	.	.	346	-3.41	7.96E-34	1.07E-30
AABR07034362	.	.	.	380	-2.99	6.46E-33	7.23E-30
Clec4d	C-type lectin domain family 4, member D	.	.	503	-2.99	6.64E-30	6.37E-27
Clec4e	C-type lectin domain family 4, member E	.	.	221	-3.73	3.7E-28	2.9E-25
Lrg1	leucine-rich alpha-2-glycoprotein 1	Y	.	1037	-2.60	3.89E-28	2.9E-25
Anxa1	annexin A1	Y	.	594	-2.82	1.52E-26	1.02E-23
Steap4	STEAP family member 4	.	.	218	-3.62	9.64E-26	5.88E-23
Fbxl5	F-box and leucine-rich repeat protein 5	.	.	462	-2.96	2.64E-24	1.48E-21
AABR07003235	.	.	.	194	-3.14	3.03E-24	1.57E-21
Slpi	secretory leukocyte peptidase inhibitor	Y	Y	168	-3.81	1.38E-23	6.62E-21
Pglyrp1	peptidoglycan recognition protein 1	Y	.	228	-3.20	1.9E-23	8.51E-21
Dgat2	diacylglycerol O-acyltransferase homolog 2	.	.	354	-3.66	1.53E-22	6.42E-20
Lyz2	lysozyme 2			9010	-1.83	2E-21	7.9E-19
Cxcr2	C-X-C motif chemokine receptor 2	Y	Y	156	-3.25	5.09E-21	1.9E-18
Il17ra	interleukin 17 receptor A	Y	Y	845	-2.01	1.81E-20	6.4E-18
Alox5ap	arachidonate 5-lipoxygenase-activating protein	Y	Y	380	-3.14	4.59E-20	1.54E-17

Table 3.3. Top 20 differentially expressed genes in comparison T17 (injury effect overtime in placebo)

Gene	Gene Description	Druggable	Drugged	base mean expression	log2 FC	p	q
Hp	haptoglobin	Y	Y	837	-5.33	2.3E-197	2.7E-193
Serpinb1a	serpin family B member 1a			912	-5.89	1.5E-176	8.9E-173
Dgat2	diacylglycerol O-acyltransferase homolog 2	.	.	333	-4.43	6.2E-144	2.5E-140
Fbxl5	F-box and leucine-rich repeat protein 5	.	.	382	-4.07	9E-143	2.7E-139
Il1r2	interleukin 1 receptor, type II	Y	Y	526	-5.35	1.5E-142	3.5E-139
Csf3r	colony stimulating factor 3 receptor (granulocyte)	Y	.	827	-4.51	3.5E-141	6.8E-138
Anxa1	annexin A1	Y	.	537	-3.65	1.3E-140	2.1E-137
S100a8	S100 calcium binding protein A8	Y	Y	2658	-4.07	1.1E-139	1.6E-136
Mmp8	matrix metallopeptidase 8 (neutrophil collagenase)	Y	Y	794	-4.60	1E-129	1.4E-126
S100a9	S100 calcium binding protein A9	Y	.	5244	-3.79	2.5E-126	3E-123
Alox5ap	arachidonate 5-lipoxygenase-activating protein	Y	Y	355	-4.07	1.4E-115	1.6E-112
Clec4d	C-type lectin domain family 4, member D	.	.	324	-4.06	1.2E-113	1.2E-110
AABR07003235	.	.	.	203	-4.71	8E-112	7.3E-109
Chi3l1	chitinase 3-like 1 (cartilage glycoprotein-39)	.	.	704	-2.68	4.6E-107	3.9E-104
Vsir	V-set immunoregulatory receptor	.	.	292	-2.24	7.55E-87	5.99E-84
Mcemp1	mast cell expressed membrane protein 1	.	.	245	-3.52	3.9E-83	2.9E-80
Pglyrp1	peptidoglycan recognition protein 1	Y	.	225	-3.77	8.19E-81	5.73E-78
Clec4e	C-type lectin domain family 4, member E	.	.	170	-4.59	2.23E-79	1.47E-76
Sbno2	strawberry notch homolog 2			234	-3.44	8.55E-79	5.35E-76
Slpi	secretory leukocyte peptidase inhibitor	Y	Y	172	-4.70	9.42E-79	5.6E-76

T18: Injury effect overtime in simvustatin treated samples

The effect of injury overtime in simvastatin treated samples was investigated by comparing all SURG samples in group 3 (13 samples) vs all PM samples in group 3 (13 samples). This comparison showed 4118 significant genes (q<0.05) between the two groups. The top twenty associated genes are reported in table 3.3, all associations are reported in supplementary file 3.1 (**T18**).

T19: Injury and blast effect overtime in placebo treated samples

The effect of injury and blast overtime in placebo treated samples was investigated by comparing all SURG samples in group 4 (3 samples) vs all PM samples in group 4 (3 samples). This comparison showed 733 significant genes (q<0.05) between the two groups. The top twenty associated genes are reported in table 3.4, all associations are reported in supplementary file 3.1 (**T19**).

Table 3.4. Top twenty differentially expressed genes in comparison T18 (injury effect overtime in treatment)

Gene	Gene Description	Druggable	Drugged	base mean expression	log2 FC	p	q
Serpinb1a	serpin family B member 1a			869.5	-5.8322	5.93E-198	6.96E-194
Csf3r	colony stimulating factor 3 receptor (granulocyte)	Y	.	923.8	-4.1641	9.15E-189	5.36E-185
Mmp8	matrix metallopeptidase 8 (neutrophil collagenase)	Y	Y	770.1	-4.1148	1.50E-182	5.86E-179
Alox5ap	arachidonate 5-lipoxygenase-activating protein	Y	Y	343.6	-3.7095	6.40E-141	1.87E-137
Hp	haptoglobin	Y	.	768.9	-5.5115	1.42E-130	3.33E-127
S100a8	S100 calcium binding protein A8	Y	Y	2435	-3.9495	1.31E-127	2.55E-124
S100a9	S100 calcium binding protein A9	Y	.	4906	-3.7308	1.08E-125	1.81E-122
Cxcr2	C-X-C motif chemokine receptor 2	Y	Y	175	-4.3768	1.86E-124	2.72E-121
Mmp9	matrix metallopeptidase 9 (gelatinase B,	Y	Y	198.6	-3.7227	1.41E-118	1.84E-115
AABR07003235	.	.	.	210.9	-4.1566	3.20E-111	3.75E-108
Il1r2	interleukin 1 receptor, type II	.	.	529.6	-5.3647	5.26E-107	5.60E-104
Scimp	chromosome 17 open reading frame 87	.	.	136.6	-3.8709	2.52E-103	2.46E-100
Dgat2	diacylglycerol O-acyltransferase homolog 2	.	.	339.4	-4.5561	1.23E-100	1.11E-97
Csf2rb	colony stimulating factor 2 receptor, beta,	.	.	182.9	-3.9591	3.23E-99	2.70E-96
Clec4d	C-type lectin domain family 4, member D	.	.	370.1	-3.7321	2.87E-94	2.24E-91
Vsir	V-set immunoregulatory receptor	.	.	309	-2.0987	9.23E-91	6.76E-88
Fbxl5	F-box and leucine-rich repeat protein 5	.	.	403.5	-3.8302	2.79E-88	1.92E-85
Ptafr	platelet-activating factor receptor	Y	Y	172.9	-3.0888	4.16E-87	2.71E-84
Steap4	STEAP family member 4	.	.	259.3	-4.5085	1.31E-86	8.10E-84
Clec4e	C-type lectin domain family 4, member E	.	.	171.8	-3.942	6.75E-85	3.95E-82

T20: Injury and blast effect overtime in simvustatin treated samples

The effect of injury and blast overtime in simvustatin treated samples was investigated by comparing all SURG samples in group 5 (6 samples) vs all PM samples in group 5 (6 samples). This comparison showed 3537 significant genes ($q<0.05$) between the two groups. The top twenty associated genes are reported in table 3.5, all associations are reported in supplementary file 3.1 (**T20**).

Table 3.5. Top twenty differentially expressed genes in comparison T19 (injury and blast effect overtime in placebo)

Gene	Gene Description	Druggable	Drugged	base mean expression	log2 FC	p	q
Il1r2	interleukin 1 receptor, type II	.	.	938.8	-5.9778	2.11E-92	1.41E-88
Serpinb1a	serpin family B member 1a			1491	-6.044	6.20E-82	2.08E-78
Csf3r	colony stimulating factor 3 receptor (granulocyte)	Y	.	1534	-4.0131	6.85E-69	1.53E-65
Hp	haptoglobin	Y	.	1368	-5.6305	7.50E-55	1.26E-51
S100a9	S100 calcium binding protein A9	Y	.	7042	-4.048	3.67E-46	4.91E-43
Fbxl5	F-box and leucine-rich repeat protein 5	.	.	600.7	-3.5459	4.78E-44	5.33E-41
Dgat2	diacylglycerol O-acyltransferase homolog 2	.	.	569.4	-4.4151	6.61E-44	6.32E-41
Cxcr2	C-X-C motif chemokine receptor 2	Y	Y	327.4	-4.3747	1.05E-43	8.76E-41
Alox5ap	arachidonate 5-lipoxygenase-activating protein	Y	Y	588.3	-4.2323	8.08E-43	6.01E-40
S100a8	S100 calcium binding protein A8	Y	Y	3662	-4.3127	1.31E-42	8.77E-40
Clec4d	C-type lectin domain family 4, member D	.	.	513.2	-3.3958	1.53E-40	9.32E-38
Chi3l1	chitinase 3-like 1 (cartilage glycoprotein-39)	.	.	1089	-2.8789	2.60E-35	1.45E-32
Csf2rb	colony stimulating factor 2 receptor, beta, l	.	.	313.3	-3.8101	1.44E-34	7.40E-32
AABR07003235	.	.	.	358.4	-4.1038	3.20E-33	1.53E-30
Steap4	STEAP family member 4	.	.	405.5	-4.364	6.96E-32	3.11E-29
Clec4e	C-type lectin domain family 4, member E	.	.	253.5	-3.9654	9.89E-32	4.14E-29
Mcemp1	mast cell expressed membrane protein 1	.	.	365.2	-3.2558	1.70E-31	6.69E-29
Anxa1	annexin A1	Y	Y	943.6	-3.6018	3.35E-31	1.25E-28
Lrg1	leucine-rich alpha-2-glycoprotein 1	Y	.	1367	-3.0204	8.91E-31	3.14E-28
Dusp1	dual specificity phosphatase 1	Y	Y	395.3	-3.0085	3.17E-30	1.06E-27

Table 3.6. Top ten differentially expressed genes in comparison T20

Gene	Gene Description	Druggable	Drugged	base mean expression	log2 FC	p	q
Csf3r	colony stimulating factor 3 receptor (granulocyte)	Y	.	1370	-4.6397	2.68E-171	2.99E-167
Serpinb1a	serpin family B member 1a			1341	-6.1896	6.89E-155	3.85E-151
Clec4d	C-type lectin domain family 4, member D	.	.	443.2	-4.2214	3.15E-130	1.17E-126
Fbxl5	F-box and leucine-rich repeat protein 5	.	.	548.5	-4.0568	1.07E-111	2.98E-108
Anxa1	annexin A1	Y	.	738	-3.7836	2.92E-110	6.52E-107
Steap4	STEAP family member 4	.	.	366.1	-5.4794	1.78E-109	3.32E-106
Dgat2	diacylglycerol O-acyltransferase homolog 2	.	.	480.2	-4.9386	6.83E-109	1.09E-105
Alox5ap	arachidonate 5-lipoxygenase-activating protein	Y	Y	532.2	-4.1714	2.34E-98	3.27E-95
Mmp8	matrix metallopeptidase 8 (neutrophil collagenase)	Y	Y	1002	-4.4548	2.41E-92	2.99E-89
Sell	selectin L	Y	Y	850.9	-2.963	6.94E-85	7.75E-82
Dusp1	dual specificity phosphatase 1	Y	Y	303.6	-3.6953	1.31E-84	1.33E-81
Csf2rb	colony stimulating factor 2 receptor, beta,	.	.	328.5	-4.6551	6.79E-82	6.32E-79
Cxcr2	C-X-C motif chemokine receptor 2	Y	Y	288.1	-5.2331	1.61E-81	1.39E-78
Clec4e	C-type lectin domain family 4, member E	.	.	220.3	-4.5126	7.01E-79	5.59E-76
Sbno2	strawberry notch homolog 2			348	-3.649	2.31E-78	1.72E-75
Srgn	serglycin	Y	Y	699.6	-2.5704	1.48E-75	1.03E-72
AABR07003235	.	.	.	297.1	-4.6316	1.72E-74	1.13E-71
Chi3l1	chitinase 3-like 1 (cartilage glycoprotein-39)	.	.	1004	-2.9195	5.80E-71	3.60E-68
Entpd1	ectonucleoside triphosphate diphosphohydrolase 1	Y	Y	217.2	-3.2155	1.05E-69	6.17E-67
Clec7a	C-type lectin domain family 7, member A	.	.	164.7	-3.7487	1.60E-69	8.96E-67

3.7.4 Comparison of changes overtime

As no treatment effects were seen in earlier analyses, the aim of the time course comparisons (T16-T20) was to identify treatment changes that may only be reflected over time in the models. The analyses are intended to identify a change in the overall trajectory of transcriptome response to injury and injury + blast in treatment groups. Very strong signals were observed in these comparisons. This is expected due to the previously described magnitude of response to trauma and blast injury. In order to characterise the genes showing differential expression over time between treatment groups, a Venn diagram was prepared (figure 3.8). The Venn diagram identified a large number of genes which were specific to placebo and treatment groups, including 447 that were unique to Injury + Blast, 855 that were unique to injury and 351 that were unique to statin treatment but shared between the injury and blast groups, totalling 1653 treatment specific genes. In total 506 genes were unique to placebo suggesting a treatment effect in the statin group, although the smaller placebo group is less powered to detect an effect.

Figure 3.9 Venn diagram comparison of differential expression changes (q<0.05) over time (T17 – T20)

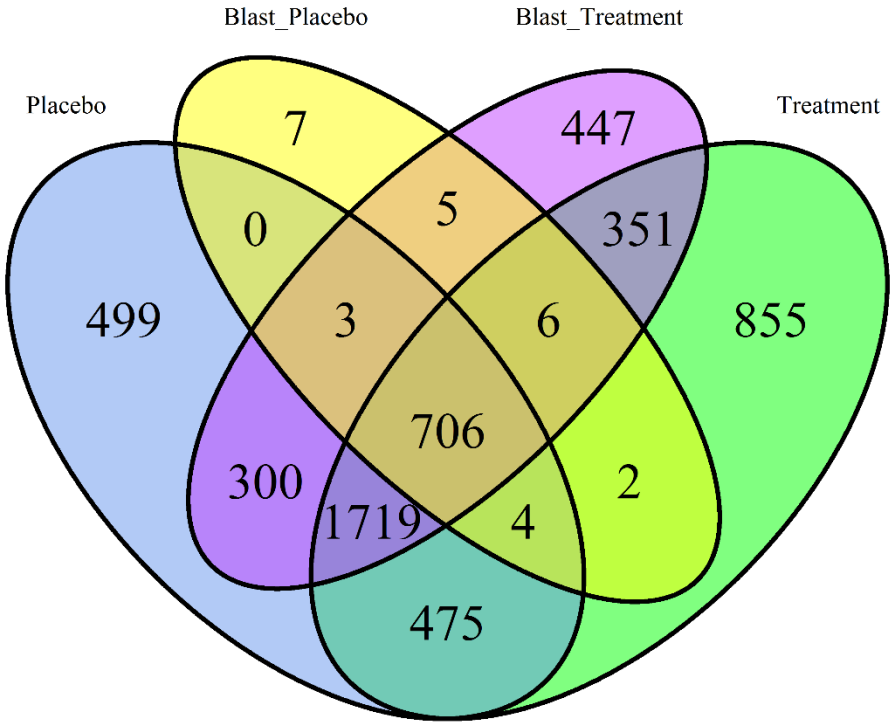

3.8 Integrated Systems Biological Pathway Analysis

3.8.1. Ingenuity Pathway analysis - time course analysis (T17-T20)

Genes with significant differential expression (q<.05) in each treatment group were compared at a pathway level to comparatively evaluate pathway enrichment. To assist mechanistic interpretation and also to reflect the tendency for genes to form co-expression networks, gene expression results were partitioned into up and down regulated responses prior to pathway analysis. Results of the pathway analysis are presented in Tables 3.1 – 3.16. Evidence for enrichment was investigated across three categories, disease and function, canonical pathways and upstream regulators. Pathways enrichment among up and down regulated genes are ordered by the strength of pathway enrichment (activation z score) across the top 10 shared pathways, followed by the top 10 pathways within each treatment group (in this case combining the injury and injury + blast groups to focus on treatment effects). All results for all pathways are reported in supplementary table 3.3. Activation Z-scores used to rank pathway association are used to find likely regulating molecules based on a statistically significant pattern match of up- and down-regulation, and also to predict the activation state of the given process, regulator or pathway.

Strong evidence of differential expression was detected in the time course analyses, pathway analysis identified many key pathways and mechanisms that are activated over time in trauma injury and blast, however at an experiment wide level, many pathways are enriched across all samples, but the different treatment comparisons show some differentiation.

3.8.2 – Treatment time course analysis – Diseases and Biofunctions

Investigation of differential gene expression in diseases and biofunctions identified a strong enrichment for genes involved in cell death and cell survival. Activation Z-scores also predict the activation state of the given processes, and thus upregulated genes promote cell death and inhibit cell survival, while down regulated genes inhibit cell death and promote cell survival. Perhaps importantly in injury with blast, enrichment of cell death and survival is lower in placebo among down regulated genes and absent in up-regulated genes. However in the injury only group, treatment and placebo are not distinguished. This suggests the possibility of an enhanced treatment response in injury and blast over injury alone.

3.8.3 – Treatment time course analysis – Canonical pathways

Investigation of differential gene expression in canonical pathways also identified differential enrichment of trauma relevant pathways between treatment and control groups, particularly in the injury and blast group.

Table 3.7. T17-T20 Disease/Function Enrichment (Top 10 shared / top 10 distinct per comparison)

Diseases and Bio Functions	T20 - Injury blast time treated - down	T20 - Injury blast time treated - up	T19 - Injury blast time placebo - down	T19 - Injury blast time placebo - up	T18 - Injury time treated - down	T18 - Injury time treated - up	T17 - injury time placebo - down	T17 - injury time placebo - up
A) Top ranked all								
Organismal death	19.5	-15.5	10.42	0	20.14	-16.5	20.06	-15.6
Morbidity or mortality	18.95	-15.3	9.579	0	19.57	-16.2	19.42	-15.4
Cell viability	-10.3	9.365	-5.8	0	-11.4	9.917	-10.6	10
Cell survival	-10	9.547	-5.67	0	-11.2	10.05	-10.5	10.13
Viral Infection	-8.87	8.111	-3.69	2.38	-8.88	8.348	-9.03	8.599
Endocytosis	-7.8	5.714	-5.88	2.062	-7.35	5.362	-7.93	5.56
Leukocyte migration	-8.22	5.757	-6.18	2.578	-7.81	5.306	-7.99	5.381
Engulfment of cells	-7.54	5.723	-6.02	2.177	-7.53	5.489	-7.92	5.061
Cell viability of tumor cell lines	-8.99	8.371	0	0	-9.84	8.785	-9.29	8.343
Cell movement of blood cells	-8.27	5.754	-6.23	0	-7.89	5.307	-8.02	5.44
B) Most differentially up regulated in treatment								
Organismal death	19.5	-15.5	10.42	0	20.14	-16.5	20.06	-15.6
Morbidity or mortality	18.95	-15.3	9.579	0	19.57	-16.2	19.42	-15.4
Cell survival	-10	9.547	-5.67	0	-11.2	10.05	-10.5	10.13
Cell viability	-10.3	9.365	-5.8	0	-11.4	9.917	-10.6	10
Motor dysfunction or movement disorder	0	-4.39	0	0	0	-4.82	0	0
Infection by HIV-1	0	8.722	0	0	0	9.073	0	8.676
HIV infection	0	8.603	0	0	0	9.016	0	8.612
Transactivation of RNA	-6.11	4.516	0	0	-6.06	4.45	-4.76	0
Survival of organism	-1.53	4.379	-0.1	0	-2.08	4.545	-2.16	0
Cell viability of tumor cell lines	-8.99	8.371	0	0	-9.84	8.785	-9.29	8.343
C) Most differentially down regulated in treatment								
Anemia	5.878	-3.68	0	N/A	6.14	-3.55	0	-3.46
Growth Failure	10.86	0	0	0	11.88	0	11.3	0
Infection of cells	0	9.014	0	1.93	-9.58	9.244	0	8.962
Cell viability of tumor cell lines	-8.99	8.371	0	0	-9.84	8.785	-9.29	8.343
Morbidity or mortality	18.95	-15.3	9.579	0	19.57	-16.2	19.42	-15.4
Cell proliferation of hematopoietic cell lines	0	3.136	-3.85	0	0	0	-5.56	0
Organismal death	19.5	-15.5	10.42	0	20.14	-16.5	20.06	-15.6
Metabolism of eicosanoid	0	0	-4.45	0	0	0	-4.33	0
Expression of RNA	-7.33	3.211	0	0.571	-7.27	3.263	-6.39	3.149
Transcription	-7.1	3.628	0	0	-7.43	3.564	-6.37	3.428

Table 3.8. T16-T20 Canonical Pathway Enrichment (Top 10 shared / top 10 distinct per comparison)

Canonical pathways	T20 - Injury blast time treated - down	T20 - Injury blast time treated - up	T19 - Injury blast time placebo - down	T19 - Injury blast time placebo - up	T18 - Injury time treated - down	T18 - Injury time treated - up	T17 - injury time placebo - down	T17 - injury time placebo - up
A) Top ranked all								
Neuroinflammation Signaling Pathway	-6.57	4.707	-4.08	2.449	-6.55	4.642	-6.79	3.8
Role of NFAT in Regulation of the Immune Response	-6.32	5.209	-3.46	2.714	-6.48	5.488	-6.16	5.396
Superpathway of Inositol Phosphate Compounds	-7.14	5.196	-3.61	0	-7.07	4.899	-6.93	5.196
Dendritic Cell Maturation	-5.66	4.583	-3.61	2.449	-5.74	4.796	-5.39	4.123
PKCθ Signaling in T Lymphocytes	-5.57	5.196	-2.65	2.828	-5.83	5.196	-5.57	5.099
3-phosphoinositide Biosynthesis	-6.4	4.796	-3.16	0	-6.48	4.583	-6.24	4.796
NF-κB Signaling	-7.21	3.441	-4.12	0	-6.79	4.025	-6.78	2.324
IL-8 Signaling	-6.71	4.359	-3.61	0	-6.86	3.638	-6.78	3.606
Phospholipase C Signaling	-5.86	4.796	-3.32	0	-5.95	4.796	-5.78	5.099
Cardiac Hypertrophy Signaling	-6.51	4.146	-2.89	0	-6.79	3.8	-6.41	3.962
B) Pathways most differentially regulated between treatment and placebo up regulated genes								
Oxidative Phosphorylation	0	6.481	0	0	0	6.325	0	6.083
Integrin Signaling	-5.69	4.747	-1.67	0	-5.98	4.426	-5.52	4.025
NF-κB Signaling	-7.21	3.441	-4.12	0	-6.79	4.025	-6.78	2.324
Superpathway of Inositol Phosphate Compounds	-7.14	5.196	-3.61	0	-7.07	4.899	-6.93	5.196
Ovarian Cancer Signaling	-4.15	2.449	0	0	-4.38	2.449	-4.15	0
UVC-Induced MAPK Signaling	-3.61	2.646	-2	0	-3.74	2.236	-3.87	0
Pyrimidine Ribonucleotides Interconversion	-2.24	2	-2.24	0	-2.45	2.646	-2.45	0
3-phosphoinositide Biosynthesis	-6.4	4.796	-3.16	0	-6.48	4.583	-6.24	4.796
Adrenomedullin signaling pathway	-5.92	4	-2.33	0	-6.41	4.146	-6.09	3.606
Phospholipase C Signaling	-5.86	4.796	-3.32	0	-5.95	4.796	-5.78	5.099
C) Pathways most differentially regulated between treatment and placebo down regulated genes								
Melanocyte Development and Pigmentation Signaling	-4.81	3	0	0	-5.39	3.317	-4.81	2.646
Aldosterone Signaling in Epithelial Cells	-4.9	3	0	0	-5	2.646	-4.69	3
EGF Signaling	-4.58	2.449	0	0	-4.9	2.236	-4.36	2
Neurotrophin/TRK Signaling	-4.69	2.449	0	0	-4.9	2.646	-4.58	2.236
VEGF Signaling	-4.49	3	0	0	-4.43	2.646	-3.96	2
Neuropathic Pain Signaling In Dorsal Horn Neurons	-4.58	3	0	0	-4.69	3.162	-4.47	2.828
PAK Signaling	-4.58	2.828	0	0	-5	3.317	-4.8	2.828
FGF Signaling	-4.26	2.236	0	0	-4.9	2	-4.38	0
Actin Cytoskeleton Signaling	-5.43	4.082	-1.13	0	-5.52	4.082	-5.15	3.962
Signaling by Rho Family GTPases	-6.09	3.962	-1.89	0	-5.92	4.2	-5.49	4.6

Table 3.9. T17-T20 Upstream Regulator Enrichment (Top 10 shared / top 10 distinct per comparison)

Upstream regulators	T20 - Injury blast time treated - down	T20 - Injury blast time treated - up	T19 - Injury blast time placebo - down	T19 - Injury blast time placebo - up	T18 - Injury time treated - down	T18 - Injury time treated - up	T17 - injury time placebo - down	T17 - injury time placebo - up
A) Top ranked all								
lipopolysaccharide	-12	5.5	-9.1	2.24	-12	6.03	-12	5.03
IFNG	-9.5	6.34	-7.4	2.16	-9.5	7.32	-9.2	6.2
sirolimus	5.2	-7.3	3.08	-5.1	5.71	-7.4	5.94	-6.8
tretinoin	-7.3	2.86	-7.1	0.98	-7.5	3.87	-7.9	3.54
IL5	-8.4	5.19	-6.1	0	-8.2	5.03	-8.9	0
IL4	-6	5.38	-3	2.73	-5.3	6.18	-5.9	6
hydrogen peroxide	-7	4.56	-5	1.24	-7.2	0	-7	4.89
TNF	-9.4	0	-7.6	0	-10	0	-9.4	0
CD40LG	-5.2	4.45	-3.5	2	-5.7	5.71	-5.1	4.66
CD3	-6	4.15	-2.1	1.24	-6	5.79	-5.9	4.44
B) Pathways most differentially regulated between treatment and placebo up regulated genes								
IL5	-8.4	5.19	-6.1	0	-8.2	5.03	-8.9	0
IRF7	-5.5	4.8	-3.2	0	-5.7	5.01	-5.5	0
Ifnar	-3.7	3.82	-2.6	0	-4	3.94	-3.9	0
SPP1	-2.4	4.06	-1.6	0	-2	3.71	-2.3	0
STAT1	-5.5	4.31	-3.3	1.39	-5.6	4.83	-5.8	0
Interferon alpha	-6.3	3.11	-5.2	0	-6.3	4.5	-6.6	0
ERBB2	-4	3.66	-3.6	0	-3.4	3.18	-3.5	0
TGFB1	-5.5	3.96	-4	1.22	-5.7	3.93	-6.7	0
IFN Beta	-2.8	3.25	-1.9	0	-3.3	3.4	-3.1	0
EBF1	-2.5	3.07	-1.1	0	-2.5	3.37	-3.1	0
C) Pathways most differentially regulated between treatment and placebo down regulated genes								
FGFR1	-2.9	0	0	0	-3.1	0	0	0
PPARGC1A	-2.4	0	-0.2	0	-3.1	0	0	0
XBP1	-4.9	0	0	0	-5.2	0	-5	0
CD247	-2.3	0	0	0	-2.7	0	0	0
salinosporamide A	2.41	0	0	0	2.61	0	0	0
miR-24-3p (and other miRNAs w/seed	2.39	0	0	0	2.59	0	0	0
miR-30c-5p (and other miRNAs w/seed	5.29	0	0	0	4.72	0	5.13	0
miR-146a-5p (and other miRNAs w/seed	3.52	0	2.65	0	3.91	0	0	0
USF1	-2	2	0	0	-2.8	2.16	0	0
IFNL1	-3.1	3.16	-2	0	-3.6	0	0	0

3.8.4 – Treatment time course analysis – Upstream regulators

Investigation of differential gene expression to identify putative upstream regulators, also identified differential enrichment of trauma relevant pathways between treatment and control groups, particularly in the injury and blast group. The drug salinosporamide A, a 20s proteasome inhibitor is notably enriched among down regulated genes in the treatment groups only, suggesting a putative treatment effect and also indicating a potential repositioning candidate.

Table 3.10. Upstream regulator results for statin class drugs

Upstream regulators	T20 - Injury blast time treated - down	T20 - Injury blast time treated - up	T19 - Injury blast time placebo - down	T19 - Injury blast time placebo - up	T18 - Injury time treated - down	T18 - Injury time treated - up	T17 - injury time placebo - down	T17 - injury time placebo - up	T16 - Surgery - down	T16 - Surgery - up
fluvastatin	-0.97	0	0	0	-1.78	0	-0.29	0	0	0
simvastatin	0.96	0	0.18	0	1.41	0	0.8	0	0.63	0
atorvastatin	-0.67	0	-1.26	0	-1.89	0	-1.28	0	-0.44	0
lovastatin	-2.51	0	0	0	-2.07	0	-2.76	0	-2.12	0

Figure 3.10. Known simvastatin regulated genes differentially expressed in response to treatment

A) Treatment results overlaid

B) Placebo results overlaid

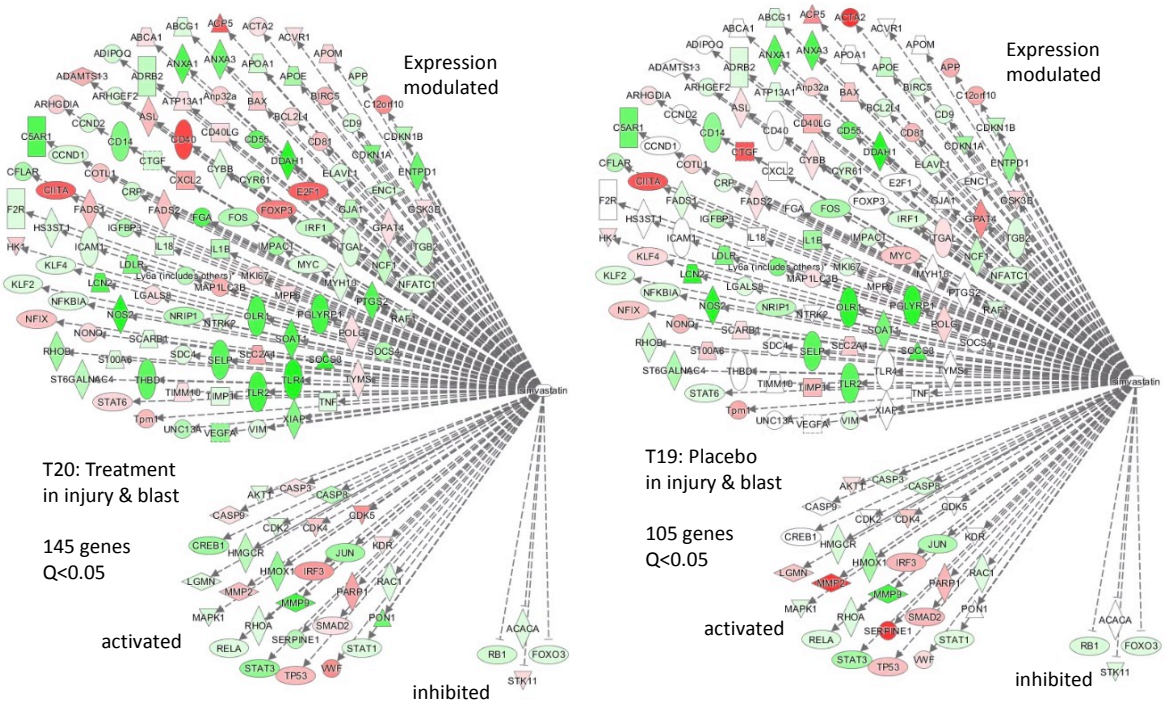

3.8.5 – Investigation of known statin responsive genes

No statin drugs were ranked among the top upstream regulators, results for all statins are shown in table 3.10. This shows that statin is predicted as an upstream regulator only among down regulated genes. Notably, simvastatin appears to exert an opposite direction of effect to other statin drugs.

A custom pathway consisting of known statin interacting genes was constructed in figure 3.10. Comparison of differential expression between treatment and placebo shows 145 and 105 differential genes respectively, further supporting a stating treatment effect on gene expression.

3.8.6 – Treatment unique differentially expressed gene list investigation

In order to focus on the differential effects between the treatment groups an additional pathway analysis was performed on the genes that were unique to treatment and placebo, indicated in the Venn diagram in Figure 3.8. Results of these analyses are presented in tables 3.11. All results for all pathways are reported in supplementary table 3.4.

Pathway analysis of the simvastatin unique gene lists showed strong differentiation between treatment and placebo groups. Strongly differentiated canonical pathway enrichments were seen in the treatment group, particularly in IL-4 signalling. In the upstream regulator analysis, strong differentiation was seen in regulation by TREM2, MS4A1 and CD9. In the disease and bio-function category, RNA processing and related processes were highlighted in the treatment group. Gene level results of all pathway analysis are available on request.

Table 3.11. Treatment/Placebo unique enrichment. A) Canonical pathways B) Upstream regulators C) Disease/Functions

A Canonical Pathway	treatment overtime	Placebo overtime
Cholecystokinin/Gastrin-mediated Signaling	4.251	2.646
Hereditary Breast Cancer Signaling	3.919	1.285
IL-4 Signaling	3.725	0.726
Sirtuin Signaling Pathway	3.674	2.202
Estrogen Receptor Signaling	3.578	1.181
Acute Myeloid Leukemia Signaling	3.534	0.677
Cell Cycle Control of Chromosomal Replication	3.497	0.576
Nur77 Signaling in T Lymphocytes	3.307	0.535
Endometrial Cancer Signaling	3.289	0.411
Neuregulin Signaling	3.227	1.093
Mismatch Repair in Eukaryotes	3.132	0.392
Role of NFAT in Regulation of the Immune Response	2.969	2.445
Huntington's Disease Signaling	2.939	1.825
Phosphatidylglycerol Biosynthesis II (Non-plastidic)	2.895	0.696
Renin-Angiotensin Signaling	2.867	1.661
Breast Cancer Regulation by Stathmin1	2.836	2.476
Adrenomedullin signaling pathway	2.753	0.717
Arginine Degradation VI (Arginase 2 Pathway)	2.692	0
Thrombopoietin Signaling	2.668	1.587
PDGF Signaling	2.638	1.06

B Upstream regulators	treatment overtime	Placebo overtime
HNF4A	5.28	5.86
TREM2	4.85	0
MS4A1	4.83	0
CD3	4.56	0
KLF3	4.18	1.31
SPP1	3.98	0
MYC	3.8	1.94
SATB1	3.69	0
IFNA1/IFNA13	3.55	0
PLAG1	3.48	0
L-dopa	3.42	0
E2F1	3.33	0
ethyl linoleate	3.33	0
RGD1560225	3.33	0
CD40LG	3.18	0
daunorubicin	3.17	0
miR-1-3p (and other miRNAs	3.17	0
ELAVL1	3.16	0
MMP3	3.12	0
3M-002	2.95	0

C Diseases and Bio Functions	treatment overtime	Placebo overtime
Processing of RNA	7.61	0
Viral Infection	6.65	4.9
Transactivation	5.59	3.91
Processing of mRNA	5.31	0
Metabolism of DNA	5.15	4.04
Proliferation of lymphatic system cells	5.1	2.31
Homeostasis of leukocytes	5.09	0
Lymphocyte homeostasis	5.08	0
Cell cycle progression of lymphoblastoid cell	5.04	0
Liver lesion	5	3.11
T cell homeostasis	4.99	0
Cell death of immune cells	4.95	0
Proliferation of blood cells	4.88	0
Transactivation of RNA	4.83	2.86
Morbidity or mortality	4.74	9.18
Organismal death	4.68	9.14
Hematopoiesis of mononuclear leukocytes	4.67	0
Proliferation of immune cells	4.65	0
DNA damage response of cells	4.56	2.4
Lymphopoiesis	4.54	0

3.9 Comparison of Rat model with QMUL Human and Rat samples

High level comparison analyses were performed between DSTL trauma injury models (T17 & T18) and QMUL human trauma data (Critical v Control; Critical MODS v Critical No MODs) from Cabrera et al (2017) and a QMUL rat model data (sham v hemorrhagic shock) from Sordi et al (2017). Results are presented in Table 3.12. Notably the rat model comparisons generally showed high correlation with human and rat models in differential expression at a pathway level (tables 3.12-3.14).

3.9.1 Human and Rat comparisons with T17-T18 Rat model – Canonical pathways

Comparison of human trauma and a QMUL rat hemorrhagic shock model with the rat trauma model showed strong enrichment across a range of pathways relevant to trauma injury, including NFAT regulation of immune response, Neuroinflammatory signalling, IL-8 and NFKB signalling. Although magnitude of enrichment varied between human and rat, the direction of effect was consistent across all pathways, supporting the representative nature of rat models in human trauma and MODs.

Table 3.12. Comparison of canonical Pathway Enrichment between human trauma (critical v control over 24h ; critical MODs v critical no MODs over 24h), rat hemorrhagic shock model (sham v hemorrhagic shock over 24h) and T17 and T18 rat models

Canonical Pathways	control over 24h - up trauma critical	over 24h - up MODS v No MODS	up QMUL SH_HS_Rat -	placebo - up T17 - injury time	treated - up T18 - injury time	control over 24h - trauma critical	over 24h - down MODS v No MODS	down QMUL SH_HS_Rat -	placebo - down T17 - injury time	treated - down T18 - injury time
NFAT in Regulation of the Immune Response	3.32	2.65	3.64	5.4	5.49	-4.8	-3.8	-4.9	-6.2	-6.5
Superpathway of Inositol Phosphate	3	3.74	4.58	5.2	4.9	-4.1	-3.6	-3.3	-6.9	-7.1
PKCθ Signaling in T Lymphocytes	2.83	2.24	3.74	5.1	5.2	-5.2	-3.7	-4.8	-5.6	-5.8
Neuroinflammation Signaling Pathway	4.36	3.32	3.41	3.8	4.64	-4	-3.3	-3.9	-6.8	-6.5
Phospholipase C Signaling	4	2.45	4.71	5.1	4.8	-4	-2.9	-3.7	-5.8	-5.9
IL-8 Signaling	4.36	3.87	4.9	3.61	3.64	-3.5	-2.6	-2.8	-6.8	-6.9
3-phosphoinositide Biosynthesis	2.65	3.61	4	4.8	4.58	-4	-3.3	-3.2	-6.2	-6.5
Cardiac Hypertrophy Signaling	3.77	3.46	6.25	3.96	3.8	-2.7	-3	-2.6	-6.4	-6.8
Dendritic Cell Maturation	3.16	2.83	3.74	4.12	4.8	-4.2	-4	-4	-5.4	-5.7
Role of NFAT in Cardiac Hypertrophy	3.21	3.32	7.35	3.36	3.5	-2.7	-2.7	-2.8	-6	-6.1
Adrenomedullin signaling pathway	3.61	3	5.49	3.61	4.15	-2.3	-2.6	-2.6	-6.1	-6.4
Integrin Signaling	3.71	4.15	3.96	4.03	4.43	-3.5	-1.6	-2.6	-5.5	-6
Tec Kinase Signaling	3	2.45	4.12	3.61	3.87	-4.4	-2.8	-3.2	-5.7	-6
CREB Signaling in Neurons	2.83	2.45	6.78	3.16	3.61	-3.2	-2.6	-2.6	-5.6	-5.7
Signaling by Rho Family GTPases	3.87	2.89	5.48	4.6	4.2	-2.1	-1	-2.8	-5.5	-5.9
NF-κB Signaling	3.36	2.65	4.12	2.32	4.03	-3.7	-2.1	-2.3	-6.8	-6.8
B Cell Receptor Signaling	3.74	2.33	4.2	3.84	3.3	-2.9	-3.2	-2.7	-5.9	-6
PI3K Signaling in B Lymphocytes	2.83	2.24	3.77	4.12	4	-3.3	-3.5	-3.5	-5.4	-5.3
D-myo-inositol-5-phosphate Metabolism	2.65	2.83	3.61	4.47	4.36	-3.2	-3	-2.2	-5.7	-5.7
Thrombin Signaling	3.16	2.33	3.53	3.61	3.36	-3.6	-3	-3.2	-5.2	-5.7

3.9.2 Human and Rat comparisons with T17-T18 Rat model – Upstream Regulators

Comparison of human trauma and a QMUL rat hemorrhagic shock model with the rat trauma model showed strong enrichment across a range of upstream regulators relevant to trauma injury (Table 3.13), including LPS, Interferon Gamma, and several interleukins. Notable differences between human and rat, included TNF upstream regulation which was absent in the up-regulated T17/T18 rat genes only but present among down regulated genes in rat and human. The significance of this is unknown, but suggests that the TNF up regulation of expression seen in human trauma and MODS is absent in the DSTL model.

Table 3.13. Comparison of upstream regulator Enrichment between human trauma (critical v control over 24h ; critical MODs v critical no MODs over 24h), rat hemorrhagic shock model (sham v hemorrhagic shock over 24h) and T17 and T18 rat models

Upstream Regulators	trauma critical control over 24h - up	MODS v No MODS over 24h - up	QMUL SH_HS_Rat - up	T17 - injury time placebo - up	T18 - Injury time treated - up	trauma critical control over 24h - down	MODS v No MODS over 24h - down	QMUL SH_HS_Rat - down	T17 - injury time placebo - down	T18 - Injury time treated - down
lipopolysaccharide	7.63	5.25	0	5.03	6.03	-5.7	-5.4	-3.7	-12	-12
IFNG	4.79	3.01	2.32	6.2	7.32	-6.6	-5	-5.6	-9.2	-9.5
tretinoin	4.91	4.13	5.36	3.54	3.87	-4.5	-3.2	-3.4	-7.9	-7.5
TNF	5.97	4.35	2.58	0	0	-4.5	-4.7	-3.9	-9.4	-10
sirolimus	-3.3	-2.3	-4.1	-6.8	-7.4	3.86	4.28	1.13	5.94	5.71
IL4	4.06	4.01	0	6	6.18	-4.6	-3.3	-3	-5.9	-5.3
LY294002	-4.2	-4.5	-6.7	0	0	5.16	3.26	3.14	7.43	7.42
phorbol myristate acetate	5.74	4.72	4.75	0	0	-2.2	-2.8	-4	-8.3	-8.5
IL5	5.52	4.49	0	0	5.03	-4.5	0	-3.6	-8.9	-8.2
IL2	4.3	3.48	0	2.51	3.3	-5.6	-2.8	-3	-6.8	-6.5
PD98059	-4.5	-5.1	-5.1	0	0	3.99	3.71	2.93	6.8	6.12
NFkB (complex)	3.5	3.78	0	0	0	-5.2	-4.7	-3.7	-7.9	-8
CD40LG	2.87	0	0	4.66	5.71	-4.7	-3.2	-3.4	-5.1	-5.7
NFE2L2	4.25	3.24	6.04	5.64	5.27	0	0	0	-5.4	-5.2
CD3	3.28	0	0	4.44	5.79	-4.1	-2.5	-2.9	-5.9	-6
STAT4	4.2	3.7	0	0	4.94	-4.3	-3.4	0	-7	-6.8
CSF2	4.93	3.77	0	0	0	-4.8	-3.5	-4.1	-6.4	-6.8
CD38	4.09	2.72	3.47	4.08	4.46	-3.2	0	0	-6.4	-5.8
1,2-dithiol-3-thione	3.29	3.2	3.5	5.92	6.09	0	-3.6	0	-4	-4.3
SB203580	-4.6	-4.1	0	0	0	3.84	3.69	2.42	7.58	7.44

3.9.3 Human and Rat comparison with T17-T18 Rat model – Diseases and Biofunctions

Comparison of human trauma, the rat hemorrhagic shock model with the rat trauma model also showed strong enrichment across a range of diseases and bio-functions relevant to trauma injury and MODs (Table 3.14). Intriguingly the DSTL T17/T18 Rat model (but not the Hemorrhagic shock model) showed strong pathway similarity with differential expression seen in MODs. This may indicate common pathology between the MODs state and the DSTL model, that could be of value for investigation of MODS. Other bio-functions including cell migration were strong in human trauma but weak in rat. By contrast human trauma showed no enrichment for RNA virus infection seen in rat.

Table 3.14. Comparison of Disease and Bio-function Enrichment between human trauma (critical v control over 24h ; critical MODs v critical no MODs over 24h), rat hemorrhagic shock model (sham v hemorrhagic shock over 24h) and T17 and T18 rat models

Diseases and Bio Functions	trauma critical control over 24h - up	MODS v No MODS over 24h - up	QMUL SH_HS_Rat - up	T17 - injury time placebo - up	T18 - Injury time treated - up	trauma critical control over 24h -	MODS v No MODS over 24h - down	QMUL SH_HS_Rat - down	T17 - injury time placebo - down	T18 - Injury time treated - down
Morbidity or mortality	-11	-11	-19	-15	-16	0	10.3	0	19.4	19.6
Organismal death	-11	-12	-19	-16	-16	0	0	0	20.1	20.1
Cell viability	6.34	6.29	0	10	9.92	-6.9	-6	-6.1	-11	-11
Cell survival	6.11	5.92	0	10.1	10.1	-7.1	-6.2	-6.1	-10	-11
Cell movement	6.43	7.24	8.42	0	0	-4.7	-5.6	-6	-11	-11
Migration of cells	5.51	6.54	8.14	0	0	-5.2	-5.9	-5.6	-11	-11
Viral Infection	6.38	6.51	0	8.6	8.35	-3.2	-3.9	0	-9	-8.9
Cell viability of tumor cell lines	5.47	4.89	0	8.34	8.79	0	-5.8	0	-9.3	-9.8
Cell movement of blood cells	4.89	5.1	0	5.44	5.31	-3.9	-5.2	-5.2	-8	-7.9
Leukocyte migration	4.7	5.04	0	5.38	5.31	-4.1	-5.2	-5.1	-8	-7.8
Cellular homeostasis	3.86	0	3.54	5.14	4.97	-4.7	-4.8	-4.9	-7.6	-7.8
Activation of cells	4.76	2.69	0	5.46	5.35	-5.7	-4.3	-3.3	-6.3	-6.6
Quantity of cells	2.39	1.91	5.16	5.25	5.11	-6.5	-3.8	-3.4	-4.9	-4.9
Infection by RNA virus	0	0	0	8.78	9.12	0	-4.9	0	-10	-10
Activation of blood cells	4.78	1.82	0	5.72	5.24	-5.3	-4.2	-3.2	-5.8	-5.8
Leukopoiesis	3.09	0	0	4.8	4.53	-6.1	-4.8	-4	-6.3	-6.8
Hematopoiesis of leukocytes	3.78	0	0	4.69	4.74	-5.4	-4.8	-4	-5.7	-6
Engulfment of cells	5.82	4.22	0	5.06	5.49	0	0	-3	-7.9	-7.5
Lymphopoiesis	3.17	0	0	4.98	4.81	-5.4	-5.3	-4	-5.3	-5.5
Activation of leukocytes	4.47	0	0	5.47	4.98	-5	-4.1	-3.2	-5.5	-5.5

4. Discussion and Conclusions

Sequencing of mRNA libraries generated from 39 paired rat model samples was successfully completed. High quality and consistent RNA-seq data was generated. Exploratory data analysis identified five samples as outliers, these were excluded from further analysis. Key findings from the analysis were as follows

- *Effects of injury and injury + blast on transcriptome expression were similar but could be differentiated and were most strongly detected in time course analyses*
- *Very few significant treatment effects on the transcriptome were seen within time-points*
- *Time course analysis showed evidence for larger differential expression in the treatment group compared to placebo*
- *Pathway analysis identified a number of trauma injury relevant pathways*
- *Putative treatment effects were identified, relating to cell death and survival processes*
- *Statin responsive genes were identified*
- *Comparison with Human trauma expression data, also showed high correlation at a pathway level*
- *TNF up regulation of expression seen in human trauma and MODS is absent in the DSTL model.*
- *The DSTL T17/T18 Rat model showed pathway similarity (Morbidity and Mortality) with differential expression seen in MODs v no MODs, this was not seen in the QMUL hemorrhagic shock rat model*

In conclusion, available data indicates that the DSTL Rat trauma study was a technical success. Power calculations indicated sufficient power to detect biological effects within time point, however this was not supported in the analysis, however time course analysis enabled the detection of both trauma injury and blast effects and putative treatment effects. Pathway level similarity (Morbidity and Mortality) between the DSTL model and human MODS samples was identified.

5. References

Anders S, Huber W. (2010) Differential expression analysis for sequence count data. Genome Biol. 2010;11(10):R106.

Benjamini Y, Hochberg Y (1995). Controlling the false discovery rate: a practical and powerful approach to multiple testing. J Royal Stat Soc, Series B 57:125-133.

BRAY, N. L., H. PIMENTEL, P. MELSTED and L. PACHTER, 2016 Near-optimal probabilistic RNA-seq quantification. Nature Biotechnology 34: 525.

Cabrera CP, Manson J, Shepherd JM, Torrance HD, Watson D, Longhi MP, Hoti M, Patel MB, O'Dwyer M, Nourshargh S, Pennington DJ, Barnes MR, Brohi, K. Signatures of inflammation and impending multiple organ dysfunction in the hyperacute phase of trauma: A prospective cohort study. PLoS medicine. 2017 Jul 17;14(7):e1002352.

Gentleman RC, VJ Carey, DM Bates, B Bolstad, M Dettling, S Dudoit, B Ellis, et al. (2004). Bioconductor: Open Software Development for Computational Biology and Bioinformatics. Genome Biology 5 (10): R80.

Gunnell, Jennifer, et al. "Acute-phase response predicts erythropoietin resistance in hemodialysis and peritoneal dialysis patients." American journal of kidney diseases 33.1 (1999): 63-72.

Guo Y, Zhao S, Li CI, Sheng Q, Shyr Y. (2014) RNAseqPS: A Web Tool for Estimating Sample Size and Power for RNAseq Experiment. Cancer Inform. 13(Suppl 6):1-5

Krämer A, Green J, Pollard Jr J, Tugendreich S. Causal analysis approaches in ingenuity pathway analysis. Bioinformatics. 2013 Dec 13;30(4):523-30.

LOVE, M. I., W. HUBER and S. ANDERS, 2014 Moderated estimation of fold change and dispersion for RNA-seq data with DESeq2. bioRxiv.

R Core Team (2012). R: A language and environment for statistical computing. R Foundation for statistical computing, Vienna, Austria. ISBN 3-900051-07-0, URL http://www.R-project.org/)

Sordi R, Nandra KK, Chiazza F, Johnson FL, Cabrera CP, Torrance HD, Yamada N, Patel NS, Barnes MR, Brohi K, Collino M. Thiemerman, C. Artesunate protects against the organ injury and dysfunction induced by severe hemorrhage and resuscitation. Annals of surgery. 2017 Feb 1;265(2):408-17.

Xiao W, Mindrinos MN, Seok J, Cuschieri J, Cuenca AG, Gao H, Hayden DL, Hennessy L, Moore EE, Minei JP, Bankey PE. A genomic storm in critically injured humans. Journal of Experimental Medicine. 2011 Dec 19;208(13):2581-90.

6. APPENDIX

APPENDIX 1- Sample Indentifiers

SampleID	Subject	Type	IndDM	Group	Treatment	Injury	Batch	Type_Group
ES72_SURG	ES72	SURG	12	Gp3	Simvastatin	Yes	1	SURG_Gp3
ES76_SURG	ES76	SURG	2	Gp4	Placebo	Blast	1	SURG_Gp4
ES77_SURG	ES77	SURG	3	Gp1	Control	No	1	SURG_Gp1
ES81_SURG	ES81	SURG	3	Gp5	Simvastatin	Blast	1	SURG_Gp5
ES82_SURG	ES82	SURG	13	Gp3	Simvastatin	Yes	1	SURG_Gp3
ES83_SURG	ES83	SURG	4	Gp5	Simvastatin	Blast	1	SURG_Gp5
ES84_SURG	ES84	SURG	14	Gp3	Simvastatin	Yes	1	SURG_Gp3
ES86_SURG	ES86	SURG	12	Gp2	Placebo	Yes	1	SURG_Gp2
ES87_SURG	ES87	SURG	3	Gp4	Placebo	Blast	1	SURG_Gp4
ES88_SURG	ES88	SURG	13	Gp2	Placebo	Yes	1	SURG_Gp2
ES90_PM	ES90	PM	5	Gp5	Simvastatin	Blast	1	PM_Gp5
ES95_PM	ES95	PM	6	Gp5	Simvastatin	Blast	1	PM_Gp5
ES100_PM	ES100	PM	1	Gp3	Simvastatin	Yes	1	PM_Gp3
ES104_PM	ES104	PM	1	Gp2	Placebo	Yes	1	PM_Gp2
ES116_PM	ES116	PM	2	Gp2	Placebo	Yes	1	PM_Gp2
ES120_PM	ES120	PM	3	Gp2	Placebo	Yes	1	PM_Gp2
ES122_PM	ES122	PM	1	Gp5	Simvastatin	Blast	1	PM_Gp5
ES123_PM	ES123	PM	2	Gp5	Simvastatin	Blast	1	PM_Gp5
ES125_PM	ES125	PM	1	Gp4	Placebo	Blast	1	PM_Gp4
ES126_PM	ES126	PM	2	Gp3	Simvastatin	Yes	1	PM_Gp3
ES127_PM	ES127	PM	3	Gp3	Simvastatin	Yes	1	PM_Gp3
ES90_SURG	ES90	SURG	5	Gp5	Simvastatin	Blast	1	SURG_Gp5
ES95_SURG	ES95	SURG	6	Gp5	Simvastatin	Blast	1	SURG_Gp5
ES100_SURG	ES100	SURG	1	Gp3	Simvastatin	Yes	1	SURG_Gp3
ES104_SURG	ES104	SURG	1	Gp2	Placebo	Yes	1	SURG_Gp2
ES116_SURG	ES116	SURG	2	Gp2	Placebo	Yes	1	SURG_Gp2
ES120_SURG	ES120	SURG	3	Gp2	Placebo	Yes	1	SURG_Gp2
ES122_SURG	ES122	SURG	1	Gp5	Simvastatin	Blast	1	SURG_Gp5
ES123_SURG	ES123	SURG	2	Gp5	Simvastatin	Blast	1	SURG_Gp5
ES125_SURG	ES125	SURG	1	Gp4	Placebo	Blast	1	SURG_Gp4
ES126_SURG	ES126	SURG	2	Gp3	Simvastatin	Yes	1	SURG_Gp3
ES127_SURG	ES127	SURG	3	Gp3	Simvastatin	Yes	1	SURG_Gp3
ES72_PM	ES72	PM	12	Gp3	Simvastatin	Yes	1	PM_Gp3
ES76_PM	ES76	PM	2	Gp4	Placebo	Blast	1	PM_Gp4
ES77_PM	ES77	PM	3	Gp1	Control	No	1	PM_Gp1
ES81_PM	ES81	PM	3	Gp5	Simvastatin	Blast	1	PM_Gp5
ES82_PM	ES82	PM	13	Gp3	Simvastatin	Yes	1	PM_Gp3
ES83_PM	ES83	PM	4	Gp5	Simvastatin	Blast	1	PM_Gp5
ES84_PM	ES84	PM	14	Gp3	Simvastatin	Yes	1	PM_Gp3
ES86_PM	ES86	PM	12	Gp2	Placebo	Yes	1	PM_Gp2
ES87_PM	ES87	PM	3	Gp4	Placebo	Blast	1	PM_Gp4
ES88_PM	ES88	PM	13	Gp2	Placebo	Yes	1	PM_Gp2
ES128_PM	ES128	PM	1	Gp1	Control	No	2	PM_Gp1
ES128_SURG	ES128	SURG	1	Gp1	Control	No	2	SURG_Gp1
ES129_PM	ES129	PM	2	Gp1	Control	No	2	PM_Gp1
ES129_SURG	ES129	SURG	2	Gp1	Control	No	2	SURG_Gp1
ES131_PM	ES131	PM	4	Gp3	Simvastatin	Yes	2	PM_Gp3
ES131_SURG	ES131	SURG	4	Gp3	Simvastatin	Yes	2	SURG_Gp3
ES133_PM	ES133	PM	5	Gp3	Simvastatin	Yes	2	PM_Gp3
ES133_SURG	ES133	SURG	5	Gp3	Simvastatin	Yes	2	SURG_Gp3
ES135_PM	ES135	PM	4	Gp2	Placebo	Yes	2	PM_Gp2
ES135_SURG	ES135	SURG	4	Gp2	Placebo	Yes	2	SURG_Gp2
ES137_PM	ES137	PM	5	Gp2	Placebo	Yes	2	PM_Gp2
ES137_SURG	ES137	SURG	5	Gp2	Placebo	Yes	2	SURG_Gp2
ES138_PM	ES138	PM	6	Gp2	Placebo	Yes	2	PM_Gp2
ES138_SURG	ES138	SURG	6	Gp2	Placebo	Yes	2	SURG_Gp2
ES139_PM	ES139	PM	6	Gp3	Simvastatin	Yes	2	PM_Gp3
ES139_SURG	ES139	SURG	6	Gp3	Simvastatin	Yes	2	SURG_Gp3
ES141_PM	ES141	PM	7	Gp2	Placebo	Yes	2	PM_Gp2
ES141_SURG	ES141	SURG	7	Gp2	Placebo	Yes	2	SURG_Gp2
ES142_PM	ES142	PM	7	Gp3	Simvastatin	Yes	2	PM_Gp3
ES142_SURG	ES142	SURG	7	Gp3	Simvastatin	Yes	2	SURG_Gp3
ES143_PM	ES143	PM	8	Gp3	Simvastatin	Yes	2	PM_Gp3
ES143_SURG	ES143	SURG	8	Gp3	Simvastatin	Yes	2	SURG_Gp3
ES147_PM	ES147	PM	9	Gp3	Simvastatin	Yes	2	PM_Gp3
ES147_SURG	ES147	SURG	9	Gp3	Simvastatin	Yes	2	SURG_Gp3
ES148_PM	ES148	PM	8	Gp2	Placebo	Yes	2	PM_Gp2
ES148_SURG	ES148	SURG	8	Gp2	Placebo	Yes	2	SURG_Gp2
ES149_PM	ES149	PM	9	Gp2	Placebo	Yes	2	PM_Gp2
ES149_SURG	ES149	SURG	9	Gp2	Placebo	Yes	2	SURG_Gp2
ES150_PM	ES150	PM	10	Gp3	Simvastatin	Yes	2	PM_Gp3
ES150_SURG	ES150	SURG	10	Gp3	Simvastatin	Yes	2	SURG_Gp3
ES151_PM	ES151	PM	11	Gp3	Simvastatin	Yes	2	PM_Gp3
ES151_SURG	ES151	SURG	11	Gp3	Simvastatin	Yes	2	SURG_Gp3
ES153_PM	ES153	PM	10	Gp2	Placebo	Yes	2	PM_Gp2
ES153_SURG	ES153	SURG	10	Gp2	Placebo	Yes	2	SURG_Gp2
ES154_PM	ES154	PM	11	Gp2	Placebo	Yes	2	PM_Gp2
ES154_SURG	ES154	SURG	11	Gp2	Placebo	Yes	2	SURG_Gp2

APPENDIX 2 – Sample RNA extraction

Sample ID	Conc (ng/µl)	RIN	A260	A280	A260/ 280	A260/ 230	Conc. Factor (ng/ul)	Cursor Pos.	Cursor abs.	340 raw	NA Type
ES72 SURG	243.2	8.5	6.081	2.87	2.12	1.44	40	260	6.063	0.107	RNA-40
ES76 SURG	291.8	8.4	7.295	3.505	2.08	1.6	40	260	7.273	0.053	RNA-40
ES77 SURG	339.3	8.5	8.483	4.086	2.08	1.64	40	260	8.463	0.222	RNA-40
ES81 SURG	263.6	8.2	6.589	3.134	2.1	1.46	40	260	6.571	-0.02	RNA-40
ES82 SURG	148.2	8.7	3.704	1.757	2.11	1.23	40	260	3.695	0.118	RNA-40
ES83 SURG	325.1	8.3	8.127	3.863	2.1	1.79	40	260	8.108	0.064	RNA-40
ES84 SURG	172.4	8.9	4.31	2.041	2.11	1.57	40	260	4.299	0.054	RNA-40
ES86 SURG	209.8	8.3	5.246	2.482	2.11	1.82	40	260	5.232	0.035	RNA-40
ES87 SURG	230.3	9	5.759	2.697	2.14	0.77	40	260	5.74	0.07	RNA-40
ES88 SURG	214.7	9.7	5.368	2.561	2.1	1.31	40	260	5.353	0.018	RNA-40
ES90 SURG	282.8	8.3	7.069	3.386	2.09	1.53	40	260	7.053	0.174	RNA-40
ES95 SURG	497.7	7.8	12.442	6.07	2.05	1.87	40	260	12.408	0.037	RNA-40
ES100 SURG	245.4	8.6	6.135	2.909	2.11	1.51	40	260	6.119	0.062	RNA-40
ES104 SURG	24.74	6.5	0.618	0.287	2.15	0.66	40	260	0.618	0.037	RNA-40
ES116 SURG	267.5	7.8	6.686	3.196	2.09	1.71	40	260	6.671	0.19	RNA-40
ES120 SURG	226	7.6	5.651	2.695	2.1	1.79	40	260	5.633	0.019	RNA-40
ES122 SURG	475.7	7.3	11.893	5.799	2.05	1.76	40	260	11.861	0.064	RNA-40
ES123 SURG	359.4	7.6	8.984	4.344	2.07	1.65	40	260	8.962	0.054	RNA-40
ES125 SURG	252.6	8.3	6.315	3.016	2.09	1.65	40	260	6.297	0.183	RNA-40
ES126 SURG	286.2	7.4	7.155	3.377	2.12	1.2	40	260	7.139	-0.04	RNA-40
ES127 SURG	266.6	7.8	6.665	3.146	2.12	1.23	40	260	6.648	0.056	RNA-40
ES72 PM	8.678	8.7	0.217	0.102	2.13	0.48	40	260	0.218	0.059	RNA-40
ES76 PM	40.67	9	1.017	0.48	2.12	0.8	40	260	1.013	-0.029	RNA-40
ES77 PM	96.86	8.7	2.422	1.143	2.12	1.17	40	260	2.413	0.112	RNA-40
ES81 PM	83.42	8.9	2.085	0.958	2.18	0.71	40	260	2.078	0.079	RNA-40
ES82 PM	27.12	?	0.678	0.327	2.07	0.37	40	260	0.674	-0.004	RNA-40
ES83 PM	26.13	8.9	0.653	0.299	2.18	0.22	40	260	0.648	0.095	RNA-40
ES84 PM	55.47	9.1	1.387	0.648	2.14	0.32	40	260	1.381	-0.019	RNA-40
ES86 PM	90.3	9	2.257	1.039	2.17	0.25	40	260	2.249	0.035	RNA-40
ES87 PM	10.94	9	0.273	0.117	2.33	0.04	40	260	0.272	0.044	RNA-40
ES88 PM	114.5	9	2.862	1.364	2.1	1.44	40	260	2.854	-0.014	RNA-40
ES90 PM	27.59	9	0.69	0.329	2.09	1.31	40	260	0.687	0.036	RNA-40
ES95 PM	332.6	9	8.316	3.947	2.11	0.96	40	260	8.293	0.049	RNA-40
ES100 PM	29.8	8.9	0.745	0.354	2.1	0.52	40	260	0.741	0.009	RNA-40
ES104 PM	6.006	9.1	0.15	0.067	2.26	0.14	40	260	0.147	0.07	RNA-40
ES116 PM	77.62	8.8	1.94	0.933	2.08	0.94	40	260	1.932	0.029	RNA-40
ES120 PM	102.1	8.5	2.554	1.203	2.12	1.34	40	260	2.547	0.058	RNA-40
ES122 PM	30.1	?	0.753	0.351	2.14	0.62	40	260	0.749	0.033	RNA-40
ES123 PM	72.98	8.9	1.825	0.865	2.11	0.87	40	260	1.82	-0.019	RNA-40
ES125 PM	117.9	8.8	2.948	1.411	2.09	1.72	40	260	2.94	0.045	RNA-40
ES126 PM	92.17	9.1	2.304	1.105	2.08	1.9	40	260	2.299	0.005	RNA-40
ES127 PM	79.59	8.3	1.99	0.97	2.05	1.57	40	260	1.984	-0.037	RNA-40

Notes

Total RNA samples were quantified by micro volume UV-Vis spectrophotometry (Instrument/kit?) and assessed for quality by electrophoresis (Instrument/kit?).


Euk Total RNA Nano1.pdf


Euk Total RNA Nano2.pdf


Euk Total RNA Nano3.pdf


Euk Total RNA Pico1.pdf

Samples ES72 PM, ES87 PM, ES104 PM all had quite a low yield, but a yield that would support the sequencing analysis. A low yield requires the input of more sample for RNA library preparation, which requires 100ng minimum. Samples sequenced from libraries with low RNA input were adjusted during the data normalisation process prior to analysis.

The RNA Integrity Number (RIN) is used as a standard measure of sample quality, with a score of 8 or over being defined by the manufacturer as the recommended limit for sequencing kit use. Based upon in-house experience routinely using samples of RIN 7.5 and having successfully prepared libraries with a RIN as low as 6.8, it was agreed to proceed as planned with the all samples including those that did not reach this requirement (e.g. ES104 SURG, ES122 SURG and ES126 SURG).

For ES104 SURG the sample was much clotted and therefore hard to re-suspend and in sample ES72 PM the white blood cell pellet was not visible. These may be reasons why the quality of these samples does not appear as good as the general set.

APPENDIX 3. NGS Transcript abundance quantification

```
kallisto quant -i Rattus_norvegicus.Rnor_6.0.cdna.all.fa_index –o ES72_SURG 1-
ES72-SURG_S4_L001_R1_001.fastq.gz 1-ES72-SURG_S4_L001_R2_001.fastq.gz 1-ES72-
SURG_S4_L002_R1_001.fastq.gz 1-ES72-SURG_S4_L002_R2_001.fastq.gz 1-ES72-
SURG_S4_L003_R1_001.fastq.gz 1-ES72-SURG_S4_L003_R2_001.fastq.gz 1-ES72-
SURG_S4_L004_R1_001.fastq.gz 1-ES72-SURG_S4_L004_R2_001.fastq.gz -t 12
```

APPENDIX 4. R Analyses

APPENDIX 4.1 R Environment setup

R environment setup for exploratory and differential expression analyses

```
# R environment setup
library(data.table)
library(tximport)
library(rhdf5)
```

```
library(pheatmap)
library(vsn)
library(RColorBrewer)
library(ggplot2)
library(gridExtra)
library(DESeq2)

> sessionInfo()
R version 3.5.0 (2018-04-23)
Platform: x86_64-w64-mingw32/x64 (64-bit)
Running under: Windows 8.1 x64 (build 9600)
Matrix products: default
locale:
[1] LC_COLLATE=English_United Kingdom.1252  LC_CTYPE=English_United Kingdom.1252
[3] LC_MONETARY=English_United Kingdom.1252 LC_NUMERIC=C
[5] LC_TIME=English_United Kingdom.1252
attached base packages:
[1] parallel  stats4    stats     graphics  grDevices utils     datasets  methods   base
other attached packages:
 [1] hexbin_1.27.2               gridExtra_2.3               ggplot2_2.2.1
 [4] RColorBrewer_1.1-2          vsn_3.48.1                  pheatmap_1.0.10
 [7] rhdf5_2.24.0                tximport_1.8.0              data.table_1.11.4
[10] DESeq2_1.20.0               SummarizedExperiment_1.10.1 DelayedArray_0.6.0
[13] BiocParallel_1.14.1         matrixStats_0.53.1          Biobase_2.40.0
[16] GenomicRanges_1.32.3        GenomeInfoDb_1.16.0         IRanges_2.14.10
[19] S4Vectors_0.18.2            BiocGenerics_0.26.0
loaded via a namespace (and not attached):
 [1] bit64_0.9-7            splines_3.5.0          Formula_1.2-3          affy_1.58.0
 [5] latticeExtra_0.6-28    blob_1.1.1             GenomeInfoDbData_1.1.0 pillar_1.2.3
 [9] RSQLite_2.1.1          backports_1.1.2        lattice_0.20-35        limma_3.36.1
[13] digest_0.6.15          XVector_0.20.0         checkmate_1.8.5        colorspace_1.3-2
[17] htmltools_0.3.6        preprocessCore_1.42.0  Matrix_1.2-14          plyr_1.8.4
[21] XML_3.98-1.11          genefilter_1.62.0      zlibbioc_1.26.0        xtable_1.8-2
[25] scales_0.5.0           affyio_1.50.0          htmlTable_1.12         tibble_1.4.2
[29] annotate_1.58.0        nnet_7.3-12            lazyeval_0.2.1         survival_2.41-3
[33] magrittr_1.5           memoise_1.1.0          foreign_0.8-70
BiocInstaller_1.30.0
[37] tools_3.5.0            stringr_1.3.1          Rhdf5lib_1.2.1         munsell_0.4.3
[41] locfit_1.5-9.1         cluster_2.0.7-1        AnnotationDbi_1.42.1   compiler_3.5.0
[45] rlang_0.2.1            grid_3.5.0             RCurl_1.95-4.10        rstudioapi_0.7
[49] htmlwidgets_1.2        labeling_0.3           bitops_1.0-6           base64enc_0.1-3
[53] gtable_0.2.0           DBI_1.0.0              knitr_1.20             bit_1.1-14
[57] Hmisc_4.1-1            stringi_1.1.7          Rcpp_0.12.17
geneplotter_1.58.0
[61] rpart_4.1-13           acepack_1.4.1

# Read Sample file in
samplefile <- fread("SampleFile.txt")
       > samplefile[1:3,]
          Subject SampleNumber       Dir            Folder  SampleID Subject Type IndDM
       Group
       1:    ES72            1 QuantKal ES72_SURG-25803893 ES72_SURG    ES72 SURG    12
       Gp3
       2:    ES76            2 QuantKal ES76_SURG-25803894 ES76_SURG    ES76 SURG     2
       Gp4
       3:    ES77            3 QuantKal ES77_SURG-25803895 ES77_SURG    ES77 SURG     3
       Gp1
            Treatment Injury Batch Type_Group
       1: Simvastatin    Yes     1   SURG_Gp3
       2:     Placebo  Blast     1   SURG_Gp4
       3:     Control     No     1   SURG_Gp1

# create object with files to read
files <- file.path(samplefile$Dir,samplefile$Folder,"abundance.h5")
names(files) <- samplefile$SampleID
# Read GTF
```

```
t2g_GTF <- fread("trx2gns_Ratv6.txt",header=FALSE)
       > t2g_GTF[1:3,]
                       V1                 V2            V3
       1: ENSRNOT00000000008.4 ENSRNOG00000000007          Gad1
       2: ENSRNOT00000000009.5 ENSRNOG00000000008          Alx4
       3: ENSRNOT00000000010.5 ENSRNOG00000000009         Tmco5b
# Subset table to take gene names for analysis
t2g_2clsGTF <- t2g_GTF[,c(1,3)]
       > t2g_2clsGTF[1:3,]
                      V1     V3
       1: ENSRNOT00000000008.4   Gad1
       2: ENSRNOT00000000009.5   Alx4
       3: ENSRNOT00000000010.5 Tmco5b

# Import gene counts
txi_GTF <- tximport(files, type = 'kallisto', tx2gene = t2g_2clsGTF, importer = fread,
countsFromAbundance = 'lengthScaledTPM')

# Convert to data frame and re-class columns to factors
samplefileDF <- as.data.frame(samplefile)
samplefileDF$Type <- as.factor(as.character(samplefileDF$Type))
samplefileDF$IndDM <- as.factor(as.character(samplefileDF$IndDM))
samplefileDF$Group <- as.factor(as.character(samplefileDF$Group))
samplefileDF$Treatment <- as.factor(as.character(samplefileDF$Treatment))
samplefileDF$Injury <- as.factor(as.character(samplefileDF$Injury))
samplefileDF$Batch <- as.factor(as.character(samplefileDF$Batch))
samplefileDF$Type_Group <- as.factor(as.character(samplefileDF$Type_Group))

# set reference levels
samplefileDF$Type <- relevel(samplefileDF$Type,"SURG")
samplefileDF$Group <- relevel(samplefileDF$Group,"Gp2")
samplefileDF$Treatment <- relevel(samplefileDF$Treatment,"Placebo")
samplefileDF$Injury <- relevel(samplefileDF$Injury,"Yes")
samplefileDF$Type_Group <- relevel(samplefileDF$Type_Group,"SURG_Gp2")
> summary(samplefileDF)
  SampleNumber       Dir               Folder            SampleID           Subject
 Min.   : 1.00   Length:78          Length:78          Length:78          Length:78
 1st Qu.:20.25   Class :character   Class :character   Class :character   Class :character
 Median :39.50   Mode  :character   Mode  :character   Mode  :character   Mode  :character
 Mean   :39.50
 3rd Qu.:58.75
 Max.   :78.00

   Type        IndDM    Group          Treatment    Injury   Batch     Type_Group
 SURG:39   1      :10   Gp2:26   Placebo    :32   Yes  :54   1:42   PM_Gp3  :14
 PM  :39   2      :10   Gp1: 6   Control    : 6   Blast:18   2:36   SURG_Gp3:14
           3      :10   Gp3:28   Simvastatin:40   No   : 6          SURG_Gp2:13
           4      : 6   Gp4: 6                                      PM_Gp2  :13
           5      : 6   Gp5:12                                      PM_Gp5  : 6
           6      : 6                                               SURG_Gp5: 6
           (Other):30                                               (Other) :12



# Setup subsets
SURG_Gp1 <- which(samplefileDF$Type_Group== "SURG_Gp1")
SURG_Gp1 <- which(samplefileDF$Type_Group == "SURG_Gp1")
SURG_Gp2 <- which(samplefileDF$Type_Group == "SURG_Gp2")
SURG_Gp3 <- which(samplefileDF$Type_Group == "SURG_Gp3")
SURG_Gp4 <- which(samplefileDF$Type_Group == "SURG_Gp4")
SURG_Gp5 <- which(samplefileDF$Type_Group == "SURG_Gp5")
PM_Gp1 <- which(samplefileDF$Type_Group == "PM_Gp1")
PM_Gp2 <- which(samplefileDF$Type_Group == "PM_Gp2")
PM_Gp3 <- which(samplefileDF$Type_Group == "PM_Gp3")
PM_Gp4 <- which(samplefileDF$Type_Group == "PM_Gp4")
PM_Gp5 <- which(samplefileDF$Type_Group == "PM_Gp5")
```

```
# Contruct DESeqDataSet
ddsTxi <- DESeqDataSetFromTximport(txi_GTF,colData = samplefileDF,design = ~ Batch + IndDM
+ Type_Group)

# remove genes with less than 10 counts
dds <- ddsTxi[ rowSums( counts(ddsTxi) ) > 10 , ]
       > dim(dds)
       [1] 16915    78

# Sample numbers
       > samplefile[,.N,by=Type]
          Type  N
       1: SURG 39
       2:   PM 39

       > samplefile[,.N,by=Treatment]
              Treatment  N
       1: Simvastatin 40
       2:     Placebo 32
       3:     Control  6

       > samplefile[,.N,by=Type_Group]
             Type_Group  N
        1:   SURG_Gp3 14
        2:   SURG_Gp4  3
        3:   SURG_Gp1  3
        4:   SURG_Gp5  6
        5:   SURG_Gp2 13
        6:     PM_Gp5  6
        7:     PM_Gp3 14
        8:     PM_Gp2 13
        9:     PM_Gp4  3
       10:     PM_Gp1  3
# RAW COUNTS
counts <- counts(dds)
```

APPENDIX 4.2 R Exploratory analysis

```
# Data transformations
# ntd: Normalized counts transformation (Shifted logarithm transformation)
# vst: variance stabilizing transformation
# rld: regularized log transformation

ntd <- normTransform(dds)
vsd <- vst(dds)
rld <- rlog(dds)

# Counts
# Raw counts
counts <- counts(dds)
# VST Normalized counts
counts_vsd <- assays(vsd)[[1]]

# Exploratory analysis plots

# Counts boxplots
png(file="CountsDist_VSD.png",width=900,height=400)
par(mar=c(8,3,1,1),las=2)
boxplot(assays(vsd)[[1]],main="Counts VSD")
dev.off()
png(file="CountsDist_RLD.png",width=900,height=400)
par(mar=c(8,3,1,1),las=2)
boxplot(assays(rld)[[1]],main="Counts RLD")
dev.off()

# Standard Deviation of Transformed data
mean_ntd <- meanSdPlot(assay(ntd))
mean_vsd <- meanSdPlot(assay(vsd))
mean_rld <- meanSdPlot(assay(rld))

# Mean SD plot VSD
png(file="MeanSD_VSD.png",width=800,height=800)
mean_vsd <- meanSdPlot(assay(vsd))
dev.off()

# Grid plot of standard deviation from mean
png(file="MeanSD.png",width=3200,height=1200)
grid.arrange(mean_ntd$gg + ggtitle("Normalized Counts")+ theme(plot.title =
element_text(hjust = 0.5,size=40),axis.text=element_text(size=20)),
                     mean_vsd$gg + ggtitle("Variance Stabilizing") +
theme(plot.title = element_text(hjust =
0.5,size=40),axis.text=element_text(size=20)),
                     mean_rld$gg + ggtitle("Regularized Log") + theme(plot.title
= element_text(hjust = 0.5,size=40),axis.text=element_text(size=20)), nrow = 1)
dev.off()

# Heatmap of sample to sample distance
# VSD heatmap
sampleDists <- dist(t(assay(vsd)))
sampleDistMatrix <- as.matrix(sampleDists)
rownames(sampleDistMatrix) <- paste(vsd$SampleID, vsd$Batch,sep="-")
#rownames(sampleDistMatrix) <- vsd$SampleID
colnames(sampleDistMatrix) <- NULL
colors <- colorRampPalette( rev(brewer.pal(9, "Blues")) )(255)
png(file="AllSamples_HM_VSD.png",width=800,height=800)
```

```
pheatmap(sampleDistMatrix,clustering_distance_rows=sampleDists,clustering_distan
ce_cols=sampleDists,col=colors)
dev.off()

# RLD heatmap
sampleDists <- dist(t(assay(rld)))
sampleDistMatrix <- as.matrix(sampleDists)
rownames(sampleDistMatrix) <- paste(rld$SampleID, rld$Batch,sep="-")
colnames(sampleDistMatrix) <- NULL
colors <- colorRampPalette( rev(brewer.pal(9, "Blues")) )(255)
png(file="AllSamples_HM_RLD.png",width=800,height=800)
pheatmap(sampleDistMatrix,clustering_distance_rows=sampleDists,clustering_distan
ce_cols=sampleDists,col=colors)
dev.off()

# Possible outliers
ES72-SURG-1
ES86-SURG-1
ES120-SURG-1
ES149-PM-2
ES86-PM-1

# PCA plots

#RLD
png(file="PCA_RLD.png",width=800,height=800)
plt <-  plotPCA (rld,  intgroup ="Type",  returnData = TRUE )
percentVar <- round ( 100 * attr (plt,"percentVar" ))
ggplot (plt,aes(PC1,PC2,color=Type))+geom_point(size=5)+ xlab(paste0 ( "PC1: "
,percentVar[ 1 ], "% variance" ))  + ylab ( paste0 ( "PC2: " ,percentVar[ 2 ],
"% variance" ))+ theme(text = element_text(size=16))
dev.off()

png(file="AllSamples_TypGP_Batch_PCA_RLD.png",width=800,height=800)
plt <-  plotPCA (rld,  intgroup =c("Type_Group","Batch"),  returnData = TRUE )
percentVar <- round ( 100 * attr (plt,"percentVar" ))
ggplot (plt,aes(PC1,PC2,color=Type_Group,shape=Batch))+geom_point(size=5)+
xlab(paste0 ( "PC1: " ,percentVar[ 1 ], "% variance" ))  + ylab ( paste0 ( "PC2:
" ,percentVar[ 2 ], "% variance" ))+ theme(text = element_text(size=16))
dev.off()

# OUTLIER
      > plt
                          PC1         PC2 group Type       name
      ES72_SURG  -219.2575791  25.1176619  SURG SURG  ES72_SURG

#VSD
png(file="AllSamples_PCA_VSD.png",width=800,height=800)
plt <-  plotPCA (vsd,  intgroup ="Type",  returnData = TRUE )
percentVar <- round ( 100 * attr (plt,"percentVar" ))
ggplot (plt,aes(PC1,PC2,color=Type))+geom_point(size=5)+ xlab(paste0 ( "PC1: "
,percentVar[ 1 ], "% variance" ))  + ylab ( paste0 ( "PC2: " ,percentVar[ 2 ],
"% variance" ))+ theme(text = element_text(size=16))
dev.off()

png(file="AllSamples_PCA_Typ_Batch_VSD.png",width=800,height=800)
plt <-  plotPCA (vsd,  intgroup =c("Type_Group","Batch"),  returnData = TRUE )
percentVar <- round ( 100 * attr (plt,"percentVar" ))
```

```
ggplot (plt,aes(PC1,PC2,color=Type_Group,shape=Batch))+geom_point(size=5)+
xlab(paste0 ( "PC1: " ,percentVar[ 1 ], "% variance" ))  + ylab ( paste0 ( "PC2:
" ,percentVar[ 2 ], "% variance" ))+ theme(text = element_text(size=16))
dev.off()
#OUTLIERS
> plt
                      PC1        PC2    group     Type_Group      name
       ES72_SURG  -19.345773  47.525827 SURG_Gp3   SURG_Gp3  ES72_SURG

> plt[which(plt[,3]=="PM_Gp2:1"),]
ES86_PM  -4.099505 17.409432 PM_Gp2:1     PM_Gp2     1  ES86_PM

# Exploratory analysis removing batch effect

# Remove Batch effect from data
vsd_btcor <- vsd
assay(vsd_btcor) <- limma::removeBatchEffect(assay(vsd_btcor), vsd_btcor$Batch)

# Counts boxplots
png(file="CountsDist_VSD_BatchCor.png",width=900,height=400)
par(mar=c(8,3,1,1),las=2)
boxplot(assays(vsd_btcor)[[1]],main="Counts VSD")
dev.off()

# Standard Deviation of VSD Transformed data
png(file="MeanSD_VSD btcor.png",width=800,height=800)
mean_vsd_btcor <- meanSdPlot(assay(vsd_btcor))
dev.off()

# Heatmap sample to sample distance
sampleDists <- dist(t(assay(vsd_btcor)))
sampleDistMatrix <- as.matrix(sampleDists)
rownames(sampleDistMatrix) <- paste(vsd_btcor$SampleID, vsd_btcor$Batch,sep="-")
#rownames(sampleDistMatrix) <- vsd_btcor$SampleID
colnames(sampleDistMatrix) <- NULL
colors <- colorRampPalette( rev(brewer.pal(9, "Blues")) )(255)
png(file="AllSamples_HM_VSD_BatchCor.png",width=800,height=800)
pheatmap(sampleDistMatrix,clustering_distance_rows=sampleDists,clustering_distan
ce_cols=sampleDists,col=colors)
dev.off()

# PCA
png(file="AllSamples_PCA_VSD_BatchCor.png",width=800,height=800)
plt <-  plotPCA (vsd_btcor,  intgroup ="Type",  returnData = TRUE )
percentVar <- round ( 100 * attr (plt,"percentVar" ))
ggplot (plt,aes(PC1,PC2,color=Type))+geom_point(size=5)+ xlab(paste0 ( "PC1: "
,percentVar[ 1 ], "% variance" ))  + ylab ( paste0 ( "PC2: " ,percentVar[ 2 ],
"% variance" ))+ theme(text = element_text(size=16))
dev.off()

png(file="AllSamples_PCA_Typ_Batch_VSD_BatchCor.png",width=800,height=800)
plt <-  plotPCA (vsd_btcor,  intgroup =c("Type_Group","Batch"),  returnData =
TRUE )
percentVar <- round ( 100 * attr (plt,"percentVar" ))
ggplot (plt,aes(PC1,PC2,color=Type_Group,shape=Batch))+geom_point(size=5)+
xlab(paste0 ( "PC1: " ,percentVar[ 1 ], "% variance" ))  + ylab ( paste0 ( "PC2:
" ,percentVar[ 2 ], "% variance" ))+ theme(text = element_text(size=16))
dev.off()
```

```
png(file="AllSamples_PCA_Typ_Group_VSD_BatchCor.png",width=800,height=800)
plt <-  plotPCA (vsd_btcor,  intgroup =c("Type","Group"),  returnData = TRUE )
percentVar <- round ( 100 * attr (plt,"percentVar" ))
ggplot (plt,aes(PC1,PC2,color=Type,shape=Group))+geom_point(size=5)+ xlab(paste0
( "PC1: " ,percentVar[ 1 ], "% variance" ))  + ylab ( paste0 ( "PC2: "
,percentVar[ 2 ], "% variance" ))+ theme(text = element_text(size=16))
dev.off()

# Exploratory analysis of batch effects removed and outlier samples removed

# Exclude samples identified
# ES86_PM
# ES86_SURG
# ES120 SURG
# ES72 SURG
# ES149 PM
SF <- samplefileDF
rem <-
sort(c(which(SF$SampleID=="ES86_SURG"),which(SF$SampleID=="ES86_PM"),which(SF$Sa
mpleID=="ES120_SURG"),which(SF$SampleID=="ES149_PM"),which(SF$SampleID=="ES72_SU
RG")))
SF <- SF[-rem,]
#select samples
files_exsams <- file.path(SF$Dir,SF$Folder,"abundance.h5")
names(files_exsams) <- SF$SampleID
# Drop Levels
SF$Type <- droplevels(SF$Type)
SF$IndDM <- droplevels(SF$IndDM)
SF$Group <- droplevels(SF$Group)
SF$Type_Group <- droplevels(SF$Type_Group)

# Import and get counts
txi_GTF_exsams <- tximport(files_exsams, type = 'kallisto', tx2gene =
t2g_2clsGTF, importer = fread, countsFromAbundance = 'lengthScaledTPM')

ddsTxi_exsams <- DESeqDataSetFromTximport(txi_GTF_exsams,colData = SF,design = ~
Batch + Type_Group)

# Remove genes with less than 10 counts
dds_exsams <- ddsTxi_exsams[ rowSums( counts(ddsTxi_exsams) ) > 10 , ]

# counts excluding samples
counts_exsams <- counts(dds_exsams)

# VSD Transformation
vsd_exsams <- vst(dds_exsams)
counts_vsd_exsams <- assays(vsd_exsams)[[1]]

# Rermove batch effect
vsd_exsams_btcor <- vsd_exsams
assay(vsd_exsams_btcor) <- limma::removeBatchEffect(assay(vsd_exsams_btcor),
vsd_exsams_btcor$Batch)
# VSD transformed counts after batch effect
counts_vsd_exsams_btcor <- assays(vsd_exsams_btcor)[[1]]

# Batch and outlier removed : plots
# Counts boxplots
png(file="CountsDist_VSD_exSams_BatchCor.png",width=900,height=400)
par(mar=c(8,3,1,1),las=2)
```

```
boxplot(assays(vsd_exsams_btcor)[[1]],main="Counts VSD")
dev.off()

# Effects of transformations on the variance
png(file="MeanSD_VSD_exSams_btcor.png",width=800,height=800)
mean_vsd_exsams_btcor <- meanSdPlot(assay(vsd_exsams_btcor))
dev.off()

# Heatmap VSD
sampleDists <- dist(t(assay(vsd_exsams_btcor)))
sampleDistMatrix <- as.matrix(sampleDists)
rownames(sampleDistMatrix) <- paste(vsd_exsams_btcor$SampleID,
vsd_exsams_btcor$Batch,sep="-")
colnames(sampleDistMatrix) <- NULL
colors <- colorRampPalette( rev(brewer.pal(9, "Blues")) )(255)
png(file="AllSamples_HM_VSD__exSams_BatchCor.png",width=800,height=800)
pheatmap(sampleDistMatrix,clustering_distance_rows=sampleDists,clustering_distan
ce_cols=sampleDists,col=colors)
dev.off()

# PCA
png(file="AllSamples_PCA_VSD_exSams_BatchCor.png",width=800,height=800)
plt <-  plotPCA (vsd_exsams_btcor,  intgroup ="Type",  returnData = TRUE )
percentVar <- round ( 100 * attr (plt,"percentVar" ))
ggplot (plt,aes(PC1,PC2,color=Type))+geom_point(size=5)+ xlab(paste0 ( "PC1: "
,percentVar[ 1 ], "% variance" ))  + ylab ( paste0 ( "PC2: " ,percentVar[ 2 ],
"% variance" ))+ theme(text = element_text(size=16))
dev.off()

png(file="AllSamples_PCA_Typ_Batch_VSD_exSams_BatchCor.png",width=800,height=800
)
plt <-  plotPCA (vsd_exsams_btcor,  intgroup =c("Type_Group","Batch"),
returnData = TRUE )
percentVar <- round ( 100 * attr (plt,"percentVar" ))
ggplot (plt,aes(PC1,PC2,color=Type_Group,shape=Batch))+geom_point(size=5)+
xlab(paste0 ( "PC1: " ,percentVar[ 1 ], "% variance" ))  + ylab ( paste0 ( "PC2:
" ,percentVar[ 2 ], "% variance" ))+ theme(text = element_text(size=16))
dev.off()

png(file="AllSamples_PCA_Typ_Group_VSD_exSams_BatchCor.png",width=800,height=800
)
plt <-  plotPCA (vsd_exsams_btcor,  intgroup =c("Type","Group"),  returnData =
TRUE )
percentVar <- round ( 100 * attr (plt,"percentVar" ))
ggplot (plt,aes(PC1,PC2,color=Type,shape=Group))+geom_point(size=5)+ xlab(paste0
( "PC1: " ,percentVar[ 1 ], "% variance" ))  + ylab ( paste0 ( "PC2: "
,percentVar[ 2 ], "% variance" ))+ theme(text = element_text(size=16))
dev.off()
```

APPENDIX 4.3 R SURG samples LRT test

```
# First data was setup as in Appendix 4.1 (R environment setup).

# Get subsets
x <- sort(c(SURG_Gp1,SURG_Gp2,SURG_Gp3,SURG_Gp4,SURG_Gp5))

#select samples
SF <- samplefileDF[x,]
files <- file.path(SF$Dir,SF$Folder,"abundance.h5")
names(files) <- SF$SampleID

# Remove outliers
rem <-
sort(c(which(SF$SampleID=="ES86_SURG"),which(SF$SampleID=="ES120_SURG"),which(SF
$SampleID=="ES72_SURG")))
SF <- SF[-rem,]

#select samples
files <- file.path(SF$Dir,SF$Folder,"abundance.h5")
names(files) <- SF$SampleID
# Drop Levels
SF$Type <- droplevels(SF$Type)
SF$IndDM <- droplevels(SF$IndDM)
SF$Group <- droplevels(SF$Group)
SF$Type_Group <- droplevels(SF$Type_Group)

# Import and get counts
txi_GTF <- tximport(files, type = 'kallisto', tx2gene = t2g_2clsGTF, importer =
fread, countsFromAbundance = 'lengthScaledTPM')

ddsTxi <- DESeqDataSetFromTximport(txi_GTF,colData = SF,design = ~ Batch +
Type_Group)

# remove genes with less than 10 counts
dds <- ddsTxi[ rowSums( counts(ddsTxi) ) > 10 , ]
> dim(dds)
[1] 14225    36
> colnames(dds)
 [1] "ES76_SURG"  "ES77_SURG"  "ES81_SURG"  "ES82_SURG"  "ES83_SURG"
"ES84_SURG"  "ES87_SURG"  "ES88_SURG"  "ES90_SURG"  "ES95_SURG"  "ES100_SURG"
[12] "ES104_SURG" "ES116_SURG" "ES122_SURG" "ES123_SURG" "ES125_SURG"
"ES126_SURG" "ES127_SURG" "ES128_SURG" "ES129_SURG" "ES131_SURG" "ES133_SURG"
[23] "ES135_SURG" "ES137_SURG" "ES138_SURG" "ES139_SURG" "ES141_SURG"
"ES142_SURG" "ES143_SURG" "ES147_SURG" "ES148_SURG" "ES149_SURG" "ES150_SURG"
[34] "ES151_SURG" "ES153_SURG" "ES154_SURG"

# Relevel reference
dds$Type_Group <- relevel(dds$Type_Group,"SURG_Gp5")
# Design
> design(dds)
~Batch + Type_Group

# LRT TEST
dds_T21_SURG_LRT <-  DESeq(dds, test = "LRT", reduced = ~ Batch)
       > dds_T21_SURG_LRT <-  DESeq(dds, test = "LRT", reduced = ~ Batch)
       estimating size factors
       estimating dispersions
```

```
       gene-wise dispersion estimates
       mean-dispersion relationship
       final dispersion estimates
       fitting model and testing
       -- replacing outliers and refitting for 83 genes
       -- DESeq argument 'minReplicatesForReplace' = 7
       -- original counts are preserved in counts(dds)
       estimating dispersions
       fitting model and testing

# Results
res_T21_SURG_LRT <- results(dds_T21_SURG_LRT)
res_T21_SURG_LRT <- res_T21_SURG_LRT[order(res_T21_SURG_LRT$padj),]

> summary(res_T21_SURG_LRT)

out of 14222 with nonzero total read count
adjusted p-value < 0.1
LFC > 0 (up)       : 0, 0%
LFC < 0 (down)     : 0, 0%
outliers [1]       : 75, 0.53%
low counts [2]     : 3, 0.021%
(mean count < 0)
[1] see 'cooksCutoff' argument of ?results
[2] see 'independentFiltering' argument of ?results
```

APPENDIX 4.4 R Differential expression analyses between experimental groups

```
# First data was setup as in Appendix 4.1 (R environment setup).

# TEST: T16 SURG CONTROL [gp1] - PM CONTROL [gp1]

# Get subsets
x <- sort(c(SURG_Gp1,PM_Gp1))
#select samples
SF <- samplefileDF[x,]
files <- file.path(SF$Dir,SF$Folder,"abundance.h5")
names(files) <- SF$SampleID
# Import and get counts
txi_GTF <- tximport(files, type = 'kallisto', tx2gene = t2g_2clsGTF, importer =
fread, countsFromAbundance = 'lengthScaledTPM')

# BATCH and Individual fixed effects
# Batch and Individual have linear combinations, only fitting Individual
ddsTxi <- DESeqDataSetFromTximport(txi_GTF,colData = SF,design = ~ IndDM +
Type_Group)

# Remove samples
rem <-
sort(c(which(SF$SampleID=="ES86_SURG"),which(SF$SampleID=="ES86_PM"),which(SF$Sa
mpleID=="ES120_SURG"),which(SF$SampleID=="ES149_PM"),which(SF$SampleID=="ES72_SU
RG")))

# remove genes with less than 10 counts
# dds <- ddsTxi[ rowSums( counts(ddsTxi) ) > 10 , ]
# > dim(dds)
# [1] 14038    17
# > colnames(dds)
 # [1] "ES90_PM"  "ES95_PM"  "ES104_PM" "ES116_PM" "ES120_PM" "ES122_PM"
"ES123_PM" "ES81_PM"  "ES83_PM"  "ES88_PM"  "ES135_PM" "ES137_PM" "ES138_PM"
"ES141_PM"
# [15] "ES148_PM" "ES153_PM" "ES154_PM"

## VSD Transformation
vsd <- vst(dds)
             png(file="SURG-GP1_PM-GP1_VSD_BXP.png",width=600,height=600)
             par(mar=c(8,3,1,1),las=2)
             boxplot(assays(vsd)[[1]],main="Counts VSD")
             dev.off()
             # Effects of transformations on the variance
             png(file="SURG-GP1_PM-GP1_VSD_DISP.png",width=600,height=600)
             meanSdPlot(assay(vsd))
             dev.off()
             #VSD HEATMAP
             sampleDists <- dist(t(assay(vsd)))
             sampleDistMatrix <- as.matrix(sampleDists)
             rownames(sampleDistMatrix) <-
paste(vsd$Subject,vsd$Group,vsd$Batch, sep="-")
             colnames(sampleDistMatrix) <- NULL
             colors <- colorRampPalette( rev(brewer.pal(9, "Blues")) )(255)
             png(file="SURG-GP1_PM-
GP1_VSD_HM_otlrExcl.png",width=600,height=600)
```

```
       pheatmap(sampleDistMatrix,clustering_distance_rows=sampleDists,clustering
_distance_cols=sampleDists,col=colors)
              dev.off()
              # VSD PCA
              png(file="SURG-GP1_PM-
GP1_VSD_PCA_otlrExcl.png",width=600,height=600)
              plt <-  plotPCA (vsd,  intgroup =c("Subject","Type_Group"),
returnData = TRUE )
              percentVar <- round ( 100 * attr (plt,"percentVar" ))
              ggplot
(plt,aes(PC1,PC2,color=Subject,shape=Type_Group))+geom_point(size=5)+
xlab(paste0 ( "PC1: " ,percentVar[ 1 ], "% variance" ))  + ylab ( paste0 ( "PC2:
" ,percentVar[ 2 ], "% variance" ))+ theme(text = element_text(size=16))
              dev.off()
       # # removing batch effect ...same individual
       vsdCP <- vsd
       assay(vsdCP) <- limma::removeBatchEffect(assay(vsdCP), vsdCP$IndDM)
       #Heatmap
       sampleDists <- dist(t(assay(vsdCP)))
       sampleDistMatrix <- as.matrix(sampleDists)
       rownames(sampleDistMatrix) <-
paste(vsdCP$Subject,vsdCP$Group,vsdCP$Batch, sep="-")
       colnames(sampleDistMatrix) <- NULL
       colors <- colorRampPalette( rev(brewer.pal(9, "Blues")) )(255)
       png(file="SURG-GP1_PM-
GP1_VSD_HM_otlrExcl_batchcor.png",width=800,height=800)
       pheatmap(sampleDistMatrix,clustering_distance_rows=sampleDists,clustering
_distance_cols=sampleDists,col=colors)
       dev.off()
       #PCA
       png(file="SURG-GP1_PM-
GP1_VSD_PCA_otlrExcl_batchcor.png",width=600,height=600)
       plt <-  plotPCA (vsdCP,  intgroup =c("Subject","Type_Group"),  returnData
= TRUE )
       percentVar <- round ( 100 * attr (plt,"percentVar" ))
       ggplot
(plt,aes(PC1,PC2,color=Subject,shape=Type_Group))+geom_point(size=5)+
xlab(paste0 ( "PC1: " ,percentVar[ 1 ], "% variance" ))  + ylab ( paste0 ( "PC2:
" ,percentVar[ 2 ], "% variance" ))+ theme(text = element_text(size=16))
       dev.off()

# Check Levels and relevel if needed
> dds$Type_Group
[1] SURG_Gp1 PM_Gp1   PM_Gp1   SURG_Gp1 PM_Gp1   SURG_Gp1
Levels: PM_Gp1 SURG_Gp1

dds$Type_Group <- relevel(dds$Type_Group,"SURG_Gp1")
# Design
> design(dds)
~IndDM + Type_Group

# DF
> dds_T16_SURGgp1_PMgp1 <- DESeq(dds,betaPrior=FALSE)
       > dds_T16_SURGgp1_PMgp1 <- DESeq(dds,betaPrior=FALSE)
       estimating size factors
       estimating dispersions
       gene-wise dispersion estimates
       mean-dispersion relationship
```

```
       final dispersion estimates
       fitting model and testing


# Results
# Treat as exploratory as there might be a strong batch effect
res_T16_SURGgp1_PMgp1 <- results(dds_T16_SURGgp1_PMgp1,contrast=c("Type_Group",
"SURG_Gp1", "PM_Gp1"))
res_T16_SURGgp1_PMgp1 <-
res_T16_SURGgp1_PMgp1[order(res_T16_SURGgp1_PMgp1$padj),]

> summary(res_T16_SURGgp1_PMgp1)

out of 11708 with nonzero total read count
adjusted p-value < 0.1
LFC > 0 (up)       : 146, 1.2%
LFC < 0 (down)     : 485, 4.1%
outliers [1]       : 0, 0%
low counts [2]     : 4994, 43%
(mean count < 13)
[1] see 'cooksCutoff' argument of ?results
[2] see 'independentFiltering' argument of ?results

# Reference level
POSITIVE VALUES == HIGHER IN SURG GROUP 1 [CONTROL]
NEGATIVE VALUES == HIGHER IN PM GROUP 1 [CONTROL]

counts(dds_T16_SURGgp1_PMgp1)[which(rownames(counts(dds_T16_SURGgp1_PMgp1))=="Cs
f3r"),which(dds_T16_SURGgp1_PMgp1$Type_Group == "SURG_Gp1")]
 ES77_SURG ES128_SURG ES129_SURG
        96        183        212
>
counts(dds_T16_SURGgp1_PMgp1)[which(rownames(counts(dds_T16_SURGgp1_PMgp1))=="Cs
f3r"),which(dds_T16_SURGgp1_PMgp1$Type_Group == "PM_Gp1")]
 ES77_PM ES128_PM ES129_PM
     952     3046     1679

#
# T17 SURG PLACEBO [gp2] - PM PLACEBO [gp2]
#
x <- sort(c(SURG_Gp2,PM_Gp2))
#select samples
SF <- samplefileDF[x,]
files <- file.path(SF$Dir,SF$Folder,"abundance.h5")
names(files) <- SF$SampleID
# REMOVE SAMPLES [add pairs of samples, as comparing SURG and PM]
rem <-
sort(c(which(SF$SampleID=="ES86_SURG"),which(SF$SampleID=="ES86_PM"),which(SF$Sa
mpleID=="ES120_SURG"),which(SF$SampleID=="ES120_PM"),which(SF$SampleID=="ES149_S
URG"),which(SF$SampleID=="ES149_PM"),which(SF$SampleID=="ES72_SURG"),which(SF$Sa
mpleID=="ES72_PM")))
SF <- SF[-rem,]
# set Individual dummy variable for linear model
> SF[order(SF$Batch,SF$Subject),c(4,7,11)]
     SampleID IndDM Batch
14   ES104_PM     1     1
25 ES104_SURG     1     1
15   ES116_PM     2     1
26 ES116_SURG     2     1
```

```
10  ES88_SURG    13     1
42    ES88_PM    13     1
51   ES135_PM     4     2
52 ES135_SURG     4     2
53   ES137_PM     5     2
54 ES137_SURG     5     2
55   ES138_PM     6     2
56 ES138_SURG     6     2
59   ES141_PM     7     2
60 ES141_SURG     7     2
67   ES148_PM     8     2
68 ES148_SURG     8     2
75   ES153_PM    10     2
76 ES153_SURG    10     2
77   ES154_PM    11     2
78 ES154_SURG    11     2

SF[order(SF$Batch,SF$Subject),7]<-c(1,1,2,2,3,3,1,1,2,2,3,3,4,4,5,5,6,6,7,7)
SF$IndDM <- droplevels(SF$IndDM)
> SF[order(SF$Batch,SF$Subject),c(4,7,11)]
     SampleID IndDM Batch
14   ES104_PM     1     1
25 ES104_SURG     1     1
15   ES116_PM     2     1
26 ES116_SURG     2     1
10  ES88_SURG     3     1
42    ES88_PM     3     1
51   ES135_PM     1     2
52 ES135_SURG     1     2
53   ES137_PM     2     2
54 ES137_SURG     2     2
55   ES138_PM     3     2
56 ES138_SURG     3     2
59   ES141_PM     4     2
60 ES141_SURG     4     2
67   ES148_PM     5     2
68 ES148_SURG     5     2
75   ES153_PM     6     2
76 ES153_SURG     6     2
77   ES154_PM     7     2
78 ES154_SURG     7     2
>
#select samples
files <- file.path(SF$Dir,SF$Folder,"abundance.h5")
names(files) <- SF$SampleID
# Drop Levels
SF$Type <- droplevels(SF$Type)
SF$IndDM <- droplevels(SF$IndDM)
SF$Group <- droplevels(SF$Group)
SF$Type_Group <- droplevels(SF$Type_Group)
# Import and get counts
txi_GTF <- tximport(files, type = 'kallisto', tx2gene = t2g_2clsGTF, importer =
fread, countsFromAbundance = 'lengthScaledTPM')
ddsTxi <- DESeqDataSetFromTximport(txi_GTF,colData = SF,design = ~ Batch + IndDM
+ Type_Group)
# remove genes with less than 10 counts
dds <- ddsTxi[ rowSums( counts(ddsTxi) ) > 10 , ]
> dim(dds)
[1] 13452    20
```

```
> colnames(dds)
 [1] "ES88_SURG"  "ES104_PM"   "ES116_PM"   "ES104_SURG" "ES116_SURG" "ES88_PM"
"ES135_PM"   "ES135_SURG" "ES137_PM"   "ES137_SURG" "ES138_PM"   "ES138_SURG"
"ES141_PM"   "ES141_SURG"
[15] "ES148_PM"   "ES148_SURG" "ES153_PM"   "ES153_SURG" "ES154_PM"
"ES154_SURG"
>

# VSD Transformation
vsd <- vst(dds)
             png(file="SURG-GP2_PM-GP2_VSD_BXP.png",width=600,height=600)
             par(mar=c(8,3,1,1),las=2)
             boxplot(assays(vsd)[[1]],main="Counts VSD")
             dev.off()
             # Effects of transformations on the variance
             png(file="SURG-GP2_PM-GP2_VSD_DISP.png",width=600,height=600)
             meanSdPlot(assay(vsd))
             dev.off()
             #VSD HEATMAP
             sampleDists <- dist(t(assay(vsd)))
             sampleDistMatrix <- as.matrix(sampleDists)
             rownames(sampleDistMatrix) <-
paste(vsd$Subject,vsd$Group,vsd$Batch, sep="-")
             colnames(sampleDistMatrix) <- NULL
             colors <- colorRampPalette( rev(brewer.pal(9, "Blues")) )(255)
             png(file="SURG-GP2_PM-
GP2_VSD_HM_otlrExcl.png",width=600,height=600)

       pheatmap(sampleDistMatrix,clustering_distance_rows=sampleDists,clustering
_distance_cols=sampleDists,col=colors)
             dev.off()
             # VSD PCA
             png(file="SURG-GP2_PM-
GP2_VSD_PCA_otlrExcl.png",width=600,height=600)
             plt <-  plotPCA (vsd,  intgroup =c("Subject","Type_Group"),
returnData = TRUE )
             percentVar <- round ( 100 * attr (plt,"percentVar" ))
             ggplot
(plt,aes(PC1,PC2,color=Subject,shape=Type_Group))+geom_point(size=5)+
xlab(paste0 ( "PC1: " ,percentVar[ 1 ], "% variance" ))  + ylab ( paste0 ( "PC2:
" ,percentVar[ 2 ], "% variance" ))+ theme(text = element_text(size=16))
             dev.off()
       # # removing batch effect
       vsdCP <- vsd
       assay(vsdCP) <- limma::removeBatchEffect(assay(vsdCP), vsdCP$Batch)
       #Heatmap
       sampleDists <- dist(t(assay(vsdCP)))
       sampleDistMatrix <- as.matrix(sampleDists)
       rownames(sampleDistMatrix) <-
paste(vsdCP$Subject,vsdCP$Group,vsdCP$Batch, sep="-")
       colnames(sampleDistMatrix) <- NULL
       colors <- colorRampPalette( rev(brewer.pal(9, "Blues")) )(255)
       png(file="SURG-GP2_PM-
GP2_VSD_HM_otlrExcl_batchcor.png",width=800,height=800)
       pheatmap(sampleDistMatrix,clustering_distance_rows=sampleDists,clustering
_distance_cols=sampleDists,col=colors)
       dev.off()
       #PCA
```

```
       png(file="SURG-GP2_PM-
GP2_VSD_PCA_otlrExcl_batchcor.png",width=600,height=600)
       plt <-  plotPCA (vsdCP,  intgroup =c("Subject","Type_Group"),  returnData
= TRUE )
       percentVar <- round ( 100 * attr (plt,"percentVar" ))
       ggplot
(plt,aes(PC1,PC2,color=Subject,shape=Type_Group))+geom_point(size=5)+
xlab(paste0 ( "PC1: " ,percentVar[ 1 ], "% variance" ))  + ylab ( paste0 ( "PC2:
" ,percentVar[ 2 ], "% variance" ))+ theme(text = element_text(size=16))
       dev.off()

# DF
dds_T17_SURGgp2_PMgp2 <- DESeq(dds,betaPrior=FALSE)
       > dds_T17_SURGgp2_PMgp2 <- DESeq(dds,betaPrior=FALSE)
       estimating size factors
       estimating dispersions
       gene-wise dispersion estimates
       mean-dispersion relationship
       final dispersion estimates
       fitting model and testing


# Results
res_T17_SURGgp2_PMgp2 <- results(dds_T17_SURGgp2_PMgp2,contrast=c("Type_Group",
"SURG_Gp2", "PM_Gp2"))
res_T17_SURGgp2_PMgp2 <-
res_T17_SURGgp2_PMgp2[order(res_T17_SURGgp2_PMgp2$padj),]

> summary(res_T17_SURGgp2_PMgp2)

out of 13452 with nonzero total read count
adjusted p-value < 0.1
LFC > 0 (up)       : 1902, 14%
LFC < 0 (down)     : 2490, 19%
outliers [1]       : 0, 0%
low counts [2]     : 1565, 12%
(mean count < 1)
[1] see 'cooksCutoff' argument of ?results
[2] see 'independentFiltering' argument of ?results

# Reference level
POSITIVE VALUES == HIGHER IN SURG GROUP 2 [PLACEBO]
NEGATIVE VALUES == HIGHER IN PM GROUP 2 [PLACEBO]

counts(dds_T17_SURGgp2_PMgp2)[which(rownames(counts(dds_T17_SURGgp2_PMgp2))=="Hp
"),which(dds_T17_SURGgp2_PMgp2$Type_Group == "SURG_Gp2")]
 ES88_SURG ES104_SURG ES116_SURG ES135_SURG ES137_SURG ES138_SURG ES141_SURG
ES148_SURG ES153_SURG ES154_SURG
        20         16         18         70         12         40         59
21         52         38
>
counts(dds_T17_SURGgp2_PMgp2)[which(rownames(counts(dds_T17_SURGgp2_PMgp2))=="Hp
"),which(dds_T17_SURGgp2_PMgp2$Type_Group == "PM_Gp2")]
ES104_PM ES116_PM  ES88_PM ES135_PM ES137_PM ES138_PM ES141_PM ES148_PM ES153_PM
ES154_PM
    2324     1725     1189     3379     2227     2431     2704     1443     3760
1285

png(file="SURG-GP2_PM-GP2_Hp_counts.png",width=600,height=600)
```

```
plotCounts(dds_T17_SURGgp2_PMgp2, gene="Hp", intgroup="Type_Group",las=1)
dev.off()

#
T18 SURG TREATMENT [gp3] - PM TREATMENT [gp3]
#
#select samples
x <- sort(c(SURG_Gp3,PM_Gp3))
SF <- samplefileDF[x,]
files <- file.path(SF$Dir,SF$Folder,"abundance.h5")
names(files) <- SF$SampleID
# REMOVE SAMPLES [add pairs of samples, as comparing SURG and PM]
rem <-
sort(c(which(SF$SampleID=="ES86_SURG"),which(SF$SampleID=="ES86_PM"),which(SF$Sa
mpleID=="ES120_SURG"),which(SF$SampleID=="ES120_PM"),which(SF$SampleID=="ES149_S
URG"),which(SF$SampleID=="ES149_PM"),which(SF$SampleID=="ES72_SURG"),which(SF$Sa
mpleID=="ES72_PM")))

SF <- SF[-rem,]
#set Individual dummy variable
> SF[order(SF$Batch,SF$Subject),c(4,7,11)]
     SampleID IndDM Batch
13   ES100_PM     1     1
24 ES100_SURG     1     1
20   ES126_PM     2     1
31 ES126_SURG     2     1
21   ES127_PM     3     1
32 ES127_SURG     3     1
5   ES82_SURG    13     1
37    ES82_PM    13     1
7   ES84_SURG    14     1
39    ES84_PM    14     1
47   ES131_PM     4     2
48 ES131_SURG     4     2
49   ES133_PM     5     2
50 ES133_SURG     5     2
57   ES139_PM     6     2
58 ES139_SURG     6     2
61   ES142_PM     7     2
62 ES142_SURG     7     2
63   ES143_PM     8     2
64 ES143_SURG     8     2
65   ES147_PM     9     2
66 ES147_SURG     9     2
71   ES150_PM    10     2
72 ES150_SURG    10     2
73   ES151_PM    11     2
74 ES151_SURG    11     2

SF[order(SF$Batch,SF$Subject),7]<-
c(1,1,2,2,3,3,4,4,5,5,1,1,2,2,3,3,4,4,5,5,6,6,7,7,8,8)
SF$IndDM <- droplevels(SF$IndDM)
> SF[order(SF$Batch,SF$Subject),c(4,7,11)]
     SampleID IndDM Batch
13   ES100_PM     1     1
24 ES100_SURG     1     1
20   ES126_PM     2     1
31 ES126_SURG     2     1
21   ES127_PM     3     1
```

```
32 ES127_SURG     3     1
5   ES82_SURG     4     1
37    ES82_PM     4     1
7   ES84_SURG     5     1
39    ES84_PM     5     1
47   ES131_PM     1     2
48 ES131_SURG     1     2
49   ES133_PM     2     2
50 ES133_SURG     2     2
57   ES139_PM     3     2
58 ES139_SURG     3     2
61   ES142_PM     4     2
62 ES142_SURG     4     2
63   ES143_PM     5     2
64 ES143_SURG     5     2
65   ES147_PM     6     2
66 ES147_SURG     6     2
71   ES150_PM     7     2
72 ES150_SURG     7     2
73   ES151_PM     8     2
74 ES151_SURG     8     2

#select samples
files <- file.path(SF$Dir,SF$Folder,"abundance.h5")
names(files) <- SF$SampleID
# Drop Levels
SF$Type <- droplevels(SF$Type)
SF$IndDM <- droplevels(SF$IndDM)
SF$Group <- droplevels(SF$Group)
SF$Type_Group <- droplevels(SF$Type_Group)
# Import and get counts
txi_GTF <- tximport(files, type = 'kallisto', tx2gene = t2g_2clsGTF, importer =
fread, countsFromAbundance = 'lengthScaledTPM')
ddsTxi <- DESeqDataSetFromTximport(txi_GTF,colData = SF,design = ~ Batch + IndDM
+ Type_Group)
# remove genes with less than 10 counts
dds <- ddsTxi[ rowSums( counts(ddsTxi) ) > 10 , ]
> dim(dds)
[1] 13874    26
> colnames(dds)
 [1] "ES82_SURG"  "ES84_SURG"  "ES100_PM"   "ES126_PM"   "ES127_PM"
"ES100_SURG" "ES126_SURG" "ES127_SURG" "ES82_PM"    "ES84_PM"    "ES131_PM"
"ES131_SURG" "ES133_PM"   "ES133_SURG"
[15] "ES139_PM"   "ES139_SURG" "ES142_PM"   "ES142_SURG" "ES143_PM"
"ES143_SURG" "ES147_PM"   "ES147_SURG" "ES150_PM"   "ES150_SURG" "ES151_PM"
"ES151_SURG"

# VSD Transformation
vsd <- vst(dds)
             png(file="SURG-GP3_PM-GP3_VSD_BXP.png",width=600,height=600)
             par(mar=c(8,3,1,1),las=2)
             boxplot(assays(vsd)[[1]],main="Counts VSD")
             dev.off()
             # Effects of transformations on the variance
             png(file="SURG-GP3_PM-GP3_VSD_DISP.png",width=600,height=600)
             meanSdPlot(assay(vsd))
             dev.off()
             #VSD HEATMAP
             sampleDists <- dist(t(assay(vsd)))
```

```
              sampleDistMatrix <- as.matrix(sampleDists)
              rownames(sampleDistMatrix) <-
paste(vsd$Subject,vsd$Group,vsd$Batch, sep="-")
              colnames(sampleDistMatrix) <- NULL
              colors <- colorRampPalette( rev(brewer.pal(9, "Blues")) )(255)
              png(file="SURG-GP3_PM-
GP3_VSD_HM_otlrExcl.png",width=600,height=600)

       pheatmap(sampleDistMatrix,clustering_distance_rows=sampleDists,clustering
_distance_cols=sampleDists,col=colors)
              dev.off()
              # VSD PCA
              png(file="SURG-GP3_PM-
GP3_VSD_PCA_otlrExcl.png",width=600,height=600)
              plt <-  plotPCA (vsd,  intgroup =c("Subject","Type_Group"),
returnData = TRUE )
              percentVar <- round ( 100 * attr (plt,"percentVar" ))
              ggplot
(plt,aes(PC1,PC2,color=Subject,shape=Type_Group))+geom_point(size=5)+
xlab(paste0 ( "PC1: " ,percentVar[ 1 ], "% variance" ))  + ylab ( paste0 ( "PC2:
" ,percentVar[ 2 ], "% variance" ))+ theme(text = element_text(size=16))
              dev.off()
       # # removing batch effect
       vsdCP <- vsd
       assay(vsdCP) <- limma::removeBatchEffect(assay(vsdCP), vsdCP$Batch)
       #Heatmap
       sampleDists <- dist(t(assay(vsdCP)))
       sampleDistMatrix <- as.matrix(sampleDists)
       rownames(sampleDistMatrix) <-
paste(vsdCP$Subject,vsdCP$Group,vsdCP$Batch, sep="-")
       colnames(sampleDistMatrix) <- NULL
       colors <- colorRampPalette( rev(brewer.pal(9, "Blues")) )(255)
       png(file="SURG-GP3_PM-
GP3_VSD_HM_otlrExcl_batchcor.png",width=800,height=800)
       pheatmap(sampleDistMatrix,clustering_distance_rows=sampleDists,clustering
_distance_cols=sampleDists,col=colors)
       dev.off()
       #PCA
       png(file="SURG-GP3_PM-
GP3_VSD_PCA_otlrExcl_batchcor.png",width=600,height=600)
       plt <-  plotPCA (vsdCP,  intgroup =c("Subject","Type_Group"),  returnData
= TRUE )
       percentVar <- round ( 100 * attr (plt,"percentVar" ))
       ggplot
(plt,aes(PC1,PC2,color=Subject,shape=Type_Group))+geom_point(size=5)+
xlab(paste0 ( "PC1: " ,percentVar[ 1 ], "% variance" ))  + ylab ( paste0 ( "PC2:
" ,percentVar[ 2 ], "% variance" ))+ theme(text = element_text(size=16))
       dev.off()

# Check Levels and relevel if needed
dds$Type_Group <- relevel(dds$Type_Group,"SURG_Gp3")
# Design
> design(dds)
~Batch + IndDM + Type_Group

# DF
dds_T18_SURGgp3_PMgp3 <- DESeq(dds,betaPrior=FALSE)
       > dds_T18_SURGgp3_PMgp3 <- DESeq(dds,betaPrior=FALSE)
       estimating size factors
```

```
       estimating dispersions
       gene-wise dispersion estimates
       mean-dispersion relationship
       final dispersion estimates
       fitting model and testing


# Results
res_T18_SURGgp3_PMgp3 <- results(dds_T18_SURGgp3_PMgp3,contrast=c("Type_Group",
"SURG_Gp3", "PM_Gp3"))
res_T18_SURGgp3_PMgp3 <-
res_T18_SURGgp3_PMgp3[order(res_T18_SURGgp3_PMgp3$padj),]

> summary(res_T18_SURGgp3_PMgp3)

out of 13874 with nonzero total read count
adjusted p-value < 0.1
LFC > 0 (up)       : 2317, 17%
LFC < 0 (down)     : 2528, 18%
outliers [1]       : 0, 0%
low counts [2]     : 2152, 16%
(mean count < 1)
[1] see 'cooksCutoff' argument of ?results
[2] see 'independentFiltering' argument of ?results


# Reference level
POSITIVE VALUES == HIGHER IN SURG GROUP 3 [TREATMENT]
NEGATIVE VALUES == HIGHER IN PM GROUP 3 [TREATMENT]

png(file="SURG-GP3_PM-GP3_Serpinb1a_counts.png",width=600,height=600)
plotCounts(dds_T18_SURGgp3_PMgp3, gene="Serpinb1a", intgroup="Type_Group",las=1)
dev.off()

#
# T19 SURG TREATMENT BLAST [gp4] - PM TREATMENT BLAST[gp4]
#
x <- sort(c(SURG_Gp4,PM_Gp4))
#select samples
SF <- samplefileDF[x,]
files <- file.path(SF$Dir,SF$Folder,"abundance.h5")
names(files) <- SF$SampleID
# Drop Levels
SF$Type <- droplevels(SF$Type)
SF$IndDM <- droplevels(SF$IndDM)
SF$Group <- droplevels(SF$Group)
SF$Type_Group <- droplevels(SF$Type_Group)
# Import and get counts
txi_GTF <- tximport(files, type = 'kallisto', tx2gene = t2g_2clsGTF, importer =
fread, countsFromAbundance = 'lengthScaledTPM')
ddsTxi <- DESeqDataSetFromTximport(txi_GTF,colData = SF,design = ~ IndDM +
Type_Group)
# remove genes with less than 10 counts
dds <- ddsTxi[ rowSums( counts(ddsTxi) ) > 10 , ]
> dim(dds)
[1] 12085     6
> colnames(dds)
[1] "ES76_SURG"  "ES87_SURG"  "ES125_PM"   "ES125_SURG" "ES76_PM"    "ES87_PM"
>
```

```
# VSD Transformation
vsd <- vst(dds)
             png(file="SURG-GP4_PM-GP4_VSD_BXP.png",width=600,height=600)
             par(mar=c(8,3,1,1),las=2)
             boxplot(assays(vsd)[[1]],main="Counts VSD")
             dev.off()
             # Effects of transformations on the variance
             png(file="SURG-GP4_PM-GP4_VSD_DISP.png",width=600,height=600)
             meanSdPlot(assay(vsd))
             dev.off()
             #VSD HEATMAP
             sampleDists <- dist(t(assay(vsd)))
             sampleDistMatrix <- as.matrix(sampleDists)
             rownames(sampleDistMatrix) <-
paste(vsd$Subject,vsd$Group,vsd$Batch, sep="-")
             colnames(sampleDistMatrix) <- NULL
             colors <- colorRampPalette( rev(brewer.pal(9, "Blues")) )(255)
             png(file="SURG-GP4_PM-
GP4_VSD_HM_otlrExcl.png",width=600,height=600)

       pheatmap(sampleDistMatrix,clustering_distance_rows=sampleDists,clustering
_distance_cols=sampleDists,col=colors)
             dev.off()
             # VSD PCA
             png(file="SURG-GP4_PM-
GP4_VSD_PCA_otlrExcl.png",width=600,height=600)
             plt <-  plotPCA (vsd,  intgroup =c("Subject","Type_Group"),
returnData = TRUE )
             percentVar <- round ( 100 * attr (plt,"percentVar" ))
             ggplot
(plt,aes(PC1,PC2,color=Subject,shape=Type_Group))+geom_point(size=5)+
xlab(paste0 ( "PC1: " ,percentVar[ 1 ], "% variance" ))  + ylab ( paste0 ( "PC2:
" ,percentVar[ 2 ], "% variance" ))+ theme(text = element_text(size=16))
             dev.off()
# Check Levels and relevel if needed
> dds$Type_Group
[1] SURG_Gp4 SURG_Gp4 PM_Gp4   SURG_Gp4 PM_Gp4   PM_Gp4
Levels: PM_Gp4 SURG_Gp4

dds$Type_Group <- relevel(dds$Type_Group,"SURG_Gp4")
# Design
> design(dds)
~IndDM + Type_Group

# DF
dds_T19_SURGgp4_PMgp4 <- DESeq(dds,betaPrior=FALSE)
       > dds_T19_SURGgp4_PMgp4 <- DESeq(dds,betaPrior=FALSE)
       estimating size factors
       estimating dispersions
       gene-wise dispersion estimates
       mean-dispersion relationship
       final dispersion estimates
       fitting model and testing

# Results
res_T19_SURGgp4_PMgp4 <- results(dds_T19_SURGgp4_PMgp4,contrast=c("Type_Group",
"SURG_Gp4", "PM_Gp4"))
res_T19_SURGgp4_PMgp4 <-
res_T19_SURGgp4_PMgp4[order(res_T19_SURGgp4_PMgp4$padj),]
```

```
> summary(res_T19_SURGgp4_PMgp4)

out of 12085 with nonzero total read count
adjusted p-value < 0.1
LFC > 0 (up)       : 190, 1.6%
LFC < 0 (down)     : 693, 5.7%
outliers [1]       : 0, 0%
low counts [2]     : 5389, 45%
(mean count < 13)
[1] see 'cooksCutoff' argument of ?results
[2] see 'independentFiltering' argument of ?results


# Reference level
POSITIVE VALUES == HIGHER IN SURG GROUP 4 [PLACEBO + BLAST]
NEGATIVE VALUES == HIGHER IN PM GROUP 4 [PLACEBO + BLAST]

png(file="SURG-GP4_PM-GP4_Il1r2_counts.png",width=600,height=600)
plotCounts(dds_T19_SURGgp4_PMgp4, gene="Il1r2", intgroup="Type_Group",las=1)
dev.off()
#
# T20 SURG TREATMENT BLAST [gp5] - PM TREATMENT BLAST [gp5]
#
x <- sort(c(SURG_Gp5,PM_Gp5))
#select samples
SF <- samplefileDF[x,]
files <- file.path(SF$Dir,SF$Folder,"abundance.h5")
names(files) <- SF$SampleID
# Drop Levels
SF$Type <- droplevels(SF$Type)
SF$IndDM <- droplevels(SF$IndDM)
SF$Group <- droplevels(SF$Group)
SF$Type_Group <- droplevels(SF$Type_Group)

# Import and get counts
txi_GTF <- tximport(files, type = 'kallisto', tx2gene = t2g_2clsGTF, importer =
fread, countsFromAbundance = 'lengthScaledTPM')

ddsTxi <- DESeqDataSetFromTximport(txi_GTF,colData = SF,design = ~ IndDM +
Type_Group)

#remove genes with less than 10 counts
dds <- ddsTxi[ rowSums( counts(ddsTxi) ) > 10 , ]
> dim(dds)
[1] 13218    12
> colnames(dds)
 [1] "ES81_SURG"  "ES83_SURG"  "ES90_PM"    "ES95_PM"    "ES122_PM"   "ES123_PM"
"ES90_SURG"  "ES95_SURG"  "ES122_SURG" "ES123_SURG" "ES81_PM"    "ES83_PM"
>
# VSD Transformation
vsd <- vst(dds)
             png(file="SURG-GP5_PM-GP5_VSD_BXP.png",width=600,height=600)
             par(mar=c(8,3,1,1),las=2)
             boxplot(assays(vsd)[[1]],main="Counts VSD")
             dev.off()
             # Effects of transformations on the variance
             png(file="SURG-GP5_PM-GP5_VSD_DISP.png",width=600,height=600)
             meanSdPlot(assay(vsd))
```

```
              dev.off()
              #VSD HEATMAP
              sampleDists <- dist(t(assay(vsd)))
              sampleDistMatrix <- as.matrix(sampleDists)
              rownames(sampleDistMatrix) <-
paste(vsd$Subject,vsd$Type,vsd$Batch, sep="-")
              colnames(sampleDistMatrix) <- NULL
              colors <- colorRampPalette( rev(brewer.pal(9, "Blues")) )(255)
              png(file="SURG-GP5_PM-
GP5_VSD_HM_otlrExcl.png",width=600,height=600)

       pheatmap(sampleDistMatrix,clustering_distance_rows=sampleDists,clustering
_distance_cols=sampleDists,col=colors)
              dev.off()
              # VSD PCA
              png(file="SURG-GP5_PM-
GP5_VSD_PCA_otlrExcl.png",width=600,height=600)
              plt <-  plotPCA (vsd,  intgroup =c("Subject","Type_Group"),
returnData = TRUE )
              percentVar <- round ( 100 * attr (plt,"percentVar" ))
              ggplot
(plt,aes(PC1,PC2,color=Subject,shape=Type_Group))+geom_point(size=5)+
xlab(paste0 ( "PC1: " ,percentVar[ 1 ], "% variance" ))  + ylab ( paste0 ( "PC2:
" ,percentVar[ 2 ], "% variance" ))+ theme(text = element_text(size=16))
              dev.off()

# Check Levels and relevel if needed
> dds$Type_Group
 [1] SURG_Gp5 SURG_Gp5 PM_Gp5   PM_Gp5   PM_Gp5   PM_Gp5   SURG_Gp5 SURG_Gp5
SURG_Gp5 SURG_Gp5 PM_Gp5   PM_Gp5
Levels: PM_Gp5 SURG_Gp5

dds$Type_Group <- relevel(dds$Type_Group,"SURG_Gp5")
# Design
> design(dds)
~IndDM + Type_Group

# DF
dds_T20_SURGgp5_PMgp5 <- DESeq(dds,betaPrior=FALSE)
       > dds_T20_SURGgp5_PMgp5 <- DESeq(dds,betaPrior=FALSE)
       estimating size factors
       estimating dispersions
       gene-wise dispersion estimates
       mean-dispersion relationship
       final dispersion estimates
       fitting model and testing

# Results

res_T20_SURGgp5_PMgp5 <- results(dds_T20_SURGgp5_PMgp5,contrast=c("Type_Group",
"SURG_Gp5", "PM_Gp5"))
res_T20_SURGgp5_PMgp5 <-
res_T20_SURGgp5_PMgp5[order(res_T20_SURGgp5_PMgp5$padj),]

> summary(res_T20_SURGgp5_PMgp5)

out of 13218 with nonzero total read count
adjusted p-value < 0.1
LFC > 0 (up)       : 1913, 14%
```

```
LFC < 0 (down)     : 2233, 17%
outliers [1]       : 0, 0%
low counts [2]     : 2050, 16%
(mean count < 2)
[1] see 'cooksCutoff' argument of ?results
[2] see 'independentFiltering' argument of ?results


# Reference level
POSITIVE VALUES == HIGHER IN SURG GROUP 5 [TREATMENT + BLAST]
NEGATIVE VALUES == HIGHER IN PM GROUP 5 [TREATMENT + BLAST]

png(file="SURG-GP5_PM-GP5_Csf3r_counts.png",width=600,height=600)
plotCounts(dds_T20_SURGgp5_PMgp5, gene="Csf3r", intgroup="Type_Group",las=1)
dev.off()
```

Annex B

RECYTMAG-65K

Normal Sample Ranges

Analyte	Sample Type & Number Tested	Strain	Mean	Range	% Detectable
G-CSF	serum 0 hr post LPS-challenge (n=40)	Sprague Dawley (SD)	0	0-0	0%
G-CSF	serum 2 hr post LPS-challenge (n=40)	SD	0	0-0	0%
G-CSF	serum 4 hr post LPS-challenge (n=40)	SD	0	0-0	0%
G-CSF	serum 8 hr post LPS-challenge (n=40)	SD	0	0-0	0%
Eotaxin	serum 0 hr post LPS-challenge (n=40)	SD	4	0-167	5%
Eotaxin	serum 2 hr post LPS-challenge (n=40)	SD	4	0-143	3%
Eotaxin	serum 4 hr post LPS-challenge (n=40)	SD	3	0-111	5%
Eotaxin	serum 8 hr post LPS-challenge (n=40)	SD	2	0-78	3%
GM-CSF	serum 0 hr post LPS-challenge (n=40)	SD	14	0-119	18%
GM-CSF	serum 2 hr post LPS-challenge (n=40)	SD	16	0-164	18%
GM-CSF	serum 4 hr post LPS-challenge (n=40)	SD	8	0-147	13%
GM-CSF	serum 8 hr post LPS-challenge (n=40)	SD	8	0-137	13%
IL-1a	serum 0 hr post LPS-challenge (n=40)	SD	11	0-238	28%
IL-1a	serum 2 hr post LPS-challenge (n=40)	SD	15	0-157	55%
IL-1a	serum 4 hr post LPS-challenge (n=40)	SD	20	0-166	58%
IL-1a	serum 8 hr post LPS-challenge (n=40)	SD	18	0-123	70%
Leptin	serum 0 hr post LPS-challenge (n=40)	SD	7894	3420-21012	100%
Leptin	serum 2 hr post LPS-challenge (n=40)	SD	8222	2976-16722	100%
Leptin	serum 4 hr post LPS-challenge (n=40)	SD	7856	3288-17370	100%
Leptin	serum 8 hr post LPS-challenge (n=40)	SD	7411	2964-15204	100%
MIP-1a	serum 0 hr post LPS-challenge (n=40)	SD	31	8-108	100%
MIP-1a	serum 2 hr post LPS-challenge (n=40)	SD	220	15-598	100%
MIP-1a	serum 4 hr post LPS-challenge (n=40)	SD	228	19-569	100%
MIP-1a	serum 8 hr post LPS-challenge (n=40)	SD	165	35-941	100%
IL-4	serum 0 hr post LPS-challenge (n=40)	SD	24	0-108	88%
IL-4	serum 2 hr post LPS-challenge (n=40)	SD	33	0-109	98%
IL-4	serum 4 hr post LPS-challenge (n=40)	SD	38	0-81	95%
IL-4	serum 8 hr post LPS-challenge (n=40)	SD	41	4-94	100%
IL-1B	serum 0 hr post LPS-challenge (n=40)	SD	492	0-5533	80%
IL-1B	serum 2 hr post LPS-challenge (n=40)	SD	522	0-3194	95%
IL-1B	serum 4 hr post LPS-challenge (n=40)	SD	368	0-2680	98%
IL-1B	serum 8 hr post LPS-challenge (n=40)	SD	258	0-1560	88%
IL-2	serum 0 hr post LPS-challenge (n=40)	SD	288	0-3710	65%
IL-2	serum 2 hr post LPS-challenge (n=40)	SD	177	0-2375	78%
IL-2	serum 4 hr post LPS-challenge (n=40)	SD	219	0-1974	83%
IL-2	serum 8 hr post LPS-challenge (n=40)	SD	164	0-1654	80%

Annex B

Analyte	Sample Type & Number Tested	Strain	Mean	Range	% Detectable
IL-6	serum 0 hr post LPS-challenge (n=40)	SD	211	0-6799	18%
IL-6	serum 2 hr post LPS-challenge (n=40)	SD	714	0-5629	63%
IL-6	serum 4 hr post LPS-challenge (n=40)	SD	1728	0-31956	80%
IL-6	serum 8 hr post LPS-challenge (n=40)	SD	608	0-4427	75%
EGF	serum 0 hr post LPS-challenge (n=40)	SD	0	0-4	13%
EGF	serum 2 hr post LPS-challenge (n=40)	SD	0	0-10	18%
EGF	serum 4 hr post LPS-challenge (n=40)	SD	3	0-59	23%
EGF	serum 8 hr post LPS-challenge (n=40)	SD	2	0-25	53%
IL-13	serum 0 hr post LPS-challenge (n=40)	SD	14	0-274	50%
IL-13	serum 2 hr post LPS-challenge (n=40)	SD	17	0-185	70%
IL-13	serum 4 hr post LPS-challenge (n=40)	SD	18	0-130	70%
IL-13	serum 8 hr post LPS-challenge (n=40)	SD	22	0-76	88%
IL-10	serum 0 hr post LPS-challenge (n=40)	SD	484	11-4738	100%
IL-10	serum 2 hr post LPS-challenge (n=40)	SD	893	110-3605	100%
IL-10	serum 4 hr post LPS-challenge (n=40)	SD	1026	118-6307	100%
IL-10	serum 8 hr post LPS-challenge (n=40)	SD	1115	70-7611	100%
IL-12p70	serum 0 hr post LPS-challenge (n=40)	SD	32	0-79	98%
IL-12p70	serum 2 hr post LPS-challenge (n=40)	SD	44	0-102	98%
IL-12p70	serum 4 hr post LPS-challenge (n=40)	SD	52	16-104	100%
IL-12p70	serum 8 hr post LPS-challenge (n=40)	SD	58	10-121	100%
IFNg	serum 0 hr post LPS-challenge (n=40)	SD	4	0-199	3%
IFNg	serum 2 hr post LPS-challenge (n=40)	SD	24	0-374	23%
IFNg	serum 4 hr post LPS-challenge (n=40)	SD	257	0-3443	35%
IFNg	serum 8 hr post LPS-challenge (n=40)	SD	138	0-2190	25%
IL-5	serum 0 hr post LPS-challenge (n=40)	SD	0	0-0	0%
IL-5	serum 2 hr post LPS-challenge (n=40)	SD	16	0-223	18%
IL-5	serum 4 hr post LPS-challenge (n=40)	SD	6	0-159	8%
IL-5	serum 8 hr post LPS-challenge (n=40)	SD	10	0-260	10%
IL-17	serum 0 hr post LPS-challenge (n=40)	SD	1	0-28	3%
IL-17	serum 2 hr post LPS-challenge (n=40)	SD	0	0-18	3%
IL-17	serum 4 hr post LPS-challenge (n=40)	SD	0	0-11	3%
IL-17	serum 8 hr post LPS-challenge (n=40)	SD	0	0-0	0%
IL-18	serum 0 hr post LPS-challenge (n=40)	SD	386	0-5523	78%
IL-18	serum 2 hr post LPS-challenge (n=40)	SD	236	0-3387	80%
IL-18	serum 4 hr post LPS-challenge (n=40)	SD	292	0-2881	90%
IL-18	serum 8 hr post LPS-challenge (n=40)	SD	243	0-2627	93%

Analyte	Sample Type & Number Tested	Strain	Mean	Range	% Detectable
MCP-1	serum 0 hr post LPS-challenge (n=40)	SD	741	331-1803	100%

Annex B

MCP-1	serum 2 hr post LPS-challenge (n=40)	SD	6122	489-15354	100%
MCP-1	serum 4 hr post LPS-challenge (n=40)	SD	5753	627-19423	100%
MCP-1	serum 8 hr post LPS-challenge (n=40)	SD	4466	795-10728	100%
IP-10	serum 0 hr post LPS-challenge (n=40)	SD	351	180-779	100%
IP-10	serum 2 hr post LPS-challenge (n=40)	SD	1592	347-2641	100%
IP-10	serum 4 hr post LPS-challenge (n=40)	SD	1950	410-3751	100%
IP-10	serum 8 hr post LPS-challenge (n=40)	SD	1662	4553331	100%
GRO/KC	serum 0 hr post LPS-challenge (n=40)	SD	216	106-412	100%
GRO/KC	serum 2 hr post LPS-challenge (n=40)	SD	11298	286->maxDC	100%
GRO/KC	serum 4 hr post LPS-challenge (n=40)	SD	5773	274->maxDC	100%
GRO/KC	serum 8 hr post LPS-challenge (n=40)	SD	3161	164-13648	100%
VEGF	serum 0 hr post LPS-challenge (n=40)	SD	73	24-413	100%
VEGF	serum 2 hr post LPS-challenge (n=40)	SD	61	25-261	100%
VEGF	serum 4 hr post LPS-challenge (n=40)	SD	76	25-291	100%
VEGF	serum 8 hr post LPS-challenge (n=40)	SD	72	30-196	100%
Fractalkine	serum 0 hr post LPS-challenge (n=40)	SD	61	28-285	100%
Fractalkine	serum 2 hr post LPS-challenge (n=40)	SD	88	23-269	100%
Fractalkine	serum 4 hr post LPS-challenge (n=40)	SD	131	22-341	100%
Fractalkine	serum 8 hr post LPS-challenge (n=40)	SD	134	31-344	100%
LIX	serum 0 hr post LPS-challenge (n=40)	SD	3664	2415-6464	100%
LIX	serum 2 hr post LPS-challenge (n=40)	SD	3929	2207-9502	100%
LIX	serum 4 hr post LPS-challenge (n=40)	SD	3450	2223-6715	100%
LIX	serum 8 hr post LPS-challenge (n=40)	SD	3125	1771-5804	100%
MIP-2	serum 0 hr post LPS-challenge (n=40)	SD	92	32-193	100%
MIP-2	serum 2 hr post LPS-challenge (n=40)	SD	944	84-3832	100%
MIP-2	serum 4 hr post LPS-challenge (n=40)	SD	492	55-3556	100%
MIP-2	serum 8 hr post LPS-challenge (n=40)	SD	524	78-4900	100%
TNFa	serum 0 hr post LPS-challenge (n=40)	SD	4	0-40	20%
TNFa	serum 2 hr post LPS-challenge (n=40)	SD	97	0-387	93%
TNFa	serum 4 hr post LPS-challenge (n=40)	SD	50	0-193	93%
TNFa	serum 8 hr post LPS-challenge (n=40)	SD	60	0-713	90%
RANTES	serum 0 hr post LPS-challenge (n=40)	SD	3568	1762-7249	100%
RANTES	serum 2 hr post LPS-challenge (n=40)	SD	3950	1607-9274	100%
RANTES	serum 4 hr post LPS-challenge (n=40)	SD	3868	1655-10414	100%
RANTES	serum 8 hr post LPS-challenge (n=40)	SD	3429	1427-8263	100%